VOLUME 37 APRIL 1959 NUMBER 4

Canadian Journal of Chemistry

Published by THE NATIONAL RESEARCH COUNCIL
OTTAWA CANADA

Canadian Journal of Chemistry

Under the authority of the Chairman of the Committee of the Privy Council on Scientific and Industrial Research, the National Research Council issues THE CANADIAN JOURNAL OF CHEMISTRY and five other journals devoted to the publication, in English or French, of the results of original scientific research. Matters of general policy concerning these journals are the responsibility of a joint Editorial Board consisting of: members representing the National Research Council of Canada; the Editors of the Journals; and members representing the Royal Society of Canada and four other scientific societies.

The Chemical Institute of Canada has chosen the Canadian Journal of Chemistry as its medium of publication for scientific papers.

Manuscripts for publication should be submitted to Dr. Léo Marion, Editor-in-Chief, Canadian Journal of Chemistry, National Research Council, Ottawa 2, Canada.
(For instructions on preparation of copy, see **Notes to Contributors** (inside back cover).)

Proof, correspondence concerning proof, and orders for reprints should be sent to the Manager, Editorial Office (Research Journals), Division of Administration and Awards, National Research Council, Ottawa 2, Canada.

Subscriptions, renewals, requests for single or back numbers, and all remittances should be sent to Division of Administration and Awards, National Research Council, Ottawa 2, Canada. Remittances should be made payable to the Receiver General of Canada, credit National Research Council.

The journals published, frequency of publication, and prices are:

Canadian Journal of Biochemistry and Physiology	Monthly	$9.00 a year
Canadian Journal of Botany	Bimonthly	$6.00 a year
Canadian Journal of Chemistry	Monthly	$12.00 a year
Canadian Journal of Microbiology	Bimonthly	$6.00 a year
Canadian Journal of Physics	Monthly	$9.00 a year
Canadian Journal of Zoology	Bimonthly	$5.00 a year

The price of regular single numbers of all journals is $2.00.

Canadian Journal of Chemistry

Issued by THE NATIONAL RESEARCH COUNCIL OF CANADA

VOLUME 37 APRIL 1959 NUMBER 4

THE REACTION OF ACTIVE NITROGEN WITH HYDROGEN BROMIDE[1]

H. B. DUNFORD AND BERNADINE E. MELANSON

ABSTRACT

The reaction of active nitrogen with hydrogen bromide was found to produce bromine and ammonium bromide as the main products, along with traces of compounds tentatively identified as bromamine, NH_2Br, and bromimine, $NHBr_2$. Hydrogen abstraction from hydrogen bromide by nitrogen atoms, imine and amine radicals can account for ammonia formation. Considerable catalysis of nitrogen atom recombination by hydrogen bromide appears to occur. A resonance transfer of the electronic energy responsible for the nitrogen afterglow to bromine with a resultant bromine emission spectrum is proposed to account for the orange reaction flame.

INTRODUCTION

In an early study Willey and Rideal (1) attributed the reactivity of active nitrogen in its reaction with hydrogen bromide to excited nitrogen molecules. However, Ewart and Rodebush (2) believed that the reactivity was due entirely to atomic nitrogen. The present paper reports the results of a more extensive investigation of the reaction.

EXPERIMENTAL

Hydrogen bromide was produced by burning the mixture obtained by bubbling cylinder hydrogen through Baker's C. P. bromine (3) which was kept at room temperature. The resultant hydrogen bromide and excess hydrogen were passed through a trap cooled with a dry ice – acetone mixture to remove moisture, and the hydrogen bromide was retained in a second trap cooled with liquid air. It was stored for use after a single bulb-to-bulb distillation.

The nitrogen was activated by a condensed discharge and was reacted with the hydrogen bromide in a fast flow system. Details of the type of apparatus have been described elsewhere (4, 5). In the present system the flow rate of molecular nitrogen was 3.64×10^{-5} mole per second at a pressure of 0.8 mm of mercury. Reaction time was 0.2 second. Condensable gases obtained as reaction products were retained in traps cooled with liquid air and analyzed after fractionation in a LeRoy still (6). The rate of salt deposition from the reaction of active nitrogen with hydrogen bromide was determined in a special series of experiments in which the salt was washed from the system with distilled water and titrated for bromide ion. The washing process eventually removed some of the metaphosphoric acid used to poison the flow system, so that when products condensable in liquid air were being analyzed, the salt was removed from the system by

[1]*Manuscript received October 7, 1958.*

A joint contribution from the Departments of Chemistry, Dalhousie University, Halifax, N.S., and the University of Alberta, Edmonton, Alberta. Based on a paper presented at the 41st Annual Conference and Exhibition of the Chemical Institute of Canada, Toronto, May 26–28, 1958.

reaction with active nitrogen. In a few experiments, products of the reaction of active nitrogen with salt were retained for analysis by placing liquid air around the second trap in the flow system.

Bromine and various mixtures of bromine – hydrogen bromide and hydrogen – hydrogen bromide were also reacted with active nitrogen. Flow rates of hydrogen and hydrogen bromide were each determined by conventional pressure–volume–time measurements. Liquid bromine was stored in a cylindrical container which was immersed in an ice–water mixture. Bromine vapor from the container was pumped through various sizes of calibrated flowmeters.

The maximum yield of hydrogen cyanide obtained from the reaction of active nitrogen with ethylene was also determined at room temperature and at 340° in order to determine the flow rate of atomic nitrogen (4). In two experiments ethylene was fed into a reaction vessel which had previously been coated with ammonium bromide.

RESULTS

The Reaction of Active Nitrogen with Hydrogen Bromide

At 80° C the reaction of active nitrogen with hydrogen bromide produced an orange flame and effectively quenched the nitrogen afterglow. As was observed earlier (2), the flame consisted of bands in the 590–600 mμ region. At 380°, the typical active nitrogen afterglow could be observed emerging from the reaction vessel at all but the highest rates of hydrogen bromide input; about two inches below the reaction vessel the afterglow was replaced by the orange flame.

A salt deposit formed on the walls of the reaction vessel in experiments conducted at 80° C. At higher temperatures, it formed only on the walls of the tubing connecting the reaction vessel to the first liquid air trap. Kjeldahl determinations and Volhard titrations indicated a 1.01:1.00 ratio (±0.01) of ammonium to bromide ions. Tests for hydrazine hydrobromide (7) were negative as were tests for oxidizing agents with potassium iodide. It was therefore concluded, in agreement with the findings of Ewart and Rodebush, that the salt was pure ammonium bromide.

The volatile products of the reaction of active nitrogen with hydrogen bromide, which were separated on the LeRoy still, were as follows. Hydrogen bromide was removed by distillation at −135° C. The rate of its recovery was determined by pressure–volume measurements and by titration with standard alkali solution. A small amount of product (A) was recovered at −90° C. Crude measurements indicated that its vapor pressure obeyed the equation $\log p_{mm} = -1.7\times10^3/T+9.0$ over the pressure range 0.01 to 0.4 mm. The material was white in the solid state, gave a negative Nessler test, and liberated iodine when warmed with frozen potassium iodide solution. Its rate of formation was of the order of 10^{-8} mole per second. Bromine was distilled at 50° C and trapped on frozen potassium iodide solution. The iodine liberated upon warming was titrated with standard thiosulphate solution. A trace of material (B) was removed after the distillation of bromine. It was white when frozen and had a vapor pressure, measured over the range 0.01 to 0.05 mm, comparable to that of hydrazine (8). However, it gave a negative test with salicylaldehyde (7). Furthermore, any hydrazine which might have been formed might be expected to react with excess hydrogen bromide to form hydrazine hydrobromide. It is proposed tentatively that A and B are bromamine, NH_2Br, and bromimine, $NHBr_2$, respectively. Neither compound has been isolated before, although the preparation of ether solutions of NH_2Br and $NHBr_2$ has been reported (9).

The rates of formation of bromine and ammonium bromide at various flow rates of

hydrogen bromide are shown in Figs. 1 and 2, respectively. The maximum rate of recovery of hydrogen cyanide from the reaction of active nitrogen with ethylene at 80° C was 8.0×10^{-6} mole per second, and this was unaffected by the presence of ammonium bromide in the reaction vessel; at 340° it was 9.0×10^{-6} mole per second.[2] Since the rate of hydrogen cyanide recovery from the reaction of active nitrogen with ethylene becomes constant above 250°, the latter figure is used as an indication of the atomic nitrogen flow rate at all temperatures.

The Reaction of Active Nitrogen with Ammonium Bromide

The flame of the reaction of active nitrogen with ammonium bromide, as observed with a pocket spectroscope, was the same as that obtained in the corresponding hydrogen bromide flame. As the salt with its orange flame was slowly swept along the flow system

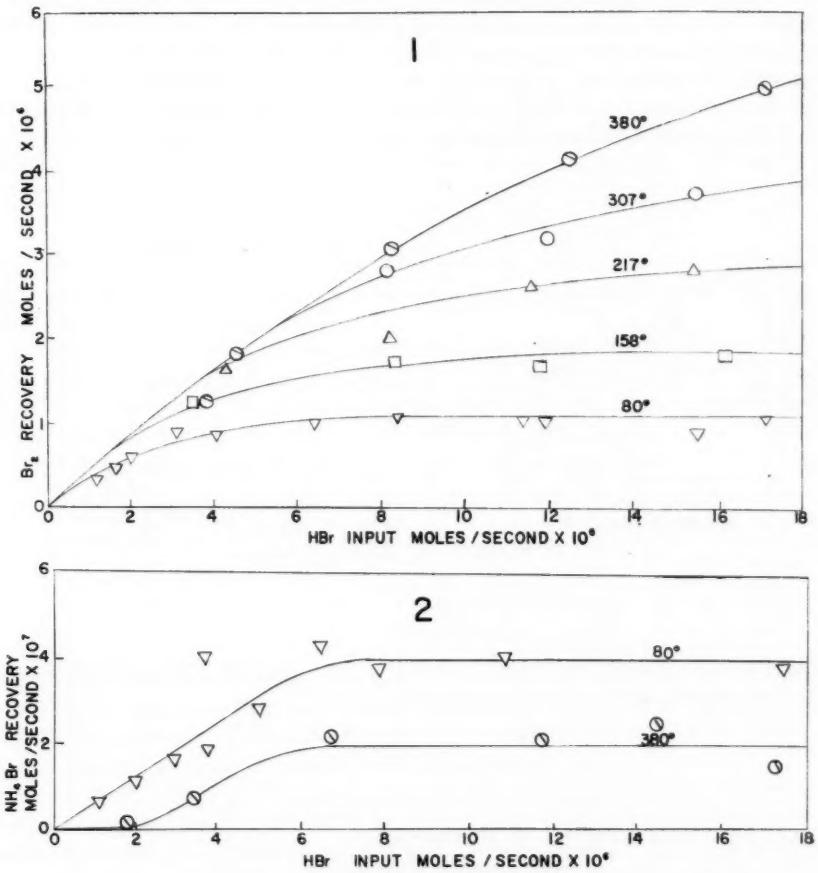

FIGS. 1 and 2.

[2] *Larger temperature coefficients from room temperature to 250° for the rate of hydrogen cyanide production from the reaction of active nitrogen with ethylene have been observed in faster flow systems (10).*

a blue glow gradually developed between the nitrogen afterglow and the orange emission. The blue glow, as observed spectroscopically, appeared as a continuum with its long wave length edge at approximately 510 mμ. In a typical experiment active nitrogen was reacted for 1 hour with 1.5×10^{-4} mole of ammonium bromide which had previously been deposited in the reaction vessel. All but a trace of the salt was destroyed and 4.2×10^{-5} mole of hydrogen bromide, 5.5×10^{-5} mole of bromine, and a trace of compound B were recovered.

The Reactions of Active Nitrogen with Bromine and Hydrogen – Hydrogen Bromide and Bromine – Hydrogen Bromide Mixtures

When bromine was fed into the active nitrogen stream no product was recovered except molecular bromine (1). However, the same orange band as that observed in the flame of active nitrogen reactions with hydrogen bromide and ammonium bromide was observed in the flame produced by the interaction of active nitrogen and bromine. Furthermore, when the input of bromine was stopped, but the flow of active nitrogen was continued, the same blue continuum, as observed in the reaction of active nitrogen with ammonium bromide was produced as the orange flame retreated rapidly.

The results of the combined additions of bromine – hydrogen bromide and hydrogen – hydrogen bromide mixtures are summarized in Fig. 3.

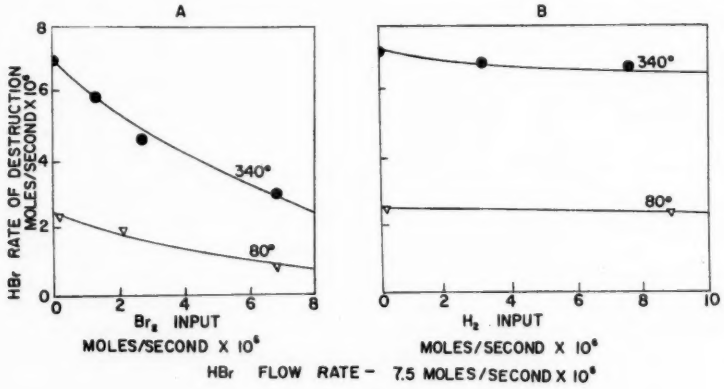

FIG. 3.

DISCUSSION

The mechanism of ammonium bromide formation proposed by Ewart and Rodebush, with added thermochemical data,[3] is as follows:

$$N + HBr \rightarrow NH + Br + 1 \text{ kcal}, \quad [1]$$

$$NH + HBr \rightarrow NH_2 + Br + 1 \text{ kcal}, \quad [2]$$

$$NH_2 + HBr \rightarrow NH_3 + Br + 17 \text{ kcal}, \quad [3]$$

[3] *All heats of reaction are calculated from the following data:*
D_{H-Br} = *87 kcal*, D_{H-H} = *104 kcal*, D_{Br-Br} = *46 kcal—Selected values of chemical thermodynamic properties. National Bureau of Standards, Washington, D.C. 1950.*
D_{N-H} = *88 kcal—Pannetier, G. and Gaydon, A. G. J. chim. phys.* **48**, *221 (1951).*
D_{NH_2-H} = *104 kcal—Swarcz, M. Chem. Revs.* **47**, *75 (1950).*
D_{N_2} = *225 kcal—Hendrie, J. M. J. Chem. Phys.* **22**, *1503 (1954).*
ΔH_f NH_3 = *11 kcal—Handbook of chemistry and physics.*
ΔH_{sub} NH_4Br = *44 kcal—Smits, A. and deLange, W. J. Chem. Soc. 2936 (1928).*

$$NH_3 + HBr \rightarrow NH_4Br + 44 \text{ kcal}, \quad [4]$$

$$2Br + M \rightarrow Br_2 + M + 46 \text{ kcal}. \quad [5]$$

There is ample evidence that atomic nitrogen is present in active nitrogen and that it is chemically reactive (11). However, if reactions [1–5] were the only ones occurring then the optimum rate of recovery of ammonium bromide would be equal to the flow rate of atomic nitrogen, and the rate of molecular bromine formation would be 1.5 times as great. Actually, the maximum recovery rates of ammonium bromide and bromine obtained at 80° C are, respectively, only 1/22 and 1/9 as great as the available supply of atomic nitrogen, as indicated by the maximum recovery of hydrogen cyanide from ethylene. At 380° the yield of ammonium bromide is still lower and the bromine recovery has climbed to 5/9 the amount of atomic nitrogen available.

Reactions of the type:

$$2NH \rightarrow N_2 + H_2 + 153 \text{ kcal}, \quad [6]$$

$$2NH_2 \rightarrow N_2 + 2H_2 + 81 \text{ kcal}, \quad [7]$$

$$N + NH \rightarrow N_2 + H + 137 \text{ kcal}, \quad [8]$$

$$N + NH_2 \rightarrow N_2 + 2H + 49 \text{ kcal}, \quad [9]$$

would have the effect of a reduction in the yields of bromine and ammonium bromide. Reaction [9], which is spin allowed for three out of every eight collisions, would be favored over the more exothermic reaction

$$N + NH_2 \rightarrow N_2 + H_2 + 153 \text{ kcal},$$

which is spin disallowed. Reactions [6–9] inclusive presumably would have very low activation energies and might occur more rapidly on the wall, since they are all free radical or atomic reactions.

However, even if every imine radical were destroyed in [8], the yield of bromine would still be too large, namely one-quarter of the available supply of atomic nitrogen. Only the possible fate of atomic hydrogen formed in [8] and [9] might reconcile the above mechanism with the experimental observations.

Atomic hydrogen, if formed, might be expected to recombine

$$2H + M \rightarrow H_2 + M + 104 \text{ kcal} \quad [10]$$

or to undergo one of the following reactions:

$$H + HBr \rightarrow H_2 + Br + 17 \text{ kcal}, \quad [11]$$

$$H + Br_2 \rightarrow HBr + Br + 41 \text{ kcal}, \quad [12]$$

$$H + Br + M \rightarrow HBr + M + 87 \text{ kcal}. \quad [13]$$

Both reactions [12] and [13] would decrease the yield of bromine. The ratio k_{12}/k_{11} is known to be about 10 over a considerable temperature range (12). Since both [11] and [12] are extremely rapid, they might be expected to consume most of the available atomic hydrogen before it could reach the reaction vessel wall.

Two rather serious objections can be raised to the mechanism outlined in [1–13]. First, an increase in the flow rate of hydrogen bromide should increase the rate of bromine formation through [1–3] and [11], yet plateaus in bromine production are observed at the two lowest temperatures at which the reaction was studied.

Second, if the above mechanism is to account for the low rate of recovery of bromine at 80°, then [8–9] followed by [12] must be remarkably efficient processes. The slope of the curve in Fig. 3A would indicate that if [12] is extensive in the present system, its

effect is largely offset by [11]; cf. the effect of added chlorine on the rate of destruction of hydrogen chloride observed by Wiles and Winkler (10). Furthermore the existence of excess active nitrogen at high flow rates of hydrogen bromide at high temperatures is not compatible with the postulate of extensive occurrence of [8–9] in the present system.

In the reaction of active nitrogen with hydrogen chloride, where hydrogen abstraction by atomic nitrogen is prohibitive energetically at lower temperatures, the initiation steps were assumed to be

$$N + HCl \rightarrow [H\text{–}Cl\text{–}N],$$
$$N + [H\text{–}Cl\text{–}N] \rightarrow N_2 + H + Cl.$$

If the corresponding initial steps occurred in the present system, then ammonia formation would proceed through the reactions

$$N + H + M \rightarrow NH + M, \qquad [14]$$
$$NH + H_2 \rightarrow NH_3, \qquad [15]$$

as first proposed by Steiner (13).

A qualitative comparison of other reactions involving atomic hydrogen in the reaction of active nitrogen with hydrogen chloride and in the present system may be of interest. In the former system considerable quantities of atomic hydrogen are liberated and largely removed through the reactions

$$H + HCl \rightarrow H_2 + Cl,$$
$$H + Cl_2 \rightarrow HCl + Cl,$$

which have activation energies of 5 and 3 kcal, respectively. In the present system, the corresponding reactions [11] and [12] both have activation energies of 2 kcal or less, and so removal of hydrogen atoms is even more rapid. Since no ammonia is formed through [14–15] in the reaction of active nitrogen with hydrogen chloride, it might appear even less likely in the present system, where the steady state concentration of atomic hydrogen is even lower. A more convincing argument perhaps is the fact that if the reactions

$$N + HBr \rightarrow [H\text{–}Br\text{–}N], \qquad [1a]$$
$$N + [H\text{–}Br\text{–}N] \rightarrow N_2 + H + Br, \qquad [16a]$$

which would be the principle source of atomic hydrogen, were predominant at 80°, then the yield of molecular bromine would be one-quarter of the available supply of atomic nitrogen, provided, as appears to be the case, that the net regeneration of hydrogen bromide from atomic hydrogen reactions is not of prime significance at 80°.

A mechanism which would appear to account for most features of the reaction satisfactorily is [1*a*] followed by

$$[H\text{–}Br\text{–}N] \rightarrow NH + Br, \qquad [1b]$$
$$N + [H\text{–}Br\text{–}N] \rightarrow N_2 + HBr. \qquad [16b]$$

Ammonia formation could proceed through [2–3].

If [16*b*] is predominant at 80°, an increase in the flow rate of hydrogen bromide would mainly increase the rate of nitrogen atom recombination. Hence the plateau in the rate of bromine production can be explained. At higher temperatures, if [1*b*] becomes increasingly important, then the temperature coefficient for bromine production, and its increased sensitivity to hydrogen bromide flow rate with increased temperature, can be

explained. It is thus not necessary to attach prime importance to reactions [6–13] in the present system.

Whether the substance which catalyzes the recombination of atomic nitrogen will be decomposed is dependent on the fraction of the recombination energy which is transmitted to the remainder of the complex. For a hydrogen bromide complex, it would appear that this fraction is less than the ratio of the bond dissociation energies of hydrogen bromide and nitrogen, namely 87/225, or 0.39, provided that the hydrogen bromide remains in its electronic ground state. For a hydrogen chloride complex, the fraction must have a minimum value of 0.46. The difference might be attributed to the relative sizes of the p orbitals of chlorine and bromine, the latter being too large to facilitate formation of a strongly bonded complex with atomic nitrogen.

There remains the problem of why the yield of ammonium bromide decreases with increasing temperature. Because of the appreciable sublimation pressure of ammonium bromide at higher temperatures (one atmosphere at 396° C), the occurrence of [4] is prevented in a hot reaction vessel. Ammonia, which at 80° would be removed rapidly from the flow system by [4], could, to a large measure, be destroyed by reaction with active nitrogen at higher temperatures. The rapid rate of reaction of active nitrogen with ammonia, even in competition with the reaction of active nitrogen with ethylene, introduced as a second reactant, has been demonstrated previously (14).

Because the bands in the 590–600 mμ region are produced as a result of the interaction of active nitrogen and pure bromine, it would appear that bromine, produced in the reactions of active nitrogen with hydrogen bromide and ammonium bromide, respectively, is responsible for the emission of the same orange band in the latter two reactions.

Ewart and Rodebush originally proposed that the transfer of two vibrational quanta from the $B\ ^3\Pi_g$ state of nitrogen to a ground state molecule of hydrogen bromide, followed by a modified $B\ ^3\Pi_g \rightarrow A\ ^3\Sigma_u^+$ transition in the active nitrogen as the cause of the orange flame. This appeared plausible as the appropriate vibrational energy spacings of the B state of nitrogen are roughly double those of the ground state of hydrogen bromide, and the selection rule for the transfer of vibrational quanta states that $v = \pm 1$ or ± 2. However, if the interaction of active nitrogen and bromine is responsible for the orange band, then an explanation in terms of a modified nitrogen afterglow is not possible, since the vibrational energy spacings of the ground state of bromine differ by a factor of approximately nine from those of the B state of nitrogen (15).

Transitions between the ground state of bromine, $X\ ^1\Sigma_g^+$, and the state $B\ ^3\Pi_{0_u^+}$ are known in both emission and absorption. A careful plot of the potential functions of both states shows that the energy corresponding to the transition from the first vibrational level of the X state of bromine to the 15th, 16th, and 17th levels of the B state matches exactly the energy emitted in the first positive bands of active nitrogen. The transition does not violate the Franck–Condon principle; furthermore, an appreciable fraction of ground state bromine molecules have $v = 1$ at 80° C. Such a resonance transfer is much more likely to occur when the energy matching is exact (16). The return transitions $15' \rightarrow 2''$, $16' \rightarrow 2''$, and $17' \rightarrow 2''$ could account for the orange emission. Transitions to the zero vibrational level of the ground state would violate the Franck–Condon principle.[4] That the emission occurs in such a selective wave length region might indicate that

[4] *The referee has pointed out the apparent violation of spin conservation in the energy transfer process proposed above. However, the* $^3\Pi$–$^1\Sigma$ *transition in the halogens appears identical with a* $^1\Sigma$–$^1\Sigma$ *transition (17). No real significance can be attached to the S and* Λ *quantum numbers, but only to* Ω *for the excited state of bromine.*

quenching of the B state bromine molecules occurs in the present system more rapidly than the exchange of vibrational quanta among B state molecules of bromine. The quenching of the B state of iodine and bromine by various gases by an induced predissociation mechanism has been observed by various authors (15).

The blue emission continuum corresponds to that observed for the two-body recombination of $^2P_{3/2}$ and $^2P_{1/2}$ bromine atoms followed by a $B \rightarrow X$ transition. The source of excited bromine atoms is not clear. Furthermore the probability of the two-body atom recombination occurring is very slight, but it appears to provide the only readily available explanation of the blue glow. The two-body recombination of atoms has been observed spectroscopically for the halogens at high temperatures (18) and for tellurium vapor in an intense discharge (19).

ACKNOWLEDGMENTS

This project was supported financially by the National Research Council. One of us (B.E.M.) is also indebted to Canadian Industries Limited for a Fellowship and to N.R.C. for a Studentship.

REFERENCES

1. WILLEY, E. J. B. and RIDEAL, E. K. J. Chem. Soc. 669 (1927).
2. EWART, R. H. and RODEBUSH, W. R. J. Am. Chem. Soc. **56**, 97 (1934).
3. ORGANIC SYNTHESES. Vol. XV. John Wiley & Sons, Inc., New York. 1935. p. 35.
4. GREENBLATT, J. and WINKLER, C. A. Can. J. Research, B, **27**, 721 (1949).
5. BLADES, H. and WINKLER, C. A. Can. J. Chem. **30**, 915 (1952).
6. LEROY, D. J. Can. J. Research, B, **28**, 492 (1950).
7. FEIGL, F. Spot tests. Nordemann Publishing Co., New York. 1939. p. 155.
8. HANDBOOK OF CHEMISTRY AND PHYSICS. Chemical Rubber Publishing Co., Cleveland. 1957.
9. COLEMAN, G. H., YAGER, C. B., and SOROOS, H. J. Am. Chem. Soc. **56**, 965 (1934).
10. WILES, D. M. and WINKLER, C. A. Can. J. Chem. **35**, 1298 (1957).
11. EVANS, H. G. V. and WINKLER, C. A. Can. J. Chem. **34**, 1217 (1956).
12. LAIDLER, K. J. Chemical kinetics. McGraw-Hill Book Company. 1950.
13. STEINER, W. Z. Elektrochem. **36**, 807 (1930).
14. FREEMAN, G. R. and WINKLER, C. A. J. Phys. Chem. **59**, 371 (1955).
15. HERZBERG, G. Spectra of diatomic molecules. 2nd ed. D. Van Nostrand Co., New York. 1950.
16. LAIDLER, K. J. The chemical kinetics of excited states. Oxford. 1955.
17. MULLIKEN, R. A. Rev. Modern Phys. **4**, 1 (1932).
18. KONDRATJEW, V. and LEIPUNSKY, A. Trans. Faraday Soc. **25**, 736 (1929).
19. ROMPE, R. Z. Physik, **101**, 214 (1936).

MEASUREMENT OF Ni^{63} WITH A 2π PROPORTIONAL COUNTER[1]

J. R. MacEwan,[2] J. U. MacEwan, and L. Yaffe

ABSTRACT

Measurement of Ni^{63}, a β^- emitter with very low maximum energy, is described. External absorption curves were determined in aluminum and a range 8.5 ± 0.5 mg/cm^2 was found. This corresponds to a maximum energy of the β radiation of 72.7 ± 2.5 kev, in reasonably good agreement with values obtained by other methods. Self-absorption curves of electrolytically deposited samples were obtained and attempts made to compare these with the theoretical predictions of Gora and Hickey.

A. INTRODUCTION

An investigation of the counting characteristics of Ni^{63}, a nuclide emitting 67-kev beta rays, was undertaken, since few precise 2π counting studies have been made in this energy range. Self-absorption measurements with Ni^{63} are particularly interesting because Gora and Hickey's (1) theoretical expressions for self-absorption in wide-angle geometries have yet to be verified for use with nuclides emitting soft beta radiation. Their general expression for self-absorption is an integrated form of equation [1], which corrects for the extra distance a particle emitted at an angle θ to a normal on the source mount surface must travel before reaching the surface.

$$[1] \qquad A(x, \theta) = \frac{a_0 \cos\theta}{k} \left(1 - e^{-\frac{kx}{\cos\theta}}\right)$$

where $A(x, \theta)$ is the detected activity of particles emitted at an angle θ from a source of thickness x, consisting of material of specific activity a_0, and k is the absorption coefficient. They have refined this treatment further to include the case where a fraction, p, of the particles incident on the source mount are scattered back towards the active volume of the counter, but were unable to include the effects of self- and back-scattering in the source. This relationship was very successfully applied by them to their results for self-absorption of C^{14} in narrow- and wide-angle geometries.

In addition, a measurement of the range of Ni^{63} beta particles in aluminum was made because it provides a check on this method for determination of maximum energies in this range as compared with beta spectrometer and other proportional counter studies.

B. EXPERIMENTAL TECHNIQUES AND RESULTS

Tracer Purification and Source Preparation

The active material used in this investigation was prepared by the irradiation of spectrographically pure nickel in the Brookhaven reactor in a position where the flux was predominantly thermal. A gamma-emitting impurity, identified as Co^{58} by scintillation spectrometry, was found. This was presumably produced by the reaction $Ni^{58}(n,p)$-Co^{58}. The cobalt was removed by dissolving the nickel in 9 *M* HCl and eluting the resulting solution through an anion exchange column (2). One passage through the column was sufficient to effect a complete separation, with the cobalt being retained on the resin.

[1]*Manuscript received October 30, 1958.*
Contribution from the Radiochemistry Laboratory, Department of Chemistry, and the Department of Metallurgy, McGill University, Montreal, Que., with financial assistance from the National Research Council, Atomic Energy Control Board, and the Defence Research Board.
[2]*Present address: Fuel Development Branch, Atomic Energy of Canada Limited, Chalk River, Ontario.*

The resulting solution was evaporated to dryness and the nickel chloride was dissolved in an ammonia – ammonium sulphate electrolysis solution. The resulting electrolyte had a nickel concentration of 0.03 moles per liter. All sources used for measurement in this investigation were prepared by electroplating nickel from aliquots of this stock solution onto copper planchets 1 in. in diameter, to give deposits 0.70 in. in diameter. Plating was carried out in rotating anode plating cells at a current density of 20 ma/cm^2. The rotational speed and anode shape were adjusted until extremely uniform deposits were obtained.

The sources were counted on an internal source proportional counter (AEP CFIS 2) with a 2π geometry. An AEP 1448 amplifier-discriminator unit, a Marconi AEP scale of 1000, and a Dynatron power supply P200A comprised the associated electronic equipment. The counter gas was C.P. methane, dried over silica gel. The long, flat plateaux (approximately 400 v long and with slopes of 0.5% per 100 v) and general stability of this equipment ensured that any small observed variations in counting rate were due solely to counting statistics. Coincidence loss corrections were made for all sources wherever necessary. The calibration curve for this correction was obtained using a multiple source technique (3).

External Absorption Curve

When an aluminum foil is placed over the source in an internal source counter, the chamber is effectively converted into an end window counter. Unless the foil is in intimate contact with the source, besides the reduction in counting rate caused by absorption in the absorber, further reductions are caused by absorption in the methane trapped between the foil and source and also by scattering of beta particles at the foil surface. It was found that these latter effects could be eliminated by laminating the aluminum absorbers onto the source with a thin layer of plastic adhesive, in this case a solution of VYNS resin in cyclohexanone. For the thinnest foils employed, the weight of aluminum was 0.23 mg/cm^2 and that of plastic about 0.06 mg/cm^2. With thicker aluminum foils the ratio of aluminum to plastic increased accordingly, and in this investigation the absorbers were considered to consist solely of aluminum. Aluminum foils with mass thicknesses of 0.23, 0.66, and 1.90 mg/cm^2 were laminated singly and in various combinations onto the source to cover the range of absorbers used, 0 to 13.5 mg/cm^2. In most cases sufficient counts were obtained at each absorber thickness to give satisfactory statistics, but in those instances where a small number of counts were obtained the accuracy of the plotted values is indicated in the usual manner.

Self-absorption Curve

To investigate the phenomenon of self-absorption of Ni^{63}, a series of active sources was prepared by electrodeposition. All sources were prepared from material of the same specific activity. The range of source thicknesses investigated varied from 0.05 to 4.50 mg/cm^2. Weights of the deposits were determined on a five-place balance sensitive to 0.005 mg. The deposits were checked for circular symmetry by measuring across several diameters and the mass thickness of the source calculated using the mean of these diameters. All observed counting rates were corrected to correspond to the same area of active surface—a correction $\leqslant 1.5\%$. Sufficient counts were obtained in all cases so that the statistical variation was negligible.

C. RESULTS AND DISCUSSION

External Abso. ption Curve

Results for the absorption of radiation in aluminum are plotted in Fig. 1. The measured

counting rates are a composite of the detected radiation from Ni^{59} ($\sim 0.02\%$) which decays by K-electron capture with the emission of a Co $K\alpha$ X-ray (4), and of Ni^{63}, which decays by emission of a 70-kev beta particle (4, 9). The low activity component has a half-thickness of 9.0 mg/cm². This value is in agreement with that given in X-ray tables for the absorption of Co $K\alpha$ X-rays of 9.4 mg/cm² and serves to identify this component as Ni^{59}. The absence of a gamma-ray background indicates that the anion exchange separation completely removed the radioactive impurity, Co^{58}. The absorption curve for the soft component, the Ni^{63} radiation, was obtained in the usual manner by deducting the Ni^{59} background from the total activity, as shown in Fig. 1. The value for the range of Ni^{63} in these experiments is estimated to be 8.5 ± 0.5 mg/cm². A 'visual method' of estimating the range from the absorption curve was employed, since a suitable standard is as yet not available in this energy range for a Feather analysis (5). Values of 0.52_3 mg/cm² and 1.33 cm²/mg were found respectively for the half-thickness and absorption coefficient of Ni^{63} beta radiation. (Since the curve is very close to a true exponential, these values can be used over most of the range.)

The value of the range found in this work for Ni^{63} is greater than that given by Wilson and Curran (6) of 6.0 mg/cm² and by Brosi *et al.* (4) of 6.6 mg/cm². However, as the individual measurements made to determine the external absorption curve can be accurately reproduced, there is no reason to suspect this new value. It is difficult to assess the accuracy of Wilson and Curran's result, as they failed to publish an absorption

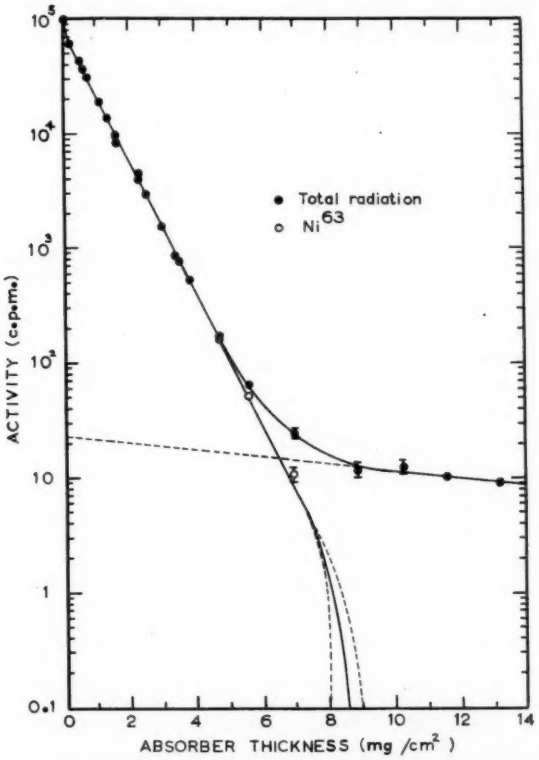

FIG. 1. Absorption curve for Ni^{63} in aluminum.

curve. Brosi *et al.* determined their range value using a Feather plot. Unfortunately they do not state which nuclide was used as a standard in the range determination. As they followed the absorption of Ni^{63} over only three decades of activity, the use of a standard having an energy spectrum different from Ni^{63} could result in an appreciable error in the estimated range. Furthermore, examination of their absorption curve shows that they did not completely eliminate the scattering phenomenon which occurs when the first absorber is placed over the source. This could also account for their low value for the range.

There are many empirical and semiempirical expressions for relating the maximum energy of a beta-ray spectrum to the observed range of these particles in aluminum. However, only Glendenin's range–energy curve (7) and Libby's range–energy relation (8) are recommended for use below 100 kev. The maximum energy of Ni^{63} beta particles obtained from these relations, using the range value found in this work, are 72.5 ± 2.5 and 72.9 ± 2.5 kev respectively.

This value is slightly higher than a recent value of 67.0 ± 0.5 kev by Preiss, Fink, and Robinson (9) but is considered to be reasonably good agreement, bearing in mind the method used. This presents additional justification for this fairly rapid, seemingly rough method and further verification of the range–energy formulae quoted above.

Self-absorption Curve

The results of the self-absorption measurements are summarized in the data plotted in Fig. 2. For convenience, the apparent specific activity, rather than the actual specific activity, of each source was plotted against the mass thickness of deposit. The apparent specific activity of the active material was arbitrarily taken as unity to simplify the comparison of these results with Gora and Hickey's theoretical expression. The experimental results are nearly identical with those obtained in a 2π geometry by Schweitzer, Stein, and Nehls (10).

In Fig. 3, three separate curves are drawn representing Gora and Hickey's theoretical self-absorption expression corresponding to values of the back-scattering factor, p, of

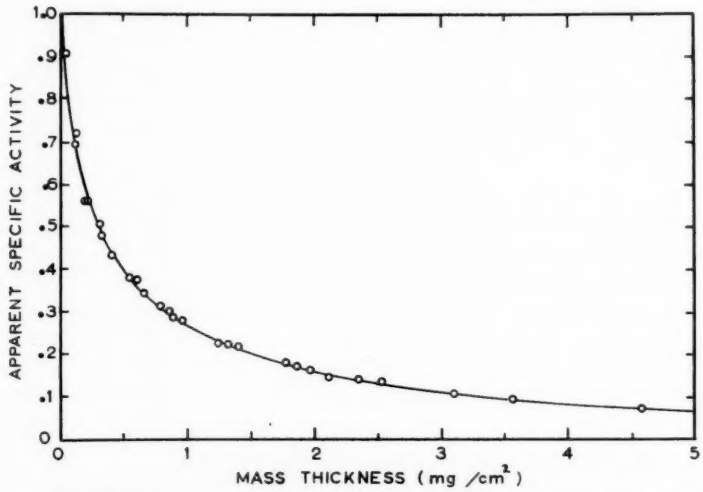

FIG. 2. Self-absorption curve for Ni^{63} in nickel—apparent specific activity plot.

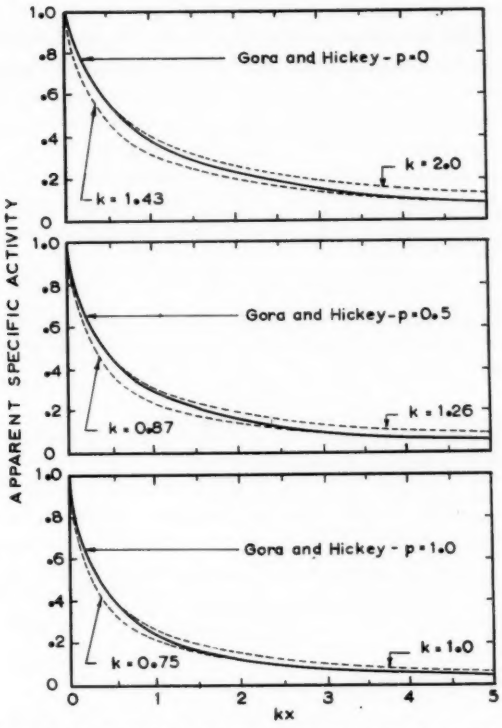

FIG. 3. A comparison of self-absorption of Ni^{63} with the theoretical curves by Gora and Hickey. Experimental data for Ni^{63} taken from Fig. 2 and shown as dotted lines for various values of R.

0.0, 0.5, and 1.0. These correspond to the respective cases where either none, half, or all the emitted particles incident on the source mount are scattered back towards the active volume of the counter. If Gora and Hickey's expression is an adequate description of the processes occurring in a source and mount, then it should be possible to make the experimental results coincide with the theoretical curve by proper selection of the back-scattering factor, p, and the absorption coefficient, k. By selecting various values of k, consistent with various parts of the experimentally determined absorption curve, it was attempted to correlate the self-absorption results shown in Fig. 2 with the theoretical curves in Fig. 3. It is apparent that the experimental results for Ni^{63} self-absorption are not consistent with the theoretical expressions. As can be observed, the correlation is improved when a correction is made for source mount back-scattering, with better correlation for the hypothetical case $p = 1.0$ than for $p = 0.5$. From this it may be concluded that for low energy beta-emitters the effects arising from self-scattering and back-scattering are important enough to invalidate any description of self-absorption in a 2π system which ignores these processes. Similar results have been obtained in conditions where 4π 'geometry' prevails (11).

When a value of the mass absorption coefficient, k, is selected to make the theoretical and experimental curves coincide for large source thicknesses, it is observed that the experimentally determined apparent specific activity decreases more rapidly than that

predicted theoretically. This suggests that the back-scattering processes in the source degrades the energy of the scattered particle, so that it is more easily absorbed in the overlying layers of atoms in the source. This is in agreement with the experimental work of Pate and Yaffe (11), who also suggest that the effect is more marked for wide-angle geometries. In addition, their results show that the back-scattering factor, p, for an infinitely thick source mount increases with decreasing energy of the beta emitter. This probably accounts for the fact that Gora and Hickey could successfully interpret their results for self-absorption of C^{14} (β^-, 0.154 Mev), while the results for Ni^{63} are inconsistent with their equations.

ACKNOWLEDGMENTS

The authors wish to express their gratitude to the Defence Research Board, the Atomic Energy Control Board, and the National Research Council for grants-in-aid.

REFERENCES

1. Gora, E. K. and Hickey, F. C. Anal. Chem. **26**, 1158 (1954).
2. Moore, G. E. and Kraus, K. A. J. Am. Chem. Soc. **73**, 9 (1951); **74**, 843 (1952).
3. Pate, B. D. and Yaffe, L. Can. J. Chem. **33**, 610 (1955).
4. Brosi, A. R., Borkowski, C. J., Conn, E. E., and Greiss, J. C., Jr. Phys. Rev. **81**, 391 (1951).
5. Feather, N. Proc. Cambridge Phil. Soc. **34**, 599 (1938).
6. Wilson, H. W. and Curran, S. C. Phil. Mag. **40**, 631 (1949).
7. Glendenin, L. E. Nucleonics, **2**, 12 (1948).
8. Libby, W. F. Anal. Chem. **19**, 2 (1947).
9. Preiss, I. L., Fink, R. W., and Robinson, B. L. J. Inorg. & Nuclear Chem. **4**, 233 (1957).
10. Schweitzer, G. K., Stein, B. R., and Nehls, J. W. J. Phys. Chem. **56**, 692 (1952).
11. Pate, B. D. and Yaffe, L. Can. J. Chem. **33**, 1656 (1955).

THE REACTIONS OF ACTIVE NITROGEN WITH ACETYLENE, METHYLACETYLENE, AND DIMETHYLACETYLENE[1]

A. SCHAVO[2] AND C. A. WINKLER

ABSTRACT

Hydrogen cyanide was the main nitrogen-containing product of all three reactions, but whereas only about one-half the available active nitrogen was converted to product in the acetylene reaction, the conversion by methyl- and dimethyl-acetylene was substantially complete. A faster-than-linear increase of HCN production with acetylene flow rate was observed at low flow rates. Similar behavior was just perceptible in the corresponding curve for methylacetylene, while no observable inflection was present with dimethylacetylene. Polymer formation was pronounced with acetylene, less so with methylacetylene, and practically absent with dimethylacetylene. Small amounts of cyanogen resulted from all three reactions, while condensable hydrocarbons were obtained in significant yields from the methyl- and dimethyl-acetylene reactions only at higher flow rates of the alkynes.

In a previous investigation (1) of the reaction of active nitrogen with acetylene, the products were found to be HCN, C_2N_2, CH_4, and H_2, together with a nitrogen-containing polymer. The conversion of active nitrogen to HCN appeared to be only about one-half that observed under optimal conditions in similar reactions with saturated and olefinic hydrocarbons. Since it was of interest to determine whether the relatively low extent of HCN formation from acetylene was characteristic of the acetylene structure, the reactions of active nitrogen with methyl- and dimethyl-acetylene have now been investigated. At the same time, some additional information was obtained about the reaction of acetylene itself.

EXPERIMENTAL

The apparatus, purification of reactants, experimental procedures, and analytical methods were similar in all essential respects to those used in previous investigations (for references, see (2)). Hydrogen cyanide and cyanogen were analyzed by titration methods, other condensable products by low temperature distillation, and non-condensable products with a mass spectrometer. A solution of ammonium hydroxide (2 *M*) was found to be effective for removing polymer from the wall of the reaction vessel, presumably because it attacked the metaphosphoric acid with which the wall was poisoned.

The flow rate of active nitrogen was estimated from the rate of production of hydrogen cyanide from ethylene at 300° C to be approximately 12 micromoles/second (3, 4).

RESULTS AND DISCUSSION

There were some rather interesting differences for the three reactions. Figure 1 shows the yields of HCN, and Fig. 2A those of C_2N_2, at different flow rates of the reactants. The relative rates of HCN production at lower flow rates, particularly from 0 to about 5 micromoles per second, were in the order acetylene < methylacetylene < dimethylacetylene. On the other hand, in the same flow rate range, the rate of production of HCN from acetylene showed a rather pronounced "induction" effect, i.e. it increased

[1]*Manuscript received November 12, 1958.*
Contribution from the Physical Chemistry Laboratory, McGill University, with financial assistance from the National Research Council of Canada.
[2]*Holder of C.I.L. Fellowship.*

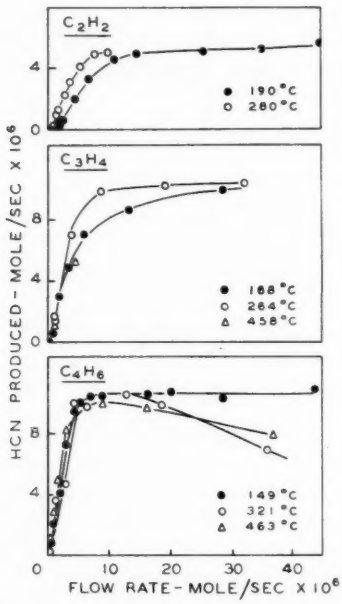

FIG. 1. Dependence of hydrogen cyanide production on the flow rates of the hydrocarbons in the reactions of active nitrogen with acetylene, methylacetylene, and dimethylacetylene.

rather markedly with flow rate, whereas similar behavior was much less evident for methylacetylene and not apparent at all in the results for dimethylacetylene. When the ratio of the rate of HCN production to flow rate of reactant is plotted against flow rate, as in Fig. 2B, the linear increase in this ratio for acetylene and possibly also for methylacetylene at the lower flow rate indicates quadratic dependence of HCN production on flow rate of hydrocarbon in this region. A similar conclusion is not possible for dimethylacetylene, although it is conceivable that it might hold for flow rates below those experimentally accessible in the present study.

Marked differences were observed also in the maximum extents to which active nitrogen could be converted to HCN in the three reactions. With acetylene, this conversion never exceeded about one-half the available active nitrogen,[3] while maximum production of HCN from methyl- and dimethyl-acetylene appeared to correspond roughly to the flow rate of active nitrogen in the system.

The yield of cyanogen was observed previously to pass through a maximum with increased flow rate of acetylene itself (1), but the same did not appear to be true with the other two acetylenes (Fig. 2A). Further, although small but significant yields of hydrogen and methane were obtained from the reaction of acetylene with active nitrogen, mass spectrometric examination showed not more than traces of these products in the non-condensables from the reaction with methylacetylene. In the reaction of dimethylacetylene, small amounts of methane (2×10^{-7} mole/second) were found only at high flow rates.

[3]*Independent experiments with acetylene in this laboratory by Mr. George have confirmed this observation for temperatures up to 400° C.*

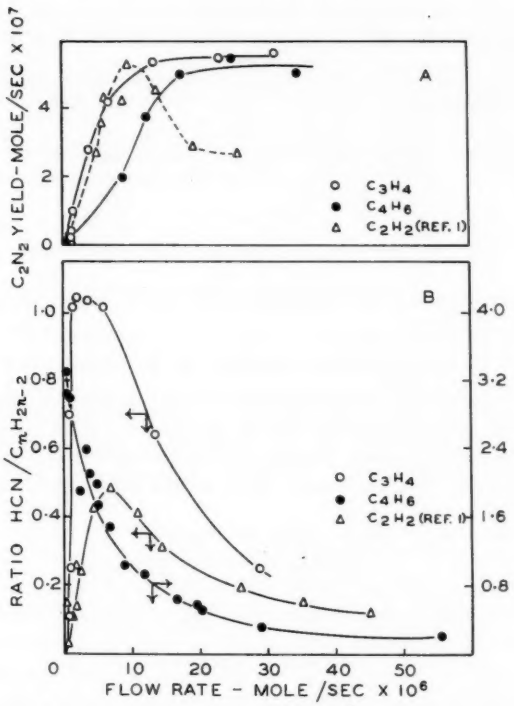

FIG. 2. A. Dependence of cyanogen production on the flow rates of the hydrocarbons in the reactions of active nitrogen with acetylene, methylacetylene, and dimethylacetylene.
B. Relation between ratio HCN/hydrocarbon and the flow rates of the hydrocarbons in the reactions of active nitrogen with acetylene, methylacetylene, and dimethylacetylene.

Other hydrocarbons were not found in more than trace amounts in the condensable products from the methyl- and dimethyl-acetylene reactions at lower flow rates. However, when the flow rates had been increased to about 10 to 20 micromoles/second, the methylacetylene reaction yielded C_2H_2 (1.7×10^{-7} mole/second), C_3H_6 (3×10^{-7} mole/second), and C_4H_8 (8×10^{-6} mole/second), while the dimethylacetylene reaction yielded C_2H_2 (1.8×10^{-7} mole/second), C_2H_6 (8×10^{-8} mole/second), C_3H_6 (2×10^{-6} mole/second), and a C_5 fraction (8×10^{-6} mole/second).

Polymer yields from the acetylene and methylacetylene reactions are shown in Table I. The amount of polymer from the reaction of dimethylacetylene was too small for quantitative estimation. Analyses of the polymers[4] showed their composition to be somewhat similar from the two reactions, with roughly 65% carbon, 27% nitrogen, and 7% hydrogen. However, the composition of the polymer probably has limited significance, since it seems likely that it would be subject to considerable variability as a result of attack by free radicals, active nitrogen, hydrogen atoms, and the parent hydrocarbon. They were all insoluble in the common solvents and were attacked only slowly by a mixture (equal volumes) of concentrated nitric and sulphuric acids.

[4]*We are indebted for these analyses to Dr. Léo Marion, Director, Division of Pure Chemistry, National Research Council, Ottawa.*

TABLE I

Yields of polymer from the reactions of acetylene and methylacetylene with active nitrogen

Acetylene		Methylacetylene	
Flow rate (mole/sec×10⁶)	Polymer yield (g/sec×10⁶)	Flow rate (mole/sec×10⁶)	Polymer yield (g/sec×10⁶)
7.6	128	1.4	22
11.0	98	6.7	65
		16.1	50

In the previous paper (1) it was suggested that HCN was produced in the acetylene – atomic nitrogen reaction by

$$C_2H_2 + N \rightarrow C_2H_2N \rightarrow HCN + CH. \quad [1]$$

However, this reaction would be endothermic and correspondingly doubtful if, as now seems likely (2), the heat of sublimation of graphite must be taken to be at least 170 kcal/mole. An alternative, which suffers no similar difficulty, would be to assume a relatively long-lived complex such that HCN might be formed by further reactions of the type

$$C_2H_2N + N \rightarrow 2HCN \quad [2]$$

$$\rightarrow 2CN + H_2 \quad [3]$$

$$2C_2H_2N \rightarrow HCN + CH \equiv C - CN + H_2 \quad [4][5]$$

$$\rightarrow HCN + H + CN + C_2H_2. \quad [5]$$

Such bimolecular processes would explain the observed greater-than-linear dependence of HCN yield on C_2H_2 flow rate at low flow rates of acetylene.

Reaction [4] is an interesting possibility, since it seems reasonable that the unsaturated nitrile should polymerize rapidly, hence account not only for formation of polymer with about the composition observed, but perhaps also for the reaction of not more than about one-half the available active nitrogen to form HCN.

The higher conversions of active nitrogen to HCN by methyl- and dimethyl-acetylene may be explained if the corresponding complexes were comparatively unstable and predominantly suffered decomposition similar to reaction [1], i.e. reactions such as:

methylacetylene:

$$C_3H_4 + N \rightarrow C_3H_4N \rightarrow HCN + C_2H_3 \quad [6]$$

$$\rightarrow HCN + C_2H_2 + H \quad [7]$$

$$\rightarrow CN + C_2H_2 + H_2, \quad [8]$$

dimethylacetylene:

$$C_4H_6 + N \rightarrow C_4H_6N \rightarrow HCN + C_3H_5 \quad [9]$$

$$\rightarrow HCN + C_3H_4 + H \quad [10]$$

$$\rightarrow HCN + C_2H_2 + CH_3 \quad [11]$$

$$\rightarrow CN + C_3H_6. \quad [12]$$

[5] *A product of mass 51, thought to be cyanoacetylene, has been observed in a mass spectrometric study of the reaction between active nitrogen and acetylene. (Private communication from Dr. J. L. Franklin, Humble Oil and Refining Company, while working at the National Bureau of Standards, Washington.)*

It is possible that polymer is formed in the methylacetylene reaction mainly by polymerization of $CH_3C \equiv C-CN$, which may be produced in a reaction similar to reaction [4]. The absence of polymer in the dimethylacetylene reaction may be ascribed to greater instability of the dimethylacetylene – nitrogen atom complex, which would not favor such a reaction.

Any radicals resulting from the foregoing reactions (e.g. C_2H_3, C_3H_5) would be expected to react rapidly with active nitrogen.

$$C_2H_3 + N \rightarrow HCN + CH_2 \quad [13]$$

$$\rightarrow CN + CH_3, \text{ etc.} \quad [14]$$

$$C_3H_5 + N \rightarrow HCN + C_2H_3 + H, \text{ etc.} \quad [15]$$

The amount of HCN formed from acetylene – nitrogen atom complexes by reactions such as [2], [4], and [5] would almost certainly be limited by interaction of the complexes or their reaction with nitrogen atoms to regenerate molecular nitrogen and the parent hydrocarbon or CH radicals. Reaction of the complex with acetylene to form polymer would also decrease the extent to which HCN may be produced. An upper limit of about one-half the active nitrogen converted to HCN is therefore not surprising, even if reaction [4] does not occur.

The absence of methane in the products from methyl- and dimethyl-acetylene is readily explained if the single carbon free radicals produced in these reactions, e.g. CH_3 and CH_2, are rapidly consumed by active nitrogen. The production of methane during the acetylene reaction suggests, therefore, that the single carbon free radical from this reaction, presumably the CH radical, is not rapidly attacked by active nitrogen. This might mean that the reaction

$$CH + N \rightarrow HCN$$

requires a three-body collision, while the corresponding reaction to form CN + H is not favored.

Cyanogen production in all three reactions is probably by recombination of CN radicals. Since the cyanogen yield from acetylene passes through a maximum, while that from the other two reactions increases steadily with flow rate of hydrocarbon, the CN radicals are probably produced directly by decomposition of the methyl- and dimethyl-acetylene complexes (e.g. reactions [8] and [12]), but indirectly from acetylene complexes by further nitrogen atom attack or interaction of complexes as in reactions [3] or [5].

The presence, in the products, of small amounts of hydrocarbons, such as C_2H_6 and C_3H_6, and the larger amounts of C_4H_8 and C_5 fraction at higher flow rates of methyl- and dimethyl-acetylene, indicate that H atom and free radical reactions occurred under these conditions. However, there would seem to be little point in attempting to detail these, since they probably bear little relation to the nitrogen reactions which are of principal concern.

It might be noted that the production of as much as 3.3 moles HCN per mole dimethyl-acetylene requires hydrogen rearrangement in the complex. Similar behavior has been indicated by the results for some other reactions of active nitrogen with hydrocarbons (2).

REFERENCES

1. VERSTEEG, J. and WINKLER, C. A. Can. J. Chem. **31**, 129 (1953).
2. EVANS, H. G. V., FREEMAN, G. R., and WINKLER, C. A. Can. J. Chem. **34**, 1271 (1956).
3. FORST, W., EVANS, H. G. V., and WINKLER, C. A. J. Phys. Chem. **61**, 320 (1957).
4. WILES, D. M. and WINKLER, C. A. J. Phys. Chem. **61**, 902 (1957).

SOME YIELDS IN THERMAL NEUTRON FISSION OF U^{233} AND Pu^{239} [1]

ROSALIE M. BARTHOLOMEW, J. S. MARTIN,[2] AND A. P. BAERG

ABSTRACT

Relative yields of Sr^{89}, Sr^{91}, Ba^{139}, Ba^{140}, and La^{141} have been measured for U^{233} and Pu^{239} thermal neutron fission. Ion exchange separations and 4π beta-counting methods were used. The following relative values were obtained for the nuclides as listed: 1.05, 1.00, 1.00, 1, and 1.10 in U^{233} fission and 0.301, 0.431, 1.07, 1, and 1.01 in Pu^{239} fission.

INTRODUCTION

Although the mass distribution of the products of U^{235} fission has been well studied and yields accurately determined for most masses, relatively few accurate measurements have been made for the fission of the nuclides U^{233} and Pu^{239}. Radiochemical studies of the fission of U^{233} have been reported by Grummitt and Wilkinson (9) in 1948 and by Steinberg *et al.* (16) in the same year. Papers reporting earlier radiochemical studies of Pu^{239} fission have been summarized by Steinberg and Freedman (13). All of the radiochemical data, with revised values for U^{233} fission yields, together with some more recent relative mass spectrometric measurements have been summarized by Steinberg and Glendenin in 1955 (14).

Mass spectrometric relative yield measurements in U^{233} fission have been reported for the isotopes of xenon, cesium, and krypton (6) and the isotopes of zirconium, molybdenum, and ruthenium (15). Similar relative values for Pu^{239} fission have been obtained for the isotopes of xenon by Fleming and Thode (5) and for the isotopes of cerium, neodymium, and cesium by Krizhansky *et al.* (11).

Absolute mass spectrometric yields for some nuclides have been obtained by the isotope dilution technique. In Pu^{239} fission preliminary values have been reported for cesium, cerium, neodymium, and samarium isotopes by Wiles *et al.* (17). Absolute values for the isotopes of neodymium and cerium are reported for U^{233} fission by Kukavadze *et al.* (12).

All of the data, both radiochemical and mass spectrometric, reported to 1958 have recently been evaluated and summarized by Katcoff (10). The radiochemical data were obtained using end-window Geiger counters and the values have an accuracy of 10–20% (14). The mass spectrometric yields have a relative accuracy, in most cases, of 1–2% and absolute values are usually accurate to 3–5% (14).

During the 1958 International Conference on the Peaceful Uses of Atomic Energy, further data have become available. These include radiochemical measurements of the heavy rare earths in Pu^{239} fission (4), absolute mass spectrometric yields for Cs^{133}, Xe^{135}, Nd^{143}, Sm^{149}, and Sm^{151} for both U^{233} and Pu^{239} fission (3), and for the isotopes of Xe and Kr in Pu^{239} fission (7). Anikina *et al.* (1) have reported absolute yields for isotopes of Sr, Cs, Ba, Ce, Nd, and Sm for U^{233} and Pu^{239} fission. They have also obtained yields of La^{139} and Eu^{153} for U^{233} fission and of Pr^{141} for fission of U^{233} and Pu^{239} using mass spectrometric methods requiring the comparison of integrated ion currents.

We have recently used improved radiochemical methods (2) to measure relative yields of Sr^{89}, Sr^{91}, Ba^{139}, Ba^{140}, and La^{141} in U^{235} fission with a reliability believed comparable

[1]*Manuscript received December 2, 1958.*
Contribution from the Chemistry and Metallurgy Division, Research Chemistry Branch, Atomic Energy of Canada Limited, Chalk River, Ontario.
Issued as A.E.C.L. No. 764.
[2]*Present address: Columbia University, New York, N.Y., U.S.A.*

with that achieved by mass spectrometric techniques. Except for the mass 91 chain the cumulative yields of these masses can better be obtained by radiochemical determination of the nuclides listed and the purpose of this work was to extend the measurements already made for U^{235} fission to fission of U^{233} and Pu^{239}.

EXPERIMENTAL

Except for several minor modifications, the procedure used for the relative yield measurements here was the same as that reported earlier (2). In the work with U^{235} relatively large samples (10 to 50 mg) of natural uranium were irradiated as the oxides in the Chalk River NRX reactor. In the present experiments with U^{233} and Pu^{239}, however, samples of about 100 μg only were sealed in quartz for the irradiations. Under these conditions it was found that up to 50% of the fission fragments were embedded in the quartz and not recovered in the subsequent dissolution. As a consequence of partial segregation of the products arising from differences in fragment ranges, very significant errors in the relative yield values were observed, even for adjacent masses. To avoid these errors from the loss of fission fragments, the fissile material was deposited as the nitrate solution on a pure iron oxide matrix (50 mg) to serve as a fragment catcher in the quartz tube. The samples were dried and heated to the oxide before sealing.

Following irradiation, the samples were crushed and dissolved in aqua regia containing small quantities (about 50 μg each) of suitable carriers, then dried, and taken up in 9 *N* hydrochloric acid. This solution was passed through an anion column to remove the Pu^{239} or U^{233} and iron together with various anionic fission products. The cations in the effluent, predominantly the alkali metals, alkaline earths and rare earths, were subsequently adsorbed on a cation column and the various species separated by elution with ammonium α-hydroxyisobutyrate. Details of the separation procedures and 4π beta-counting methods have been given in ref. 2. All yield calculations were based on half-lives as quoted in the same reference.

In the absolute beta counting of Sr^{89} and Y^{91} small corrections (usually less than 1%) were made for the presence of 27.7-year Sr^{90} and its 64.8-hour Y^{90} daughter. To make these corrections it was assumed that the ratio of yields Sr^{90}/Sr^{89} is 1 for U^{233} fission and 1.5 for Pu^{239} fission, while the Sr^{91}/Sr^{90} yield ratio was assumed to be 1 for U^{233} and 0.9 for Pu^{239} fission.

RESULTS AND DISCUSSION

The relative yield values obtained are listed in Table I, each set of experiments being divided into two groups: one for the Ba^{139}/Ba^{140} ratios and the other for the ratios of Sr^{89}, Sr^{91}, and La^{141} to Ba^{140}. In Table II the values of Table I have been combined and converted to absolute values on the basis of selected yields for mass 140 as given by Katcoff (10). The errors quoted reflect only the precision of the values given in Table I. Included for comparison in Table II are the relevant yields quoted in refs. 10 and 14.

U^{233}

In U^{233} fission the value of 5.60% for the yield of Ba^{140} corresponds to that of Ce^{140} determined mass spectrometrically by Kukavadze *et al.* (12). We make the reasonable assumption that the yields of Ce^{140} and Ba^{140} are equivalent. With this assumption our results for Sr^{89} and Sr^{91} are somewhat lower than those reported for these masses in ref. 14. The Zr^{91} yield of ref. 14 is based on relative mass spectrometric data fitted together with the aid of earlier radiochemical yields for Sr^{89}, Zr^{95}, Mo^{99}, and Ru^{103} to give a yield curve for the light mass group (15). The discrepancies with the present

TABLE I

Relative yields in thermal neutron fission of U^{233} and Pu^{239}

	Expt.	Ba^{140}	Ba^{139}	La^{141}	Sr^{89}	Sr^{91}
U^{233}	1	1	1.00_4			
	2	1	0.99_5			
	3	1	0.99_7			
	4	1	0.99_9			
	5	1		1.10_7	1.04_6	0.99_7
	6	1		1.10_8	1.07_8	1.02_2
	7	1		1.08_7	1.01_9	0.99_4
	8	1		1.10_7	1.05_1	0.99_6
Pu^{239}	1	1	1.06_8			
	2	1	1.07_9			
	3	1	1.06_0			
	4	1	1.07_0			
	5	1		1.00_4	0.29_1	0.41_7
	6	1		0.99_3	0.30_6	0.43_2
	7	1		1.02_3	0.31_0	0.43_8
	8	1		1.03_2	0.29_7	0.43_8

TABLE II

Yields normalized to selected values for Ba^{140}

	Ba^{140}	Ba^{139}	La^{141}	Sr^{89}	Sr^{91}
U^{233}	5.60	5.59	6.17	5.87	5.61
Standard deviation		0.02	0.05	0.12	0.06
Data of ref. 14*	5.6 Ce^{140}			6.1	6.09 Zr^{91}
Pu^{239}	5.68	6.07	5.75	1.71	2.45
Standard deviation		0.04	0.09	0.04	0.05
Data of ref. 10	5.68	5.7	5.2 Ce^{141}	1.9	2.4 Y^{91} 3.0%

*The original data, based on 6.0% for Ba^{140} (16), are renormalized to 5.6% for this nuclide.

results are, however, probably within the associated errors.

Anikina *et al.* (1) have reported values of 5.91 and 5.57% respectively for La^{139} and Pr^{141}. These values are based on mass spectrometer integrated ion currents and are to be compared with 5.59 and 6.17% respectively for Ba^{139} and La^{141} relative to 5.6% for Ba^{140}. The differences are greater than the quoted errors allow and no explanation for the discrepancies is obvious.

Pu^{239}

In Pu^{239} fission the yield of Ba^{140} given by Steinberg and Glendenin (14) was 5.36%. This value was increased to 5.68% by Katcoff (10) to make the total yields 100% each for the light and heavy groups. The preliminary mass spectrometric values of Wiles *et al.* (17) indicate a yield of 7.36% for Ce^{140}. On the other hand, Krizhansky *et al.* (11) have made relative measurements of the cerium isotopes which agree well with those of Wiles *et al.* except at mass 140. Accepting the absolute values of Wiles *et al.* for masses other than Ce^{140} and combining these with the relative values of Krizhansky *et al.*, the Ce^{140} absolute yield becomes 5.63%, which agrees well with that selected by Katcoff for Ba^{140}.

The yields of Ba^{139}, Ce^{141}, Sr^{89}, and Sr^{91} quoted in ref. 10 are from the data of Steinberg *et al.* (13, 14) normalized to a value of 5.68% for Ba^{140}. Comparison of these yields with those obtained here shows agreement within the experimental errors. The integral mass spectrographic value of 6.02% for Pr^{141} given by Anikina *et al.* (1) is greater than the value (5.75%) we obtained for La^{141}. The difference is larger than the quoted errors

and also larger than could reasonably be attributed to independent formation of Ce^{141}. The value for Sr^{91} found here is in good agreement with that of ref. 10. There is, however, a large difference between it and the values for Y^{91} (10, 14) implying a high independent yield for the latter. The difference seems excessive but may possibly arise from a short-lived isomeric state in Sr^{91} which feeds Y^{91}. Evidence for such chain branching has already been given by Grummitt and Milton (8) for U^{235} fission.

REFERENCES

1. ANIKINA, M. P., ARON, R. M., GORSHOV, V. K., IVANOV, R. N., KRIZHANSKY, L. M., KUKAVADZE, G. M., MOURIN, A. N., REFORMATSKY, I. A., and ERSHLER, B. V. Second United Nations International Conference on the Peaceful Uses of Atomic Energy, Paper No. 2040 (1958).
2. BAERG, A. P. and BARTHOLOMEW, R. M. Can. J. Chem. **35**, 980 (1957).
3. BIDINOSTI, D. R., FICKEL, H. R., and TOMLINSON, R. H. Second United Nations International Conference on the Peaceful Uses of Atomic Energy, Paper No. 201 (1958).
4. BUNNEY, L. R., SCADDEN, E. M., ABRIAM, J. O., and BALLOU, N. E. Second United Nations International Conference on the Peaceful Uses of Atomic Energy, Paper No. 644 (1958).
5. FLEMING, W. H. and THODE, H. G. Can. J. Chem. **34**, 193 (1956).
6. FLEMING, W. H., TOMLINSON, R. H., and THODE, H. G. Can. J. Phys. **32**, 522 (1954).
7. FRITZE, K., MCMULLEN, C. C., and THODE, H. G. Second United Nations International Conference on the Peaceful Uses of Atomic Energy, Paper No. 187, rev. 1 (1958).
8. GRUMMITT, W. E. and MILTON, G. M. J. Inorg. Nucl. Chem. **5**, 93 (1957).
9. GRUMMITT, W. E. and WILKINSON, G. Nature, **161**, 520 (1948).
10. KATCOFF, S. Nucleonics, **16**, 78 (1958).
11. KRIZHANSKY, L. M., MALY, Y., MURIN, A. N., and PREOBRAZHENSKY, B. K. Soviet J. Atomic Energy, **2**, 334 (1957).
12. KUKAVADZE, G. M., ANIKINA, M. P., GOLDIN, L. L., and ERSHLER, B. V. Conference of the Academy of Sciences of the U.S.S.R. on the Peaceful Uses of Atomic Energy (English translation), p. 125 (July 1955).
13. STEINBERG, E. P. and FREEDMAN, M. S. National Nuclear Energy Series, Div. IV. Vol. 9. McGraw-Hill Book Company, Inc., New York. 1951. Paper 219.
14. STEINBERG, E. P. and GLENDENIN, L. E. International Conference on the Peaceful Uses of Atomic Energy. Vol. 7. United Nations, New York. 1956. p. 614.
15. STEINBERG, E. P., GLENDENIN, L. E., INGHRAM, M. G., and HAYDEN, R. J. Phys. Rev. **95**, 867 (1954).
16. STEINBERG, E. P., SEILER, J. A., GOLDSTEIN, A., and DUDLEY, A. U.S. Atomic Energy Comm. Rept. MDDC-1632 (1948).
17. WILES, D. M., PETRUSKA, J. A., and TOMLINSON, R. H. Can. J. Chem. **34**, 227 (1956).

PROTONATION OF THE CARBONYL GROUP

II. THE BASICITIES OF SUBSTITUTED BENZALDEHYDES[1]

K. YATES[2] AND ROSS STEWART

ABSTRACT

The basicities of seven meta- and para-substituted benzaldehydes have been determined by a spectrophotometric method in sulphuric acid media. The simple Hammett relation does not hold for these bases but a good correlation exists between pK_{BH^+} and σ^+. The effects of substitution on the wavelengths of maximal ultraviolet absorption in benzaldehyde are compared with those in acetophenone.

The basicity of *o*-tolualdehyde was determined in an attempt to estimate the steric effects of ortho substitution. The effects of symmetrical trisubstitution on the basicity of benzaldehyde and acetophenone are compared and discussed.

INTRODUCTION

In connection with studies of the protonation of ketones reported previously (1) and of carboxylic acids to be reported soon, we have determined the effects of ring substitution on the basicity of benzaldehydes. In determining the strengths of these very weak bases we have again followed the approach used by Hammett in his classical investigations (2) utilizing the concept of the H_0 acidity function. This has the advantage of yielding basicity values which are absolute in so far as they are based on dilute aqueous solution as the standard state. Pratt and Matsuda (3) determined relative basicities of some oxygen-containing organic bases in benzene solution by their effect on acid catalyzed reactions. Gordy and Stanford (4) have also determined relative basicities of similar compounds by a spectroscopic method. Wepster (5) has used a number of physical and chemical properties to determine base strengths of substituted nitrobenzenes.

EXPERIMENTAL

Commercially available benzaldehydes were purified either by vacuum distillation under a small positive pressure of nitrogen or by several recrystallizations. *o*-Tolualdehyde was prepared from *o*-bromotoluene by the method of Smith and Nichols (6). (B.p. 89°/22 mm, $n_D^{24} = 1.5410$. Lit. b.p. 72°/6 mm, and $n_D^{25} = 1.5430$ (7).) Stock solutions of these compounds in the range 10^{-2}–10^{-3} molar were titrated against standard alkali immediately after use and found to be free of the corresponding benzoic acids.

Sulphuric acids of various concentrations were prepared by dilution of Fisher C.P. reagent grade sulphuric acid (95.0% min.). Further solutions up to 99.9% were prepared by mixing the above with 30% fuming sulphuric acid (Baker & Adamson Reagent). Determination of the H_0 values of these acids and the preparation of suitably absorbing solutions of the aldehydes in them is described in Part I of this series.

The extinction coefficients of these solutions at various concentrations of sulphuric acid were determined at two wavelengths with quartz cells of 1 cm path length using a Beckman Model DU Spectrophotometer, whose cell compartment was maintained at 25±0.1° by means of thermospacers. The sulphuric acids were tested for optical clarity in the regions used and a solvent blank of the same concentration as that containing the aldehyde was used. Ultraviolet absorption spectra of the aldehydes in 44.0% and

[1]*Manuscript received November 12, 1958.*
Contribution from the Department of Chemistry, University of British Columbia, Vancouver.
[2]*Holder of N.R.C. studentships, 1957–59.*

95.5% acids measured with a Cary Model 14 Recording Spectrophotometer were used to locate the wavelengths of maximal absorption of the unprotonated (λ_u) and protonated (λ_1) forms. These are listed in Table I.

TABLE I

Absorption spectra of substituted benzaldehydes

Substituent	In 44.0% H_2SO_4			In 95.5% H_2SO_4		
	λ_{max} (mμ)	log ϵ_{max}	$\Delta\lambda_u$ (mμ)	λ_{max} (mμ)	log ϵ_{max}	$\Delta\lambda_1$ (mμ)
m-Chloro	250	3.89	−1	297	4.16	1
p-Chloro	263	4.18	12	316	4.37	20
p-Nitro	270	4.13	19	282	4.25	−14
p-Methoxy	290	3.87	39	344	4.23	48
Hydrogen	251	4.08	0	296	4.36	0
o-Methyl	260	4.26	9	302	4.48	6
m-Methyl	258	4.03	7	301	4.27	5
p-Methyl	264	4.14	13	313	4.43	17

The pK_{BH^+} values were determined by the method of Davis and Geissman (8) as follows: The extinction coefficients $\epsilon(\lambda_u)$ and $\epsilon(\lambda_1)$ of the two species were measured in at least 12 different concentrations of acid. The function $[\epsilon(\lambda_1)-\epsilon(\lambda_u)]$ which is linearly related to the fraction ionized was plotted against H_0. At the inflection point of this curve it can be shown that the fraction ionized equals the fraction un-ionized, hence $\log (c_{BH^+}/c_B) = 0$ and $H_0 = pK_{BH^+}$. In all cases a sigmoid titration type curve was obtained and the inflection point taken as the mid-point of the "straight" portion. The results of a typical determination are shown in Fig. 1. The advantages and limitations of the method are discussed by the above authors. In cases where λ_1 is very close to λ_u or where $\epsilon(\lambda_1) \gg \epsilon(\lambda_u)$ we have found that smooth curves cannot be obtained. The method fails for *m*-nitrobenzaldehyde and the second decimal in the pK_{BH^+} value of the *p*-nitro isomer is of doubtful significance.

Because of the possibility of chemical change other than protonation occurring in the strongly acid solutions the absorption spectra of the aldehydes in 95.5% acid were repeated after 1 hour's standing. They were found to undergo no appreciable change and on subsequent dilution the spectra reproduced closely those of control solutions in dilute acid. The possibility of sulphonation in very high concentrations is not serious, since this region is not in a critical part of the curve. However, to minimize any such effects all measurements used in determining pK_{BH^+} were taken as rapidly as possible after the addition of the acids.

RESULTS AND DISCUSSION

Effects of Meta and Para Substitution on Basicity

The values of pK_{BH^+} for the substituted benzaldehydes are listed in Table I and are plotted as a function of σ (9), the Hammett substituent constant in Fig. 2. It can be seen that the correlation is rather poor even if only meta and para substituents are considered (open circles). The 2,4,6-substituted compounds (closed circles) will be discussed in a later section. The four points through which the dotted line is drawn represent those substituents which are not able to supply electrons to the positively charged conjugate acid by direct resonance with the group and hence are expected to obey the Hammett equation (10),

$$\log (K/K_H) = \rho\sigma.$$

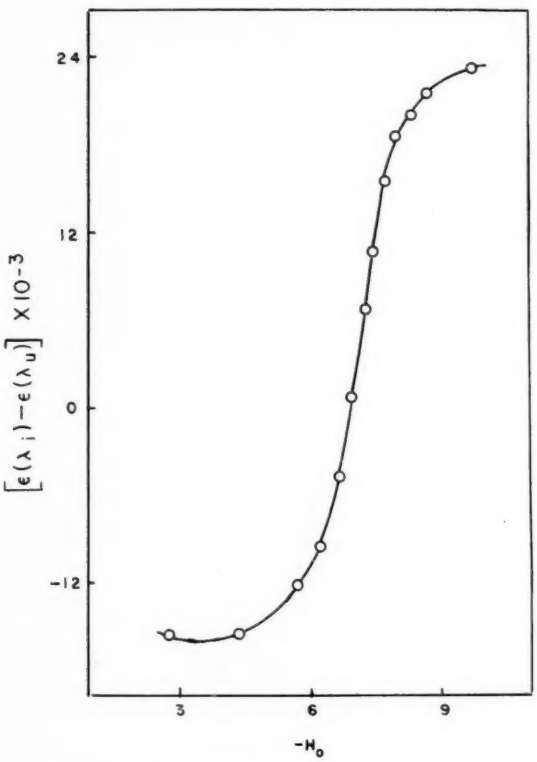

FIG. 1. The function $[\epsilon(\lambda_i)-\epsilon(\lambda_u)]\times 10^{-3}$ plotted against $-H_0$ for *p*-chlorobenzaldehyde.

The other three points represent para substituents which are able to do this owing to contributions from structures like II.

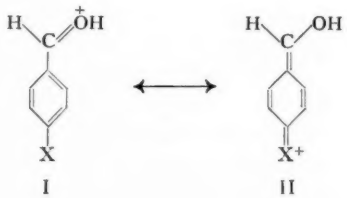

I II

The latter substituents thus give higher basicities than their σ values predict owing to increased stabilization of the conjugate acid.

Several investigators (11) have noted that substituents such as *p*-methoxy are able to stabilize carbonium ions to a much greater extent than is indicated by their σ values, and σ^+ values have been derived (12) for groups which are able to supply electrons for use in reactions where a positive charge is developed in conjugation with the group. Figure 3 shows a plot of pK_{BH^+} of the same seven compounds against σ^+. A good linear correlation ($r = 0.994$) now exists for both meta and para points.

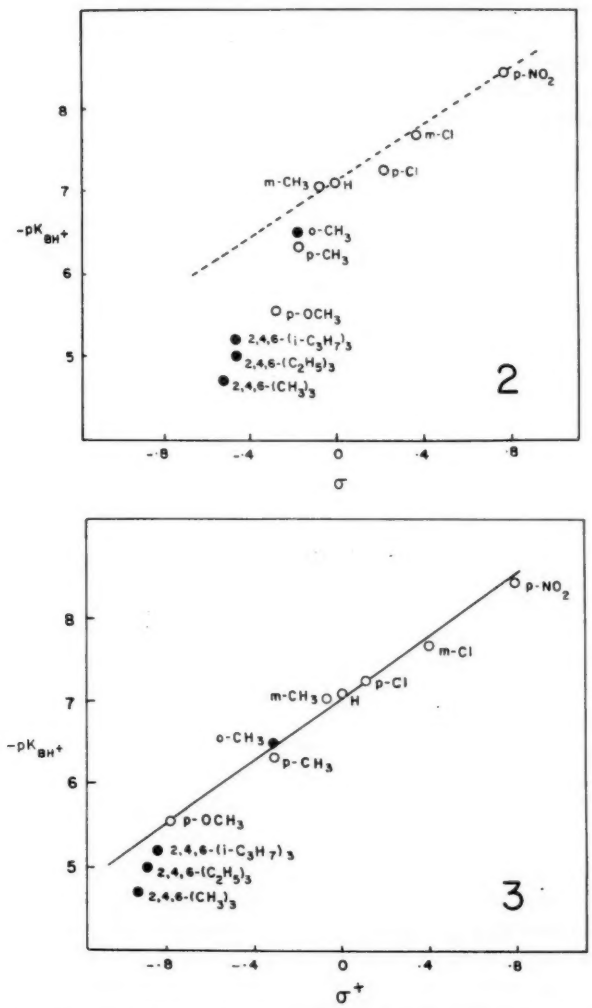

FIG. 2. $-pK_{BH^+}$ for substituted benzaldehydes plotted against Hammett's σ constants.
FIG. 3. $-pK_{BH^+}$ for substituted benzaldehydes plotted against Brown's σ^+ constants.

As might be expected these results are very similar to those obtained with substituted acetophenones (1) in which similar resonance effects are possible. However, two points of difference arise. In the case of the ketones the basicity of the *p*-methoxy group was found to be lower than that predicted by the σ^+ value. Similar deviations for alkoxy groups have been noted by other workers (13). The above deviation was explained on the basis that solvent–solute hydrogen-bonding for such groups should be particularly strong in sulphuric acid with a consequent increase in σ^+, thus lowering the basicity. The point for the analogous *p*-methoxybenzaldehyde, however, falls on a good straight line through all the other points. This is surprising, since the solvent effects discussed

previously (1) should be at least as strong for benzaldehydes. The possibility of protonation occurring at the methoxy rather than the formyl group was considered but rejected for two reasons:

1. The spectral changes of *p*-methoxybenzaldehyde in sulphuric acid parallel those of other benzaldehydes and acetophenones, i.e. a pronounced red shift on protonation. If protonation occurred preferentially at the methoxy group the change would be expected to be in the opposite direction as in the case of anilines which undergo a blue shift on protonation (14).

2. The evidence of other workers (3, 4) indicates that alkyl aryl ethers are considerably less basic than aromatic aldehydes and ketones. This difference should be even more pronounced where there is an electron-withdrawing formyl group para to the alkoxyl group as shown below:

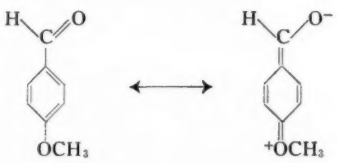

III IV

The second point of difference between the two series is the magnitude of the reaction constant. The ρ value obtained from the meta and para points in Fig. 3 is 1.85 (least squares calculations used throughout), whereas the value for acetophenones is 2.17 (neglecting the point for *p*-methoxy). The larger ρ for the acetophenone series compared to the benzaldehyde series suggests that the charge is more localized on the ketone carbon atom of the former than on the aldehyde carbon of the latter (15). A similar effect occurs in the solvolysis of α-phenylethyl chloride compared to the benzyl compound (16).[3] The greater localization of charge in the cases of the ketone conjugate acid and the α-phenylethyl carbonium ion can be rationalized in terms of steric hindrance of the methyl group to solvation in the cations.

Effects of Substitution on the Ultraviolet Spectra

Forbes *et al.* (17) have shown in a recent series of papers that para substitution of benzaldehydes produces displacements of the wavelength of maximum absorption (π–π^* transitions) relative to that of the parent compound. These displacements are directly related to those produced by similar substitution in nitrobenzenes and acetophenones and it was suggested that this proportionality is primarily due to the similarity of resonance effects on the transition energies in all three types of compounds. In Figs. 4*a* and 4*b* the wavelength displacements produced by the introduction of substituents in benzaldehyde ($\Delta\lambda_u$) and its conjugate acid ($\Delta\lambda_l$) are taken from Table I and plotted against the corresponding values for acetophenones. Since most of Forbes' measurements were taken in neutral solvents, it is interesting to see that a good correlation ($r = 0.981$) still exists for the unprotonated forms (Fig. 4*a*). Despite the large change in medium the slope of the line (0.88) is close to that observed by Forbes, although the wavelength shifts appear to be more pronounced in 44.0% sulphuric acid. This indicates that, although medium effects on the spectra are rather large, they are similar for both types of carbonyl compound.

An equally good correlation ($r = 0.984$) is found for the conjugate acids (Fig. 4*b*,

[3]*We are grateful to the referee for drawing this to our attention.*

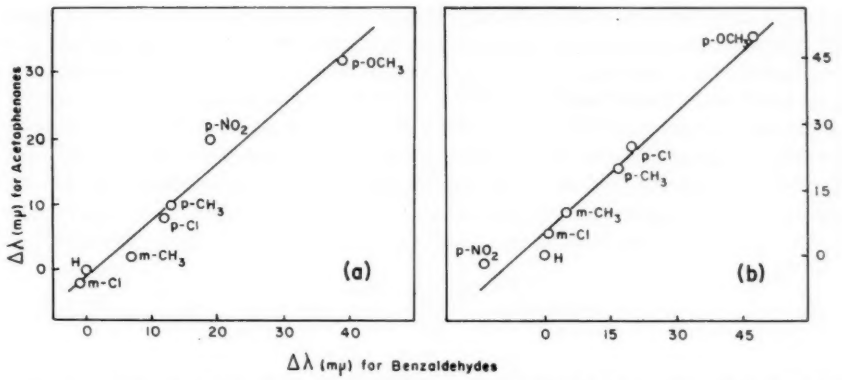

FIG. 4. Wavelength displacements of the principal ultraviolet band obtained on introducing substituents (*a*) into acetophenone and benzaldehyde and (*b*) in the conjugate acids of acetophenone and benzaldehyde.

slope = 0.90) and the displacements are now in the approximate order of the ability of the groups to donate electrons by resonance. The fact that the slopes of the lines in Figs. 4*a* and 4*b* are approximately unity indicates that resonance is of comparable importance in the acetophenone and benzaldehyde series being possibly slightly more important in the latter case. A further indication of this is the fact that those groups which can donate electrons by resonance (*p*-methoxy, *p*-methyl, *p*-chloro) produce *a slightly larger* increase in basicity when substituted in benzaldehyde than when substituted in acetophenone. This is despite the greater over-all ρ for the acetophenones.

Steric Effects of Alkyl Groups

It is interesting to compare the effect of methyl substitution in different positions on the basicities of benzaldehydes as shown in Table II and Figs. 2 and 3. It is apparent that ortho methyl substitution produces an increase in basicity roughly comparable to para substitution. Symmetrical trimethyl substitution as in 2,4,6-trimethylbenzaldehyde results in a greatly enhanced basicity as shown in Fig. 3, where we have assumed the sigma value for 2,4,6-trialkyl substitution to be $\Sigma\sigma^+$ para (21). The extent of deviation of the three alkyl groups ($CH_3 > C_2H_5 > i\text{-}C_3H_7$) is in the order of decreasing size possibly reflecting decreasing extents of steric hindrance to solvation of the cations. If the latter effect was unimportant the three points would all presumably deviate even farther from the straight line.

TABLE II

pK_{BH^+} values of substituted benzaldehydes

Substituent	$-pK_{BH^+}$	Substituent constants*	
		σ	σ^+
m-Chloro	7.68	0.373	0.399
p-Chloro	7.26	0.227	0.114
p-Nitro	8.45	0.778	0.790
p-Methoxy	5.54	−0.268	−0.778
Hydrogen	7.10	0.0	0.0
o-Methyl	6.50	—	—
m-Methyl	7.06	−0.069	−0.066
p-Methyl	6.32	−0.170	−0.311
2,4,6-Trimethyl†	4.7	—	—
2,4,6-Triethyl†	5.0	—	—
2,4,6-Triisopropyl†	5.2	—	—

*Refs. 9 and 12.
†Ref. 22.

Braude and Sondheimer (18) among others (19) have used changes in electronic spectra and dipole moments to estimate the steric effects of two ortho methyl groups on the coplanarity of the carbonyl group and the benzene ring for both benzaldehydes and acetophenones. Their results as shown in Table III indicated a mean rotation of about 15–20° for 2,4,6-trimethylbenzaldehyde. (The amount of π orbital overlap is reduced by an amount which varies as $\cos^2\theta$ (20).) The process studied by Braude and Sondheimer in evaluating the extent of steric interference was the absorption of a photon to give the excited state crudely represented by VI. The oxygen atom as a result of bearing an increased negative charge should be larger than the oxygen atom in V.

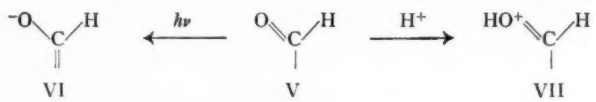

VI V VII

The protonation reaction on the other hand results in a positively charged oxygen atom as in VII which should be smaller than the oxygen in V, smaller at least in the direction at right angles to the O—H bond axis. The greater degree of coplanarity thus allowed the conjugate acid compared to the neutral aldehyde and the consequent increased resonance with the ring may explain the enhanced basicity of 2,4,6-trimethylbenzaldehyde.

TABLE III

Steric effects of 2,4,6-trimethyl substitution in benzaldehyde and acetophenone (18)

Compound	θ_ϵ*	θ_μ†	μ_{obs} (D)	μ_{calc} (D)	pK_{BH^+}
Benzaldehyde	0°	0°	2.92	2.92	−7.1
2,4,6-Trimethylbenzaldehyde	22°	15°	2.96	2.99	−4.7 (22)
Acetophenone	0°	0°	2.96	2.96	−6.15 (1, 22)
2,4,6-Trimethylacetophenone	63°	62°	2.81	3.03	−7.9 (22)

*Mean interplanar angle calculated from ratio of observed ϵ of K band to that expected in a uniplanar system (Braude and Sondheimer (18)).

†Mean interplanar angle calculated from observed dipole moment data (18).

It is interesting to compare the effects of similar substitution on the basicity of acetophenone. Table III shows that the observed dipole moment of 2,4,6-trimethylacetophenone is much lower than the calculated value and approaches the value for saturated ketones (μ = 2.75 D for acetone (18)) unlike mesitaldehyde whose observed dipole moment is close to the calculated value. This indicates that the contribution of dipolar resonance structures such as VIII is greatly reduced by steric inhibition. This is due to the bulky acetyl methyl which overlaps the ortho groups much more than does the

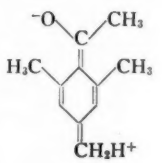

VIII

carbonyl oxygen. In support of this the mean interplanar angle θ calculated from ultra-

violet spectra is 63°. This should result in drastic reduction of π-orbital overlap involving the carbonyl group and the ring. In agreement with this the basicity of 2,4,6-trimethylacetophenone (22) is found to be 1.75 log units less than the parent compound, whereas the inductive effects alone of three methyl groups would normally be expected to increase the basicity. The shrinking of the carbonyl group as a result of protonation, which we discussed above as an explanation for the enhanced basicity of 2,4,6-trimethylbenzaldehyde, is not an important factor in the case of the ketones. Here it is the ketone methyl which is largely responsible for the steric repulsions rather than the carbonyl group as for the aldehydes.

ACKNOWLEDGMENT

The financial aid of the National Research Council is gratefully acknowledged.

REFERENCES

1. STEWART, R. and YATES, K. J. Am. Chem. Soc. **80**, 6355 (1958).
2. FLEXSER, L. A., HAMMETT, L. P., and DINGWALL, A. J. Am. Chem. Soc. **57**, 2103 (1935). FLEXSER, L. A. and HAMMETT, L. P. J. Am. Chem. Soc. **60**, 885 (1938). HAMMETT, L. P. and DEYRUP, A. J. J. Am. Chem. Soc. **54**, 2721 (1932).
3. PRATT, E. F. and MATSUDA, K. J. Am. Chem. Soc. **75**, 3739 (1935).
4. GORDY, W. and STANFORD, S. C. J. Chem. Phys. **8**, 170 (1940).
5. WEPSTER, B. M. Rec. trav. chim. **76**, 335, 337 (1957).
6. SMITH, L. J. and NICHOLS, J. J. Org. Chem. **6**, 489 (1941).
7. HASS, H. B. and BENDER, M. L. Org. Syntheses, **30**, 99 (1950).
8. DAVIS, C. T. and GEISSMAN, T. A. J. Am. Chem. Soc. **76**, 3507 (1954).
9. JAFFE, H. H. Chem. Revs. **53**, 191 (1953).
10. HAMMETT, L. P. Physical organic chemistry. McGraw-Hill Book Company, Inc., New York. 1940. Chap. VII.
11. PEARSON, D. E., BAXTER, J. F., and MARTIN, C. J. J. Org. Chem. **17**, 1511 (1952). KOCHI, J. K. and HAMMOND, G. S. J. Am. Chem. Soc. **75**, 3445 (1953). JARUZELSKI, J. J., DENO, N. C., and SCHREISHEIM, A. J. Org. Chem. **19**, 155 (1954).
12. DENO, N. C. and EVANS, W. L. J. Am. Chem. Soc. **79**, 5804 (1957). BROWN, H. C. and OKAMOTO, Y. J. Am. Chem. Soc. **80**, 4979 (1958).
13. BROWN, H. C. and OKAMOTO, Y. J. Am. Chem. Soc. **79**, 1913 (1957). See also WILES, L. A. Chem. Revs. **56**, 329 (1956).
14. MATSEN, F. A. *In* Chemical applications of spectroscopy. *Edited by* A. Weissberger. Interscience Publishers Ltd., London. 1956. p. 671.
15. TAFT, R. W. and LEWIS, I. C. J. Am. Chem. Soc. **80**, 2436 (1958).
16. BERLINER, E. and SHIEH, N. J. Am. Chem. Soc. **79**, 3849 (1957).
17. FORBES, W. F. Can. J. Chem. **36**, 1350 (1958). DEARDEN, J. C. and FORBES, W. F. Can. J. Chem. **36**, 1362 (1958). FORBES, W. F. and LECKIE, I. R. Can. J. Chem. **36**, 1371 (1958).
18. BRAUDE, E. A. and SONDHEIMER, F. J. Chem. Soc. 3754 (1955).
19. KADESH, R. G. and WELLER, S. W. J. Am. Chem. Soc. **63**, 1310 (1941). KLEVENS, H. B. and PLATT, J. R. J. Am. Chem. Soc. **71**, 1714 (1949). BRAUDE, E. A., SONDHEIMER, F., and FORBES, W. F. Nature, **173**, 117 (1954).
20. COULSON, C. A. Conference on quantum mechanical methods in valence theory. U.S. Government Printing Office. 1951. p. 47.
21. TAFT, R. W. *In* Steric effects in organic chemistry. *Edited by* M. S. Newman. John Wiley & Sons, Inc., New York. 1956. p. 577 ff.
22. PAUL, M. A. and LONG, F. A. Chem. Revs. **57**, 1 (1957). SCHUBERT, W. M. and ZAHLER, R. E. J. Am. Chem. Soc. **76**, 1 (1954).

THE REACTION OF METHYL RADICALS WITH FORMALDEHYDE[1]

S. TOBY[2] AND K. O. KUTSCHKE

ABSTRACT

Azomethane was photolyzed in the presence of up to 30 mole per cent formaldehyde and formaldehyde-d_2 at temperatures from 80° C to 180° C. The value of the activation energy for the abstraction reaction with methyl radicals was found to be 6.2 kcal mole^{-1} for CH_2O and 7.9 kcal mole^{-1} for CD_2O. The results indicated that the formyl radical was stable over the temperature range studied.

INTRODUCTION

This work was undertaken to provide data on a reaction which is of considerable interest in mechanisms of oxidation. Kodama and Takezaki (1) have reacted methyl radicals, produced by the thermal decomposition of azomethane at 310° C, with formaldehyde. They cite a value of 5.63 kcal per mole for the activation energy of the abstraction reaction; however, very little experimental data was given. It seemed desirable to investigate this reaction more fully.

EXPERIMENTAL

The methyl radicals were produced by photolysis of azomethane (2) using standard photochemical procedures. The optical system consisted of a Hanovia S-500 medium pressure mercury arc, two quartz lenses which produced an approximately parallel beam of light, and a Corning 5860 filter used with two filters of clear Pyrex glass. This combination gave radiation at approximately 3660 Å with an intensity of about 10^{14} quanta cm^{-3} sec^{-1} (using azomethane as an actinometer). A photocell was used to measure relative absorption.

The reaction cell was a cylindrical quartz vessel of volume 189 cm^3 connected to a magnetic stirrer, two Wood's alloy cutoffs (3), and a quartz spiral manometer. The whole was situated in an insulated box, the temperature of which could be kept constant within 1° C up to 200° C. Experiments were done at temperatures from 80° C (below which formaldehyde readily polymerizes) to 180° C (above which azomethane decomposes thermally).

The thermostatted section of the apparatus was connected to a conventional gas analysis system. After an experiment the non-condensable products were passed through a solid nitrogen trap into a gas burette via a small mercury diffusion pump backed by a Toepler pump. Carbon monoxide was oxidized over cupric oxide at 260° C and measured as carbon dioxide. The remaining mixture of nitrogen and methane was analyzed mass spectrometrically. Ethane was distilled through a Ward still at −180° C and its purity checked by the mass spectrometer.

Azomethane, supplied by Dr. L. C. Leitch of these laboratories, was distilled *in vacuo*, the center fraction being retained. Mass spectrometric analysis detected no impurity. Formaldehyde monomer was prepared by repeated distillation of α-polyoxymethylene (4), the only impurity being a trace of CO_2. The formaldehyde was stored at liquid nitrogen temperature. Illumination of pure formaldehyde produced less than 0.01% photodecomposition in a time comparable to the normal experiment. There was no detectable dark reaction between formaldehyde and azomethane.

[1]*Manuscript received December 8, 1958.*
Contribution from the Division of Pure Chemistry, National Research Council, Ottawa, Canada.
Issued as N.R.C. No. 5085.

[2]*National Research Council of Canada Postdoctorate Fellow 1955–1957. Present address: Department of Chemistry, Rutgers University, New Brunswick, N.J., U.S.A.*

Formaldehyde-d_2, supplied by Dr. L. C. Leitch (5), contained 99.4% atom per cent deuterium. In the case of runs using formaldehyde-d_2, methanes-d_0 and -d_1 were formed. It was confirmed that there was no deuterium exchange when the non-condensables were left in the CuO furnace for an hour.

Up to 5% of the azomethane was decomposed, and up to 2% of the formaldehyde was allowed to react. The azomethane concentration was kept at approximately two millimoles per liter corresponding to pressures of about 50 mm. The light intensity was not intentionally varied, but two arcs which had a difference of 20% in their output were used.

RESULTS AND DISCUSSION

The results of experiments with CH_2O are given in Table I and with CD_2O in Table II. They are consistent with the following reaction scheme:

$$CH_3N_2CH_3 \xrightarrow{h\nu} 2CH_3 + N_2, \quad [0]$$

$$2CH_3 \rightarrow C_2H_6, \quad [1]$$

$$CH_3 + CH_3N_2CH_3 \rightarrow CH_4 + CH_2N_2CH_3, \quad [2]$$

$$CH_3 + CH_2O \rightarrow CH_4 + CHO, \quad [3]$$

$$CH_3 + CHO \rightarrow CH_4 + CO. \quad [4]$$

TABLE I

Photolysis of mixtures of azomethane and formaldehyde

T, °K	[Azo] moles/liter $\times 10^4$	[CH_2O] moles/liter $\times 10^4$	Time, sec.	Absorption, %	Rate $\times 10^{10}$ moles liter^{-1} sec^{-1}				$R_{CO}/\{R^{\frac{1}{2}}_{C_3H_6}[CH_2O]\}$, $l^{\frac{1}{2}}M^{-\frac{1}{2}}s^{-\frac{1}{2}}$
					N_2	CH_4	C_2H_6	CO	
357.5	19.4	0.871	3600	16.0	72.3	19.2	26.3	5.2	0.12
357	18.7	1.03	7200	15	74.0	22.1	20.1	6.7	0.14$_8$
358	19.1	1.21	4500	18	70.2	22.3	27.1	8.3	0.13
357	20.4	2.58	4500	17.9	75.0	33.7	25.2	15.6	0.12
356.5	19.6	4.34	3600	17	96.1	54.9	28.0	29.4	0.13
363	23.4	1.57	5460	19.5	90.1	30.4	18.8	9.7	0.14
366	19.0	0.942	3600	17	73.4	23.5	14.9	7.1	0.19$_4$
371	20.1	4.78	3600	18	102	82.4	20.4	38.7	0.18
390	19.4	0.415	3300	17.9	83.2	25.6	7.2	3.5	0.32
389.5	19.9	0.819	2520	18	87.4	30.1	6.1	6.5	0.32
390	20.1	0.976	3600	17	107	46.0	18.2	11.2	0.27
389	21.7	1.08	5400	18.4	90.1	34.8	8.8	7.6	0.24
389	19.8	1.84	3060	17.7	83.4	43.1	7.2	15.1	0.31
389.5	19.1	2.24	3660	18.4	88.7	40.0	7.6	15.4	0.25
389	20.8	3.70	3900	18	80.5	55.7	9.7	26.9	0.23$_8$
387	20.2	4.37	4200	17	102	75.5	11.3	36.6	0.25
389	19.6	8.80	4200	17.3	101	99.8	7.3	60.1	0.25
389	19.1	12.7	3600	16.5	100	112	4.7	74.1	0.27
409	21.6	1.76	7200	20	76.6	42.0	3.7	12.0	0.36
412	23.1	1.37	4560	20.2	84.7	41.2	2.6	10.3	0.47
425.5	19.3	1.11	7380	15.2	72.3	45.1	2.2	16.3	0.52
432	22.8	1.26	3480	20.6	92.4	46.5	1.8	10.8	0.70
432.5	22.0	1.24	3600	20.7	92.4	47.7	1.7	11.2	0.69$_4$
457.5	17.6	1.15	7200	17.3	77.6	47.9	1.0	10.1	0.86
456.5	21.5	1.37	2460	20.6	92.9	51.0	1.5	11.1	0.65$_8$
452.5	20.2	7.88	3600	19.4	114	121	1.6	67.4	0.68
450.5	20.8	7.93	5400	20.5	112	121	0.81	65.0	0.91
452	20.2	10.1	3600	19.7	110	137	0.76	78.9	0.90
451	20.6	11.3	4200	20	111	150	0.85	86.1	0.83

TABLE II

Photolysis of mixtures of azomethane and formaldehyde-d_2

T, °K	[Azo] moles/-liter $\times 10^4$	[CD_2O] moles/-liter $\times 10^4$	Time of run, sec.	Absorption, %	Rate $\times 10^{10}$ moles liter^{-1} sec^{-1} N_2	CH_4	CH_3D	C_2H_6	CO	$R_{CH_4}/\{R^{\frac{1}{2}}_{C_2H_6}[Azo]\}$, $l^{\frac{1}{2}}M^{-\frac{1}{2}}s^{-\frac{1}{2}}$	R_{CH_3D}/R_{CO}	$\{R_{CH_3D}-R_{CO}\}/\{R^{\frac{1}{2}}_{C_2H_6}[CD_2O]\}$, $l^{\frac{1}{2}}M^{-\frac{1}{2}}s^{-\frac{1}{2}}\times 10^2$	$\{R_{CH_3D}-R_{CO}[Azo]\}/R_{CH_4}[CD_2O]$
350.5	21.9	1.48	4200	19	117	14.0	2.0	54.9	0.96	0.00866	2.1	0.97	1.1
361	18.8	0.58	3900	15	107	16.8	0.7	44.7	0.3	0.0133	2	1.1	0.8
362	20.0	2.09	4200	17.3	108	17.3	3.5	38.8	1.5	0.0139	2.3	1.5	1.1
362.5	19.4	2.40	3900	18	107	16.6	4.0	42.1	1.8	0.0132	2.1	1.4	1.1
360.5	20.3	4.13	4200	17.5	103	19.9	7.9	42.9	3.3	0.0150	2.4	1.7	1.1
357.5	21.6	8.03	3600	19.5	108	21.6	14.7	42.6	6.7	0.0154	2.2	1.5	0.99
359	21.7	8.12	3500	19	110	21.4	14.6	42.8	6.9	0.0150	2.1	1.5	0.96
374.5	19.7	1.58	4500	16.7	113	22.1	3.6	32.3	1.5	0.0198	2.3	2.3	1.2
387	18.5	1.79	5100	17	103	24.2	4.8	22.4	1.8	0.0278	2.7	3.6	1.3
405.5	19.3	1.02	5400	17.5	109	32.9	3.0	12.6	1.3	0.0481	2.4	4.8	0.98
401	19.6	1.13	5460	16.9	110	31.3	3.3	11.1	1.4	0.0478	2.3	4.8	1.0
402.5	20.3	2.07	5400	18.2	113	31.5	6.1	12.9	2.4	0.0432	2.5	5.0	1.1$_5$
401	20.3	3.34	4500	19	109	39.0	12.8	12	4.1	0.055	3.1	7.2	1.4
403	19.6	7.16	4800	18	110	36.0	24.9	12.7	9.1	0.0517	2.7	6.2	1.2
403	19.9	9.24	3600	18.9	118	34.5	30.2	11.9	12.0	0.0504	2.5	5.7	1.1
425.5	18.5	1.15	5580	17.1	106	38.3	34.2	5.0	1.5	0.0929	2.2	7.4	0.79
453.5	18.4	0.68	6600	17.4	113	50.2	2.0	2.7	1.0	0.168	2.4	11	0.6
454	18.7	1.22	7200	17	116	52.1	3.9	2.8	1.9	0.167	2.6	12	0.7
453	17.7	1.79	5400	18	111	46.4	6.4	2.5	2.6	0.166	2.4	13.5	0.82
452.5	17.9	5.50	6300	18	115	47.0	22.2	2.5	8.7	0.165	2.5$_5$	15.5	0.94
452.5	18.3	9.43	7500	19	119	45.3	35.8	2.6	11.6	0.157	2.4$_5$	14	0.91
452.5	18.1	11.4	5400	19.4	120	44.5	43.4	2.6	18.2	0.152	2.4	14	0.95

Some experiments were performed in which azomethane was photolyzed alone. In this case

$$\frac{k_2}{k_1^{\frac{1}{2}}} = \frac{R_{CH_4}}{R^{\frac{1}{2}}_{C_2H_6}[Azo]}.$$

This same rate expression holds when CD_2O was present, since all methane formed in reaction [2] is undeuterated. A plot of log $k_2/k_1^{\frac{1}{2}}$ against the reciprocal of the absolute temperature is shown in Fig. 1. The presence of up to 30 mole % CD_2O is seen to have no effect on the value of log $k_2/k_1^{\frac{1}{2}}$. The slope of the best straight line through the points leads to a value of 8.4 ± 0.3 kcal mole^{-1} for E_2, assuming E_1 is zero. This differs from the value of 7.6 obtained by Jones and Steacie (2) and 7.3 by Ausloos and Steacie (6) but agrees with the value obtained by Wenger (7).

A conventional treatment of the results gives

$$\frac{k_3}{k_1^{\frac{1}{2}}} = \left(\frac{R_{CH_4}-R_{CO}}{R^{\frac{1}{2}}_{C_2H_6}} - \frac{k_2}{k_1^{\frac{1}{2}}}[Azo]\right)\frac{1}{[CH_2O]}.$$

The results obtained were not sufficiently accurate to use this expression, since it involves the difference between two quantities which, in this case, are of similar magnitude. The CH_2O results may be treated by assuming a steady state of formyl radical concentration. In this case

$$\frac{k_3}{k_1^{\frac{1}{2}}} = \frac{R_{CO}}{R^{\frac{1}{2}}_{C_2H_6}[CH_2O]}.$$

This rate expression is approximately constant at constant temperature with up to 30-fold changes in CH_2O concentration, as shown in Table I. A plot of log $k_3/k_1^{\frac{1}{2}}$ against $1/T$ is given in Fig. 2 and the least mean square line is given by

$$k_3/k_1^{\frac{1}{2}} = 780 \exp[-(6200 \pm 300)/RT] \text{ (mole liter}^{-1})^{-\frac{1}{2}} \text{ sec}^{-\frac{1}{2}}.$$

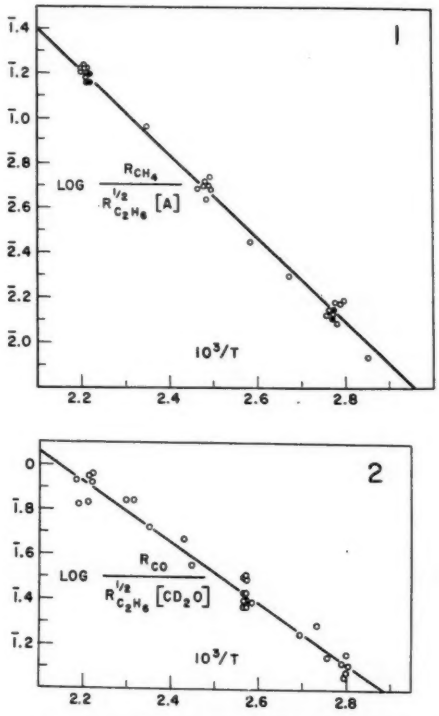

FIG. 1. Arrhenius plot for the reaction $CH_3 + CH_3N_2CH_3$: ● azomethane alone, ○ variable amounts CD_2O present; see text.
FIG. 2. Abstraction of hydrogen from CH_2O by methyl radicals.

The only published result with which this may be compared is the value of 5.63 kcal mole^{-1} for E_3 given by Kodama and Takezaki (1).

In the case of the CD_2O experiments the rate equations give directly

$$\frac{k_3'}{k_1^{\frac{1}{2}}} = \frac{R_{CH_3D} - R_{CO}}{R^{\frac{1}{2}}_{C_2H_6}[CD_2O]}$$

and

$$\frac{k_3'}{k_2} = \frac{R_{CH_3D} - R_{CO}}{R_{CH_4}} \frac{[Azo]}{[CD_2O]}.$$

These expressions are plotted in Fig. 3 and give

$$k_3'/k_1^{\frac{1}{2}} = 960 \exp[-(7900 \pm 300)/RT] \text{ (mole/liter)}^{-\frac{1}{2}} \text{ sec}^{-\frac{1}{2}}$$

and

$$k_3'/k_2 = 0.48 \exp(590 \pm 300/RT) \text{ (mole/liter)}^{-\frac{1}{2}} \text{ sec}^{-\frac{1}{2}}$$

respectively. From Fig. 1

$$k_2/k_1^{\frac{1}{2}} = 1700 \exp[-(8400\pm300)/RT] \text{ (mole/liter)}^{-\frac{1}{2}} \text{ sec}^{-\frac{1}{2}},$$

hence

$$k_3'/k_1^{\frac{1}{2}} = 810 \exp[-(7800\pm400)/RT] \text{ (mole/liter)}^{-\frac{1}{2}} \text{ sec}^{-\frac{1}{2}},$$

in satisfactory agreement with the former value. The values $E_3 = 6.2$, $E_3' = 7.9$ kcal mole^{-1} may be compared with the corresponding activation energies for the abstraction reaction with acetaldehyde and acetaldehyde-*d* as found by Ausloos and Steacie (8). They obtained $E = 6.8$, $E' = 7.9$ kcal mole^{-1} for the corresponding reactions.

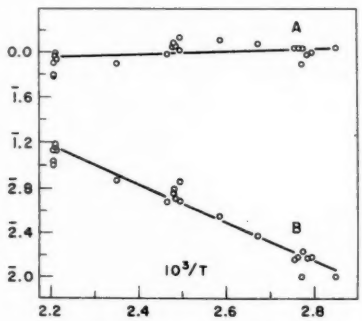

FIG. 3. Abstraction of deuterium from CD_2O by methyl radicals: A: $\log\{(R_{CH_3D}-R_{CO})/R_{CH_4}[CD_2O]\}$ vs. $10^3/T$; B: $\log\{(R_{CH_3D}-R_{CO})/R^{\frac{1}{2}}_{C_2H_6}[CD_2O]\}$ vs. $10^3/T$.

In Fig. 4 the amounts of the products of the CD_2O experiments are plotted as a function of CD_2O concentration. It can be seen that the amount of CH_3D and CO formed increases linearly with CD_2O concentration. There is, however, no corresponding decrease

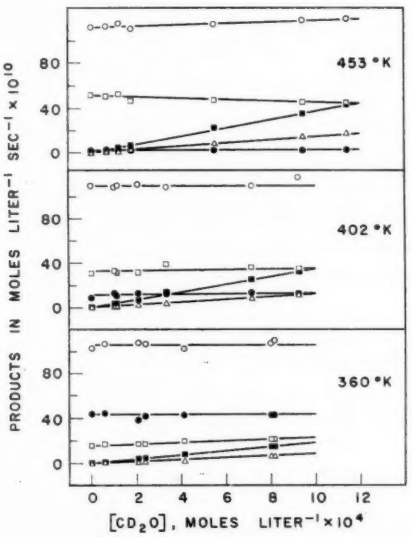

FIG. 4. Products of CD_2O experiments as functions of formaldehyde-d_2 concentration: ○ N_2, ● C_2H_6, □ CH_4, ■ CH_3D, △ CO.

in the amounts of CH_4 and C_2H_6 formed. Since the amount of azomethane photolyzed shows no appreciable increase with CD_2O (as shown by the N_2 formed), the source of the extra methyl radicals is not apparent. It is possible that fewer addition products of CH_3 + azomethane were formed in the presence of CD_2O but this could not be verified. The corresponding graph for the CH_2O runs is not given, since the light intensity was not constant. However, it may be seen from Table I that the increase in CH_4 and CO production at constant temperature has no corresponding decrease in C_2H_6 production.

Other Fates for the Formyl Radical

The addition reaction corresponding to the disproportionation reaction [4] is

$$CH_3 + CHO \rightarrow CH_3CHO. \qquad [5]$$

No acetaldehyde was found by mass spectrometric analysis of the products, however. If any acetaldehyde were formed it seemed likely that it would copolymerize with the excess CH_2O. The residues from several runs were therefore collected and tested with Leys reagent, which will detect 0.1% acetaldehyde in CH_2O solution (9). The tests were negative and from this it can be inferred that reaction [4] occurs at least four times as fast as reaction [5] under the conditions studied.

For the CD_2O experiments $k_5'/k_4' = R_{CH_3D}/R_{CO} - 2$. The value of R_{CH_3D}/R_{CO} is reasonably constant with CD_2O concentration and with temperature as shown in Table II. The results give $k_5'/k_4' \simeq 0.4$. These findings agree with those of Lossing (10), who found that reaction [4] was much faster than reaction [5] at 55° C.

No hydrogen was found in the products. This does not rule out the occurrence of

$$CHO \rightarrow CO + H \qquad [6]$$

because any H formed would probably undergo addition rather than abstraction reactions with azomethane, since CH_3 adds to azomethane approximately five times as fast as it abstracts from it in the temperature range employed (2). Reaction [6] is thought not to have occurred, however, for the following reasons.

In the CD_2O experiments it was found that the CH_3D/CO ratio was approximately 2.4 regardless of temperature or CD_2O concentration. E_6 is at least 12 kcal mole^{-1} (11), which is undoubtedly much higher than E_3 or E_4. If an appreciable fraction of the carbon monoxide were formed by reaction [6] then it would be expected that the CH_3D/CO ratio would decrease as the temperature increased, and this is not in accordance with the results obtained. Hence reaction [6] is slow up to at least 180° C.

Other possible fates for the formyl radical were

$$2CHO \rightarrow (CHO)_2, \qquad [7]$$

$$2CHO \rightarrow CO + CH_2O. \qquad [8]$$

The residues of several experiments were collected and analyzed mass spectrometrically for glyoxal with negative results, ruling out the appreciable occurrence of reaction [7] in the system studied. Reaction [8] could not be directly checked, however; its occurrence would not be in accordance with the rate law found.

ACKNOWLEDGMENTS

The authors wish to thank Dr. E. W. R. Steacie for his interest in this work and Miss Bernice Thornton and Mrs. K. O. Kutschke for the mass spectrometer analyses.

REFERENCES

1. KODAMA, S. and TAKEZAKI, Y. J. Chem. Soc. Japan, **73**, 13 (1952).
2. JONES, M. H. and STEACIE, E. W. R. J. Chem. Phys. **21**, 1018 (1953).
3. TOBY, S. and KUTSCHKE, K. O. Rev. Sci. Instr. **28**, 470 (1957).
4. STAUDINGER, H. *et al.* Ber. **64**, 398 (1931).
5. BANNARD, R. A., MORSE, A. T., and LEITCH, L. C. Can. J. Chem. **31**, 351 (1953).
6. AUSLOOS, P. and STEACIE, E. W. R. Can. J. Chem. **32**, 593 (1954).
7. WENGER, F. and KUTSCHKE, K. O. To be published.
8. AUSLOOS, P. and STEACIE, E. W. R. Can. J. Chem. **33**, 31 (1955).
9. WALKER, J. F. Formaldehyde. 2nd ed. Reinhold Publishing Corp., New York. 1953.
10. LOSSING, F. P. Can. J. Chem. **35**, 305 (1957).
11. CALVERT, J. G. J. Phys. Chem. **61**, 1206 (1957).

THE STABLE ALKYLATION PRODUCTS OF ORGANONITROSOHYDROXYLAMINES[1]

M. V. George, R. W. Kierstead, and George F Wright

ABSTRACT

The stable alkylation products of alkyl and aryl nitrosohydroxylamines seem to exist in a hitherto unknown structure, the diimide dioxide linkage. The alternative possibility is the alkyl diazotate monoxide structure, but the latter cannot account for the pure methane evolved when the substances are treated with methyl halide Grignard reagent. The principal products of this reaction with Grignard reagents are diimide monoxides formed subsequently by addition of an equivalent of reagent with elimination of the original alkoxy group as its magnesium salt. Nitration of N-methyl-N′-phenyldiimide dioxide shows that in salt-forming media (nitric–sulphuric) the N_2O_2R group is electrically negative, but dipole moment studies show that it is highly degenerate. This resonance stabilization is not unexpected in view of the high stability of the diimide dioxides in acidic media.

The first nitrosohydroxylamines were prepared (1) by reaction of nitric oxide with substances containing an active methylene group in presence of ethanolic sodium hydroxide. Typical is the reaction with acetone which may be postulated as follows:

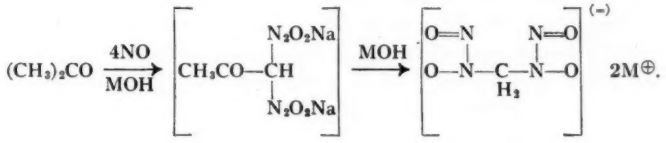

I

The second, more orthodox, method of preparation involved the nitrosation of an arylhydroxylamine (2), and led to the preparation of salts such as ammonium phenylnitrosohydroxylaminate (cupferron). The free acids are rather unstable.

When the silver salts of these nitrosohydroxylamines (II, M = Ag) are treated with alkyl iodides two products, designated α and β, are formed. The β isomers may be desig-

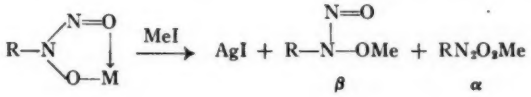

II

nated as the nitroso derivatives of hydroxylamine O-ethers, since they give a positive Liebermann test and some may be synthesized by nitrosation of the O-alkylhydroxylamines (3, 4).

The structure of the α derivative was not proved. Hantzsch (5) suggested structures III or IV while Bamberger and Ekecrantz (6) suggested either IV or V. To this list may be added VI, although it is in conflict with one structure proposed for nitroso dimers (7, 8, 9, 10, 11).

There are two claims that nitroso dimers are best represented by structure VI or charge-distorted modification of it. An X-ray diffraction study (8) of tribromonitroso-

[1]*Manuscript received October 14, 1958.*
Contribution from the Chemistry Department, University of Toronto, Toronto, Ontario.

Can. J. Chem. Vol. 37 (1959)

benzene has been interpreted in terms of a central plane containing two nitrogen and two oxygen atoms, but it is doubtful whether this definition is justified when six bromine atoms are present. A more specific claim (10) that the *cis* and *trans* isomers of VI (R = Me) have been isolated may be interpreted in terms of polymorphism. Moreover, there is no convincing reason to expect that substances having structure VI would show the instability characteristic of nitroso, carboxylic, or peroxidic dimers. For these reasons we prefer to exclude VI for consideration as a nitroso dimer, and to include it among the possible structures of the α-alkylated nitrosohydroxylamines.

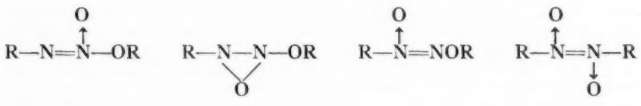

III IV V VI

In view of present knowledge structure III is inadmissable because it may clearly be assigned to isonitramines (12). The postulation of structures IV or V is justified by the observation (13) that basic hydrolysis of the methyl derivative of phenylnitrosohydroxylamine regenerates the salt (II, M = Na or K). We have extended this observation by hydrolysis of the dimethyl α derivative of the salt I using hydrazine as the basic reagent. Subsequent precipitation by use of sodium or barium hydroxide yields the appropriate salt of I rather than of methylene dinitramine (14).

Thus hydrolytic evidence favors IV or V rather than III, but it should be noted that VI is not excluded by this criterion since the alkylazoxy linkage is known to react with alkalis (15). The principal evidence favoring IV and V in contrast to VI has been presented by Bamberger (6, 13), who reduced methyl phenylnitrosohydroxylaminate and its *p*-bromo analogue. Reduction with zinc and acetic acid was said to give diazonium salts, while neutral reduction with aluminum amalgam gave the methyl ester of benzenediazotic acid. However, identification seems to have been accomplished only by odor and color tests. Only when the reduction was alkaline (4% sodium amalgam) was phenylhydrazine or its *p*-bromo analogue characterized in favor of structures IV and V rather than VI. But alkaline conditions also would yield sodium phenylnitrosohydroxylaminate by hydrolysis. Since this salt is easily reduced to phenylhydrazine, Bamberger's argument is not entirely convincing.

In order to evaluate further the criterion of reduction for a choice between structures IV, V, and VI we have applied alternative reducing agents to the methyl derivative of phenylnitrosohydroxylamine. We have found, like Bamberger, that the substance is fairly resistant. It is practically unchanged by reagents like titanous chloride in acetic anhydride, aqueous sodium bisulphite, aqueous sodium arsenite, and aqueous (47%) hydriodic acid, although a 4% yield of aniline was obtained from the latter reaction. A 24% yield of aniline was obtained, together with unchanged reagent and unidentifiable material, by catalytic reduction with platinum. But also, the alkaline reagent, sodium hydrosulphite, gave a 4% yield of phenylhydrazine together with a 65% recovery of the original substance. In fact the only reduction which might support Bamberger's contention for IV and V is that with lithium aluminum hydride which gives a 40% yield of phenylhydrazine. However, the latter reductant must be considered together with Grignard reagents which it resembles in its behavior.

Treatment of the methyl α derivative from phenylnitrosohydroxylamine with methyl halide Grignard reagent by the Kohler modification of the Zerewitinoff analysis (16)

shows that one equivalent of pure methane is liberated easily. Enough may be collected at room temperature for demonstration of an uncontaminated infrared spectrum. The analysis shows also that 1.5 equivalents of Grignard reagent are added during the process. Since it has been shown that the isolable reaction product is fixed as its magnesium salt (and therefore cannot easily undergo further reaction), the evidence for active hydrogen would seem to exclude IV or V as possible structures, but not VI with its methylene group adjacent to an azoxy linkage. Accordingly VI (R = C_6H_5, R′ = Me) is now designated for the α derivative of phenylnitrosohydroxylamine, and it is named N-phenyl-N′-methyldiimide dioxide.*

When methylphenyldiimide dioxide (VII, R = H) is treated with an excess of bromotoluene Grignard reagent in ethyl ether the significant product is N-4-tolyl-N′-phenyldiimide N′-oxide (17) (XII, R′ is *p*-tolyl). When an excess of VII is used to ensure complete consumption of the Grignard reagent both methanol and toluene (IX, R′ = tolyl) can be isolated. On the basis of this information the reaction may be formulated as follows:

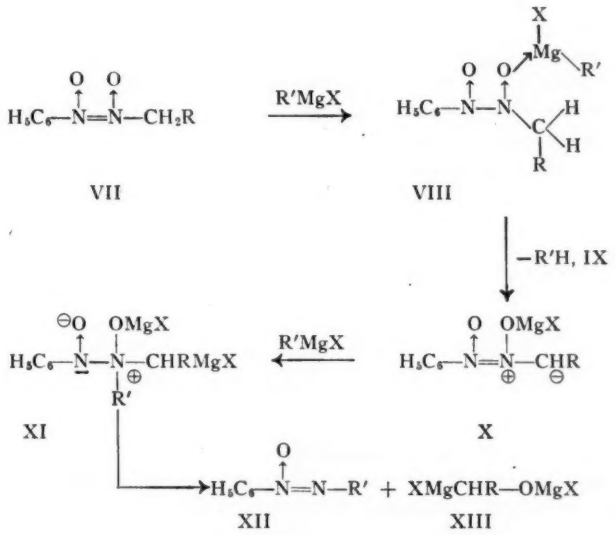

Although either of the oxide linkages might be expected to co-ordinate with the Grignard reagent only the co-ordination shown in VIII would seem to be propitious for elimination of R′H, IX. The remaining dipolar fragment, X, should then co-ordinate and add Grignard reagent to give XI, from which XIII (R = H) (finally leading to methanol) and XII would be produced. It is noteworthy that none of the isomeric N′-4-tolyl-N-phenyldiimide N′-oxide (the structure of which was proved (17) by facile bromination in the phenyl substituent) was found among the reaction products.

**It has become evident that the nomenclature of azo and azoxy compounds is inadequate for communication among chemists. A revision has been suggested (15), but this in turn cannot be used to describe structures such as VI. Consequently we suggest that azo compounds be designated by the Chemical Abstracts classification, N,N′-diimide (R—N=N—R′), that azoxy compounds be called diimide oxides (or monoxides), and that substances with structures corresponding to VI be called diimide dioxides. For example the α- and β-4-chlorophenylazoxybenzenes would be renamed N-phenyl-N′-[4-chlorophenyl]diimide N-oxide and N′-oxide respectively. From this adaptation of amine oxide nomenclature it becomes simple to describe the unsymmetrical azo and azoxy compounds as well as our diimide dioxides.*

When an otherwise comparable experiment is carried out by use of methyl chloride Grignard reagent the isolable product, besides unchanged VII, would then be designated as N-methyl-N′-phenyldiimide N′-oxide. This oily product (XII, R′ = Me) has been characterized by analysis and by reaction with lithium aluminum hydride which converts it to the previously known N-methyl-N′-phenyldiimide. The structure of XII (R′ = Me) is assigned principally by analogy with XII (R′ = tolyl), but also it might be expected that the structure isomeric with XII (in which the amine oxide group is vicinal to the methylene group) would liberate methane from methyl halide Grignard reagent. Actually the product (XII, R′ = Me) was very sluggish in this respect and only 0.3 equivalent could be discovered under the forced conditions of pyridine solvent at 100° C.

The yield of XII is always low (when R′ = Me, 14%) and this circumstance is not unexpected in view of the known reactivity of N-oxides toward Grignard reagents. For example the free N-oxide group in VIII would be expected to oxidize Grignard reagent, leading to reduction products. Presumably such reactions would be slower than the series shown as VII → XIII. In order, then, to rationalize the low yields of diimide monoxides from the dioxides in terms of side reactions with the Grignard reagent we have chosen an especially difficult example. The addition of N-methyl-N′-phenyldiimide dioxide to an equivalent of benzyl chloride Grignard reagent in diethyl ether gives a yield not exceeding 7% of the monoxide. About 40% of the diimide dioxide is recovered indicating that much of VIII or X does not react further, and that some of the Grignard reagent is consumed in reactions not included in the formulation VII → XIII. The recovery of at least 7% of a derivative of benzaldehyde from the remaining complex mixture indicates that reduction of the monoxide has occurred subsequent to its formation.

$$C_6H_5N_2OCH_2C_6H_5 \xrightarrow{RMgX} ROMgX$$

$$+$$

$$H_5C_6{-}\overset{H}{\underset{|}{C}}{=}N{-}N{-}C_6H_5 \xleftarrow{\text{rearr.}} H_5C_6{-}N_2{-}CH_2{-}C_6H_5$$

This latter reaction seems to be a significant one because reversal of addition (Grignard reagent into diimide dioxide) only raises the monoxide yield to 10%. However, threefold dilution under the latter conditions raises this yield to 14%. Moreover, equivalent addition into a tube containing a downward-pitched screw which conveys its contents into a dry-ice bath within 1 minute, Fig. 1, raises the final yield of diimide monoxide to 20%. It would appear from these experiments that low yield of diimide monoxide is partly due to reaction of XI (or some XII formed in the system before hydrolysis) with Grignard reagent. This conclusion is not vitiated by the 25% yield to be obtained when benzyl chloride Grignard reagent in diethyl ether is added slowly to the whole of N-methyl-N′-phenyldiimide in dioxane. It may be expected that the dibenzylmagnesium which remains in solution after precipitation of magnesium halides is less reactive toward XI or XII than is the whole Grignard reagent.

There are contradictions in the literature with respect to the structure that we have assigned to XII (R′ = benzyl). The diimide monoxide produced by this reaction has also been obtained by the peracid oxidation of benzaldehyde phenylhydrazone, XIV (18). Of the three possible structures which may be written, Bergmann *et al.* favored the epoxy arrangement XVII; but later two independent groups of workers favored the

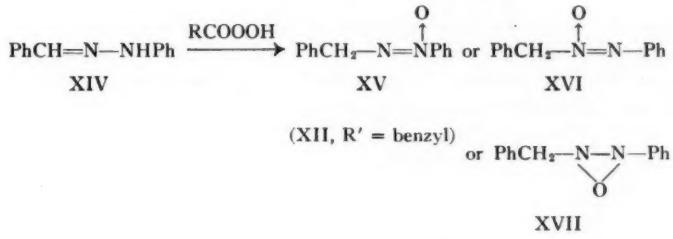

structure N-benzyl-N′-phenyldiimide N-oxide, XVI. One group (19) based its contention on bromination to N-benzyl-N′-*p*-bromophenyldiimide N-oxide, but a repetition (20) of this bromination was unsuccessful. The other group (21) approved XVI because a reaction of XIV with ethyl chloride Grignard reagent yielded diphenylamidine, XIX, but their argument is unconvincing. Indeed the formation of XIX may be explained at least as well on the basis of XV.

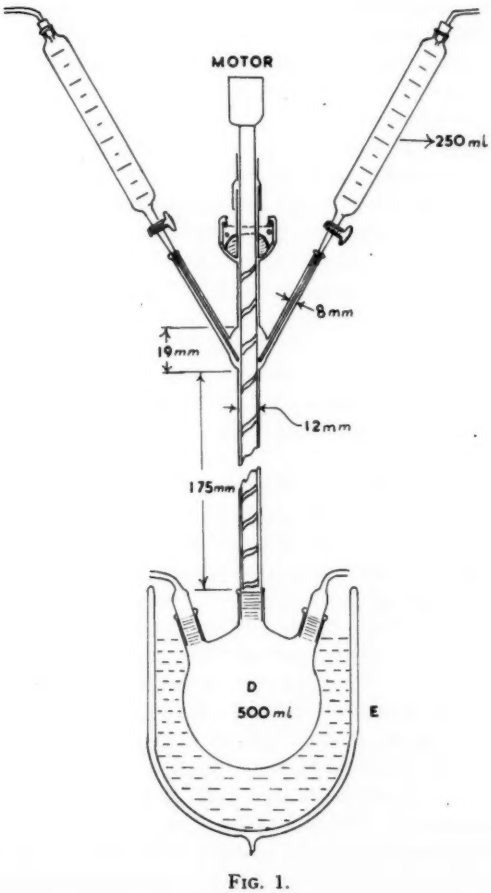

FIG. 1.

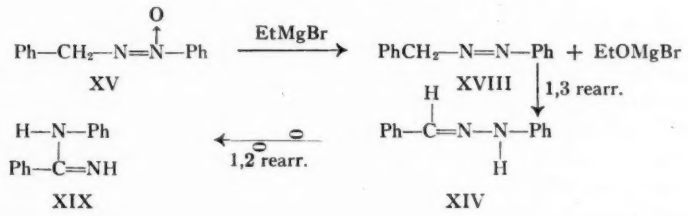

As may be seen by this formulation the reduction of XV → XIX is accomplished by the oxidation of Grignard reagent. By contrast the mechanism of Witkop and Kissman does not include the necessary oxidation step. On the other hand their mechanism does include reactions involving active hydrogen, although Witkop and Kissman searched for and could not find ethane. Lack of evidence for active hydrogen under normal conditions of Grignard treatment is confirmed by our results, although we did observe the formation of gas indicative of active hydrogen under forcing conditions (i.e. with prolonged reaction at 100° C when N-methylmorpholine was used as the reaction medium). This behavior is not unexpected when substances like XVIII, XIV, and XIX are present. For example acetone anil can be made to show the presence of active hydrogen (22). In summary it may be said that neither Pausacker nor Witkop and their co-workers have any real evidence for designation of XVI as the structure for the peroxidation product of benzaldehyde phenylhydrazone.

Actually this conclusion was drawn some years ago (19) by Lythgoe and his co-workers after preparation of both 4-chlorobenzylphenyldiimide monoxides by peroxidation of 4-chlorobenzylphenyldiimide. The product corresponding to XV was geoisomerized to the peroxidation product of 4-chlorobenzaldehyde. Also this chloro analogue of XV was brominated to give the 3-bromo-4-chlorobenzyl analogue, whereas the peroxidation product corresponding with XVI was brominated to give N-4-chlorobenzyl-N′-4-bromophenyldiimide N′-oxide.

Thus by the standard proof (17) Lythgoe and his co-workers have demonstrated the structure (XV) as the product that we obtain from phenylmethyldiimide dioxide and benzyl chloride Grignard reagent. This demonstration is not vitiated by the possibility that a modernized version of structure XVII may also explain part of the experiments of Lythgoe and his co-workers.

The behavior of Grignard reagents with N-methyl-N′-phenyldiimide dioxides provides an explanation for the action of lithium aluminum hydride in terms of the reaction sequence VII → XII inclusive, where the metal hydride replaces Grignard reagent. Moreover the heterogeneous reductants mentioned by Bamberger should behave as metal hydrides and also give N-phenyldiimide N-oxide (XII, R′ = H) initially, which ultimately would be reduced to the phenylhydrazine that eventually is obtained.

It should be noted that the nomenclature devised for diimide dioxides does not imply that characteristic properties may be specified for this group alone. In all instances at least one alkyl group must be attached to a nitrogen and no diimide dioxide has been prepared in which both organic groups attached to nitrogen are aromatic. For example an attempt to oxidize 4,4′-dichlorodiphenyldiimide to the dioxide with boiling 40% nitric acid leads only to 4,4-dichloronitrodiphenyldiimide oxide (23). On the other hand both organic groups attached to nitrogens may be aliphatic. Traube (1) prepared N,N′-methylene-bis-[N-methyldiimide]tetroxide and the ethyl homologue by treatment of the silver salt of methylene-bis-nitrosohydroxylamine (I) with the alkyl iodides. We have

prepared the 2-chloroethyl analogue (XX) by the same method taking advantage of the unusual stability of these substances toward prolonged boiling with 70% nitric acid in order to destroy the unstable isomer, di-2-chloroethyl methylene-bis-nitrosohydroxylaminate (XXI). We have also prepared methylene-bis-[methyldiimide]tetroxide and its

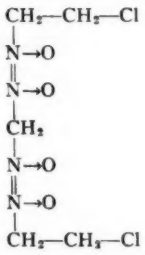

XX

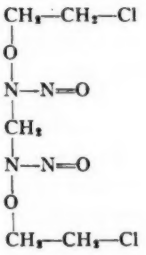

XXI

ethyl analogue by treatment of the sodium or ammonium salt of I with dialkyl sulphate but in this event the nitroso isomers corresponding with XXI evidently are destroyed *in situ*, since the tetroxides corresponding with XX are isolated in a pure state.

The chemical reactions of these aliphatic diimides have been examined by use of methylene-bis-[methyldiimide]tetroxide but they are not very informative. Pyrolysis gives methanol, nitrous oxide, and carbon, while alkaline hydrolysis gives formic acid, methanol, and nitrous acid. Treatment with bromobenzene Grignard reagent gives a small yield of benzophenone phenylhydrazone. On the other hand treatment with methyl iodide Grignard reagent under analytical conditions (Soltys machine) shows that reaction in isoamyl ether is limited to evolution of gas indicative of two equivalents of active hydrogen. A precipitate is formed immediately, which accounts for the fact that only 0.1 equivalent of Grignard reagent is found additionally to be consumed in the system.

The infrared spectra through the 1600–600 cm^{-1} range have been determined for a series of diimide dioxides, the monoxides derived from them, some oxime methyl ethers, and some methyl isonitramines (III). These spectra are shown in Table I. Among this limited number of examples two bands may be assigned tentatively to the motion of the diimide dioxide linkage. The first of these is a weak to medium absorption at 1194–1210 cm^{-1}, while the other is a consistently strong band at 995–1018 cm^{-1}. These bands are not observed among the other candidates of Table I. On the other hand the spectra of diimide dioxides are noticeably transparent in the 1000–700 cm^{-1} range whereas the O-ethers and the isonitramines show considerable absorption in this region. Although such spectral evidence cannot of itself be considered to be definitive, it does seem to confirm the chemical evidence that structure VI, and not III, IV, or V, is correct for α methylation derivatives of nitrosohydroxylamines.

The behavior of the alkyldiimide dioxide linkage as an aromatic substituent is of interest. Despite the inertness of this diimide dioxide linkage it may be displaced by forced bromination, and 4-bromonitrobenzene is obtained when N-methyl-N′-4-nitrophenyldiimide dioxide is treated in this manner. The oxidizing action of the alkyldiimide dioxide linkage may be involved, since N-methyl-N′-4-nitrophenyldiimide dioxide may be converted in part to nitrobenzene by prolonged reflux in ethanol. This reduction finds its counterpart in the oxidation of the ethanol to acetaldehyde.

TABLE I

Infrared spectra in the 1600–600 cm^{-1} region as liquids (L), solutions in carbon disulphide and carbon tetrachloride (S), in Nujol mulls (M), or in potassium bromide pellets (P)

Substance	Method																						
N-Methyl-N′-phenyldiimide dioxide	L	1590 W		1475 S	1430 S	1312 **M**	1294 **M**	1197 **M**		1100 **M**		1042 **S**	1014 **S**										
N-Methyl-N′-4-chlorophenyl-diimide dioxide	S			1486 S	1464 S	1308 M		1200 **M**		1095 S		1050 S	1015 S										
N-Benzyl-N′-phenyldiimide dioxide	S	1595 W		1472 S	1430 S	1305 W	1290 W	1210 W		1095 W		1036 S	1008 S										
N-N′-Dibenzyldiimide dioxide	S	1600 W		1486 S	1438 S	1325 M	1285 S	1210 W				1034 S	1018 S										
N-Methylene-bis-(N′-methyl-diimide) dioxide	M		1515 **M**	1482 S	1428 S	1315 M	1292 S	1205 **M**		1086 S		1040 S	995 S					795 S					
N-Methylene-bis-(N′-ethyl diimide) dioxide	M		1515 **M**	1482 S	1428 S	1315 **M**	1286 S	1194 **M**		1086 S		1040 S	1008 S					784 **M**					
N-Methylene-bis-(β-chloro-ethyldiimide) dioxide	M		1520 **M**	1488 S	1430 S	1320 W	1280 S	1194 **M**		1085 S		1032 S	1018 S					783 **M**					
N-Methyl-N′-phenyldiimide N′-monoxide	L	1605 **M**	1495 S	1452 **M**	1425 **M**	1320 S	1308 S		1160 W	1108 W	1070 **M**	1025 S		926 **M**				775 S		688 S			
N,N′-Diphenyldiimide monoxide	L	1595 W	1478 S	1455 M	1440 S	1330 S	1300 S		1164 M	1095 W	1072 M	1025 M		925 M				762 S		682 S			
N-Phenyl-N′-tolyldiimide N-monoxide	L	1605 **M**	1495 S	1458 **M**	1440 S	1325 **M**	1294 S		1165 **M**	1096 W	1070 **M**	1022 **M**		925 W				771 S		685 S			
N-Phenyl-N′-tolyldiimide N′-monoxide	L	1600 **M**	1500 S	1460 S	1447 S	1330 **M**	1295 **M**		1165 M	1098 W	1075 W	1027 W		922 W				763 S		684 S			
N-Benzyl-N′-tolyldiimide N′-monoxide	P	1602 **M**	1470 S	1440 M	1430 S	1310 S	1298 S		1170 W		1064 M	1022 **M**		918 **M**				775 S		680 S			
Benzophenone oxime O-methyl ether[a]	L	1595 W	1570 W	1498 **M**	1450 S	1428 W		1307 M		1168 M		1054 S	1032 S	1001 W		918 W			845 W	772 S	738 W	693 S	
syn-Benzaldoxime O-methyl ether[b]	L	1600 M	1589 W	1493 W	1450 M	1427 W		1312 M		1169 M		1055 S	1030 M	1002 W		919 S			845 M	757 S	747 S	692 S	
Benzophenone oxime N-methyl ether[a]	S			1490 **M**	1440 S					1169 **M**			1033 W	1001 W								704 **M**	
Diisopropyl isonitramine	L		1550 S		1470 **M**		1388 **M**	1330 **M**	1239 S	1177 W	1142 **M**				963 **M**	920 S	906 S					702 **M**	
Di-*n*-propyl isonitramine	L		1558 S		1472 **M**	1432 **M**	1382 W	1338 **M**	1239 S		1145 VW			1005 W	947 S		890 W					699 **M**	
Di-*n*-butyl isonitramine	L		1555 S		1465 **M**	1432 **M**	1379 W	1344 **M**	1240 S	1162 VW	1145 W			1005 W	959 **M**	942 **M**	887 **M**					695 **M**	

[a]Prepared according to Semper, L. and Lechertadt, L. Ber. **51**, 928 (1918).
[b]Prepared according to Aurvens, K. V. and Otters, B. Ber. B, **57**, 446 (1924).

The dissimilarity of the diimide dioxide linkage with that of the monoxides may be observed by nitration of N-methyl-N′-phenyldiimide dioxide. It is well known (24) that aromatic diimide monoxides are slowly nitrated, and almost not at all in the aromatic ring adjacent to the N → O linkage. However when substitution in this NO-adjacent ring does occur the group enters in the meta position (25). By contrast N-methyl-N′-phenyldiimide dioxide is nitrated rapidly in nitric – sulphuric acid mixture. As would be expected from this rapidity the 58% yield of this rapid nitration is predominantly (81%) the para isomer. Only 7% is found as the meta isomer and 12% as the ortho isomer.

The meta isomer could not be hydrogenolized satisfactorily to metanitroaniline but its positional isomerism seems to be proved by the tin – hydrochloric acid reductions of the ortho and para isomers to ortho- and para-nitroaniline respectively. Moreover the para isomer may be reduced to the amine which can be diazotized and then converted to N-methyl-N′-4-chlorophenyldiimide dioxide. This compound has been synthesized (2) from 4-chlorophenylnitrosohydroxylamine.

The crystallography of this 4-chloro analogue has been examined carefully in connection with a single crystal study now in progress. Incidental to this study it has been found that this typical diimide dioxide is monomeric. It has also been found that, unlike nitramines (26), the "atom polarization" of N-methyl-N′-4-chlorophenyldiimide dioxide is normal in the sense that it amounts to only a few per cent of the total (P_{E+A}) distortion polarization in a weak electric field. However the orientation polarization seems to present an anomaly.

From the formal structural representation of the diimide dioxide linkage one may draw an analogy with the nitro group. The dipole moment studies (Table II) might at

TABLE II

Electrical polarizations of some diimide dioxides in benzene at 20±0.05° C

Diimide dioxide	Polarization values				Solid dielectric			
	α	β (neg.)	P_T, cc	R_D, cc	d_4^{20}	ϵ	P_{E+A}, cc	μ, Debyes
N-Methyl-N′-phenyl	8.03	.307	267	42.8[a]				3.26
N-Methyl-N′-(4-nitrophenyl)	7.23	.437	309	50.1[a]	1.465[c]	2.815	50.7	3.50
N-Methyl-N′-(2-nitrophenyl)	15.47	.424	614	47.9[a]				5.19
N-Methyl-N′-(3-nitrophenyl)	8.11	.424	342	48.1[a]				3.74
N-Methyl-N′-(4-chlorophenyl)	4.55	.397	200	46.3[b]	1.470[c]	3.020	50.9	2.69
				48.6[a]	1.470[d]			
N-Benzyl-N′-phenyl	5.72	.317	299		1.392[c]	2.780	61.0	3.36
N-Benzyl-N′-benzyl	4.60	.315	267		1.292[c]	2.834	71.1	3.05
N′,N′-Methylene-bis-N-methyl[e]	11.36	.228	342	37.9[b]				3.80

[a]Extrapolated n_0^{20} of solutions. [b]Calc. for $n_\alpha+n_\beta+n_\gamma/3$ of solid. [c]Air displacement. [d]Flotation in zinc chloride. [e]Dioxane used instead of benzene as solvent.

first inspection seem to confirm this analogy. This $N_2O_2CH_3$ group might then be assigned the group moment 3.26 D, negative with respect to hydrogen, just as the nitro group moment is 4.0 D, negative according to the orientation polarization of nitrobenzene. Actually the observed moment (3.74 D) of N-methyl-N′-3-nitrophenyldiimide dioxide is approximate to the value calculated from $\mu_{resultant} = (m_1^2+m_2^2+2m_1m_2 \cos \theta)^{\frac{1}{2}} = 3.69$ D, where m_1 and m_2 are the group moments of $N_2O_2CH_3$ and NO_2, and θ is 120° C. However the calculated value for N-methyl-N′-4-nitrophenyl diimide dioxide (0.74 D) is widely divergent from the observed moment of 3.50 D. Likewise, a calculation

of moment for N-methyl-N′-2-nitrophenyldiimide dioxide (θ = 60° C) gives μ = 6.29 D which is considerably higher than the observed value (5.19 D). A comparable discrepancy is found for N-methyl-N′-4-chlorophenyldiimide dioxide which shows a moment of 2.64 D, about one Debye greater than that expected by calculation.

If one reconsiders the $N_2O_2CH_3$ group in respect of these discrepancies it is apparent that a simple analogy with the nitro group is not valid, and this distinction may be seen in the geometry of the group. One may depict *cis* and *trans* forms and would expect distinct physical and chemical differences. However, the variation in structure probably is more subtle than can be expressed by this simple geometry.

cis *trans*

It would appear from the results of Table II that the group moment of the diimide dioxide group is subject to wide variation depending on the substituents that may be attached to it. This variation is best explained in terms of N–N bond rotation, in which the anharmonicity is a function of the group substituent to the diimide dioxide linkage. Of course this concept conflicts with the orthodox doubly bonded diimide structure, but it is doubtful that the diimide dioxides should assume such a structure. Indeed, it would appear that the adjacent positive charge of a diimide dioxide structure such as XXII is somewhat anomalous and is better explained as a resonance hybrid of XXIII*a* and *b*.

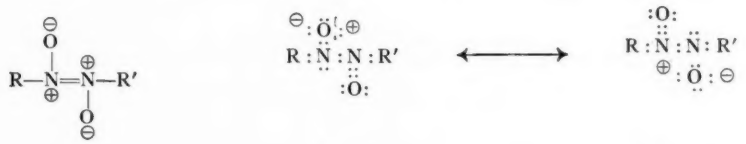

XXII XXIII*a* XXIII*b*

The resonance formulation is not intended to depict *trans* planarity; indeed the rotameric conformation of XXIII is thought to account for the apparent anomalies among the nitro and chloro derivatives described above. Certainly the conformation is not *trans* as shown in XXIII because in this event the electric moment of N,N′-dibenzyldiimide dioxide would be zero instead of 3.05 D (Table II).

The authors are grateful to Messrs. Myers and Bedard, Canadian Armament Research and Development Establishment, for the determinations of infrared absorption. They acknowledge extensive financial aid from the Defence Research Board of Canada.

EXPERIMENTAL*

N-Methyl-N′-phenyldiimide Dioxide

To a mixture of cupferron (160 g, 0.6 mole) and sodium bicarbonate (140 g, 1 mole) in 1160 ml of water was added 210 g (1 mole) of dimethyl sulphate during 7 hours with stirring. Cooling with a water bath was necessary. After 15 subsequent hours of stirring

Melting points have been corrected against appropriate standards (Can. J. Technol. **34, 89 (1956)). X-Ray diffraction patterns are recorded, using* CuK_α (Ni *filtered) radiation, in Ångstroms at relative intensities* $[I/I_1]$.

at 20° C the deep-red system was extracted with a total of 1500 ml of diethyl ether. This extract, dried with calcium chloride, was distilled finally at 0.5 mm to yield 119 g of oil, b.p. 98–100° C, which partially solidified. This product was diluted by addition with ½ volume of petroleum ether, b.p. 40–60° C, then cooled, and finally filtered. The solid was crystallized from 3.5 l. of petroleum ether (b.p. 40–60° C) and cooled to give 94 g, m.p. 37.5–39° C (60%). A similar recrystallization raised the melting point to 39.5–40.5° C. Absorption in the ultraviolet region showed λ_{max} at 262 mμ; E_{max} 10,690. The X-ray diffraction pattern was [10] 3.48; [9] 4.78; [7] 4.14; [6] 7.16; [5] 4.17; [4] 6.58; [3] 3.13; [2] 2.89, 3.38; [1] 5.19, 3.17, 3.09, 2.85, 2.61.

When this substance was heated to 100° C with 85% sulphuric acid or chlorosulphonic acid it was recovered unchanged. Likewise it was unaffected by 6 hours' treatment with acetic anhydride at 200° C.

Hydrazine Phenylnitrosohydroxylaminate

A mixture of 4.56 g (0.03 mole) of N-methyl-N′-phenyldiimide dioxide and 3.0 g (0.06 mole) of 100% hydrazine hydrate was refluxed for 17 hours, then cooled, and diluted with 15 ml of absolute ethanol. Several crystal crops totalling 3.40 g (66%, m.p. 127–128° C) were combined and crystallized from 90 ml of absolute ethanol, 2.61 g (51%) of the salt, m.p. 127–128° C (decomp.); recrystallized, m.p. 128.5–129° C. Calc. for $C_6H_{10}O_2N_4$: C, 42.3; H, 5.92; N, 32.9. Found: C, 42.3; H, 6.02; N, 33.8. Acidification of 0.25 g in 3 ml of water by 3 ml of 12% hydrochloric acid gave 1.6 g (77%), m.p. 56.5–58° C, of phenylnitrosohydroxylamine. After crystallization from 5 ml of petroleum ether (b.p. 40–60° C) the product, m.p. 58–59° C, was characterized by mixture melting point. The presence of hydrazine was demonstrated by treatment of the salt with aqueous picric acid. The hydrazine picrate melted at 182–183° C.

Reduction of N-Methyl-N′-phenyldiimide Dioxide

(*a*) *Catalytic reduction.*—A solution of 3.8 g (0.025 mole) in 50 ml of absolute ethanol with Adams catalyst absorbed 2 moles of hydrogen and then yielded aniline, b.p. 180–184° C (756 mm), which was characterized as acetanilide, 0.43 g, 24%, m.p. 112–114° C. Also 12% of the original dioxide was recovered unchanged.

(*b*) *By hydriodic acid.*—After 2 days' reflux of 1.0 g (0.0066 mole) in 3 ml of 47% hydriodic acid, 0.76 g (76%) of the original dioxide was recovered unchanged. An ether extract of the remainder was treated with oxalic acid in ether to give 4.6 mg (0.25%) of aniline oxalate, m.p. and m.m.p. 153.5–155.5° C.

(*c*) *By sodium hydrosulphite.*—A mixture of 0.99 g (0.0065 mole) in 8 ml of ethanol and 6.8 g (0.039 mole) of sodium hydrosulphite in 20 ml of water was heated with stirring at 80° C for 45 minutes. Extraction with diethyl ether yielded 65% of the unchanged starting material. The aqueous–alcoholic solution was concentrated under reduced pressure and the residue was extracted by ether to give 90 mg of oil. Treatment with picric acid yielded 104 mg (4.7%) of crude phenylhydrazine picrate, m.p. 135–137° C, which was crystallized from benzene, m.p. and m.m.p. 145.5° C.

(*d*) *By lithium aluminum hydride.*—A solution of 0.99 g (0.0065 mole) in 25 ml of dry ether was added to a solution of 0.813 g (0.0215 mole) of lithium aluminum hydride in 25 ml of the same diethyl ether with stirring during 20 minutes at 20° C. After a subsequent 30-minute stirring time the system was treated with 5 ml of 10% aqueous sodium hydroxide and then extracted with ether to yield 0.4 g of an oil. Distillation at 125–130° C (18 mm) gave 0.23 g (40%) of phenylhydrazine, characterized by conversion to *p*-chlorobenzaldehyde phenylhydrazone, m.p. and m.m.p. 125–126° C.

Bromination of N-Methyl-N′-phenyldiimide Dioxide

A mixture of N-methyl-N′-phenyldiimide dioxide (3.04 g, 0.02 mole) with 8 g (0.05 mole) of bromine in 10 ml of carbon disulphide was refluxed with 150 mg of iron filings for 15 hours. Subsequent steam distillation (4 l.) yielded 1.06 g, m.p. 68.5–71.5° C, which was crystallized from 7 ml of ethanol, and 0.48 g (6.1%, m.p. 89.8–90.8° C) of crude 1,2,3,5-tetrabromobenzene, crystallized further from ethyl acetate, m.p. 99–99.7° C. Calc. for $C_6H_2Br_4$: C, 18.3; H, 0.51. Found: C, 18.3; H, 0.73. Chloroform extraction of the steam distillation residue gave 0.51 g, m.p. 219–220° C, crystallized from dioxane, m.p. 221.6–221.9° C. This substance was not identified. Calc. for $C_7H_3Br_4$: C, 21.7; H, 0.75. Found: C, 21.1; H, 0.75.

N-Methyl-N′-4-nitrophenyldiimide Dioxide

To a chilled solution of 10.6 ml (0.26 mole) of 99% nitric acid and 45.3 ml (0.846 mole) of 100% sulphuric acid was added 19.8 g (0.13 mole) of N-methyl-N′-phenyldiimide dioxide during 15 minutes with constant stirring at 0° C. After a short time of warming to room temperature the system was poured into 400 g of crushed ice. Filtration removed 25.5 g which was twice crystallized from carbon tetrachloride to yield 12 g (47%) of the para–nitro derivative, m.p. 152–153° C. Calc. for $C_7H_7N_3O_4$: C, 42.6; H, 3.58; N, 21.3. Found: C, 42.7; H, 3.33; N, 20.8. The X-ray diffraction pattern was [10] 3.18; [8] 7.76, 7.49; [6] 4.69; [5] 5.04; [3] 3.68, 3.52; [2] 11.1; [1] 2.31; [0.5] 2.16. The ultraviolet absorption in ethanol gave λ_{max} at 243 mμ, 330 mμ with E_{max} 10,970 and 567 respectively. The substance was recovered unchanged after 12 hours at 200° C with acetic anhydride.

An unsuccessful attempt was made to prepare this compound by peroxidation of methyl 4-nitrobenzenediazotate (27). This ester was prepared via the silver salt from 4-nitrobenzenediazonium sulphate by Bamberger's method but the 2 g obtained from 6.9 g of *p*-nitroaniline was used without characterization because of its tendency toward decomposition. The orange-yellow solid (0.011 mole) was mixed with 15 ml of acetic acid and 9 ml of 30% hydrogen peroxide and kept at 0° C for 12 hours, then at 25° C for 2 days. Upon treatment with 150 ml of water and extraction with ether 1.11 g of red-brown solid was obtained upon evaporation. This solid was developed on a chromatoplate (28) (prepared from 80% silica gel and 20% plaster of Paris at 120° C) together with *p*-nitrophenol and also N-methyl-N′-4-nitrophenyldiimide dioxide. The developer was 18:1 benzene–acetone. By means of a sulphuric – nitric acid spray (95:5) only *p*-nitrophenol and not the diimide dioxide could be detected.

A mixture of 2.51 g (0.013 mole) of N-methyl-N′-4-nitrophenyldiimide dioxide and 9.2 g (0.078 atom) of granulated tin was treated with 18.8 ml (0.188 mole) of concentrated hydrochloric acid during 25 minutes. After 40 minutes of reflux the system was cooled and treated with 20 g of sodium hydroxide in 40 ml of water and then steam-distilled. From the distillate was obtained 0.89 g, m.p. 135–140° C, of *p*-phenylenediamine which was crystallized from benzene, m.p. and m.m.p. 139–140° C, 0.3 g (22%).

N-Methyl-N′-4-aminophenyldiimide Dioxide

A mixture of the para–nitro derivative (0.97 g, 0.0049 mole) and 15 ml of hydroiodic acid (sp. gr. 1.5) was heated under reflux for 15 minutes. After 12 hours at 20° C the system was diluted with 20 ml of water to precipitate 0.25 g (26%) of unchanged starting material, m.p. 152–153° C, after crystallization from carbon tetrachloride.

The amine (0.19 g, m.p. 171–172.5° C, 23%) was precipitated by addition of alkali to pH 8. It was crystallized from ethanol (95%), m.p. 176.5–176.8° C. The X-ray diffraction

pattern was [10] 4.81; [9] 3.51; [7] 4.25; [5] 3.47; [4] 7.56, 3.03; [2] 6.58, 5.86, 5.26, 2.05; [1] 2.93, 2.61. Calc. for $C_7H_9N_3O_2$: C, 50.3; H, 5.43; N, 25.1. Found: C, 50.7; H, 5.35; N, 25.5.

4-Chlorophenylhydroxylamine (2)

To a refluxing system comprised of 180 g (1.14 mole) of 4-chloronitrobenzene in 1200 ml of ethanol and 24 g (0.45 mole) of ammonium chloride in 300 ml of water was added 300 g (4.6 atom) of zinc dust in 10-g lots. One-minute periods of addition and stirring were alternated with 1-minute periods of reflux until the color of the reaction mixture passed its lightest stage of brown and began once more to darken. The residual zinc dust was quickly filtered hot. Steam distillation of the filtrate gave 50 g (30.5%), m.p. 83–83.5° C.

N-Methyl-N'-4-chlorophenyldiimide Dioxide

(*a*) *From N-Methyl-N'-4-aminophenyldiimide dioxide.*—To a suspension of N-methyl-N'-4-aminophenyldiimide dioxide (100 mg, 0.006 mole) in 0.8 ml of concentrated hydrochloric acid plus 0.5 ml of water at 0° C was slowly added a solution of 50 mg of sodium nitrite in 0.3 ml of water. To the orange-yellow reaction mixture at 0° C was then added 90 mg of cupric chloride in 0.75 ml of concentrated hydrochloric acid during 20 minutes. The system was then slowly warmed to 20° C and subsequently heated at 60° C for 10 minutes. When the mixture was cooled 60 mg (54%) of N-methyl-N'-4-chlorophenyldiimide dioxide separated, m.p. 70–71° C. After crystallization from petroleum ether (b.p. 40–60° C) a mixture melting point (71–72° C) with an authentic specimen (2) was not depressed. The X-ray diffraction pattern was [10] 5.34; [9] 3.52; [8] 3.36; [6] 3.71; [5] 4.36; [4] 4.92; [3] 6.28; [2] 2.19, 1.91; [1] 6.51, 2.94, 2.59, 2.51, 2.44, 2.22.

(*b*) *From 4-chlorophenylhydroxylamine.*—A solution of 50 g (0.348 mole) of 4-chlorophenylhydroxylamine in 335 ml of ethanol was acidified (2) with 135 ml of 2 *N* hydrochloric acid and the stirred system was held at 5° C. Then 24.6 g (0.356 mole) of sodium nitrite in saturated aqueous solution was added during 30 minutes. The precipitate was filtered off, washed with water, and, partially dried, was suspended in a solution of 80.5 g (0.761 mole) of sodium bicarbonate in 935 ml of water. The stirred suspension was treated with 45 ml (0.475 mole) of methyl sulphate. After 40 minutes the system was chilled and filtered. The crude product (54 g) was dissolved in a minimum of boiling ethanol. The hot filtrate was chilled to remove 4-chlorophenyl-bis-diimide (9.4 g, 23.9%). The filtrate was steam-distilled and 17.5 g (m.p. 69–70° C, 27%) of N-methyl-N'-4-chlorophenyldiimide dioxide was obtained from the ether extract of the distillate. After crystallization from petroleum ether (b.p. 40–60° C) it melted at 73.1–74.6° C. Rod-shaped crystals suitable for X-ray diffraction studies were obtained from *p*-cymene; they cleaved well along (100), (001), and (102).

The refractive indices were measured by the crushed crystal immersion method (29) as α, 1.49, about 10° C from (010), while β is 1.67 along (001), and γ is 1.78 about 20° C from (100). The density by flotation in aqueous zinc chloride at 29° C is 1.476, while by the air-displacement method (30) it is 1.470. Calculations of the polarization (from $\alpha+\beta+\gamma$ divided by 3) gave 46.2 cc in contrast to 50.9 cc obtained from $\epsilon = 3.020$ by dielectric constant measurement of the pelleted solid (31).

Zero level Weissenberg photographs of crystals mounted on the *b*-axis (in capsules because of sublimation) were carried out with CuK_α radiation giving constants: $a = 17.20 \pm 0.04$ Å, $b = 3.91 \pm 0.01$ Å, and $c = 13.11 \pm 0.04$ Å of a monoclinic cell with $\beta = 108.0 \pm 0.2°$ C. Since this corresponds with a cell volume of $(838$ Å$)^3$ and the molecular volume

is calculated as (210 Å)^3 there are four molecules per unit cell. Molecular weight by the Rast method was determined at 190 (calc., 186.6).

Examination of Weissenberg photographs showed no extinctions on (*hkl*), but (*oko*) reflections were found only when $k = 2n$ and (*hol*) reflections only when $l = 2n$. The space group is therefore assigned at $P2_{1/c}$. Structure factors have been determined (32).

p-Chloroaniline

Although N-methyl-N′-4-chlorophenyldiimide dioxide was unaffected by hydriodic acid at 100° C for 30 minutes, reduction was effected in a mixture of 0.56 g (0.003 mole) of the substance with 2.14 g (0.018 atom) of granulated tin to which 3.7 ml (0.095 mole) of concentrated hydrochloric acid was added during 3 minutes. Subsequently the system was maintained at 90–100° C for 30 minutes and at 20° C for 12 hours. After treatment with 6 g of sodium hydroxide in 6 ml of water the system was ether-extracted. Evaporation of the extract left 105 mg, m.p. 60–68° C, which was crystallized from petroleum ether (b.p. 40–60° C), 50 mg (13%) of *p*-chloroaniline characterized by m.p. and m.m.p. of 68.5–70° C.

4-Nitrobromobenzene

A system comprised of 0.98 g (0.005 mole) of N-methyl-N′-4-nitrophenyldiimide dioxide, 1.6 g (0.01 mole) of bromine, 100 mg of iron filings, and 5 ml of carbon disulphide was refluxed for 3 hours and then steam-distilled. The cooled distillate (220 ml) yielded 0.14 g, m.p. 67.6–69.5° C, of crude 4-nitrobromobenzene which was crystallized from ethanol, m.p. 113–115° C, 90 mg (9%), and then from commercial hexane, m.p. and m.m.p. 122.7–123.3° C.

Nitrobenzene

When a solution of N-methyl-N′-4-nitrophenyldiimide dioxide (2.56 g, 0.013 mole) in 50 ml of 95% ethanol was refluxed for 41 hours the cooled system precipitated 1.31 g (51%) of starting material, m.p. 152–153.5° C. Distillation of the filtrate gave 0.26 g of an oil, b.p. 78° C (10 mm), which on redistillation was shown to be nitrobenzene (0.23 g, 14%, b.p. 208–212° C at 756 mm, n_D^{20} 1.55256, m.p. and m.m.p. 6–7° C).

In an experiment, identical except for the addition of 0.1 g of concentrated sulphuric acid and for a 120-hour reflux, only 13% of starting material was recovered and 48% of nitrobenzene was obtained. Additionally a precipitate was formed in a trap containing acid – alcoholic 2,4-dinitrophenylhydrazine solution which surmounted the reflux condenser. This was proved by mixture melting point to be acetaldehyde 2,4-dinitrophenylhydrazone, m.p. 162–164° C.

N-Methyl-N′-3-nitrophenyldiimide Dioxide

The mother liquor (1100 ml) from which the N-methyl-N′-4-nitrophenyldiimide dioxide was removed (see above) was concentrated to a volume of 250 ml and then cooled to give 5.2 g, m.p. 103–111° C. A second crop (1.18 g, m.p. 108–113° C) was obtained by concentrating the filtrate and then eluting it on a Doucil column (1 in. × 14 in.) by means of 450 ml of 1:1 Commercial hexane – carbon tetrachloride. The combined eluates gave 6.38 g which was crystallized from 400 ml of benzene, 1.04 g (4%) of N-methyl-N′-3-nitrophenyldiimide dioxide, m.p. 128–132° C. Recrystallization from methanol raised this melting point to 133–134° C. Calc. for $C_7H_7N_3O_4$: C, 42.6; H, 3.58; N, 21.3. Found: C, 42.3; H, 3.50; N, 21.4. The X-ray diffraction pattern was [10] 3.23; [3] 7.86; [2] 4.65; [1] 4.25, 3.94, 3.70; [0.5] 6.10, 5.27. The ultraviolet absorption in ethanol at 23° C showed λ_{max} at 254 Å with E_{max} 15,350.

N-Methyl-N′-2-nitrophenyldiimide Dioxide

The eluted Doucil column (see above) was further eluted, now with carbon tetrachloride (450 ml) and then with chloroform (400 ml). These eluates gave 2.22 g, m.p. 52–60° C, and 0.55 g, m.p. 62–66° C, respectively. The combination was crystallized from a 1:1 mixture of benzene and petroleum ether (b.p. 40–60° C), 1.9 g 7.4%, m.p. 60–64° C. A similar recrystallization raised this melting point to 66.5–67.3° C. Calc. for $C_7H_7N_3O_4$: C, 42.6; H, 3.58; N, 21.3. Found: C, 42.3; H, 3.67; N, 20.9. The X-ray diffraction pattern was [10] 4.13, 3.52; [9] 7.79; [8] 5.81, 4.87, 3.87, 3.39; [6] 5.21, 2.54; [5] 4.64; [4] 3.05; [1] 7.08, 6.44. The ultraviolet absorption in ethanol at 23° C was λ_{max} 258, 289 Å with E_{max} 10,830 and 9,415 respectively.

A system comprised of 100 mg (0.0005 mole) of this isomer with 0.37 g (0.0031 atom) of granulated tin and 0.75 ml of concentrated hydrochloric acid was refluxed for 40 minutes. The cooled system, treated with 1.2 g of sodium hydroxide in 8 ml of water was ether extracted. The extract contained 35 mg, m.p. 93–97° C. This was crystallized from benzene, m.p. 100–101° C (14 mg, 26%), and then was characterized by m.p. and m.m.p. (100–102° C) as orthophenylenediamine.

N,N′-Dibenzyldiimide Dioxide

This substance was prepared in 38% yield, m.p. 58–59° C, from N-benzylhydroxylamine (33) by the previously reported procedure (3). The X-ray diffraction pattern was [10] 4.53; [8] 4.10; [7] 3.16; [6] 5.38, 4.71; [5] 3.96, 3.10; [4] 2.36; [3] 2.60; [2] 7.0; [1] 2.24, 2.91, 3.29, 3.58.

A 4% solution in benzene showed bands with the following per cent transmission (% *T*) at the recorded frequency in cm^{-1}: (89) 494, (90) 555, (86) 601, (51) 710, (66) 741, (91) 835.

N-Benzyl-N′-phenyldiimide Dioxide

To a solution of sodium ethoxide (1.38 g Na in 50 ml of absolute ethanol, 0.06 mole) was slowly added 9.3 g (0.06 mole) of cupferron. After further addition of 7.59 g (0.06 mole) of freshly distilled benzyl chloride the system was refluxed for 210 minutes. Removal of the solvent under reduced pressure left a brown residue which was extracted by diethyl ether. The evaporated extract was crystallized from a hexane–ether mixture, 2.28 g (16.7%), m.p. 80–81° C. Calc. for $C_{13}H_{12}N_2O_2$: C, 68.4; H, 5.31; N, 12.3. Found: C, 68.6; H, 5.42; N, 12.2. The X-ray diffraction pattern was [10] 4.25; [9] 5.75; [8] 3.90; [7] 4.60, 4.73; [6] 4.10; [5] 3.55, 3.17; [4] 5.06; [3] 3.26, 2.36; [2] 3.38, 3.44, 3.03; [1] 2.93.

Action of Grignard Reagents on Diimide Dioxides

(*a*) ***In the Soltys apparatus.***—N-Methyl-N′-phenyldiimide dioxide was studied by the reported procedure (34) in isoamyl ether with methyl iodide Grignard reagent in the same solvent which was distilled from sodium and then from methyl iodide Grignard reagent under nitrogen. The system evolved gas at 25° C but in order to complete the reaction it was heated by boiling water bath for 10 minutes prior to and 10 minutes after the addition of aniline. The active hydrogen was found to be 0.88 and 1.01 equivalent for two determinations in which "addition" of reagent was 1.66 and 1.59 equivalent. In a separate determination the gas was collected before the addition of aniline and was shown to be methane, free from ethane, by infrared absorption in a gas cell with potassium bromide windows: 3205 (W), 2916 (M), 2814 (S), 2786 (S), 1341 (M), 1328 (M), 1290 (S), 1258 (M), 1023 (M) cm^{-1}. Under comparable conditions the gas from N-methyl-N′-phenyldiimide N′-monoxide did not appear to be evolved at 25° C, and at 100° C it did not exceed 0.3 equivalent, although pyridine was the solvent. N,N′-Dibenzyldiimide

dioxide (9) in isoamyl ether medium showed 0.7 active hydrogen and 0.3 equivalent of Grignard addition. In the better solubilizing medium, N-methylmorpholine, the active hydrogen was 1.5 and the equivalent of Grignard addition was 1.9. The gas evolved was proved by infrared absorption to be only methane. A simple Zerewitinoff determination in pyridine (finally at 100° C) gave 0.4 active hydrogen. N-Benzyl-N′-phenyldiimide dioxide in isoamyl ether medium showed 0.5 active hydrogen and 0.7 equivalent of Grignard addition, whereas the determination in N-methylmorpholine showed 1.9 equivalent each of hydrogen and Grignard addition. The gas evolved was entirely methane (infrared). A Zerewitinoff determination in pyridine at 100° C showed 0.2 equivalent of active hydrogen.

(*b*) *N,N′-Diphenyldiimide monoxide.*—An ether solution (265 ml, 0.1 *N*, 0.027 mole) of bromobenzene Grignard reagent was added slowly to a solution of N-methyl-N′-phenyldiimide dioxide (2.6 g, 0.0172 mole) in 50 ml of diethyl ether during 150 minutes with constant stirring. Subsequently the system was treated with 100 ml of saturated ammonium sulphate. The ether phase was steam-distilled (0.93 g of unidentified oil in the distillate) and the residue was extracted by diethyl ether. Distillation of this red extract gave a 0.69-g fraction, b.p. 80–120° C (0.6 mm), and a 1.18-g fraction, b.p. 115–130° C (0.6 mm). The latter fraction, crystallized from 4 ml of petroleum ether (b.p. 40–60° C) gave 0.58 g, m.p. 34.5–35.5° C (17%), of diphenyldiimide monoxide identified by mixture melting point (35–36° C) after recrystallization from 4 ml of methanol.

(*c*) *N-Methyl-N′-phenyldiimide N′-oxide.*—Methyl chloride Grignard reagent (185 ml, 0.21 *N*, 0.0389 mole) was added slowly to a stirred solution of 4.2 g (0.0276 mole) of N-methyl-N′-phenyldiimide dioxide in 50 ml of diethyl ether during 3 hours at 20° C. After subsequent decomposition by means of 100 ml of saturated ammonium sulphate a deep-red solid (37 mg, m.p. 126–127° C decomp.) separated from the ether layer. This unidentified solid melted at 140.5° C after crystallization from benzene (60.8% C, 3.70% H). The ether layer was steam-distilled. Ether extraction of the steam distillate removed 2 g of a yellow oil, the higher boiling fraction of which (b.p. 106° C at 1 mm) was 14% of unchanged starting material, m.p. 37–39° C, while the lower boiling fraction gave 0.90 g (b.p. 90–106° C at 16 mm). Crystallization from petroleum ether, b.p. 40–60° C, gave 0.54 g (14%) of N-methyl-N′-phenyldiimide N′-monoxide, m.p. −3 to 0° C. Two similar crystallizations raised this melting point to 6.5–8.5° C, n_D^{20} 1.556. Calc. for $C_7H_8N_2O$: C, 61.7; H, 5.85; N, 20.6. Found: C, 61.9; H, 6.18; N, 20.7. The brown viscous residue from steam distillation (1.27 g) was not identified.

(*d*) *N-Methyl-N′-phenyldiimide.*—To a stirred solution of 180 mg (0.0047 mole) of lithium aluminum hydride in 10 ml of absolute diethyl ether was added 180 mg (0.0013 mole) of N-methyl-N′-phenyldiimide N′-monoxide during 10 minutes. After 35 minutes of subsequent stirring 1 ml of water was added and the system was filtered. The ether extract of the filtrate, dried over magnesium sulphate, was mixed with 3 ml of ether containing 180 mg of anhydrous oxalic acid to give 95 mg, m.p. 138–139° C, of crude methylphenyldiimide oxalate. Two crystallizations from absolute ethanol gave 36 mg (13%), m.p. 145–146° C, which did not depress the melting point of an authentic specimen (35, 36).

(*e*) *N-4-Tolyl-N′-phenyldiimide N′-monoxide.*—To a solution of 3.8 g (0.025 mole) of N-methyl-N′-phenyldiimide dioxide in 50 ml of dry diethyl ether was slowly added during 4 hours at 25° C 200 ml of 0.185 *N* *p*-bromotoluene Grignard reagent (0.037 mole). Then 100 ml of saturated aqueous ammonium chloride solution was added. Evaporation of the separated non-aqueous layer left a red liquid which was steam-distilled. Ether

extraction of the distillate (250 ml) gave 60 mg of *p,p'*-bitolyl. Ether extraction of the steam distillation residue gave 4.75 g of oil which was distilled, the first fraction (b.p. 100–120° C, 0.5 mm) of which was more bitolyl (total 0.21 g, 6%) identified after methanol crystallization by m.p. and m.m.p., 118–119° C. The higher boiling fraction (2.85 g, b.p. 120–150° C at 0.5 mm) was crystallized from methanol, 2.23 g, m.p. 42–48° C. Two further crystallizations raised the melting point to 50–51° C (1.67 g, 31.5%), and a mixture melting point with an authentic specimen (17) was not depressed. The X-ray powder diagram was [10] 4.35; [9] 3.72; [8] 4.62; [7] 7.49; [6] 3.05; [5] 6.52; [4] 3.15; [3] 5.27; entirely identical with that of the authentic sample but appreciably different from that of N-4-tolyl-N'-phenyldiimide N-monoxide, also prepared by Bigiavi and Sabatelli, [10] 4.67; [9] 3.95; [8] 3.34; [7] 9.34; [6] 3.65; [5] 4.17; [4] 5.34; [3] 5.65; [2] 4.98; [1] 3.49. In a separate experiment the mixture of 0.048 mole of *p*-bromotoluene Grignard reagent and 0.032 mole of the diimide dioxide reacted for 2 hours at 20° C. A Gilman test 1 (37) for excess Grignard reagent was then negative. The red oil obtained after hydrolysis was dried and distilled through a 10-plate column to give 2.04 g, b.p. 40–70° C (756 mm), and 1.65 g, b.p. 70–115° C (756 mm), as well as 5.34 g, b.p. 100–140° C at 10 mm. The first fraction was redistilled, 0.44 g (43%), b.p. 50–60° C, and identified as methanol by its *p*-nitrobenzoate, m.p. and m.m.p. 95–96° C. The second fraction was redistilled, b.p. 100–110° C (756 mm), 0.43 g (12% as toluene) which was converted to 2,4,6-trinitrotoluene, m.p. and m.m.p. 80–81° C for characterization.

(*f*) *N-Benzyl-N'-phenyldiimide N'-oxide.*—The best preparation involved the addition of 100 ml of 0.2 *N* benzyl chloride Grignard reagent in diethyl ether (0.02 mole) to a dioxane solution of N-methyl-N'-phenyldiimide dioxide (1.53 g, 0.01 mole in 50 ml) during 90 minutes. Then 25 ml of saturated aqueous ammonium chloride was added. The white solid which separated was filtered off and its quantity was augmented by chilling the non-aqueous layer at 0° C for 12 hours, 0.54 g (25%) as N-benzyl-N'-phenyldiimide N'-monoxide, m.p. 198–199° C decomp. This melting point was not depressed by admixture with a sample prepared according to Lynch and Pausacker (19). Moreover the X-ray diffraction patterns were identical: [10] 3.90; [9] 5.60; [8] 4.40; [7] 8.98; [6] 4.20; [5] 4.82; [4] 5.40; [3] 3.44; [2] 10.3; [1] 3.66. Calc. for $C_{13}H_{12}N_2O$: C, 73.6; H, 5.70; N, 13.2. Found: C, 73.8; H, 5.34; N, 13.2.

Preparations in diethyl ether alone were less successful. The yield by adding Grignard reagent to an equimolar amount of the diimide dioxide in 65 ml of ether was 10%, which was lowered to 7% by reversing the order of addition, while threefold dilution with consequent longer addition time gave 14% yield. The best yield in diethyl ether (20%) was obtained by adding equivalent amounts at equivalent concentrations of the reagents from two burettes into a tube in which a downward pitched screw conveyed the mixture to a dry-ice-cooled trap within 1 minute of the time of introduction.

The other products of these reactions are of interest. The red oil remaining after evaporation of the filtered non-aqueous part of the hydrolyzate showed at least 6 constituents when examined on a chromatoplate (28). Column chromatography of the red oil on alumina (100–150 mesh activated at 150° C for 10 hours) eluted by benzene gave 3.18 g which was rechromatographed similarly to give 2.74 g that yielded 0.51 g (19%) of bibenzyl (m.p. and m.m.p. 51–52° C) by crystallization from methanol. The methanolic filtrate on treatment with 2,4-dinitrophenylhydrazine reagent gave 0.58 g (m.p. 227–228° C, 7%) of crude benzaldehyde 2,4-dinitrophenylhydrazone, identified by m.p. and m.m.p. (234–236° C) after crystallization from benzene.

Elution of the alumina columns by chloroform gave a liquid (1.99 g) which was crystal-

lized from petroleum ether (b.p. 40–60° C) to give unchanged starting material, m.p. 38–39° C, 1.85 g, 40%, characterized by mixture melting point.

A modification of the preparation of N-benzyl-N′-phenyldiimide N′-oxide was made by filtration of the reaction system. To a stirred solution of 6.1 g (0.04 mole) of N-methyl-N′-phenyldiimide dioxide in 50 ml of absolute diethyl ether was added 0.06 mole of benzyl chloride Grignard reagent (300 ml, 0.2 *N*) during 2 hours. The system was filtered under nitrogen to remove the white precipitate from the ultimately red solution. Hydrolysis of this filtrate by addition of 50 ml of saturated aqueous ammonium chloride gave 3.6 g of viscous oil after drying and evaporation of the ether. Treatment of this oil with 15 ml of hexane precipitated 0.1 g (1.2%) of N-benzyl-N′-phenyldiimide N′-oxide, m.p. 198–199° C after crystallization from toluene, authenticated like the main bulk of this product by mixture melting point and infrared spectra.

The hexane-soluble portion of the oil was chromatographed on alumina to yield by hexane elution 0.6 g (10%) of unchanged methylphenyldiimide dioxide (m.p. 38–39° C) and then by carbon tetrachloride elution 0.1 g (1.3%, m.p. 154–155° C after crystallization from cyclohexane) of benzaldehyde phenylhydrazone, authenticated by mixture melting point and infrared spectra.

The white precipitate from the reaction system was hydrolyzed by treatment with 75 ml of saturated aqueous ammonium chloride. The ether extract of the hydrolyzate, evaporated and then dissolved in hot toluene, yielded 1.2 g (14%) of N-benzyl-N′-phenyldiimide N′-oxide, m.p. 198–199° C. Evaporation of the mother liquors left 4.5 g of unidentified red oil.

Solvolysis of N-Benzyl-N′-phenyldiimide N′-Monoxide

A mixture of 0.5 g (0.00236 mole) of the monoxide and 5 ml of glacial acetic acid (13) was gently refluxed for 15 minutes and then poured into 25 g of crushed ice. The system, neutralized by addition of sodium bicarbonate, was ether-extracted. Evaporation left an oil (0.76 g) from which 0.28 g (42%) of benzaldehyde 2,4-dinitrophenylhydrazone (m.p. and m.m.p. 235–236° C) was isolated by treatment with 2,4-dinitrophenylhydrazine reagent.

Analysis of N-Benzyl-N′-phenyldiimide N′-Monoxide in the Soltys Machine

By the technique used for analysis of methylphenyldiimide dioxide the N-benzyl-N′-phenyldiimide N′-monoxide did not react at all at room temperature; at 100° C it yielded only 0.5 active hydrogen and 0.7 equivalent of addition. Consequently the isoamyl ether was replaced by N-methylmorpholine (dried over solid potassium hydroxide, then barium oxide, and distilled under nitrogen, b.p. 136–136.5° C). In this reaction medium 1.9 equivalent of active hydrogen and 1.9 equivalent of addition were observed, after 20 minutes at 100° C. No gas was evolved at 25° C. A Zerewitinoff determination at 100° C in pyridine showed 0.3 equivalent of active hydrogen.

N′,N′-Methylene-bis-[N-ethyldiimide]tetroxide

A solution of 45 g (0.294 mole) of monoammonium methylene-bis-nitrosohydroxylaminate (1) in 140 ml of 8% aqua ammonia was stirred during 24 hours while 88.5 ml (0.675 mole) of diethyl sulphate was added gradually, the pH being maintained at 8 by addition of more ammonia. The precipitate which was filtered off weighed 8.2 g, m.p. 145° C, after it was dried and washed with chloroform. This 15% molar yield of ammonium N-ethyl-N′-diimidomethylnitrosohydroxylaminate dioxide could be purified by rapid solution in 40 ml of water at 70° C, followed by quick cooling to avoid decom-

position with evolution of colorless gas. The recovery was 41% of that added, m.p. 150.1–150.6° C decomp., but a second crop, m.p. 149° C, could be obtained by dilution of the liquors with ethanol. Calc. for $C_3H_{11}N_5O_4$: C, 19.8; H, 6.13; N, 38.6. Found: C, 19.9; H, 6.40; N, 38.1.

The reaction liquor from which the ammonium salt precipitated was treated during 7 hours with 50 ml of diethyl sulphate and sufficient ammonia to maintain the pH at 8. The clear solution was then extracted three times with chloroform and these extracts were vacuum evaporated to leave 10 g of gummy solid which was treated with 10 ml of 68% nitric acid. After the strenuous evolution of nitrogen oxides had ceased the hot solution was cooled and neutralized by strong alkali. The crystals (4.4 g, m.p. 75.8–76.3° C) were N′,N′-methylene-bis-[N-ethyldiimide]tetroxide.

This compound also was obtained when 2.96 g (0.014 mole) of the ammonium salt described above was dissolved in 10 ml of water with 12 ml of 10% aqueous sodium hydroxide (0.03 mole) and was treated during 24 hours with 3.9 ml (0.03 mole) of diethyl sulphate. The product (1.3 g) was crystallized from 95% ethanol (1.5 ml per g) 0.68 g, m.p. 78.9° C. More of the same compound was obtained (0.4 g) by concentration of the mother liquors followed by fume-off with hot nitric acid. Calc. for $C_5H_{12}N_4O_4$: N, 29.2. Found: N, 29.6.

The methyl analogue was prepared in the same manner but with less complication because the ammonium salt did not precipitate. Consequently a 33% yield, m.p. 136° C, could be obtained within one day. The X-ray diffraction diagram was [10] 5.88; [9] 3.87; [8] 3.80; [7] 3.12; [6] 3.58; [5] 5.21; [4] 2.60; [3] 3.23; [2] 3.96, 3.35; [1] 2.40, 2.32, 2.36.

N,N′-Methylene-bis-methyldiimide tetroxide, m.p. 136° C, may be crystallized from 70% nitric acid in which it is quite stable, even during several hours at the boiling point of this medium. The density at 20° C of the solid substance is 1.368 (flotation) in comparison with 1.378 calculated from the following X-ray data. The crystal is orthorhombic pyramidal with $a = 14.38 \pm 0.04$ Å, $b = 15.16 \pm 0.04$ Å, $c = 7.16 \pm 0.02$ Å when crystallized from benzene. Reflections (Weissenberg) are found in (*hkl*) only when $h+k$, $k+l$, and $l+h$ are even; in (*hol*) only when $h = 2n$, $l = 2n$, and $h+l = 4n$; in (*okl*) only when $k = 2n$, $l = 2n$, and $k+l = 4n$. Hence the space group is $C_{2v}^{19}(F_{ddm})$. There will be eight molecules per unit cell with a twofold molecular symmetry axis. Since the volume of the unit cell is 1561 Å^3, the total number of electrons is 688. The absorption coefficient for CuK_α radiation is thus 12.6 cm^{-1}.

The crystals are twinned parallel to the *b*-axis and are strongly piezoelectric, indicating lack of centrosymmetry. The refractive indices measured by the crushed crystal technique are $\alpha = 1.38$, $\beta = 1.445$, $\gamma = 1.48$, so $\alpha+\beta+\gamma/3 = 1.44$. A tentative orientation was chosen and structure factors were determined (38).

N,N′-Methylene-bis-[N-β-chloroethyldiimide]tetroxide

A suspension of 2.23 g (0.0146 mole) of monoammonium methylene-bis-nitrosohydroxylaminate in 50 ml of water was treated with water until solution was complete. To this solution was added 4.96 g (0.0202 mole) of silver nitrate in 25 ml of water. The silver salt was filtered off, washed twice with water, and thrice with absolute ethanol. It was then suspended in 30 ml of absolute ethanol and 5.55 g (0.029 mole) of 1-chloro-2-iodoethane was added. After 5 days the silver iodide was filtered off and washed with absolute ethanol. Evaporation of the filtrate left 2.16 g which was treated with 2 ml of 68% nitric acid to destroy the nitroso compounds. After the strenuous reaction had subsided the system was diluted with water and the crystals were filtered off, 1.20 g

(37%), m.p. 87.8–89.5° C, not raised by crystallization from ethanol (5 ml per g). Calc. for $C_5H_{10}N_4O_4Cl_2$: N, 21.4. Found: N, 21.8.

Bromobenzene Grignard Reagent with Methylene-bis-[methyldiimide]tetroxide

Into 75 ml (0.1375 mole) of bromobenzene Grignard reagent under nitrogen at 0° C was added 3.28 g (0.02 mole) of the powdered tetroxide during 30 minutes with strong gas evolution. The brownish-red system was filtered to remove a gummy mass from which, after hydrolysis, 0.50 g (15%) of the tetroxide was recovered by decomposition of the remainder with 70% nitric acid, m.m.p. 134° C. The filtered reaction mixture was hydrolyzed by 12% hydrochloric acid and the dried non-aqueous layer was distilled, finally at 130° C (20 mm) to remove 2.02 g of biphenyl. Continuation gave a distillate, b.p. 140–240° C (9 mm), which was dissolved in 4 ml of ethanol, 0.71 g, m.p. 126–130° C. This 13% yield of benzophenone phenylhydrazone was twice crystallized from ethanol, m.p. 133–133.5° C, not depressed by admixture with the authentic compound.

Pyrolysis of Methylene-bis-[methyldiimide]tetroxide

The substance decomposed smoothly when 4.92 g (0.03 mole) was heated during 2 hours at 210–220° C. After 15 minutes at 245° C the distillate was converted by means of *p*-nitrobenzoyl chloride to 1.68 g (89%) of the methyl ester. The pyrolysis residue (0.32 g, 93%) was carbon. Analysis of the evolved gas showed that 86% was nitrous oxide.

Qualitative and Quantitative Tests with Methylene-bis-[methyldiimide]tetroxide

A Barger–Rast molecular weight determination in camphor was 163, calc. 164. The substance was unaltered by treatment with acid hydrogen peroxide during 7 hours, and it did not react after 12 hours in methanol with sodium borohydride, but a vigorous reaction occurred with lithium aluminum hydride. However, no products could be isolated from the latter reaction. No reaction occurred with benzaldehyde, *p*-nitrobenzaldehyde, cyclohexanone, urea, but a vigorous reaction occurred with hot phenylhydrazine. No recognizable product was obtained. The alkaline hydrolysis of the tetroxide yielded methanol, formic acid, nitrous acid, and perhaps some hydrogen cyanide either with 30% aqueous sodium hydroxide or with sodium ethoxide.

The active hydrogen determination was carried out in the Soltys machine by the prescribed procedure (34) in isoamyl ether for 20 minutes at 100° C, but it was observed that a precipitate formed immediately upon addition of the reagent and a red solution was formed which faded upon heating. The active hydrogen was found to be 1.9 equivalent. The amount of Grignard reagent which underwent an addition reaction was only 0.1 equivalent, undoubtedly due to the insolubility of the original precipitate from which methane was evolved.

Electrical Polarization Studies

Dielectric constants and specific volumes of either benzene or (in one instance) dioxane solution were carried out as described previously (39, 40) and calculations were made by the method of Halverstadt and Kumler (41). The distortion polarization was determined either from refractive index, additive refractions, or by direct determination with the solid substance (31). Densities were determined by an air-displacement method (30) or by flotation. The results are shown in Table II.

Infrared Spectra

The spectra have been obtained with a Perkin–Elmer 21 spectrometer by Messrs. Bedard and Myers of Canadian Armament Research and Development Establishment,

Quebec, Que., to whom we are indebted. The samples were studied as Nujol mull (M), as solutions in carbon tetrachloride and carbon disulphide (S), or, whenever possible, as liquids (L) and these notations are made in Table I, where the principal wave numbers in the significant range are recorded.

REFERENCES

1. TRAUBE, W. Ann. **300**, 81 (1898).
2. BAMBERGER, E. and BAUDISCH, O. Ber. **42**, 358 (1909).
3. BEHREND, R. and KÖNIG, E. Ann. **263**, 218 (1891).
4. LINDER, R. Ann. **275**, 133 (1893).
5. HANTZSCH, A. Ber. **31**, 177 (1898).
6. BAMBERGER, E. and EKECRANTZ, T. Ber. **29**, 2412 (1896).
7. HAMNICK, D. U., NEW, R. G. A., and SUTTON, L. E. J. Chem. Soc. 742 (1932).
8. FENIMORE, CH. P. J. Am. Chem. Soc. **72**, 3226 (1950).
9. DARWIN, C. and HODGKIN, D. C. Nature, **166**, 827 (1950).
10. GOWENLOCK, B. G. and TROTMAN, J. J. Chem. Soc. 4190 (1955).
11. SMITH, J. W. J. Chem. Soc. 1124 (1957).
12. KINGDON, W. R. and WRIGHT, G. F. J. Am. Chem. Soc. **72**, 1030 (1950).
13. BAMBERGER, E. Ber. **31**, 574 (1898).
14. LAMBERTON, A. H. Quart. Revs. **V**, 75 (1951).
15. LANGLEY, B. W., LYTHGOE, B., and RAYNER, L. S. J. Chem. Soc. 4191 (1952).
16. KOHLER, E. P., STONE, J. F., and FUSON, R. C. J. Am. Chem. Soc. **49**, 3181 (1927).
17. BIGIAVI, D. and SABATELLI, V. Gazz. chim. ital. **57**, 557 (1927).
18. BERGMANN, M., ULPTZ, R., and WITTE, CH. Ber. **56**, 679 (1923).
19. LYNCH, B. M. and PAUSACKER, K. H. J. Chem. Soc. **3**, 2517 (1953).
20. BROUGH, J. N., LYTHGOE, B., and WATERHOUSE, P. J. Chem. Soc. **4**, 4069 (1954).
21. WITKOP, B. and KISSMAN, H. M. J. Am. Chem. Soc. **75**, 1975 (1953).
22. SHORT, W. F. and WATT, J. S. J. Chem. Soc. **2**, 2293 (1930).
23. CALM, A. and HEUMANN, K. Ber. **13**, 1185 (1880).
24. BIGELOW, L. Chem. Revs. **9**, 117 (1931).
25. VALORI, B. Atti. accad. Lincei, **22**, II, 125 (1913).
26. GEORGE, M. V. and WRIGHT, G. F. J. Am. Chem. Soc. **80**, 1200 (1958).
27. BAMBERGER, E. Ber. **28**, 225 (1895).
28. ALLENTOFF, N. and WRIGHT, G. F. Can. J. Chem. **35**, 900 (1957).
29. BUNN, C. W. Chemical crystallography. Oxford University Press, London. 1946. p. 63.
30. GEORGE, M. V. and WRIGHT, G. F. Can. J. Chem. **36**, 189 (1958).
31. MEREDITH, C. C., WESTLAND, L., and WRIGHT, G. F. J. Am. Chem. Soc. **79**, 2385 (1957).
32. DONOVAN, R. G. M.A. Thesis, University of Toronto. 1954.
33. JONES, L. W. and SNEED, M. C. J. Am. Chem. Soc. **39**, 674 (1917).
34. ORGANIC ANALYSES. Vol. I. Interscience Publishers, Inc., New York. 1953. p. 155.
35. KNORR, L. Ber. **39**, 3265 (1906).
36. KNORR, L. and WEIDEL, A. Ber. **42**, 3523 (1909).
37. GILMAN, H. and SCHULZE, F. J. Am. Chem. Soc. **47**, 2002 (1925).
38. BINNIE, W. P. Defence Research Board Postdoctoral Research Report (available from G. F Wright by request).
39. MEREDITH, C. C. and WRIGHT, G. F. Can. J. Technol. **33**, 182 (1955).
40. SIPOS, J. C., SAWATZKY, H., and WRIGHT, G. F. J. Am. Chem. Soc. **77**, 2759 (1955).
41. HALVERSTADT, I. F. and KUMLER, W. D. J. Am. Chem. Soc. **64**, 2988 (1942).

THE ELECTRONIC STATES OF *CIS*- AND *TRANS*-ACETYLENE[1]

H. HOWARD AND G. W. KING

ABSTRACT

The electronic energy levels of *cis*- and *trans*-bent planar centrosymmetric acetylene molecules, with $\angle CCH = 120°$ and $r_{CC} = 1.383$ Å, have been calculated by the LCAO/-ASMO/CI procedure. The lowest energy state that can spectroscopically combine with the linear ground state is found to be of symmetry class A_u belonging to the *trans*-bent molecule and to lie at 4.58 ev above the ground state. This compares favorably with the experimentally observed electronic transition of lowest energy which is of type $(^1A_u - ^1\Sigma_g^+)$ and at 5.24 ev. The lowest-energy allowed transition to a *cis*-bent state of these dimensions is at 9.39 ev, and hence this may not form part of the unanalyzed system of bands in the 2000–1500 Å region, as has been suggested. However, a transition to a *trans*-bent state of type $(^1B_u - ^1\Sigma_g^+)$ is predicted to fall in this region. The energies of other electronic states are discussed in relation to the observed absorption systems of acetylene.

INTRODUCTION

The molecular orbitals method has been successful in predicting the geometry and energy of electronic states of simple and highly symmetric molecules. Such orbitals are commonly constructed by linear combination of appropriate atomic orbitals (LCAO/MO method). Qualitative, empirical extensions to more complex systems have been made in which the stereochemistries of electronically excited molecular states are also considered; in papers on this subject by Walsh (1) and Mulliken (2) the acetylene molecule is considered in some detail as an example. It is known experimentally (3, 4) that the absorption bands of acetylene in the 2400–2000 Å region are due to a transition from a linear ground state of $^1\Sigma_g^+$ symmetry, with $r_{CC} = 1.202$ Å, to a *trans*-bent planar excited state of A_u electronic symmetry (point group C_{2h}) with $r_{CC} = 1.383$ Å and $\angle CCH = 120°$. Thus the excited molecule resembles an ethylene molecule with two *trans* hydrogen atoms missing.

We report, in this paper, the results of calculations of the electronic energy levels of *cis*- and *trans*-bent planar acetylene molecules, belonging to symmetry point groups C_{2v} and C_{2h} respectively, both with the same carbon–carbon bond length as in the A_u state above and with 120° carbon–hydrogen bond angles. Insofar as the approximations which it has been necessary to make are valid, the calculations reveal patterns of energy levels that are helpful in identifying further optical transitions involving bent excited states and which enable comparisons to be made with the predictions of Walsh and Mulliken. Ross (5) has already calculated the energy levels of the linear molecule by a similar method, and by using his values a comparison can be made between the experimental and theoretical energy of the $(^1A_u - ^1\Sigma_g^+)$ transition. This is of especial interest, since the latter quantity is a difference in energies obtained from independent calculations on two models of quite different geometry and electronic structure, and hence this provides a stringent test of the accuracy of these methods of calculation.

THEORY

The basic LCAO/MO procedure is well known (see 6, 7) and is presented in outline here to illustrate its application to this problem.

We consider specifically N of the electrons in a molecule; these may be all the electrons

[1]*Manuscript received December 22, 1958.*
Contribution from the Burke Chemical Laboratories, Hamilton College, McMaster University, Hamilton, Ontario.

or a certain fraction of these, called "valence electrons" which are significantly disturbed by light absorption or change in geometry. An orthonormal set of single-electron molecular wave functions $\phi_{t\nu}(\mathbf{r}_\nu)$ are constructed, $\mathbf{r}_\nu$ being the position vector of the νth electron. 2^N possible determinantal antisymmetrized product (ASMO) wave functions, each satisfying the Pauli principle, can be constructed for the N-electron system. These have the normalized form.

$$[1] \qquad \Phi_p = (N!)^{-\frac{1}{2}} \, |\phi_0(q_0) \; \phi_1(q_1) \; \ldots \ldots \; \phi_N(q_N)|$$

where only terms in the leading diagonal are written between bars. q_ν is a scalar product of $\mathbf{r}_\nu$ with basic spin vectors α or β.

Suitable linear combinations of the functions [1] can be classed as eigenfunctions of the squared spin angular momentum operator S^2;

$$[2] \qquad \Omega^S = \sum_{q,p} a_{q,p} \, \Phi_p^S$$

where the a's are coefficients.

The total Hamiltonian operator H for the N-electron system may be written

$$[3] \qquad H = \mathrm{H}^\circ + \sum_{\nu \neq \mu}^{N} e^2/r_{\nu\mu}$$

where

$$\mathrm{H}^\circ = \sum_{\nu=1}^{N} H^\circ_\nu(\mathbf{r}_\nu),$$

$H^\circ_\nu(\mathbf{r}_\nu)$ being the single-electron operator for the νth electron in a potential field due to the nuclei plus non-valence electrons, and the second term in [3] represents the inter-electronic repulsion between the valence electrons. We seek the best approximations to the eigenvalues E_k of H in the variational form

$$[4] \qquad \int \Psi_k^{S*} \, H \, \Psi_k^S \, d\tau$$

for the lowest energy state and states orthogonal to this, where in general the Ψ_k are combinations of the linearly independent AP Ω^S; in practice a finite number m of these are taken in each combination.

$$[5] \qquad \Psi_k^S = \sum_m b_{km} \, \Omega_m^S.$$

The MOs ϕ_i are each generally formed by linear combination of some n AOs,

$$[6] \qquad \phi_i = \sum_n c_{in} \chi_n.$$

The LCAO/SCF method (8) is an iterative process for evaluating [4]; the coefficients c_{in} in [6] and an effective Hamiltonian H^* in [4] are varied to minimize the energy, subject to retaining orthonormality of the MOs. This method is most readily applied when Ψ_k consists of a single AP Φ_p, such as in ground-state closed-shell molecular configurations; it gives a good approximation to the best MOs for such states.

In the alternative LCAO/MO/CI procedure used here, approximate MOs are constructed from analytic AOs in equation [6], and the best Ψ_k of type [5] determined variationally. Large determinantal secular equations are obtained, which can generally be factored into blocks along the leading diagonal if the molecule has symmetry and the

ϕ_t are constructed so as to transform like irreducible representations of the appropriate symmetry point group.

The single-electron form of H° in [3] and the orthogonality of the ASMO Φ_p in [1] lead to elements of type

$$[7] \qquad E_i' = \int \Omega_i^{S*} H \, \Omega_i^S \, d\tau$$

along the principal diagonals of the secular determinants; these are first approximations to the eigenvalues of H, and the simple LCAO/MO treatment consists in evaluating these. The E_i' are necessarily approximate because the ASMO functions employed are, in general, only approximations to exact wave functions. This is corrected by introducing Configuration Interaction (CI), this term being applied when the off-diagonal elements of the secular determinants, of form

$$[8] \qquad \int \Omega_i^{S*} \left| \sum_{\nu \neq \mu}^{N} e^2/r_{\nu\mu} \right| \Omega_m^S \, d\tau,$$

are evaluated and the eigenvalues of H are obtained by solution of the full secular determinants.

The integrals [7] and [8] can all be evaluated by standard methods (9).

APPLICATION TO ACETYLENE

In linear acetylene, six electrons constitute the carbon–carbon bond; excitations of either one or two of these give rise to the energetically low excited states (5). In the approximation used here, the corresponding set of six electrons in the *cis*- and *trans*-bent molecules were taken as valence electrons. Of the remaining eight, the carbon 1*s*-electrons were taken merely to screen their respective nuclei, reducing the net charge to $+4e$; the hydrogen atoms and their electrons were neglected (see (5) for comments on the validity of this approximation; a similar justification should apply here). Exchange and repulsion effects between the valence electrons and those contributed by each carbon atom to a carbon–hydrogen bond were included in the calculation.

Apart even from non-planar states of acetylene, there are an infinite possible number of geometrical configurations for planar states, with different combinations of bond lengths and angles. The only geometric data available for a bent state are those for the *trans*-bent A_u state (3, 4) and were used as a basis for our calculations. In both the *cis*- and *trans*-bent models, the carbon–carbon bond length was taken as 1.383 Å, and sp^2-hybridized carbon atomic orbitals were used in forming the molecular orbitals, the hydrogen atoms being formally attached at C–C–H angles of 120°. The use of these specific dimensions does not restrict the applicability of the results as much as would appear at first sight, since what is essentially a 3-electron carbon–carbon bond in the A_u state, similar to that found in benzene, recurs in other excited configurations. In any case, for other electronic states with different actual dimensions, these calculations give excitation energies to such vibronic energy levels as have approximately the dimensions used here, in accordance with the Franck–Condon principle.

Real, normalized Slater AOs were used for the carbon $n = 2$ atomic orbitals, of form:

$$a_s = (\delta^5/3\pi)^{\frac{1}{2}} r_a \exp(-\delta r_a)$$

$$\left.\begin{matrix} a_x = \\ a_y = \\ a_z = \end{matrix}\right\} (\delta^5/\pi)^{\frac{1}{2}} r_a \exp(-\delta r_a) \left\{\begin{matrix} x_a \\ y_a \\ z_a \end{matrix}\right.$$

centered on each of the carbon atoms a and b. The z-axes on each atom projected towards each other, and the x-axes were perpendicular to the molecular plane. δ was assigned the value 1.59.

The a_s Slater function is nodeless; a better form for the 2s orbital is one that is orthogonal to the corresponding 1s orbital;

$$a_s^\circ = (a_s - 0.21284\, a_{1s})/0.9771.$$

This form was used in evaluating all mononuclear integrals in which the 2s orbital occurred, for which it gives significantly improved values. The sp^2-hybridized AOs were:

$$\chi_1 = (3)^{-\frac{1}{2}}(a_s + 2^{\frac{1}{2}}a_z) \qquad \chi_2 = (3)^{-\frac{1}{2}}(b_s + 2^{\frac{1}{2}}b_z)$$
$$\chi_3 = a_x \qquad \chi_4 = b_x$$
$$\chi_5 = 3^{-\frac{1}{2}}a_s - 6^{-\frac{1}{2}}a_z - 2^{-\frac{1}{2}}a_y \qquad \chi_6 = 3^{-\frac{1}{2}}b_s - 6^{-\frac{1}{2}}b_z \mp 2^{-\frac{1}{2}}b_y$$
$$\chi_7 = 3^{-\frac{1}{2}}a_s - 6^{-\frac{1}{2}}a_z - 2^{-\frac{1}{2}}a_y \qquad \chi_8 = 3^{-\frac{1}{2}}b_s - 6^{-\frac{1}{2}}b_z \pm 2^{-\frac{1}{2}}b_y$$

where the orbitals χ_7 and χ_8 were taken as pointing towards the hydrogen atoms, the upper and lower signs referring to *trans-* and *cis*-states respectively. The sets of LCAO/MOs constructed from these AOs which span the irreducible representations of point groups C_{2h} and C_{2v} are shown in Table I, together with their appropriate symmetry representations.† The N_i are normalizing factors.

TABLE I

LCAO/MOs for *cis-* and *trans*-bent acetylene

MO	Description	Symmetry classification C_{2v}	Symmetry classification C_{2h}
$\phi_0 = (2N_0)^{-\frac{1}{2}}(\chi_1+\chi_2)$	$(\sigma_g.2sp^2)$	a_1	a_g
$\phi_1 = (2N_1)^{-\frac{1}{2}}(\chi_3+\chi_4)$	$(\pi_u.2p)$	b_2	a_u
$\phi_2 = (2N_2)^{-\frac{1}{2}}(\chi_5-\chi_6)$	$(2sp^2)$	b_1	b_u
$\phi_3 = (2N_3)^{-\frac{1}{2}}(\chi_5+\chi_6)$	$(2sp^2)$	a_1	a_g
$\phi_4 = (2N_4)^{-\frac{1}{2}}(\chi_3-\chi_4)$	$(\pi_g.2p)$	a_2	b_g
$\phi_5 = (2N_5)^{-\frac{1}{2}}(\chi_1-\chi_2)$	$(\sigma_u.2sp^2)$	b_1	b_u

ϕ_3^* (*cis*) $= 1.0005(\phi_3 - 0.09602\,\phi_0)$.
ϕ_3^* (*trans*) $= 1.0061(\phi_3 - 0.10972\,\phi_0)$.
ϕ_5^* (*cis*) $= 1.0481(\phi_5 + 0.29939\,\phi_2)$.
ϕ_5^* (*trans*) $= 1.03628(\phi_5 + 0.26228\,\phi_2)$.

The MOs ϕ_0 and ϕ_3, also ϕ_2 and ϕ_5, belong to the same symmetry species in both *cis-* and *trans*-models and are not orthogonal to each other. Properly orthogonal forms of ϕ_3 and ϕ_5 are shown starred at the bottom of Table I. The lack of orthogonality between ϕ_0 and ϕ_3 is small, and could be ignored in many parts of the calculation; but the orthogonalized forms of ϕ_3 were used, for example, in calculating the orbital energies ϵ_3 described below. The orthogonalized ϕ_5^* orbitals were used throughout in evaluating integrals. The description in the table indicates the AOs from which the MOs are formed, and also the corresponding MOs of the linear molecule. This description will be retained for convenience in discussing ϕ_3^* and ϕ_5^* orbitals.

AP wave functions were constructed in determinantal form [1] from these MOs by the principles outlined in the previous section: these could be classified according to the

†*Detailed character tables, tables of direct products, and correlations between representations of these groups for acetylene are given in reference (3), p. 2711. Walsh (1) makes a slightly different classification of the C_{2v} species: as a result his symmetry species b_1 and b_2 are interchanged with respect to these used here. Where Walsh's conclusions are mentioned (see discussion, later) his symbols are changed to accord with the definitions used here, which appear more generally accepted in the literature: see (10).*

symmetry of the occupied MOs under the appropriate point groups. Only combinations corresponding to singlet states were used as Ω functions [2]. Then the integrals [4] break down into sums of integrals over electrons in MOs, of form

$$\text{"Orbital Energy"} \quad \epsilon_a = \int \phi_a^*(\nu)[H^\circ_\nu(\mathbf{r}_\nu)]\phi_a(\nu)\, d\tau_\nu$$

$$\zeta_{bd}^{ac} = \int\int \phi_a^*(\nu)\,\phi_b^*(\mu)[e^2/r_{\nu\mu}]\phi_c(\nu)\,\phi_d(\mu)\, d\tau_\nu\, d\tau_\mu.$$

The former type of integral only arises in evaluation of the diagonal elements of the determinants. The latter type can be expanded into sums of integrals over AOs. These were evaluated independently from the tables of Kotani (11) and Kopineck (12) by five-point Lagrangian interpolation, the separate values being in excellent agreement. Certain mononuclear integrals were obtained from formulae given by Barnett and Coulson (13) and Roothan (14).

The orbital energy integrals ϵ_a require special mention. Their evaluation is discussed in detail by Ross (5) in an appendix to his paper. The operator involved can be split into two parts,

$$H^\circ_\nu = T^\circ_\nu + U^\circ_\nu.$$

U°_ν is the potential energy operator for the νth electron and contains terms representing nuclear attraction and exchange and repulsion with the carbon–hydrogen bond electrons. The evaluation of integrals over this operator is straightforward, since each integral splits up into a sum of integrals over AOs, and these are all to be found in the tables referred to above. However, as Ross shows, it is not easy to get satisfactory values for integrals involving the kinetic energy operator T°_ν when analytic Slater atomic orbitals are used, even when these are in properly orthogonalized form. Here we did not explicitly evaluate the kinetic energy integrals, but took the kinetic energies of $2s$- and $2p$-electrons to be equal in Slater AOs. Such an assumption is merely the most reasonable one to make in the circumstances; it is admitted that a different choice of kinetic energies could alter the final energy levels by some 2- or 3-electron volts. However, it enabled immediate comparison to be made with the results of Ross for the linear molecule; and since in this comparison only differences in energies are involved, there is some cancellation of such errors in the same direction as may be introduced by our assumption.

For each of the four symmetry classes of both *cis*- and *trans*-acetylene the necessary matrix elements were calculated between the ground state and between all excited states which differed in configuration from the ground state in the assignment of either one or two electrons, and which had energies lying, in first approximation, within approximately 50 ev of the ground state. The calculations were pursued in duplicate, by each author, to minimize error. Eight large determinantal equations were obtained, of orders ranging between 10 and 14. The lower roots of these were obtained using a Bendix D-15G digital computer, for which a subroutine for evaluating matrices by diagonalization was available. The computer was programmed to substitute series of possible values for the roots in the equations and evaluate the resultant matrices. Graphical interpolation gave the roots as values where the matrix equalled zero. While mathematically inelegant, this method can be recommended for speed and simplicity.

RESULTS

The calculated energies of the lower electronic states of *cis*- and *trans*-bent acetylene are given in Tables II and III. All values are relative to the energy of the ground $^1\Sigma_g^+$

state of the linear molecule, obtained by recalculation from the figures of Ross.* The energies "no CI" and "CI" are relative to Ross' corresponding 6-electron calculation results. Allowance has been made for the change in nuclear repulsion energy in going from the linear to the bent carbon–carbon nuclear separation.

TABLE II

Calculated energy levels for *trans*-bent acetylene

Symmetry	Configuration	Energy levels	
		No CI	CI
A_u	$(a_g\sigma_g 2sp^2)^2(a_u\pi_u 2p)(b_u 2sp^2)^2(a_g 2sp^2)$	4.77	4.58 ev
A_g	$(a_g\sigma_g 2sp^2)^2(a_u\pi_u 2p)^2(b_u 2sp^2)^2$	4.83	4.65
B_u	$(a_g\sigma_g 2sp^2)^2(a_u\pi_u 2p)^2(b_u 2sp^2)(a_g 2sp^2)$	14.18	6.70
A_g	$(a_g\sigma_g 2sp^2)^2(b_u 2sp^2)^2(a_g 2sp^2)^2$	6.46	8.12
B_g	$(a_g\sigma_g 2sp^2)^2(a_u\pi_u 2p)(b_u 2sp^2)(a_g 2sp^2)^2$	8.31	9.02
A_u	$(a_g\sigma_g 2sp^2)^2(a_u\pi_u 2p)^2(b_u 2sp^2)(b_g\pi_g 2p)$	11.92	10.81
A_g	$(a_g\sigma_g 2sp^2)^2(a_u\pi_u 2p)^2(a_g 2sp^2)^2$	11.48	11.63
B_g	$(a_g\sigma_g 2sp^2)^2(a_u\pi_u 2p)^2(a_g 2sp^2)(b_g\pi_g 2p)$	15.08	14.53
B_u	$(a_g\sigma_g 2sp^2)^2(a_u\pi_u 2p)(b_u 2sp^2)^2(b_g\pi_g 2p)$	16.69	18.78

TABLE III

Calculated energy levels for *cis*-bent acetylene

Symmetry	Configuration	Energy levels	
		No CI	CI
A_1	$(a_1\sigma_g 2sp^2)^2(b_2\pi_u 2p)^2(a_1 2sp^2)^2$	7.33	7.23 ev
B_1	$(a_1\sigma_g 2sp^2)^2(b_2\pi_u 2p)^2(b_1 2sp^2)(a_1 2sp^2)$	16.31	9.39
B_2	$(a_1\sigma_g 2sp^2)^2(b_2\pi_u 2p)(b_1 2sp^2)^2(a_1 2sp^2)$	12.65	10.24
A_2	$(a_1\sigma_g 2sp^2)^2(b_2\pi_u 2p)(b_1 2sp^2)(a_1 2sp^2)^2$	10.67	11.63
A_1	$(a_1\sigma_g 2sp^2)^2(b_1 2sp^2)^2(a_1 2sp^2)^2$	12.80	11.71
A_2	$(a_1\sigma_g 2sp^2)^2(b_2\pi_u 2p)^2(a_1 2sp^2)(a_2\pi_g 2p)$	12.91	14.32
A_1	$(a_1\sigma_g 2sp^2)^2(b_2\pi_u 2p)^2(b_1 2sp^2)^2$	13.85	14.93
B_2	$(a_1\sigma_g 2sp^2)^2(b_2\pi_u 2p)^2(b_1 2sp^2)(a_2\pi_g 2p)$	16.29	15.44
B_1	$(a_1\sigma_g 2sp^2)(b_2\pi_u 2p)^2(b_1 2sp^2)(a_1 2sp^2)^2$	20.87	22.23

In general, the off-diagonal elements in the secular determinants are small compared to the E_l'; consequently, single configurations [2] dominate in most excited states after applying CI, and the simple MO description in the tables for the electronic states can be retained. Extensive configurational mixing does occur in the lowest electronic states of B_1 and B_u symmetry, leading to considerable depression of energy after CI. Here the MO description is not accurate but is retained for convenience.

The treatment only gives approximate energies for higher electronic states of a given symmetry class, but these could be readily calculated from the secular determinants, and some are included in the tables. The results are shown graphically in Fig. 1, which also shows the lower linear state energy levels calculated by Ross. The left-hand side shows the levels before, and the right-hand side after, CI is applied.

Experimentally, the lowest energy transition observed in absorption for gaseous acetylene is that mentioned in the Introduction, a (^1A_u–$^1\Sigma_g^+$) transition at 5.24 ev (3, 4). The calculated energy of 4.58 ev compares favorably with this; furthermore, these calculations agree that a ^1A_u *trans*-bent state is the lowest to which transition is allowed from the ground state. The MO description for this ^1A_u state agrees with that predicted by

**We thank Dr. Ross for correspondence about this.*

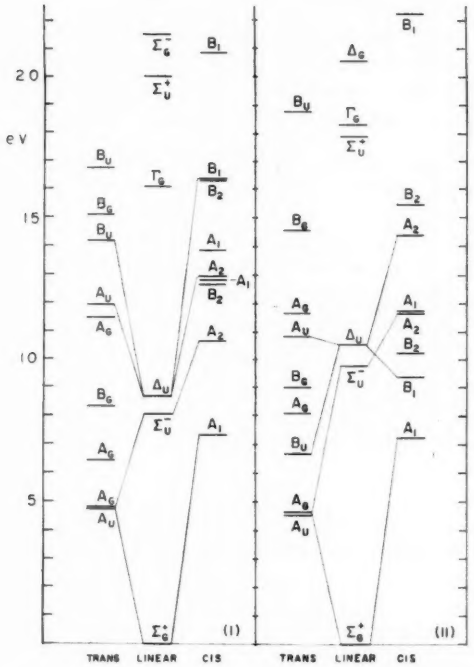

FIG. 1. Energy levels for bent and linear acetylene (i) before CI, (ii) after CI. Correlations are shown here between the lower energy states.

Ingold and King (3) from general valency arguments, by Walsh (1) from MO correlation diagrams, and by Mulliken (2) from analogy with the electronically similar nitrogen and carbon monoxide molecules. However, Walsh correlates this state with a linear Δ_u state; Fig. 1 shows correlation with a linear Σ_u^- state, which is lower in energy than Δ_u according to Ross; this order is preferred by Mulliken.

Acetylene exhibits complex absorption in the 2000–1550 Å region, which is especially intense and of different appearance below 1725 Å (15), indicating the presence of an additional electronic transition here. The bands in this region have not been analyzed: however, Wilkinson (16) has found that discrete absorption bands in the 1520–1280 Å region can be assigned to two Rydberg transitions and two transitions to excited states called *B* and *C*, both of the latter lying some 9.2 ev above the ground state and being *trans*-bent, their band structure being similar to that for the $(^1A_u - ^1\Sigma_g^+)$ transition mentioned above. There is also some evidence that state *C* is planar and state *B* non-planar.

Electronic transitions from the ground state to planar, *trans*-bent A_u and B_u states are allowed; the former being a perpendicular-type transition, the latter possessing both perpendicular and parallel components. The calculated $(^1B_u - ^1\Sigma_g^+)$ transition energy is 6.70 ev; this would correspond to absorption in the 2000–1550 Å region. Wilkinson, following Mulliken's predictions of a ^1B_u state at 8.6 ev, discusses its identification with his '*B*' state, but finds an insufficiency of parallel bands in the spectrum to justify this assignment. We suggest that the $(^1B_u - ^1\Sigma_g^+)$ transition is responsible for the strong

absorption around 1725 Å, and that much of the absorption around 2000–1800 Å is due to the tail of the lowest (^1A_u–$^1\Sigma_g^+$) transition, which, on Franck–Condon grounds, has an intensity maximum in this region. It is possible that Wilkinson's state *B* may correlate with some planar state which cannot formally combine with the ground state, such as the A_g state at 8.1 ev; when this is bent out of plane (coming under symmetry class '*A*' of the C_2 point group) it can combine with the ground state in a perpendicular-type transition. However, the observed high absorption coefficient does mitigate this possibility. The lowest allowed transition to a *cis*-state is calculated to be ($^1B_1$–$^1\Sigma_g^+$)* at 9.4 ev, and although it must be remembered that this figure does not necessarily correspond to the electronic origin of a transition, it is rather high to be used to explain the 2000–1550 Å absorption as due to transition to a *cis*-state.

ACKNOWLEDGMENTS

We are most grateful to Professor D. P. Craig of University College, London, for helpful correspondence on this problem. We are also indebted to the National Research Council for financial support.

REFERENCES

1. WALSH, A. D. J. Chem. Soc. 2288 (1953).
2. MULLIKEN, R. S. Can. J. Chem. **36**, 10 (1958).
3. INGOLD, C. K. and KING, G. W. J. Chem. Soc. 2708 (1953).
4. INNES, K. K. J. Chem. Phys. **22**, 863 (1954).
5. ROSS, I. G. Trans. Faraday Soc. **48**, 973 (1952).
6. MULLIKEN, R. S. J. chim. phys. **46**, 497 (1949).
7. CRAIG, D. P. Proc. Roy. Soc. A, **200**, 474 (1950).
8. ROOTHAN, C. C. J. Revs. Modern Phys. **23**, 69 (1951).
9. CONDON, E. U. and SHORTLEY, G. H. The theory of atomic spectra. Cambridge University Press, London. 1935.
10. HERZBERG, G. Infrared and Raman spectra of polyatomic molecules. D. Van Nostrand Company, Inc., New York. 1945.
11. KOTANI, M., AYAO, A., EIICHI, I., and TOSAKU, K. Tables of molecular integrals. Maruzen Company, Ltd., Tokyo. 1955.
12. KOPINECK, H. J. Z. Naturforsch. **5a**, 420 (1950); **6a**, 177 (1951).
13. BARNETT, M. P. and COULSON, C. A. Trans. Roy. Soc. A, **243**, 221 (1951).
14. ROOTHAN, C. C. J. J. Chem. Phys. **19**, 1445 (1951).
15. PRICE, W. C. and WALSH, A. D. Trans. Faraday Soc. **41**, 381 (1945).
16. WILKINSON, P. G. J. Mol. Spectroscopy, **2**, 387 (1958).

**See previous footnote about the symmetry species of cis-bent states.*

QUANTITATIVE GAS CHROMATOGRAPHY OF REACTION PRODUCTS FROM THE CATALYTIC OXIDATION OF ETHYLENE[1]

C. H. AMBERG, E. ECHIGOYA,[2] AND D. KULAWIC

ABSTRACT

A simple two-stage gas chromatograph is described which employs only one detector for both effluent streams. It was designed specifically for the routine quantitative analysis of mixtures of ethylene oxide, carbon dioxide, and ethylene in the presence of water vapor and a large excess of air, and for concentrations down to 0.2% by volume of individual components.

INTRODUCTION

The routine quantitative analysis of products from the catalytic oxidation of ethylene is of considerable interest in this laboratory for operations both on the bench and pilot plant scale. It was desirable, in particular, to evolve a method by which both the selectivity of the catalyst and the total conversion of ethylene could be computed exclusively from the analytical data furnished by one gas sample. The indirect titration methods frequently employed for the analysis of ethylene oxide and carbon dioxide (following absorption in Lubatti's reagent and sodium hydroxide, respectively) have disadvantages in that they are not suitable for low gas concentrations and in that two separate gas samples have to be collected. Moreover, information about two components only is thus obtained.

A two-stage gas chromatographic apparatus has been constructed which is able to analyze quantitatively the amounts of ethylene oxide, carbon dioxide, and ethylene in a 10-cc sample of moist air. Analysis on a single column and at invariant temperatures has not proved feasible, chiefly because of the generally high retention time of ethylene oxide and water relative to that of air, carbon dioxide, and ethylene.

EXPERIMENTAL

Apparatus

The apparatus was modelled on that of Simmons and Snyder (1) in which two chromatographic columns could be run alternately in series and in parallel. The flow scheme in the present instance was rearranged so as to enable the effluent from both columns to be detected by one thermal conductivity cell only (see Fig. 1). Column lengths and flow rates were adjusted so that peaks passing through opposite sides of the cell K would not interfere with each other. By reversing the polarity of the bridge output at appropriate times, all recorded peaks were made to point in the same direction.

The columns were made of $\frac{1}{4}$-in. coiled copper tubing. Column 1 was 15 ft long and packed with 32.8 g of *n*-octadecane supported on Celite 545 in the ratio 40:100 w/w. The Celite had been size-graded by flotation as described by James and Martin (2). Celite is to be preferred to firebrick, because it was found to cause less tailing of the ethylene oxide bands. Column 2, 7.5 ft in length, was packed with 27.1 g of 35- to 80-mesh silica gel (Davison No. 12).

Helium was used as the carrier gas at an inlet pressure of 31 p.s.i.g.; it was first led through a silica gel drying column. Both streams were vented to the atmosphere at the rate of 90 cc/min as measured by the soap film method. The accuracy of these measure-

[1]*Manuscript received November 20, 1958.*
Contribution from the Division of Applied Chemistry, National Research Council, Ottawa, Canada.
Issued as N.R.C. No. 5084.
[2]*National Research Council Postdoctorate Fellow 1957–1959.*

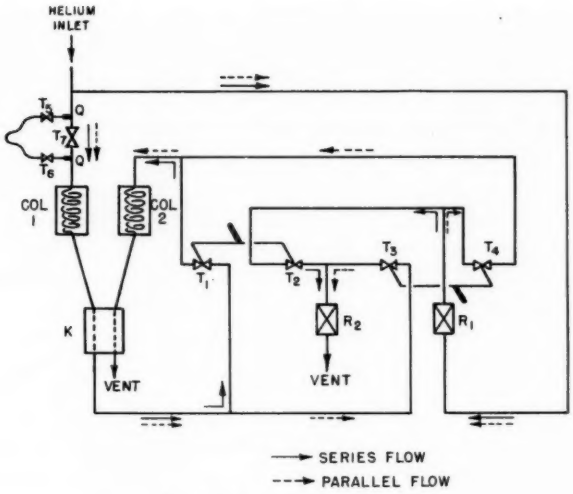

FIG. 1. Schematic flow diagram.

ments was ±0.5%. However, to adjust the dummy flow resistances, needle valves R_1 and R_2 (1), it was found more expedient to employ a Fisher and Porter Flowrator. This resulted in possible 1–2% differences in flow rate between the two streams, still sufficient to give a base line change of no more than 10 μv on changing the flow pattern from series to parallel flow.

A thermal conductivity cell (Gow-Mac Co., Model 9285) served as the detector, K, in conjunction with a recording potentiometer that could be attenuated from 20 mv to 1 mv full scale deflection. A bridge current of 200±0.2 ma was maintained with a 6-v lead storage battery.

The assembly also included Hoke toggle valves T_1 to T_4, which were joined by handles as indicated by the "double pole switches" in Fig. 1. This facilitated the instantaneous change of flow pattern.

Samples were introduced by means of a calibrated 10-cc doser. This consisted of a ¼-in. copper U-tube furnished with toggle valves T_5 and T_6, and a pair of bayonet fittings (Crawford Co., Swagelok), which enabled the doser to be inserted into the gas stream across bypass valve T_7.

The whole unit with the exception of the doser was constructed to fit into a water bath, 1 ft deep by 1 ft in diameter; this was thermoregulated at 30±0.05° C. Figure 2 gives a general view of the apparatus. Temperature and pressure regulating devices are not shown. Additional needle valves, not included in Fig. 1, simply serve to isolate the unit during shutdown. The two glass fittings at the vents on the left can be connected to flowmeters; a Flowrator is shown in position in one of them.

Procedure

To analyze a sample, the doser is evacuated and then flushed with reactor gas. Before insertion, the open ends at T_5 and T_6 must be pumped free of sample, since the calibrated volume is contained between T_5 and T_6. The introduction of an additional volume of air is of no consequence, but the volume of atmospheric carbon dioxide contained therein appears as a positive intercept on the peak height axis of the calibration curve (*v.i.*).

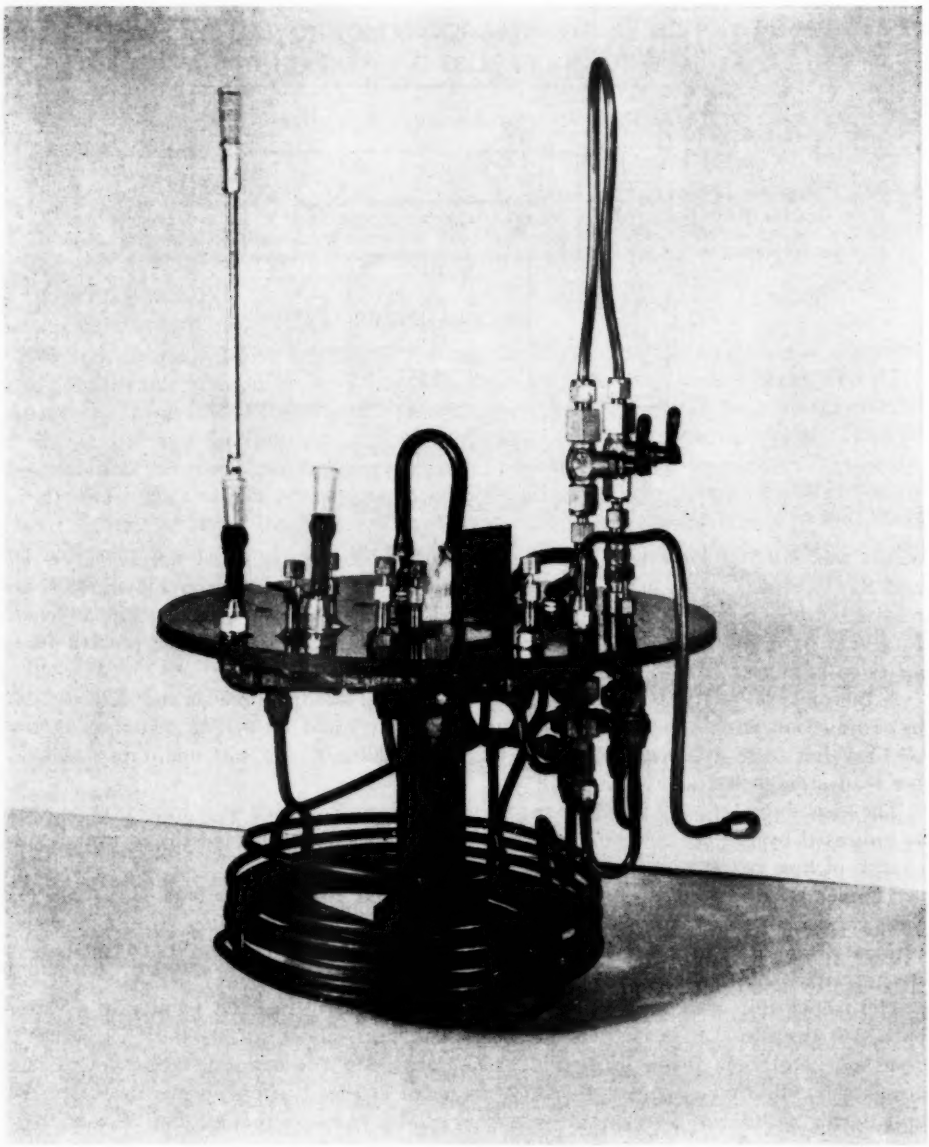

FIG. 2. View of the apparatus.

The sample is introduced with the instrument set for series flow. After 5.5 minutes the flow pattern is switched to parallel flow. At this point ethylene oxide and water are still partitioning in column 1, while carbon dioxide and ethylene are partitioning in column 2, the air having already passed through both columns and out to atmosphere.

Ethylene oxide is now recorded. It is followed by a clearly delineated water front. No

attempt was made to evaluate water quantitatively because of poor and irreproducible peak formation. Both vapors are vented without entering the silica gel column; this is an essential step, since they would otherwise contaminate the gel.

After reversal of the polarity of the bridge output, carbon dioxide and ethylene elute from column 2 and are recorded. Under the conditions indicated it takes 25 minutes to complete a run.

Calibrations

Calibrations were performed with the separate gases by means of four open-ended pipettes ranging from 0.078 to 0.72 cc in volume. These consisted of different lengths of 2-mm steel tubing soldered onto hypodermic syringe needles. They were flushed with the gas to be calibrated, closed at one end with a finger, and inserted into the evacuated doser through a rubber serum cap. Finally, air was allowed to flush the remaining gas into the doser. Corrections to normal pressure and a convenient standard temperature had to be applied.

This relatively simple method has not been used before to our knowledge; we feel, therefore, that its reliability merits discussion in some detail. Table I shows the results of calculating the best straight line by the method of least squares. The precision of the slopes and intercepts was calculated at the 95% confidence level.

TABLE I

Linear calibrations (peak height vs. gas volume)

Gas	Approx. sensitivity, moles/mv $\times 10^6$	Confidence limit,* ±%	Intercept, cc	Confidence limit,* ±cc
C_2H_4O	4	0.4	0.0038	0.0018
CO_2	8	0.8	−0.014	0.0037
C_2H_4	11	0.6	0.0012	0.0027

*At the 95% level.

The two main sources of error during calibration are probably loss by diffusion from the needle during transfer and loss through incomplete transfer into the calibrated part of the doser. The first of these was calculated to be about 0.001 cc/sec, 1 second being the approximate maximum time of transfer. The other factor was of the same order of magnitude or less, as established by separate experiments.

Loss errors of this type to some extent invalidate the use of the method of least squares which is based on random distribution of errors. For this reason the calibration line for ethylene oxide was recalculated using highest values only. This changed the value of the slope by less than one part in 10^4 and reduced the intercept by 0.001 cc, neither change being significant.

It is possible that all calibration lines were slightly curved (3), the degree of curvature being reflected in part by the confidence limits in Table I. For ethylene oxide and ethylene satisfactory results were obtained by assuming linear relationships and by drawing a parallel line through the origin, i.e. assuming the intercepts to be due to calibration losses only. For ethylene, at any rate, a zero intercept fell within the calculated limits.

The curvature of the carbon dioxide line was somewhat more marked. Also, the negative intercept was too large to be accounted for by atmospheric carbon dioxide alone. Hence, a calibration curve was obtained graphically and fitted by a quadratic equation. The resulting intercept of −0.0036 cc agreed closely with blank determinations using atmospheric air. The final curve had to be corrected for the atmospheric carbon

dioxide contained in the calibrated volume of the doser.

Calibrations were frequently checked using one pipette only. After a shutdown, 3–5% drifts in the slopes towards equilibrium values were found over as much as a 2-day period, after which sensitivities remained steady within 1%.

The instrument has been in use for approximately seven months with its original columns, during which time over 1000 runs have been carried out. It was found beneficial to purge the columns every 6–8 weeks at 50–60° C for several hours. Although there is some uncertainty regarding the initial period, no significant deterioration has been observed over the past 5 months. Variations in the final sensitivity value, once stability had been reached after a new start, were found to be about ±3%.

Performance

The best way to evaluate the accuracy of the apparatus was to analyze synthetic mixtures of ethylene oxide, carbon dioxide, and ethylene. A conventional B.E.T. apparatus was used to measure out the gas volumes into a 1-l. calibrated bulb. Air was admitted at atmospheric pressure and the mixture displaced from the bulb by mercury.

Table II shows a series of such tests in the order in which they were carried out. It is believed that deviations here were due to experimental errors in measuring out the gas mixtures at least as much as they were due to fluctuations in the analyzer. This is borne out by the following observations.

(1) Agreement was excellent where only one gas was handled. With increasing experience this was equally true for two gases, but some deviations occurred when three gases were involved.

(2) To exclude any possibility of mutual interference, separate tests were made during calibrations with a pipette. No sign of interference was discovered. Therefore, although no unambiguous standard was available with an accuracy known to be substantially higher than that expected of the analyzer, we estimate an approximate accuracy of ±5%, where the gas concentrations are in the 0.2 to 0.3% region. This will improve to at least ±2% for concentrations of 1% and higher.

TABLE II

Analysis of synthetic mixtures

Calculated from pressure–volume data, % by volume			Gas chromatographic analysis, % by volume		
C_2H_4O	CO_2	C_2H_4	C_2H_4O	CO_2	C_2H_4
0.57	—	—	0.57	—	—
1.20	—	—	1.20	—	—
—	—	2.21	—	—	2.24
1.02	2.17	3.32	1.09	2.17	3.34
0.48	1.52	2.53	0.50	1.46	2.52
0.64	1.24	2.37	0.61	1.28	2.41
0.85	1.33	—	0.84	1.40	—
—	1.20	—	—	1.20	—
1.09	1.20	2.54	1.11	1.20	2.57
0.92	1.15	2.64	0.89	1.20	2.68
—	—	2.41	—	—	2.42
—	—	2.38	—	—	2.38
0.55	0.60	4.55	0.59	0.52	4.57
0.61	0.72	4.87	0.63	0.72	4.97
0.64	0.65	4.93	0.63	0.69	5.02
—	0.30*	—	—	0.30	—
0.31	0.34*	—	0.31	0.35	—
0.36	0.35*	—	0.37	0.37	—

*Atmospheric carbon dioxide removed from air. Correction of 0.035% was applied in all other cases.

Finally, inspection of Table III will give some indication of the precision of the apparatus in the analysis of reactor gas. To make this as unbiased a selection as possible, *all* the results of an arbitrary, continuous 30-day period are given for those cases where more than one analysis had been carried out for a given set of reaction parameters. Each of the nine runs shown was done on the same bench reactor under different conditions. It should be noted that most of the ethylene oxide concentrations in the table are near the lower limit considered practicable for our instrument in its present form.

TABLE III

Analysis of the products from a bench reactor

Run	Interval between samples, hours	% Composition		
		C_2H_4O	CO_2	C_2H_4
A	0	0.26	0.36	4.32
	1	0.26	0.37	4.38
B	0	0.53	0.96	3.82
	2	0.59	1.03	3.71
	2	0.53	0.90	3.87
C	0	0.22	0.32	2.52
	2	0.22	0.34	2.46
	1	0.23	0.33	2.49
D	0	0.17	0.29	2.73
	19	0.16	0.26	2.72
E	0	0.27	0.40	4.42
	2.5	0.26	0.41	4.49
F	0	0.26	0.36	5.60
	1	0.24	0.35	5.56
G	0	0.26	0.46	5.94
	1	0.26	0.44	6.00
	17	0.25	0.39	6.01
H	0	0.25	0.41	4.41
	18	0.24	0.42	4.38
I	0	0.28	0.52	2.50
	18	0.31	0.52	2.56

Again, it is difficult to assign responsibility for the fluctuations in the results. Undoubtedly some are due to variations in reactor conditions, as is suspected, for instance, in run G. At any rate, they allow approximate outside limits of repeatability to be estimated. These limits are at least equal to, and probably somewhat better than, the expected limits of accuracy specified above.

ACKNOWLEDGMENT

The authors wish to thank Mr. W. Thayer for valuable help in the construction of the apparatus and, in particular, for suggesting the use of bayonet fittings for sample introduction.

REFERENCES

1. SIMMONS, M. C. and SNYDER, L. R. Anal. Chem. **30**, 32 (1958).
2. JAMES, A. T. and MARTIN, A. J. P. Biochem. J. **50**, 679 (1951).
3. KEULEMANS, A. I. M., KWANTES, A., and RIJNDERS, G. W. A. Anal. Chim. Acta, **16**, 29 (1957).

THE SURFACE ENERGY OF TOBERMORITE[1]

STEPHEN BRUNAUER, D. L. KANTRO, AND C. H. WEISE

ABSTRACT

The total surface energy (or surface enthalpy) of a calcium silicate hydrate, tobermorite, having the composition of $Ca_5Si_2O_7 \cdot 2H_2O$, was determined at 23.5° C. The tobermorite was obtained from the room-temperature hydration of tricalcium silicate, Ca_3SiO_5, or β-dicalcium silicate, β-Ca_2SiO_4, two of the most important constituents of portland cements. The hydration reactions were carried out in three different ways, and 14 preparations were obtained. For each preparation the heats of solution in a mixture of nitric acid and hydrofluoric acid were measured at 23.5° C, and the surface areas were determined by the B.E.T. method, using water vapor at 25° C as the adsorbate. The cross-sectional area of the adsorbed water molecule was taken to be 11.4 Å^2. The surface energy of tobermorite at 23.5° C was found to be 386±20 ergs/cm^2. It is close to the geometric mean of the surface energies of calcium hydroxide and hydrous amorphous silica, previously reported.

Nitrogen adsorption did not measure the true surface area of most tobermorite preparations. This was indicated by negative surface energy values in a number of instances.

INTRODUCTION

Tricalcium silicate and β-dicalcium silicate are two of the most important constituents of portland cement, together making up about three-fourths of a portland cement by weight. In experiments reported earlier (4, 5, 8) the two silicates were hydrated at room temperature by three methods: (*a*) in a small steel ball mill, (*b*) in paste form, and (*c*) in a polyethylene bottle rotated on a wheel. The stoichiometry of the hydration of β-dicalcium silicate by all three methods was represented by the equation

$$2\beta\text{-}Ca_2SiO_4 + 4H_2O = Ca_5Si_2O_7 \cdot 3H_2O + Ca(OH)_2 \qquad [1]$$

and the stoichiometry of the hydration of tricalcium silicate by methods (*b*) and (*c*) was represented by the equation

$$2Ca_3SiO_5 + 6H_2O = Ca_5Si_2O_7 \cdot 3H_2O + 3Ca(OH)_2. \qquad [2]$$

The same calcium silicate hydrate, tobermorite, was produced in all five cases. Only the ball-mill hydration of tricalcium silicate produced a different calcium silicate hydrate, afwillite (4), which is not discussed in the present paper but will be discussed in a future publication.

Among the three methods of hydration, method (*b*) is of especial importance, because it attempts to simulate the hydration of portland cement in concrete and mortar. In paste hydration, both tricalcium silicate and dicalcium silicate produce tobermorite, and there is ample evidence that in the hydration of portland cements both silicates produce tobermorite. In all probability, the properties of concrete and mortar are determined to a greater extent by the properties of tobermorite than by the properties of any of their other constituents.

Although in the above reactions the calcium silicates were mixed with distilled water, lime saturation was established at an early stage of hydration, after which the reaction proceeded in a saturated calcium hydroxide solution. Under these conditions, the calcium silicate hydrate obtained was the high-lime end member of a series of hydrates designated by Taylor (13) as calcium silicate hydrate (I) or CSH (I). Because of the similarity of this hydrate to the natural mineral tobermorite (12), in the earlier papers (4, 5, 8) it was called tobermorite and, in the absence of general agreement on nomenclature, that

[1]*Manuscript received December 15, 1958.*
Contribution from the Research and Development Laboratories, Portland Cement Association, Skokie, Illinois.

Can. J. Chem. Vol. 37 (1959)

name will be retained here. Bernal (3) proposed the structural formula $Ca_2[SiO_2(OH)_2]_2 \cdot [Ca(OH)_2]$ for this compound.

The natural mineral tobermorite and some of its synthetic varieties are well crystallized substances, but the tobermorite obtained in the room-temperature hydration of tricalcium silicate or β-dicalcium silicate was poorly crystallized, exhibiting only three X-ray diffraction lines (8). The tobermorite was also very finely divided; its specific surface area in the 14 preparations used in the present experiments ranged from 244 to 376 meters^2/g. Because of the colloidal nature of the hydrate, its equilibrium water vapor pressure varied with water content in a continuous rather than stepwise manner. At a vapor pressure of 8×10^{-3} mm of mercury the water content was about 2.8 moles, at 5×10^{-4} mm it was about 2.1 moles per mole of tobermorite.

The method used for the determination of surface energy (or, more strictly, surface enthalpy) was similar to that used for the determination of the surface enthalpies of amorphous silica and hydrous amorphous silica (10); namely, the heat-of-solution method. Heats of solution at three different concentrations, water content, and surface area were measured for each preparation, and the composition was determined by chemical and X-ray analysis. From these data, the heat of solution, water content, and surface area of the tobermorite were calculated. The results were then subjected to a least squares analysis to evaluate the surface energy and other parameters.

EXPERIMENTAL

Materials

The preparation of tricalcium silicate was described in an earlier paper (7), and that of β-dicalcium silicate in another (11). The analyses of the two silicates were given in the latter paper.

Details of the three methods of hydration were also given in earlier papers; one described ball-mill hydration (4), another paste hydration (5), and a third one hydration in the polyethylene bottle (8). All hydrations were carried out in a constant-temperature room, kept at 23.5±0.5° C. The hydration products were dried either at a vapor pressure of 5×10^{-4} mm of mercury (the vapor pressure of ice at −78° C) or at 8×10^{-3} mm of mercury (the equilibrium pressure of $Mg(ClO_4)_2 \cdot 2H_2O$ and $Mg(ClO_4)_2 \cdot 4H_2O$). The methods of drying were described in previous papers (4, 7).

Fourteen preparations (batches) were made, as shown in Table I. C-17 and C-18

TABLE I

Hydration of calcium silicates

Batch designation	Calcium silicate	Method of hydration	Time of hydration	Vapor pressure of drying
C-17	Ca_3SiO_5	Paste	17 months	5×10^{-4}
C-18	Ca_3SiO_5	Paste	17 months	8×10^{-3}
C-23	β-Ca_2SiO_4	Paste	17 months	5×10^{-4}
C-24	β-Ca_2SiO_4	Paste	17 months	8×10^{-3}
D-28	β-Ca_2SiO_4	Ball-mill	46 days	5×10^{-4}
D-35	Ca_3SiO_5	Bottle	47 days	5×10^{-4}
D-40	β-Ca_2SiO_4	Bottle	162 days	5×10^{-4}
D-42	Ca_3SiO_5	Bottle	49 days	5×10^{-4}
D-43	Ca_3SiO_5	Bottle	49 days	8×10^{-3}
D-47	β-Ca_2SiO_4	Ball-mill	63 days	5×10^{-4}
D-49	Ca_3SiO_5	Bottle	49 days	5×10^{-4}
D-50	Ca_3SiO_5	Bottle	49 days	5×10^{-4}
D-51	β-Ca_2SiO_4	Ball-mill	47 days	5×10^{-4}
D-52	β-Ca_2SiO_4	Ball-mill	64 days	5×10^{-4}

were the same paste divided into two parts, one part dried at 5×10^{-4}, the other at 8×10^{-3} mm pressure. The same was true of C-23 and C-24. D-42 and D-43 were also the same preparation; however, when the slurry was divided into two parts, a slight separation of the constituents occurred, as evidenced by chemical analysis.

Each batch was analyzed for calcium oxide, silicon dioxide, aluminum oxide, carbon dioxide, and loss on ignition, with results shown in Table II, columns 2 to 6. The magnesium oxide, sodium oxide, sulphur trioxide, and boric oxide contents were assumed to be the same as in the unhydrated calcium silicates. The methods of analysis used were reported before (7).

TABLE II

Analyses of hydration products* (ignited weight basis)

1 Batch No.	2 CaO	3 SiO_2	4 Al_2O_3	5 Ignition loss	6 CO_2	7 Other analyses
	%	%	%	%	%	
C-17	72.92	25.98	0.07	20.48	0.35	
C-18	72.92	25.98	0.07	23.22	0.50	
C-23	64.45	34.22	0.12	11.54	0.26	30.65% β-Ca_2SiO_4
C-24	64.45	34.22	0.12	13.60	0.32	30.65% β-Ca_2SiO_4
D-28	63.19	33.95	0.15	16.53	0.40	1.01% Fe, 0.06% FeO, 0.41% Fe_2O_3
D-35	72.53	26.41	0.12	19.09	0.14	3.73% Ca_3SiO_5
D-40	64.26	34.48	0.08	11.70	0.40	30.75% β-Ca_2SiO_4
D-42	73.93	25.15	0.09	20.42	0.12	3.06% Ca_3SiO_5
D-43	72.80	26.66	0.10	22.17	0.11	3.06% Ca_3SiO_5
D-47	62.43	33.41	0.11	17.48	0.59	1.93% Fe, 0.05% FeO, 0.03% Fe_2O_3
D-49	71.15	28.11	0.12	18.92	0.26	3.42% Ca_3SiO_5
D-50	72.79	26.02	0.14	19.76	0.14	3.99% Ca_3SiO_5
D-51	62.75	33.36	0.11	16.78	0.37	1.72% Fe, 0.34% FeO, 0.14% Fe_2O_3
D-52	63.22	33.51	0.11	18.10	0.38	1.31% Fe, 0.16% FeO, 0.12% Fe_2O_3

*All Ca_3SiO_5 preparations contained 0.23% MgO and 0.08% Na_2SO_4, and all β-Ca_2SiO_4 preparations 0.22% MgO, 0.06% Na_2SO_4, and 0.53% B_2O_3.

Because in the ball-mill hydration of dicalcium silicate some iron was rubbed off the steel balls, the ball-mill batches were analyzed for free, ferrous, and ferric iron. The method used was a modification of that proposed by Wesly (14). The results are shown in Table II, column 7.

Eight of the batches contained some unhydrated tricalcium silicate or dicalcium silicate. The amounts of these were determined by X-ray quantitative analysis, using magnesium hydroxide as an internal standard, as described before (8). The results are shown in Table II, column 7.

All the analytical results in Table II are given on ignited weight basis; i.e., the sum of the component oxides of the *ignited* batch is taken as 100%. The composition of each batch was calculated, with the results shown in Table III. The excess water, given in column 6, is the water in the tobermorite in excess of two molecules per molecule. Thus, the composition of the tobermorite in C-17 was $Ca_3Si_2O_7.2.08H_2O$, in C-18 it was $Ca_3Si_2O_7.2.79H_2O$.

Measurements

The method of determination of the heats of solution was described before (10, 11). Three sample weights were used: approximately 0.7, 1.0, and 1.3 g. The calorimeter acid was a mixture of 8 ml of 49.4% hydrofluoric acid with sufficient 2 *N* nitric acid added to make the total weight 420 g.

The surface areas were measured by the B.E.T. method (6), using water vapor and

TABLE III

Compositions of the hydration products (ignited weight basis)*

1 Batch No.	2 $Ca_3Al_2O_6 \cdot 6H_2O$	3 $CaCO_3$	4 $Ca(OH)_2$	5 $Ca_3Si_2O_7 \cdot 2H_2O$	6 Excess H_2O
	%	%	%	%	%
C-17	0.27	0.80	47.87	70.67	0.46
C-18	0.27	1.14	47.62	70.67	3.11
C-23	0.45	0.59	14.62	63.91	0.00
C-24	0.45	0.73	14.52	63.91	2.02
D-28	0.56	0.91	19.77	92.07	0.37
D-35	0.45	0.32	44.92	69.14	0.12
D-40	0.29	0.91	13.70	64.52	0.21
D-42	0.34	0.27	49.55	66.08	0.71
D-43	0.38	0.25	45.04	69.89	3.14
D-47	0.41	1.34	19.69	91.39	1.32
D-49	0.45	0.59	39.74	73.73	0.58
D-50	0.52	0.32	45.90	67.96	0.66
D-51	0.41	0.84	20.49	90.80	0.70
D-52	0.41	0.86	20.82	91.20	1.89

*The composition of each batch also includes the data of Table II, column 7, which were not repeated in this table. However, Fe_2O_3 is in the form of $Fe_2O_3 \cdot H_2O$ under the drying conditions employed. In addition, all Ca_3SiO_5 preparations contained 0.33% $Mg(OH)_2$ and 0.08% Na_2SO_4, and all β-Ca_2SiO_4 preparations 0.32% $Mg(OH)_2$, 0.06% Na_2SO_4, and 0.94% H_3BO_3.

nitrogen as adsorbates. Water vapor adsorption was measured gravimetrically at 25° C and nitrogen adsorption volumetrically at −195.8° C.

RESULTS

The heats of solution of the seven batches of hydrated tricalcium silicate are given in Table IV, and those of the seven batches of hydrated β-dicalcium silicate in Table V. From each heat value, the heat of solution of tobermorite was calculated by correcting for the heats of solution of the other substances present in the batch. The heats of solution of tricalcium aluminate hexahydrate, calcium carbonate, magnesium hydroxide, and boric acid were given in an earlier paper (7), and those of tricalcium silicate, β-dicalcium silicate, and sodium sulphate in another (11). The heats of solution of free iron, ferrous oxide, and ferric oxide monohydrate in the nitric acid – hydrofluoric acid mixture were found to be 1450, 360, and 255 cal/g, respectively. The 1.0- and 1.3-g samples of ball-mill hydrated β-dicalcium silicate usually contained some undissolved ferric oxide at the end of the calorimetric runs. Appropriate corrections were made for this in the calculations.

The heats of solution of 0.2, 0.3, 0.4, 0.5, 0.7, and 0.9 g of calcium hydroxide in the acid mixture were found to be 439.1, 437.3, 435.6, 435.6, 441.3, and 447.3 cal/g, respectively. Each value is the average of four to seven determinations. The results can be represented by two intersecting straight lines. The increase in heat of solution at higher concentrations is caused by the precipitation of calcium fluoride (11).

In the calculation of the heat of solution of tobermorite, it was assumed that the heats of solution of the constituents of the hydration products were additive. The correction for the deviation from additivity will be discussed later.

The specific surface areas of the 14 batches of hydration products are shown in Table VI. The adsorption area of a nitrogen molecule was taken to be 16.2 Å^2, and that of a water molecule 11.4 Å^2. The reasons for adopting the latter value were given in an earlier paper (8). Only the areas obtained by water vapor adsorption were used, for reasons to be discussed later.

TABLE IV

Heats of solution of tricalcium silicate hydration products

Weight, g	Heat of solution, cal/g	Weight, g	Heat of solution, cal/g	Weight, g	Heat of solution, cal/g
C-17		D-35			
0.6812	461.07	0.7113	474.21	1.2916	450.91
0.7101	459.49	0.7162	475.53	1.2972	449.57
0.7513	461.59			1.3052	452.75
		1.0109	473.89	1.3118	451.55
1.0226	460.66	1.0178	476.01	D-49	
1.0274	459.65	1.0270	474.74	0.7022	476.93
1.0299	460.10			0.7034	472.10
		1.3350	476.04	0.7072	476.11
1.3069	461.21	1.3556	475.93	0.7102	473.44
1.3285	461.90	D-42		0.7209	475.88
C-18		0.6862	470.44		
0.6950	445.87	0.6950	466.06	0.9852	475.28
0.6980	446.54	0.7354	466.27	1.0090	473.21
0.7042	443.72			1.0136	474.08
0.7236	443.90	0.9952	468.20	1.0502	472.92
0.7258	436.84	1.0024	469.45		
0.7366	440.86	1.0478	466.93	1.3000	473.51
				1.3016	473.29
1.0086	442.60	1.3008	467.55	1.3086	473.82
1.0118	440.93	1.3152	467.32	1.3162	473.05
1.0232	441.88	1.3264	468.16	D-50	
1.0294	442.53	D-43		0.6958	470.26
1.0358	441.65	0.6844	449.97	0.7055	470.36
		0.6950	449.67	0.7166	469.70
1.2834	443.49	0.7258	447.93		
1.2966	440.88	0.7427	451.86	0.9960	470.01
1.3052	442.78			0.9986	469.85
1.3332	441.92	0.9920	449.46	1.0013	470.62
1.3369	441.98	0.9980	451.21		
1.3448	440.58	1.0178	450.89	1.3000	470.13
		1.0298	450.48	1.3065	469.47

In the calculation of the specific surface area of tobermorite from the specific surface area of the hydration products, it was assumed that all of the surface resided in tobermorite. The error introduced by this approximation was negligible except possibly for the ball-mill hydrated dicalcium silicate batches. Because of the prolonged grinding, in these batches about 2% of the total surface area was contributed by calcium hydroxide. Nevertheless, no attempt was made to correct the area, for two reasons. In the first place, a reliable determination of the surface area of the calcium hydroxide could not be made (8). In the second place, the slight error introduced by overestimating the tobermorite surface was partly compensated by a simultaneous overestimation of the heat of solution of tobermorite. This was because not only the surface area but also the surface energy of calcium hydroxide was neglected. As will be seen later, the results obtained for the four ball-mill hydrated batches agreed very well with those obtained for the 10 other batches.

DISCUSSION

Analysis of Data

After the heat of solution, the specific surface area, and the water content of the tobermorite in each sample of each batch were calculated, the data were subjected to a least squares analysis, similar to that described in an earlier paper (10). The main

TABLE V

Heats of solution of β-dicalcium silicate hydration products

Weight, g	Heat of solution, cal/g	Weight, g	Heat of solution, cal/g	Weight, g	Heat of solution, cal/g	Weight, g	Heat of solution, cal/g
C-23		1.0158	480.19	1.0070	492.86		
0.6900	497.33	1.1656	477.79	1.0114	491.34	0.9918	475.82
0.6999	497.82			1.0150	493.72	0.9924	479.82
0.7006	497.99	1.2812	478.36	1.0250	491.93	1.0000	477.63
0.7160	495.56	1.2954	478.95			1.0022	476.85
0.7390	497.27	1.3056	480.26	1.3018	492.78	1.0106	475.96
		1.3059	481.86	1.3148	495.30		
0.9996	497.05	1.3072	479.73	1.3244	496.04	1.2984	477.18
1.0164	495.02	D-28		1.3267	493.99	1.3003	477.66
1.0221	495.49	0.6386	475.87	1.3267	494.44	1.3076	481.11
1.0291	494.94	0.6752	475.21	D-47		1.3204	476.12
1.0371	494.95	0.8326	475.00	0.6976	472.36	D-52	
		0.9648	474.83	0.6994	474.22	0.7004	465.63
1.3152	496.05			0.7166	474.36	0.7054	464.64
1.3216	495.55	1.3136	474.77			0.7134	465.10
1.3224	495.98	1.4196	475.23	0.9950	469.85	0.7138	461.94
1.3242	497.13	1.5233	473.70	1.0086	470.91		
1.3442	498.84	D-40		1.0128	470.67	0.9996	463.07
C-24		0.6853	498.12			1.0036	463.53
0.6214	479.91	0.7162	495.60	1.2964	469.51	1.0040	464.35
0.6716	479.77	0.7344	493.20	1.3084	470.29	1.0074	463.14
0.7032	480.55	0.7374	491.60	D-51		1.0092	462.73
0.7154	480.92	0.7384	492.00	0.6978	478.31		
0.7158	479.50	0.7531	494.60	0.7012	481.14	1.2994	461.49
				0.7036	477.77	1.3034	461.20
1.0074	479.79	1.0039	494.45	0.7088	479.35	1.3108	461.38
1.0092	478.47	1.0053	490.27	0.7138	480.06	1.3280	460.67

difference was that an additional parameter was used in the present treatment, to correct for the non-additivity of the heats of solution.

In an investigation of the heat of decomposition of tricalcium silicate into β-dicalcium silicate and calcium oxide (11), it was found that the heat of solution of an equimolar mixture of β-dicalcium silicate and calcium oxide in the acid mixture was not equal to the sum of the heats of solution of the two components dissolved individually. A similar non-additivity was expected and found for the heats of solution of tobermorite

TABLE VI

Specific surface areas of hydration products

Batch No.	By water adsorption ($meters^2/g$)	By nitrogen adsorption ($meters^2/g$)
C-17	171.5, 172.7	76.6
C-18	135.7	44.3
C-23	170.8, 172.3	35.8
C-24	134.5	
D-28	220.7, 221.4, 212.7, 210.0	217.4, 222.0
D-35	214.6, 214.6, 220.7, 223.7	119.2, 123.4
D-40	174.9, 176.9, 173.8, 174.6	95.0, 86.1
D-42	191.0, 191.7	85.4
D-43	167.6	
D-47	191.0, 191.7, 188.7, 189.8	144.6
D-49	233.3, 232.9, 227.2, 222.2	
D-50	196.7, 198.6, 202.4, 199.7	
D-51	220.3, 219.2, 224.1, 222.6	
D-52	197.1, 192.0	

and calcium hydroxide. Since a separate determination of this effect would have been extremely laborious, it was evaluated from the data of the present experiments as a parameter in the least squares calculations.

The parameters were evaluated from the experimental data in three different ways. The heats of solution were determined at three sample weights, 0.7, 1.0, and 1.3 g; and in the first evaluation, the data obtained for each weight were treated separately. The three equations employed were of the form

$$[3] \qquad H_{ijk}+w_jh-A_j\epsilon_s-c_jX_k = H_k$$

where H_{ijk} is the heat of solution, in cal/g of $Ca_3Si_2O_7\cdot 2H_2O$, of the ith sample of the jth batch, having weight k;

w_j is the "excess water" content of the jth batch (Table III, column 6) in g/g of $Ca_3Si_2O_7\cdot 2H_2O$;

h is the average heat evolved, in cal/g of water, when $Ca_3Si_2O_7\cdot 2H_2O$ reacts with water to form a tobermorite of higher water content;

A_j is the average specific surface area of the jth batch in meters^2/g of $Ca_3Si_2O_7\cdot 2H_2O$;

ϵ_s is the average surface energy (or surface enthalpy) of $Ca_3Si_2O_7\cdot 2H_2O$ in cal/-meters^2;

c_j is the total calcium oxide in the hydration products in the jth batch, in g/g of $Ca_3Si_2O_7\cdot 2H_2O$;

X_k is the non-additivity correction factor for a sample having weight k, expressed in cal/g of calcium oxide; and

H_k is the heat of solution, in cal/g of $Ca_3Si_2O_7\cdot 2H_2O$, of a sample of weight k, having zero surface and zero excess water.

The term c_jX_k is the correction to the heat of solution of tobermorite, caused by non-additivity of the heats of solution of the hydration products. The value of c_j is approximately 1 for all hydrated tricalcium silicate batches and approximately 2/3 for all hydrated dicalcium silicate batches.

A least squares analysis of the data led to the results shown in Table VII, columns 2 and 3. Actually, three values were obtained for each of the parameters h, ϵ_s, and X (one for each sample weight), and the values given in column 2 are the weighted means of the three values.

TABLE VII

Results of least squares analyses

1	2	3	4	5	6	7
	Individual weight		Five-parameter		Six-parameter	
Parameter	Weighted mean	Standard error	Weighted mean	Standard error	Weighted mean	Standard error
$H_{0.7}$ (cal/g of $Ca_3Si_2O_7\cdot 2H_2O$)	455.5	4.0	453.7	1.2	450.9	1.1
$H_{1.0}$ (cal/g of $Ca_3Si_2O_7\cdot 2H_2O$)	448.7	3.1	446.9	1.1	450.3	1.1
$H_{1.3}$ (cal/g of $Ca_3Si_2O_7\cdot 2H_2O$)	451.0	2.0	452.1	1.2	451.5	1.1
X (cal/g of CaO)	10.6	1.8			11.1	1.2
h (cal/g of H_2O)	420.4	14.9	419.0	9.7	422.2	9.9
ϵ_s (cal/meters^2)	0.0927	0.0072	0.0929	0.0036	0.0914	0.0048
ϵ_s (ergs/cm^2)	388	30	389	15	383	20

The values of X for the 0.7-, 1.0-, and 1.3-g samples were found to be 7.2 ± 4.6, 14.6 ± 3.6, and 9.8 ± 2.4 cal/g of calcium oxide, respectively. In the second evaluation

of the parameters, the heat of solution of tobermorite was recalculated for each sample, using the appropriate values of c and X for correction. The equation then was of the form

[4] $$H'_{ijk}+w_jh-A_j\epsilon_s = H_k$$

where $H'_{ijk} = H_{ijk}-c_jX_k$. All terms in eq. [4] have the same meaning as in eq. [3]. In the second evaluation, the data for all weights were used together. The results for the five parameters are given in Table VII, columns 4 and 5.

As the data in the previous paragraph show, the errors in $X_{0.7}$, $X_{1.0}$, and $X_{1.3}$ are so large that, actually, the three parameters may be equal. In the third evaluation it was assumed that the parameter X was the same for all three weights. The equation used was of the form of eq. [3]; the data for all weights were used together, and six parameters were calculated. The results are shown in Table VII, columns 6 and 7.

The values of the parameters, and even of the standard errors, obtained in the five- and six-parameter calculations are very close to each other. There is little to choose between them; consequently, the mean value estimates are probably as good as any that can be obtained from the present data.

The Surface Energy of Tobermorite

1. The surface energy of tobermorite obtained in the room temperature hydration of tricalcium silicate or β-dicalcium silicate and having a composition of $Ca_3Si_2O_7\cdot 2H_2O$ is 386 ± 20 ergs/cm² at 23.5° C. The qualification in this statement as to the source of tobermorite is probably essential. It was stated in the Introduction that the tobermorite obtained in the room-temperature hydration of the two calcium silicates was a poorly crystallized substance exhibiting only three X-ray diffraction lines. Better crystallized tobermorites of the same composition can be prepared in a variety of ways, and their surface energies may be different from the value reported here.

The surface energy value of 386 ergs/cm² is intermediate between the surface energies of calcium hydroxide and hydrous amorphous silica (silanol), 1180 and 129 ergs/cm², respectively (9, 10). This was expected, for two reasons: the calcium silicate hydrate is chemically intermediate between calcium hydroxide and hydrous silica, and it is also intermediate structurally. The calcium hydroxide consisted of nearly perfect crystals (9), the hydrous silica was completely amorphous (10), and the tobermorite was very poorly crystallized. Actually, the surface energy of tobermorite is very close to the geometric mean of the surface energies of calcium hydroxide and hydrous amorphous silica.

The standard error of 20 ergs/cm² is an estimate of the precision of the experimental measurements and not of the accuracy of the surface energy value. The least squares analysis evaluates the random errors but not the systematic errors. For example, if the area of an adsorbed water molecule, 11.4 Å², is in error by 5%, the surface energy value is also in error by 5%, from this factor alone.

2. To present a clearer picture of the consistency of the results, in Fig. 1 the variation of the heat of solution of $Ca_3Si_2O_7\cdot 2H_2O$ with specific surface area is shown for the 1.0-g samples. The average heat of solution of the tobermorite in each preparation was calculated, and the results were corrected (1) for the excess water by using $h = 420$ cal/g of water, and (2) for non-additivity by using $X = 11.1$ cal/g of calcium oxide (Table VII). C-17 and C-18 had the same specific surface area; the arrows in the figure indicate which point belongs to which preparation. The same is true of C-23 and C-24, and D-42 and D-43.

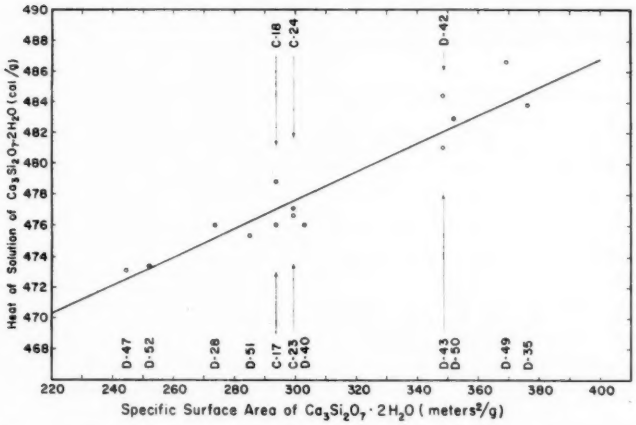

FIG. 1. Variation of the heat of solution of $Ca_3Si_2O_7 \cdot 2H_2O$ with specific surface area for 1.0-g samples.

The straight line drawn in Fig. 1 is a theoretical curve, based on $H_{1.0} = 450$ cal/g of $Ca_3Si_2O_7 \cdot 2H_2O$, and $\epsilon_s = 0.092$ cal/meters². Although the points are scattered, the line appears to be a good representation of the results. Similar data for the 0.7-g samples show somewhat more scatter and those for the 1.3-g samples somewhat less. The point that falls farthest from the straight line is 2.6 cal/g too high (D-49). Such deviations may come about by slight differences in the body structure or somewhat greater differences in surface structure. (The 2.6 cal/g is 0.58% of the heat of solution of the body of tobermorite, and 7.6% of the energy of the surface of the tobermorite in D-49.) However, probably, the real reason is random variation caused by accumulation of the errors in all measurements. This is seen from the results for the pairs C-17 and C-18, and D-42 and D-43. Each of these pairs was a single preparation divided into two parts and dried at different vapor pressures (Table I). As Fig. 1 shows, the difference between the heats of solutions is 2.8 cal/g for the first pair and 3.4 cal/g for the second, the drier preparation giving the lower value for the first pair, and the higher value for the second.

As Fig. 1 shows, only 4 of the 14 preparations had heats of solution deviating from the theoretical value by more than 1.0 cal/g. The average of the absolute values of the deviations is 1.1 cal/g. This corresponds to 0.24% of the heat of solution of the body of tobermorite or to 3.8% of the surface energy. Thus, even if all variation in the heat of solution is ascribed to variation in body structure, or in surface structure, the conclusion is that *both the body structure and the surface structure of tobermorite are highly reproducible.* The different starting materials (tricalcium silicate and β-dicalcium silicate) and the different methods of hydration (ball-mill, paste, bottle) produced a tobermorite of the same body structure and the same surface structure. The method of preparation, however, appears to have an effect on the specific surface area. Tobermorite obtained in ball-mill hydration seems to have the smallest specific surface, and that produced in bottle hydration, the largest.

There is no variation of ϵ_s with specific surface area within the experimental error. Similar result was obtained by Benson and co-workers (1, 2) for sodium chloride. The areas of their samples varied from 1 to 50 meters²/g.

3. The tobermorite formed in the room-temperature hydration of tricalcium silicate

or β-dicalcium silicate has probably three molecules of water of hydration per molecule, rather than two (5, 8). It would be of considerable interest to know the surface energy of $Ca_3Si_2O_7 \cdot 3H_2O$, but the difficulties in its experimental determination would be very great. This is because the binding energies of combined water and adsorbed water overlap. At a water vapor pressure of 8×10^{-3} mm of mercury, tobermorite contains 2.8 moles of water per mole, of which 2.54 moles are combined water and 0.26 moles adsorbed water (8). At a higher vapor pressure, tobermorite would contain more combined water and more adsorbed water.

A rough estimate of the surface energy of $Ca_3Si_2O_7 \cdot 3H_2O$ can be made on the basis of the following considerations. Tobermorite is a layer crystal, like the clay minerals. At a vapor pressure of 5×10^{-4} mm of mercury, it contains two moles of combined water per mole, and the distance between the layers is 9.3 Å. At a vapor pressure of 8×10^{-3} mm the distance between the layers is 10.4 Å, indicating that the third mole of combined water, or at least a part of it, is between the layers. On the other hand, in the surface area determinations water vapor does not penetrate between the layers; it measures the external surface areas of the tobermorite crystallites (8). If *all* of the third mole of combined water were between the layers, the surface energy of $Ca_3Si_2O_7 \cdot 3H_2O$ would be only slightly different from that of $Ca_3Si_2O_7 \cdot 2H_2O$.

The opposite extreme would be if all of the third mole of combined water were on the surface. In earlier work, it was found that the surface energy of calcium hydroxide was 130 ergs/cm² lower than that of calcium oxide (9), and the energy of the surface of hydrous amorphous silica (silanol) was 130 ergs/cm² lower than that of amorphous silica (siloxane) (10). It seems, therefore, reasonable to assume that a mole of combined water on the surface of $Ca_3Si_2O_7 \cdot 2H_2O$ would lower the surface energy by about 130 ergs/cm².

It follows from the above considerations that *the surface energy of tobermorite having a composition of* $Ca_3Si_2O_7 \cdot 3H_2O$ *falls in the range* 320 ± 70 *ergs/cm², and probably it is not far from the upper limit of the range.*

4. The tobermorite crystallites are very thin sheets. The dimensions of the sheets are of the order of several thousand Angstrom units, the thickness is only two or three unit cells (20 to 30 Å). It was shown in an earlier work (8) that the specific surface area can be calculated from crystal structure and density data. If the sheets are all two unit cells thick, the area should be 377 meters²/g, and if they are all three unit cells thick, it should be 251 meters²/g.

On the basis of water vapor adsorption, the specific surface area of the tobermorite in D-47 is 244 and that in D-35 is 376 meters²/g (Fig. 1). All other area values fall between these limits. Thus, the indication from the water adsorption results is that all tobermorite crystallites are two or three unit cells thick; and the indication from the crystallographic data is that water adsorption measures the true surface of tobermorite.

In contrast with this, with one exception (D-28), nitrogen adsorption indicates smaller specific surface areas (Table VI), ranging down to 21% of the area measured by water (C-23). That nitrogen does not measure the true surface of tobermorite can be seen from the following considerations. As Fig. 1 shows, the heat of solution of the tobermorite in D-35 is about 8 cal/g larger than that of the tobermorite in D-28, but the surface area of the former is only about half as large, as measured by nitrogen adsorption (Table VI). This would indicate a *negative* surface energy, an absurdity. Several other pairs of preparations would, likewise, lead to negative surface energy values.

The probable explanation for the low nitrogen areas is that aggregation of the tober-

morite crystallites, or rolling of the sheets, or both together prevent nitrogen molecules from reaching some parts of the surface that are accessible to water molecules.

The Heat of Hydration, h

1. The heat evolved when $Ca_3Si_2O_7 \cdot 2H_2O$ reacts with liquid water at 23.5° C to form a hydrate of higher water content was evaluated from data on preparations ranging in water content from 2.0 to 2.8 moles per mole of tobermorite. It was stated before that of the 2.8 moles, 2.54 moles were chemically combined and 0.26 moles were adsorbed water. The latter value corresponds to a surface coverage of about 18%. The fact that at 8×10^{-3} mm vapor pressure this adsorbed water remains on the surface indicates that the free energy of binding of the 0.26 moles of adsorbed and 0.54 moles of combined water to $Ca_3Si_2O_7 \cdot 2H_2O$ is the same. It seems a fair approximation to assume that the heat of binding is, likewise, the same. Thus, the value of $h = 420$ cal/g of water is probably a good value for the heat of hydration, especially since 11 of the 14 preparations were dried at 5×10^{-4} mm pressure, at which the amount of adsorbed water is negligible.

If it is assumed that the heat of hydration of $Ca_3Si_2O_7 \cdot 2H_2O$ is the same for the uptake of the entire additional mole of water, it follows that

$$Ca_3Si_2O_7 \cdot 2H_2O(c) + H_2O(1) = Ca_3Si_2O_7 \cdot 3H_2O(c), \quad \Delta H_{296.6} = -7600 \text{ cal.} \qquad [5]$$

The value of ΔH was rounded off to the nearest 100 cal. The heat evolved is intermediate between the heat of hydration of calcium oxide to calcium hydroxide, 15,620 cal (9), and the heat of hydration of siloxane to silanol, 4660 cal (10).

2. The heat of solution of $Ca_3Si_2O_7 \cdot 3H_2O$ having zero surface can be calculated from the data of Table VII. For 0.7-, 1.0-, and 1.3-g samples it is 406.4, 402.9, and 405.9 cal/g of $Ca_3Si_2O_7 \cdot 3H_2O$, respectively.

ACKNOWLEDGMENTS

The authors are greatly indebted to Dr. Paul Seligmann for deriving the complicated statistical equations, to Dr. Fred Ordway for valuable discussion of the paper, to Messrs. E. E. Pressler and E. LaBonde for most of the analytical data, and to Miss Edith Turtle for most of the X-ray data.

REFERENCES

1. BENSON, G. C. and BENSON, G. W. Can. J. Chem. **33**, 232 (1955).
2. BENSON, G. C., SCHREIBER, H. P., and VAN ZEGGEREN, F. Can. J. Chem. **34**, 1553 (1956).
3. BERNAL, J. D. Proceedings of the Third International Symposium on the Chemistry of Cement. London. 1952. p. 216.
4. BRUNAUER, S., COPELAND, L. E., and BRAGG, R. H. J. Phys. Chem. **60**, 112 (1956).
5. BRUNAUER, S., COPELAND, L. E., and BRAGG, R. H. J. Phys. Chem. **60**, 116 (1956).
6. BRUNAUER, S., EMMETT, P. H., and TELLER, E. J. Am. Chem. Soc. **60**, 309 (1938).
7. BRUNAUER, S., HAYES, J. C., and HASS, W. E. J. Phys. Chem. **58**, 279 (1954).
8. BRUNAUER, S., KANTRO, D. L., and COPELAND, L. E. J. Am. Chem. Soc. **80**, 761 (1958).
9. BRUNAUER, S., KANTRO, D. L., and WEISE, C. H. Can. J. Chem. **34**, 729 (1956).
10. BRUNAUER, S., KANTRO, D. L., and WEISE, C. H. Can. J. Chem. **34**, 1483 (1956).
11. BRUNAUER, S., KANTRO, D. L., and WEISE, C. H. J. Phys. Chem. **60**, 771 (1956).
12. CLARINGBULL, G. F. and HEY, M. H. Mineral. Mag. **29**, 960 (1952).
13. TAYLOR, H. F. W. J. Chem. Soc. 3682 (1950).
14. WESLY, W. Chemiker-Ztg. **68**, 106 (1944).

THE OXIDATION OF SOME TERMINAL-SUBSTITUTED POLYHYDRIC ALCOHOLS BY ACETOBACTER SUBOXYDANS[1]

L. HOUGH,[2] J. K. N. JONES, AND D. L. MITCHELL

ABSTRACT

Various terminal-substituted pentitols and hexitols, which possessed either the L-*lyxo*- or the D-*ribo*-configuration at the three contiguous carbon atoms adjacent to the terminal carbon atom, were oxidized to ketoses by *Acetobacter suboxydans*. The terminal hydroxyl group of the polyol was replaced by -H, -*O*Me, -*S*Et, and -*O*Ac groups; several 1,1-dithioacetal derivatives of aldoses were also tested. The preparation of 1-*O*-acetyl-DL-galactitol, 1-deoxy-1-*S*-ethyl-D-arabitol, and 6-deoxy-6-*S*-ethyl-L-sorbose are described. 6-Deoxy-6-*S*-ethyl-L-sorbose was prepared by the microbiological oxidation of 1-deoxy-1-*S*-ethyl-D-glucitol.

INTRODUCTION

The oxidation of unsubstituted sugar alcohols by proliferating cells of *Acetobacter suboxydans* has resulted in the formulation of the Bertrand–Hudson rule for oxidations occurring within the pH range of 5–6.5 (1, 2). Thus a polyol with the D-*erythro* configuration (I) is oxidized mainly at the secondary alcohol group adjacent to the terminal primary alcohol to give a ketose (II). Many examples of this reaction have been reported (3, 4, 5, 6, 7, 8). More recently, cell-free extracts have been used for the oxidation of some polyols in an alkaline environment (optimum pH 7.8), although the reaction is less specific since polyols possessing either the L-*threo*- (III) or D-*erythro*- (I) configurations were utilized (9).

Investigation of the microbiological oxidation of various ω-deoxy-sugar alcohols at pH 5–6.5 has shown that ω(*n*)-deoxy-polyols with the D-*erythro* configuration at the carbon atoms (*n*-2) and (*n*-3) (where *n* equals the number of carbons in the chain) (e.g. VI and VII) gave copper reducing products even when the favorable D-*erythro* configuration was absent at the other end of the chain (10, 11). This configuration is present in L-fucitol (6-deoxy-L-galactitol) (IV), which has been shown to be oxidized at carbon 4 to give 1-deoxy-D-*xylo*-3-hexulose (L-fuco-4-ketose) (V). Hudson, Stewart, and Richtmyer reconciled this evidence with the known specificity of the organism by suggesting that the secondary alcohol at carbon 5 of 6-deoxy-L-galactitol (IV), which can be considered as a *C*-methyl derivative of a pentitol, serves at the enzyme surface in a capacity similar to the primary alcohol of an unsubstituted acyclic polyol. We have investigated the specificity of this microbiological oxidation with a view to the preparation of 3-hexuloses and 3-pentuloses.

A limited number of polyols which possess the favorable D-*ribo*- (VI) or L-*lyxo*- (VII) configuration adjacent to a substituent other than hydroxyl at the terminal carbon atom have been tested as substrates for *A. suboxydans* and some gave reducing products. The substituents included a hydrogen atom (ω-deoxy), ω-*O*-methyl, ω-deoxy-ω-*S*-ethyl, and an ω-*O*-acetyl group. All of the unbranched polyols except 1-deoxy-1-*S*-ethyl-L-arabitol were oxidized to reducing products, which unlike the polyols gave bright yellow or orange spots with *p*-anisidine hydrochloride on paper chromatograms. Similar color reactions were reported for 2-*O*-methyl-3-hexuloses (12) and more commonly for 2-hexuloses (13). Although 1-deoxy-L-arabitol (5-deoxy-L-lyxitol) was oxidized by *A. suboxydans*

[1]*Manuscript received December 9, 1958.*
Contribution from the Department of Chemistry, Queen's University, Kingston, Ontario, and the Department of Organic Chemistry, The University, Bristol 8, England.
[2]*Present address: Department of Organic Chemistry, The University, Bristol 8, England.*

(11) to give a reducing product that resulted in a typical ketose reaction with *p*-anisidine hydrochloride, the substitution of a thioethyl group for a hydrogen atom at carbon-1 in this molecule completely inhibited the oxidation. However, in the cases of 6-deoxy-L-galactitol and 6-deoxy-6-*S*-ethyl-L-galactitol, both substrates yielded reducing compounds in moderate yields. Terminal-branched polyols like diethyldithioacetals (aldose mercaptals) were also tested but they did not appear to be oxidized by *A. suboxydans*, thus supporting the observations of Hudson (1) and Iselin (14).

Estimates of the amounts of reducing sugars formed from the oxidation of various substrates by *A. suboxydans* were made by copper-reduction measurements on aliquots taken from the culture medium at various times during incubation. However, this determination was found to be unsatisfactory when the substrate contained sulphur and unexpectedly high reducing values were obtained; ω-deoxy-ω-thioethyl polyols and dithioacetals reduced the copper reagent when tested in control solutions. An approximate reducing value was obtained by subtracting a 'control reducing value' from the reducing value of the medium which was being tested for biochemical oxidation. The reducing values reported by Bollenback and Underkofler for sugar dithioacetals, when they were used as substrates for *A. suboxydans*, were most likely due to the oxidation of the sulphur atom(s) by the copper reagent (11).

The finding that 6-substituted derivatives of L-galactitol, such as 6-deoxy-L-galactitol (L-fucitol), 1,6-dideoxy-L-galactitol (1,6-dideoxy dulcitol (10)), and 6-deoxy-6-*S*-ethyl-L-galactitol were oxidized by *A. suboxydans* prompted an investigation of the preparation and oxidation of similar derivatives. Two possible synthetic routes to 3-hexuloses might use either L-galactose or DL-galactitol (dulcitol) as starting compounds.

Preferential esterification of the primary alcohol group at carbon 6 of D-galactose and D-glucose has been accomplished by Duff (15, 16) using 50% acetic acid at 100° C. Acetylation of DL-galactitol under slightly modified conditions followed by chromatography on charcoal (25) yielded a crystalline monoacetate as the major product. Periodate

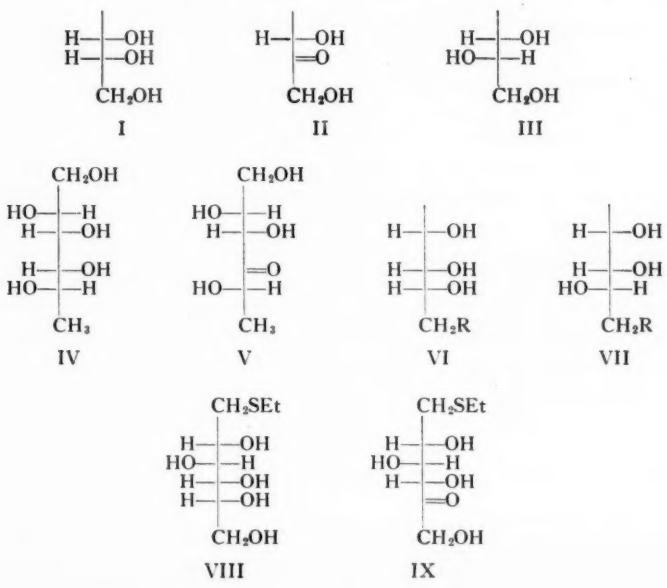

oxidation experiments revealed that esterification had taken place at one of the primary alcohol groups, and the compound was therefore identified as 1-*O*-acetyl-DL-galactitol (6-*O*-acetyl-DL-galactitol). Since only one-half of the DL-galactitol derivative, the D-isomer (i.e. 6-*O*-acetyl-L-galactitol), can be utilized by *A. suboxydans*, a lower copper reducing value would be anticipated from this substrate than from an L-isomer, such as 6-deoxy-L-galactitol, and this has been verified experimentally.

The oxidation product of 1-deoxy-1-*S*-ethyl-D-glucitol (VIII) has been identified conclusively as 6-deoxy-6-*S*-ethyl-L-sorbose (IX), since after conversion to the 2,3-*O*-isopropylidene derivative, reductive desulphurization gave 6-deoxy-L-sorbose which was characterized as the derived phenylosazone.

At the present time, structural studies are in progress on the products formed by oxidation with *A. suboxydans* of 6-deoxy-6-*S*-ethyl-L-galactitol and 1-*O*-acetyl-DL-galactitol. From the known specificity of the microorganism, these products are probably derivatives of 3-hexuloses.

EXPERIMENTAL

Solutions were concentrated under reduced pressure (*ca.* 15 mm). Optical rotations were determined in water at 23°±3° C unless otherwise stated. Paper chromatography was carried out by the descending method (17) on Whatman No. 1 filter paper using the following solvent systems (v:v): (*a*) ethyl acetate – acetic acid – water (9:2:2); (*b*) ethyl acetate – acetic acid – formic acid – water (18:3:1:4); (*c*) butan-1-ol–ethanol–water (40:11:19); and (*d*) butan-1-ol–pyridine–water (10:3:3). Paper electrophoresis was carried out on Whatman No. 3 filter paper impregnated with 0.05 *M* borate buffer (pH 9.2 at 1800 volts for 1.5 hours). Reducing compounds were detected on paper chromatograms and paper electrophoretograms by the *p*-anisidine hydrochloride reagent (13). Non-reducing compounds were detected on paper chromatograms with an alkaline silver nitrate reagent (18) and on paper electrophoretograms by 3% (w:v) lead tetra-acetate in absolute benzene (19). The rate of movement on paper chromatograms is quoted relative to that of rhamnose (R_{Rh} value). On paper electrophoretograms the mobilities are quoted relative to that of D-glucose (M_G value), and are corrected for endosmosis from the rate of movement of tetra-*O*-methyl-D-glucose relative to the D-glucose standard.

Acetobacter suboxydans (A.T.C.C. No. 621) was kindly supplied by Dr. N. K. Richtmyer. The stock culture was grown on agar slopes on a medium consisting of sorbitol (5%, w:v), yeast extract (0.5% w:v),* and potassium dihydrogen phosphate (0.05% w:v) (10). The substituted polyols under examination (Table II) were made up as a broth containing the polyol (1–3%, accurately weighed), yeast extract (0.5% w:v), potassium dihydrogen phosphate (0.05% w:v), and were fortified with sorbitol (0.1% w:v). Control solutions, made up in duplicate, contained the above constituents except the substituted polyol. The solutions (10 ml) in 75-ml conical flasks were autoclaved (15 p.s.i., 20 minutes), cooled to room temperature, and inoculated with a 72 hours' culture of *A. suboxydans* grown on sorbitol (1 drop). The flasks were stored without agitation at 27° C.

At intervals, an aliquot sample (*ca.* 2 ml) was removed from the medium with a sterile pipette and a little examined directly on paper chromatograms and paper electrophoretograms. The remainder (1 ml) was deproteinized and the reducing power estimated using Somogyi's microcopper reagent (20). Solutions of the sulphur-containing polyols

**Difco Laboratories Inc., Detroit, Michigan, U.S.A.*

were made up to identical concentration for copper-reduction estimation. The reducing values of the two control solutions were then subtracted from the reducing value of the medium containing the sulphur-containing polyols under biochemical test. The reducing values are quoted in moles of reducing sugar (calculated as L-sorbose)/100 moles of polyol.

The results are shown in Table II. The 1,1-diethyldithioacetals of D-arabinose, D-glucose, D-galactose, and the 1,1-dibenzyldithioacetal of D-arabinose were not oxidized by *A. suboxydans* as revealed by the copper-reducing power of the culture medium and the absence of any products on paper chromatograms.

Preparation of Substrates

2-Amino-2-deoxy-D-glucitol and 2-acetamido-2-deoxy-D-glucitol were prepared by borohydride-reduction of the respective aldoses according to the method of Bragg and Hough (21). 5-Deoxy-D-ribitol and 5-*O*-methyl-D-ribitol were prepared from D-ribono-1→4-lactone (22). 1-Deoxy-1-*S*-ethyl-polyols were prepared from the corresponding aldose diethyldithioacetals by partial desulphurization with aged Raney nickel (23).

1-Deoxy-1-S-ethyl-D-arabitol

D-Arabinose diethyldithioacetal (3.0 g) was partially desulphurized (23) to yield 57% of product melting at 124–125° C, and with $|\alpha|_D^{28}$ 13°±1° (*c*, 1.1). Anal. Calc. for $C_7H_{16}O_4S$: C, 42.8; H, 8.2; S, 16.3. Found: C, 43.1; H, 8.2; S, 16.7.

1-Deoxy-1-S-ethyl-D-arabitol Tetraacetate

1-Deoxy-1-*S*-ethyl-D-arabitol was acetylated with acetic anhydride in pyridine. The product crystallized when it was poured into a slurry of chipped ice and water, and it was collected by filtration. Recrystallization from aqueous ethanol yielded flakes that melted at 58° C, and with a $|\alpha|_D$ 38°±4° (*c*, 1.3, chloroform). Anal. Calc. for $C_{15}H_{24}O_8S$: C, 49.4; H, 6.6; S, 8.8. Found: C, 49.8; H, 6.8; S, 8.2.

1-O-Acetyl-DL-galactitol (6-O-Acetyl-DL-galactitol, 1-O-Acetyl-dulcitol)

Dulcitol (100 g) was heated under reflux with 50% acetic acid (100 ml) for 36 hours at 80° C (15, 16). Upon cooling, most of the unreacted dulcitol was recovered by filtration and the soluble acetates were obtained as a white residue upon removal of the solvent. Paper chromatographic examination of the residue indicated at least four constituents which had R_{Rh} values of 0.96, 1.23 (major constituent), 1.90, and 2.22 (solvent *a*). The mixture (55 g) was fractionated on a short charcoal column (10×12 cm) of Ultrasorb S.C.* 120–240 (24, 25). Elution was then carried out stepwise with successive fractions (3 liters) of water, and 1.5, 3, 5, 8, 12.5, and 25% ethanol; the major constituent was found in the 8% ethanol fraction. This fraction was filtered, deionized with Amberlite resins (IR-120 (H) and IR-400 (carbonate)) at 5° C, and concentrated to dryness. The product (18 g—low yield due to an accident) after recrystallization from ethanol melted at 131–133° C and possessed a strong adsorption peak in the infrared at ν_{max} 1745 cm^{-1} (nujol). Sorbitol hexaacetate gave an absorption peak at ν_{max} 1748 cm^{-1} and D-glucose diethyldithioacetal possessed a double-peaked adsorption at ν_{max} 1730 and ν_{max} 1750 cm^{-1}. Anal. Calc. for $C_8H_{16}O_7$: C, 42.9; H, 7.2; OAc, 19.2. Found: C, 43.0; H, 7.1; OAc, 19.7.

Structural Determination by Periodate Oxidation Experiments

Oxidations were carried out in the dark at 18° C.

**British Carbo Norit Union Ltd., West Thurrock, Gray's, Essex, England.*

The sample (23 mg) was dissolved in water (21 ml) containing 0.3 *M* sodium metaperiodate solution (4 ml). At intervals, aliquots (2 ml) were withdrawn for either the determination of periodate consumption or the estimation of formic acid liberated (26). Formaldehyde was estimated on aliquots that were diluted 10-fold prior to the estimation (27).

TABLE I

The periodate oxidation of 1-*O*-acetyl-DL-galactitol

Hours	0.08	0.25	0.5	2.25	4.0	28
Periodate uptake*	3.7	3.9	3.9	4.0	4.0	
Formic acid*		2.9		2.8		2.8
Formaldehyde*	0.95		0.95		0.95	

*Moles/mole of 1-*O*-acetyl-DL-galactitol.

*6-Deoxy-6-S-ethyl-*L*-sorbose Phenylosazone*

A culture medium containing 1-deoxy-1-*S*-ethyl-D-glucitol was oxidized for 10 days with *A. suboxydans*. A portion of the solution was deproteinized, deionized with Amberlite resins (IR-120 (H) and IR-4B (OH)), and concentrated to a syrup. The components were separated by paper chromatography (Whatman 3MM) in the usual way (solvent *c*). Some of the syrupy ketose (18 mg) was dissolved in a mixture of phenylhydrazine (0.1 ml), acetic acid (0.1 ml), and water (0.5 ml), and heated in a water bath at 70° C for 3 hours. The phenylosazone (18 mg) was washed first with water, followed by benzene, and was finally recrystallized from aqueous ethanol to give a product melting at 185–190° C. Anal. Calc. for $C_{20}H_{26}N_4O_3S$: C, 59.7; H, 6.5; N, 13.9. Found: C, 59.6; H, 6.5; N, 13.7.

*Reductive Desulphurization to 6-Deoxy-*L*-sorbose (via the O-Isopropylidene Derivative)*

A solution of 6-deoxy-6-*S*-ethyl-L-sorbose (0.20 g) in acetone (20 ml) containing concentrated hydrochloric acid (0.2 ml) was shaken at room temperature for 2.5 hours

TABLE II

Substrates			Products						
			Copper-reducing power (days)						
	R_{RA}[a]	M_G[b]	3	5	6	14	21	R_{RA}[a,d]	M_G[d]
5-Deoxy-D-ribitol	1.2	0.75	81.5[c]	—	91	72	—	1.7 (Y)[f]	0.89
5-Deoxy-L-lyxitol	1.2	0.83	—	—	—	—	—	1.6 (Y)	0.89
6-Deoxy-L-galactitol (L-fucitol)	1.1	0.95	17.6	—	38	—	50	1.3 (Y)	0.80
5-*O*-Methyl-D-ribitol	1.3	0.72	6.7	—	15.4	22.9	24.4	1.8 (Y)	0.81
6-*O*-Acetyl-DL-galactitol	1.2	—	—	26	—	21.8	—	1.6[g](Y)	—
2-Amino-2-deoxy-D-glucitol	—	—	—	6.9	—	6.9	—	Nil	—
2-Acetamido-2-deoxy-D-glucitol	0.82	—	51	—	—	57	—	0.75 (Y)	—
1-Deoxy-1-*S*-ethyl derivative of:									
-D-Glucitol	1.6	—	19	—	87	116	116	2.1 (Y)	—
-L-Arabitol	1.8	0.85	—	—	—	—	—	Nil	—
-D-Arabitol	1.8	0.83	71	—	75	82	92	2.6 (O)[e]	0.84
-D-Galactitol	1.6	0.84	16	—	24	27	31	2.1 (Y)	0.88

[a]Solvent (*b*) detected with silver nitrate – sodium hydroxide reagent.
[b]Detected with lead tetraacetate reagent.
[c]Moles of reducing substance/100 moles of substrate.
[d]Detected with *p*-anisidine hydrochloride reagent.
[e]Orange color with *p*-anisidine hydrochloride (O).
[f]Yellow color with *p*-anisidine hydrochloride (Y).
[g]Detected with resorcinol reagent (13).

followed by neutralization with silver carbonate. The filtrate was concentrated to a syrup which was non-reducing and moved on paper chromatograms at a rate considerably faster than the original ketose. The *O*-isopropylidene derivative (0.12 g) was dissolved in ethanol containing freshly prepared Raney nickel W-2 catalyst (6 ml settled volume) (28) and was heated under reflux for 4 hours. After cooling and filtering free of nickel, a syrup (97 mg) was obtained which had $|\alpha|_D$ 18°±2° (*c*, 1.2, ethanol). (Lit. for 2,3-*O*-isopropylidene-L-sorbose $|\alpha|_D$ 17.9° (29).)

A solution of the syrupy *O*-isopropylidene compound (61 mg) was dissolved in a mixture of phenylhydrazine (0.1 ml), acetic acid (0.1 ml), and water (2 ml), and heated in a water bath at 70° C for 3 hours. The phenylosazone which crystallized from the solution during heating was collected by filtration and washed with cold water followed by ether. Its melting point (175–180° C) was not depressed when admixed with an authentic specimen prepared from 6-deoxy-L-sorbose (30). (Lit. melting point 183–185° C (29) and 168–172° C (9).) The infrared adsorption spectra of the derived and authentic specimens were identical over the frequency range of 600–4000 cm^{-1}.

ACKNOWLEDGMENTS

The authors wish to thank Dr. N. K. Richtmyer of the National Institute of Arthritis and Metabolic Diseases, National Institute of Health, Bethesda, Maryland, for cultures, and Mr. D. J. Anderson for a specimen of sorbitol hexaacetate. One of us (D.L.M.) thanks the Ontario Research Foundation for a scholarship.

REFERENCES

1. Hann, R. M., Tilden, E. B., and Hudson, C. S. J. Am. Chem. Soc. **60**, 1201 (1938).
2. Bertrand, G. Ann. chim. **3** (8), 209, 287 (1904).
3. Whistler, R. L. and Underkofler, L. A. J. Am. Chem. Soc. **60**, 2507 (1938).
4. Bosshard, W. and Richstein, T. Helv. Chim. Acta, **18**, 959 (1935).
5. Stewart, L. C., Richtmyer, N. K., and Hudson, C. S. J. Am. Chem. Soc. **71**, 3532 (1949).
6. Pratt, J. W., Richtmyer, N. K., and Hudson, C. S. J. Am. Chem. Soc. **74**, 2210 (1952).
7. Stewart, L. C., Richtmyer, N. K., and Hudson, C. S. J. Am. Chem. Soc. **74**, 2206 (1952).
8. Pratt, J. W. and Richtmyer, N. K. J. Am. Chem. Soc. **77**, 6326 (1955).
9. Arcus, A. C. and Edson, N. L. Biochem. J. **64**, 385 (1956).
10. Richtmyer, N. K., Stewart, L. C., and Hudson, C. S. J. Am. Chem. Soc. **72**, 4934 (1950).
11. Bollenback, G. N. and Underkofler, L. A. J. Am. Chem. Soc. **72**, 741 (1950).
12. Jones, J. K. N. J. Am. Chem. Soc. **78**, 2855 (1956).
13. Hough, L., Jones, J. K. N., and Wadman, W. H. J. Chem. Soc. 1702 (1950).
14. Iselin, B. J. Biol. Chem. **175**, 997 (1948).
15. Duff, R. B. J. Chem. Soc. 4730 (1957).
16. Duff, R. B. Biochem. J. **70**, 515 (1958).
17. Partridge, S. M. Biochem. J. **42**, 238 (1948).
18. Trevelyan, W. E., Proctor, D. P., and Harrison, J. S. Nature, **166**, 444 (1950).
19. Buchanan, J. G., Dekker, C. A., and Long, A. G. J. Chem. Soc. 3162 (1950).
20. Somogyi, M. J. Biol. Chem. **160**, 61, 69 (1945).
21. Bragg, P. D. and Hough, L. J. Chem. Soc. 4347 (1957).
22. Hough, L., Jones, J. K. N., and Mitchell, D. L. Can. J. Chem. **36**, 1720 (1958).
23. Jones, J. K. N. and Mitchell, D. L. Can. J. Chem. **36**, 206 (1958).
24. Hughes, R. C. and Whelan, W. J. Chem. & Ind. 884 (1958).
25. Andrews, P., Hough, L., and Powell, D. B. Chem. & Ind. 658 (1956).
26. Hough, L., Taylor, T. J., Thomas, G. H. S., and Woods, B. M. J. Chem. Soc. 1212 (1958).
27. O'Dea, J. F. and Gibbons, R. A. Biochem. J. **55**, 580 (1953).
28. Organic syntheses. Vol. 21. John Wiley & Sons, Inc., New York. 1941. p. 15.
29. Müller, H. and Reichstein, T. Helv. Chim. Acta, **21**, 263, 1023 (1938).
30. Hough, L. and Jones, J. K. N. J. Chem. Soc. 4052 (1952).

MYCOCHRYSONE

I. ISOLATION, PROPERTIES, AND PRELIMINARY CHARACTERIZATION[1]

G. READ,[2] P. SHU,[3] L. C. VINING, AND R. H. HASKINS

ABSTRACT

Mycochrysone, an orange-red crystalline pigment, has been isolated from in vitro cultures of an inoperculate discomycetous fungus. It possesses quinonoid properties and forms a monoquinoxaline derivative. At least two phenolic or enolic groups are present, one of which is in the *peri* position to a quinone carbonyl. Reduction of the pigment with a zinc dust – zinc chloride mixture gives perylene, together with some hydroperylenes. The pigment shows limited antibiotic activity.

An inoperculate discomycete, designated PRL 1252, which was isolated from a diseased *Pinus sylvestris* seedling, produces an orange-red pigment when grown in vitro on an agar-solidified nutrient medium. The mold probably cannot be identified accurately until its sexual stage is discovered in nature and the organism, for the present, remains unnamed (9). For this reason it is not possible to follow the customary practice of naming the pigment after the species designation and the name "mycochrysone" has therefore been chosen. Cultures grown on a Difco potato dextrose agar were found to give the best yields of pigment, which appeared as sheaves of bright orange needles in the mycelial exudate and in the surrounding medium.

When pigment yield appeared optimal by visual inspection, the cultures were harvested, freeze-dried, and defatted with petroleum ether. The extract yielded a pale yellow thermolabile oil with an infrared spectrum characteristic of a triglyceride ester. The pigment was extracted from the residue by repeated leaching with chloroform at room temperature in the dark, since in solution it is thermolabile and photosensitive. The extracts, upon careful concentration, gave an orange-red microcrystalline solid in a yield of 4% of the total dry weight of mycelium and agar. Paper chromatographic examination suggested that the pigment contained only a single component. Recrystallization from hot solvents usually resulted in gel formation but analytically pure samples, which decomposed slowly when heated above 180° C, were obtained by concentrating cold chloroform solutions as in the initial extraction. Recrystallization by concentrating cold ethereal solutions frequently gave a dimorphic form as short orange-brown rods which decomposed slowly above 200° C and which could be converted to the orange-red modification by recrystallization from chloroform.

Mycochrysone was found to inhibit the two Gram-positive bacteria *Bacillus subtilis* and *Staphylococcus aureus* but showed no activity against a typical Gram-negative bacterium (*Escherichia coli*), a yeast (*Candida albicans*), or a filamentous fungus (*Penicillium roqueforti*).

Determinations of molecular weight by the Rast method were unsatisfactory owing to decomposition of the pigment, but a value of 370 was obtained by isothermal distillation (4). This was in good agreement with values of 358 and 367 for the reduction equivalent obtained by measuring hydrogen uptake over palladized asbestos. Tests for

[1]*Manuscript received January 2, 1959.*
Contribution from the National Research Council of Canada, Prairie Regional Laboratory, Saskatoon, Saskatchewan.
Issued as N.R.C. No. 5080.
[2]*National Research Council of Canada Postdoctorate Fellow, 1957–1959.*
[3]*Present address: Biochemical Research Section, Lederle Laboratories Division, American Cyanamid Company, Pearl River, New York.*

nitrogen, halogens, and sulphur were negative, and elemental analyses best fitted a formula of $C_{20}H_{14}O_7$. No C- or O-methyl groups were detected; a Zerewitinoff determination corresponded to 2.66 active hydrogens per mole.

In concentrated sulphuric acid, a deep blue solution was formed. Dilution with water precipitated an amorphous dark red solid, distinct from the original pigment, which could not be crystallized and appeared heterogeneous when chromatographed on paper. A similar product was deposited after a few minutes from the orange-red solution given by the pigment in cold concentrated hydrochloric acid, or on warming an alcoholic solution with dilute mineral acid. Since no reducing sugars could be detected after the latter treatment, the pigment is not a simple glycoside. Mycochrysone dissolved readily in aqueous alkali to form a purple solution. It could be recovered unchanged when precipitated with acetic acid after a short interval in sodium bicarbonate but above pH 9 degradation was rapid. Prolonged exposure in solution to even slightly alkaline conditions (pH 7.2) caused extensive decomposition. The product formed was heterogeneous and has not been investigated further.

Solutions of mycochrysone were reduced by sodium hydrosulphite or zinc and dilute acid. The uptake of 1 mole of hydrogen over palladium catalyst was rapid and when the leuco compound so formed was reoxidized by exposure to air, the original pigment was regenerated. The recovery was not quantitative. This readily reversible reduction, together with positive ethylenediamine and indole tests (11), indicates that a quinone group is present. With titanium trichloride a methanolic solution of mycochrysone gave a violet color which faded to a violet-brown; in methanol containing pyridine a red-brown color was obtained after shaking and subsequently a brown precipitate formed. Such reactions are shown by 1,2-quinones and by 1,4-quinones with a hydroxyl group in either the 2-position or *peri* to one of the quinone carbonyls (17). An inconclusive Craven test (7) was obtained, but the purple and brown color with boroacetic anhydride and ferric chloride, respectively, provide evidence for a *peri*-hydroxyl group in the chromophore. The boroacetate derivative could not be isolated, and it appeared to be degraded when allowed to stand in the reaction medium. With methanolic lead acetate the pigment formed a purple precipitate, suggesting that a second, more acidic group is also present. This is supported by the solubility in bicarbonate, a property not associated with chelated *peri*-hydroxyl groups. Although an accurate pK value for this group could not be obtained because of the instability of the pigment in alkali, the pH of a solution in 80% methanol after rapid neutralization with 0.5 moles of alkali was 7.75. Since this would represent a minimum value for the pK_1 of the most acidic hydroxyl, the group is too weakly ionized to be a 2-hydroxy-1,4-quinone but must be activated to some extent. Brockmann and Muxfeldt (3) report a pK of 4.65 and 4.8 for lawsone and despeptidoactinomycin, respectively, in 50% dimethylformamide, while Schwarzenbach and Suter (13) give pK's of 2.73 and 5.18 for 2,5-dihydroxybenzoquinone in water. Under very mild conditions the pigment gave a yellow-brown quinoxaline, $C_{26}H_{18}O_5N_2$, decomposing above 229° C. Considered with the absence of a strongly dissociated acidic group in the molecule the ease with which this reaction occurred suggested that an *o*-quinone, and not a 2-hydroxy group adjacent to a quinonoid carbonyl, was present.

Zinc dust reduction gave only traces of volatile material. Better yields were achieved by fusion with zinc dust in a zinc chloride – sodium chloride eutectic mixture (6). The products were partially separated by chromatography on alumina and the major fraction found to be perylene, obtained in a yield of 13%. A second component with a typical phenanthrene absorption spectrum was shown to be identical with an authentic sample

of hexahydroperylene. This ultraviolet evidence has been used previously by Hua-chih and Conrad-Billroth (10) to show that the hydroperylene has structure I but the fact appears to have been overlooked in more recent publications (5, 19). The remaining component was a volatile oil with an ultraviolet spectrum characteristic of a highly substituted naphthalene. During the preparation of authentic hexahydroperylene considerable amounts of a volatile by-product with very similar spectral properties were obtained. Analyses indicate a formula $C_{20}H_{22}$, and considering its origin there is little doubt that this is a hitherto unreported decahydroperylene. Since the bathochromic displacement of the absorption spectrum is considerably greater than that of a 1,8-disubstituted naphthalene, the compound is assigned the structure II, and it is clear that, contrary to the report of Zinke and Benndorf (18), products intermediate between octa- and tetradeca-hydroperylene are formed. Since these hydroperylenes are readily obtained from perylene by reduction, no significance is attached to their presence in the product from zinc dust fusion of the pigment. Moreover, the formation of perylene by this treatment does not restrict the carbon skeleton of the pigment to that of perylene, for under these conditions derivatives of 1,1′-dinaphthyl would also be expected to give a fully condensed ring hydrocarbon (12, 14). The possibility of naphthalene derivatives dimerizing is more remote, although, under the experimental conditions used, β-naphthoquinone did give a trace of perylene. The absence of an aromatic central ring in a perylene skeleton is suggested by the failure to obtain mellitic acid upon oxidation of the pigment with concentrated nitric acid (8).

On the basis of the above facts, the partial structure III is proposed for mycochrysone. This accommodates all of the carbon atoms and suggests a close structural relationship between the pigment and 4,9-dihydroxyperylene-3,10-quinone, isolated by Anderson and Murray from the fruiting bodies of the fungus *Daldinia concentrica* (1).

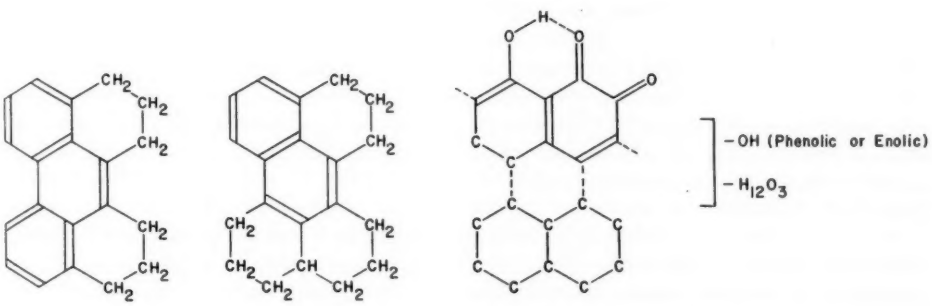

(I) (II) (III)

EXPERIMENTAL

Production

Petri dishes (9 cm diameter) containing potato dextrose agar (Difco) were inoculated at 5 to 8 well-separated points with blocks (*ca.* 0.5 cm cube) of agar and mycelium from 7-day-old cultures. Incubation was carried out for 7 days at 28° C, followed by 14 days at room temperature (20–25° C). Crystals of the pigment appeared among the dark mycelium after 7 to 10 days. On suitable liquid media, in shaken flasks, growth of the organism was more rapid and profuse, but under these conditions no mycochrysone could be detected.

Isolation

The freeze-dried mycelium and agar (143 g) from 160 plates were macerated in a Waring blendor with petroleum ether (1 liter) and the mixture kept for 12 hours at room temperature before filtering. The solvent was then evaporated to give a pale yellow oil (1.7 g) which decomposed on attempted distillation at 90° C at 0.05 mm.

Analar chloroform (3 liters) was added to the residue and the suspension was kept in the dark for 3 days at room temperature. The orange solution was filtered and concentrated to about 700 ml on a rotary evaporator to precipitate the pigment as orange microcrystalline needles. The extraction was repeated and the filtrate was added to the initial concentrate and again evaporated to about 700 ml. After the mixture had been left to stand at 4° C overnight the product (4.27 g) was filtered off and dried (100° C, high vacuum). On treatment of the residual mycelium and agar with a further 6 liters of chloroform in two extractions, as above, an additional 1.48 g of pigment was obtained.

Prepared in this way the pigment gave a single zone (R_f 0.60) when examined by circular chromatography on formamide-treated paper with chloroform as mobile phase. It was considered sufficiently pure for most experiments. After two crystallizations from chloroform by the same technique used in the initial isolation, the pigment decomposed slowly above 180° C. Found: C, 65.31, 65.67, 65.74; H, 3.82, 4.08, 3.68; active hydrogen (Zerewitinoff) 0.72%; no nitrogen, halogen, methoxy, or terminal methyl. Calculated for $C_{20}H_{14}O_7$: C, 65.57; H, 3.85; 3 active hydrogens, 0.82%. Ultraviolet absorption in ethanol λ_{max} 236, 307, and 438 mμ; log ϵ 4.50, 3.62, and 3.78, respectively.

The purified pigment was soluble in methanol, ethanol, and acetone, fairly soluble in benzene, chloroform, ether, and water, but insoluble in petroleum ether or carbon disulphide.

Quinoxaline

o-Phenylenediamine (200 mg) in ethanol (15 ml) was added to a solution of the pigment (100 mg) in hot ethanol (25 ml) and the reactants refluxed for 15 minutes. The quinoxaline separated after a few minutes as brown prisms, decomposing slowly above 223° C. Two recrystallizations from ether gave the product as yellow-brown prisms decomposing slowly above 229° C. Found: C, 71.11; H, 3.87; N, 6.05%. Calculated for $C_{26}H_{18}O_5N_2$: C, 71.22; H, 4.14; N, 6.39%.

Attempts to prepare analytical samples of this derivative from methanolic solutions invariably gave a product with a lower decomposition point (from 210° C). Such samples gave lower values on analysis for C, H, and N, and it is concluded that under these conditions a small amount of oxidative degradation takes place.

When a methanolic solution containing mycochrysone and an excess of *o*-phenylenediamine, or an ethereal solution of the reactants together with anhydrous sodium sulphate, was kept for 12 hours at room temperature (2), it was shown by paper chromatography using formamide-treated paper and benzene as mobile phase that mycochrysone (R_f 0.05) had been completely converted to the quinoxaline (R_f 0.50).

Molecular Weight Determinations

Isothermal distillation in acetone solution at 45° C using cholesterol as a standard gave a value of 370 for the molecular weight. The experiment was carried out in the dark. Microhydrogenations using 5% palladium–asbestos catalyst in ethanol at room temperature and atmospheric pressure showed a rapid uptake of hydrogen corresponding to reduction equivalents of 358 and 367. Under these conditions a further slow reduction took place.

Antibiotic Properties

Activity against bacteria and fungi was tested using the streak-dilution assay (15) on Waksman's glucose-broth supplemented agar (16). A stock solution containing 1 mg/ml of mycochrysone was prepared in 50% aqueous ethanol. Subsequent dilutions were made in sterile distilled water and aliquots of the suspension were mixed immediately with the cooled but still molten agar to give a range of final concentrations. Suspensions of the test organisms were streaked over the surface of the agar plates. *Staphylococcus aureus* v. *pyogenes* (PRL M2), *Bacillus subtilis* (PRL R2), *Escherichia coli* (PRL B44), and *Candida albicans* (ATCC 10231) were incubated at 37° C. Complete suppression of growth was obtained with the *Staphylococcus* at 5 μg/ml and with the *Bacillus* at 15 μg/ml. The remainder of the organisms and *Penicillium roqueforti* (PRL 1763), which was incubated at 28° C, were not inhibited at the highest concentrations tested (100 μg/ml). Controls included in the assay demonstrated that inhibition was not due to solvent toxicity.

Zinc Chloride – Zinc Dust Fusion (Typical Run)

A stirred solution of mycochrysone (49 mg) in acetone (5 ml) and zinc dust (1 g) was evaporated to dryness by an air stream so that a fine precipitate of the pigment adhering to the zinc was obtained.

Zinc dust (3.5 g) was stirred into a melt of zinc chloride (4.0 g) and sodium chloride (0.8 g). On cooling, the mass was broken up, ground into a fine powder, and divided into two equal portions. One was intimately mixed with the pigment-coated zinc and added in equal portions to five small test tubes. The second half of the melt was divided similarly, placed on top of the first layer, and tamped firmly down.

The reactants were heated at 210° C for 4 minutes and subsequently at 310° C for 5 minutes. The froth formed on top of the melts during the heating was dispersed with glass rods. On cooling, the zinc and zinc chloride were dissolved in hot, dilute hydrochloric acid. The aqueous suspension was extracted with benzene (4×100 ml) and the extract evaporated to dryness, redissolved in petroleum ether – benzene (95:5), and chromatographed on a column (7×1.5 cm) of alkaline alumina (Brockmann Grade I). Two fluorescent fractions were collected, the first eluted with petroleum ether – benzene (95:5), and the second with petroleum ether – benzene (50:50). The second fraction was evaporated to dryness and sublimed in high vacuum to give perylene (4.4 mg, 13%), m.p. 272–274° C, undepressed on admixture with an authentic sample. Found: C, 95.44; H, 4.85%. Calc. for $C_{20}H_{12}$: C, 95.21; H, 4.79%.

The first fraction was found to contain a mixture of an oil and a solid. The products from several fusions were combined and sublimed. The solid fraction was separated from the oil by trituration with petroleum ether and purified by a further sublimation (110° C at 0.01 mm). The compound, m.p. 176–182° C (softening at 168° C), gave ultraviolet and infrared spectra indistinguishable from an authentic sample of hexahydroperylene (m.p. 178–184° C), and the melting point on admixing the two compounds showed no depression.

β-Naphthoquinone (50 mg) under the same conditions gave perylene (0.14 mg, 0.35%).

Decahydroperylene

Perylene (100 mg) was reduced in a benzene and alcohol solution with sodium (1 g). The conditions differed from those employed by Zinke and Benndorf (19) only in that the reaction was completed in 45 minutes. Chromatography of the product on a column (8×1.4 cm) of cationotropic alumina (Brockmann Grade I) gave the following fractions:

(*a*) Petroleum ether eluate. Colorless oil (b.p. 110° C at 0.02 mm) (59 mg). Found: C, 91.44; H, 8.39%. Calc. for $C_{20}H_{22}$: C, 91.55; H, 8.45%. Ultraviolet absorption spectrum shows λ_{max} 240, 265, 274, and 299 mμ; log ϵ 4.52, 3.38, 3.41, and 3.40, respectively.

(*b*) Petroleum ether – benzene (98:2) octahydroperylene (8 mg).

(*c*) Petroleum ether – benzene (95:5) hexahydroperylene (7 mg), m.p. 178–184° C.

ACKNOWLEDGMENTS

The authors wish to express their appreciation to Dr. O. Vaartaja, Forest Pathology Laboratory, Canada Department of Agriculture, Saskatoon, Saskatchewan, for the culture of the fungus under study which was received February 12, 1953, and to Dr. W. A. Taber of this laboratory for determining the antimicrobial activity of mycochrysone.

REFERENCES

1. Anderson, J. M. and Murray, J. Chem. & Ind. 376 (1956).
2. Anslow, W. K. and Raistrick, H. Biochem. J. **32**, 687 (1938).
3. Brockmann, H. and Muxfeldt, H. Chem. Ber. **89**, 1379 (1956).
4. Childs, C. E. Anal. Chem. **26**, 1963 (1954).
5. Clar, E. Aromatische Kohlenwasserstoffe. Springer-Verlag. 1952. p. 284.
6. Clar, E. Chem. Ber. **72**, 1645 (1939).
7. Craven, R. J. Chem. Soc. 1605 (1931).
8. Duewell, H., Johnson, A. W., MacDonald, S. F., and Todd, A. R. J. Chem. Soc. 485 (1950).
9. Haskins, R. H., Shu, P., and Vining, L. C. Paper presented before the Botanical and Mycological Societies of America at Storrs, Connecticut. 1956.
10. Hua-chih, C. and Conrad-Billroth, H. Z. physik. Chem. **20**, 333 (1933).
11. Karius, H. and Mapstone, G. E. Chem. & Ind. 266 (1956).
12. Marschalk, C. Bull. soc. chim. [4] **43**, 1388 (1928).
13. Schwarzenbach, G. and Suter, H. Helv. Chim. Acta, **24**, 617 (1941).
14. Thomas, D. G. and Nathan, A. H. J. Am. Chem. Soc. **70**, 331 (1948).
15. Waksman, S. A. and Reilly, H. C. Ind. Eng. Chem., Anal. Ed. **17**, 556 (1945).
16. Waksman, S. A. The actinomycetes. Chronica Botanica Co., Waltham, Mass. 1950. p. 195.
17. Weygand, F. and Csendes, E. Chem. Ber. **85**, 45 (1952).
18. Zinke, A. and Benndorf, O. Monatsh. Chem. **59**, 241 (1932).
19. Zinke, A. and Benndorf, O. Monatsh. Chem. **64**, 87 (1934).

THEORY OF THE TRANSIENT PHASE IN AN ENZYME SYSTEM INVOLVING TWO ENZYME–SUBSTRATE COMPLEXES

THE CASE OF THE FORMATION OF PRODUCTS FROM THE FIRST COMPLEX[1]

LUDOVIC OUELLET[2] AND JAMES A. STEWART[3]

ABSTRACT

A theoretical treatment is worked out for the kinetic scheme

$$E + S \rightleftarrows ES_1 \rightarrow ES_2 + P_1$$
$$ES_2 \rightarrow E + P_2$$

in which the concentration of P_1 is followed. The steady-state and transient phase equations are obtained subject to the condition that the substrate concentration is greatly in excess of the enzyme concentration. The conditions under which evidence in favor of this mechanism can be obtained from experimental data are discussed. Under certain conditions, the weight of the enzyme corresponding to one active site can be determined. Methods for the evaluation of the different constants are described.

INTRODUCTION

The description of the transient phase of an enzyme–substrate system in cases involving one enzyme–substrate complex or two consecutive enzyme–substrate complexes with products appearing as a result of the decomposition of the last complex has been given previously (1, 2). In certain cases, such as the hydrolysis of esters by chymotrypsin (3) or by trypsin (4), there are indications that the release of products involves two steps, one for the release of the alcohol and one for the release of the acid. Following the rate of appearance of the first-appearing product is often possible (if the alcohol is a phenol, for example, and can be determined colorimetrically), and could provide additional useful information on the mechanism of the reaction. The purpose of this paper will be to discuss such a case in more detail than has been done previously (5).

THEORY

Let us consider the system

$$\underset{e_0-y_1-y_2}{E} + \underset{s_0}{S} \underset{k_{-1}}{\overset{k_1}{\rightleftarrows}} \underset{y_1}{ES_1} \xrightarrow{k_2} \underset{y_2}{ES_2} + \underset{p_1}{P_1}.$$

$$\underset{y_2}{ES_2} \xrightarrow{k_3} E + \underset{p_2}{P_2}.$$

In most cases the concentration of the substrate s_0 is much larger than the concentration of the enzyme e_0, so that s_0 can be considered constant during the transient phase. The following differential equations describe the system:

$$[1] \qquad \dot{y}_1 = k_1 s_0(e_0 - y_1 - y_2) - (k_{-1} + k_2)y_1,$$

$$[2] \qquad \dot{y}_2 = k_2 y_1 - k_3 y_2,$$

[1]*Manuscript received August 22, 1958.*
Contribution from the Chemistry Department, the University of Ottawa, Ottawa, Canada.
[2]*Present address: Université Laval, Quebec, Canada.*
[3]*Present address: Laboratories of the Food and Drug Directorate, Department of National Health and Welfare, Ottawa, Canada.*

[3] $$\dot{p}_1 = k_2 y_1,$$

[4] $$\dot{p}_2 = k_3 y_2.$$

Steady State

The steady state equations are obtained by setting $\dot{y}_1$ and $\dot{y}_2$ equal to zero. This leads to

[5] $$\dot{p}_1 = \dot{p}_2 = \frac{k_1 k_2 k_3 e_0 s_0}{k_1 s_0 (k_2+k_3)+k_3(k_{-1}+k_2)}$$

which can be reduced to the following classical form of Michaelis and Menten (6)

[6] $$\dot{p}_1 = \frac{V s_0}{K'_m + s_0}$$

where V, the maximum rate is given by

[7] $$V = \frac{k_2 k_3 e_0}{k_2+k_3}$$

and K'_m, the experimental Michaelis constant is

[8] $$K'_m = \frac{k_3}{k_2+k_3}\,\frac{k_{-1}+k_2}{k_1}.$$

It should be noticed that if $k_3 \gg k_2$, the complex ES_2 exists only in very small amounts and the steady state description of the system is given by

[9] $$V = k_2 e_0$$

[10] $$K'_m = (k_{-1}+k_2)/k_1 = K_m$$

corresponding to the case of a single complex.

Transient Phase

Eliminating y_2 between equations [1] and [2] leads to

[11] $$\ddot{y}_1+(k_1 s_0+k_{-1}+k_2+k_3)\dot{y}_1+[k_1 s_0(k_2+k_3)+k_3(k_{-1}+k_2)]y_1-k_1 k_3 e_0 s_0 = 0,$$

which can be written as

[12] $$\ddot{y}_1+P\dot{y}_1+Qy_1-R = 0.$$

It has been shown previously (2) that the case $P^2-4Q < 0$, leading to periodic solutions, is not particularly interesting because the period is longer than the transient phase. In the cases where $P^2-4Q > 0$, the solution of equation [12] is

[13] $$y_1 = (R/Q)+M e^{Ft}+N e^{Gt}$$

where

[14] $$F = \tfrac{1}{2}[-P+\sqrt{(P^2-4Q)}]$$

[15] $$G = \tfrac{1}{2}[-P-\sqrt{(P^2-4Q)}]$$

and M and N are constants to be determined from the boundary conditions that at time zero, $y_1 = 0$ and $\dot{y}_1 = k_1 e_0 s_0$.

This leads to the following values for M and N

[16] $$M = -(R/Q)\,\frac{k_3 G+Q}{k_3(G-F)},$$

[17] $$N = (R/Q)\frac{k_3F+Q}{k_3(G-F)}.$$

Inserting the value of y_1 into equation [3] and integrating one obtains for the value of p_1 as a function of time

[18] $$p_1 = \frac{k_2Rt}{Q}+\frac{k_2M}{F}(e^{Ft}-1)+\frac{k_2N}{G}(e^{Gt}-1).$$

When t is sufficiently large, so that the terms e^{Ft} and e^{Gt} become negligible (F and G are always negative),

[19] $$p_1 = \frac{k_2Rt}{Q}-\frac{k_2M}{F}-\frac{k_2N}{G}.$$

It is evident that equation [19] is the proper integrated form of equation [5] for an open system in which s_0 is maintained constant.

A qualitative plot of the function represented by equation [18] is shown in Fig. 1. The initial exponential rise is due to the term $(k_2N/G)(e^{Gt}-1)$ of the expression. The approach to steady state, with decreasing rate is due to $(k_2M/F)(e^{Ft}-1)$. The relative magnitudes of these two terms depend on the relative magnitudes of F and G. As all the quantities involved are positive, G will usually be larger than F, and e^{Gt} will approach 0 more rapidly than e^{Ft}, whilst the coefficient of e^{Gt} containing F/G will be smaller than the coefficient of e^{Ft} containing G/F. This condition suggests that the e^{Ft} term will be easier to detect, experimentally, than the e^{Gt} term.

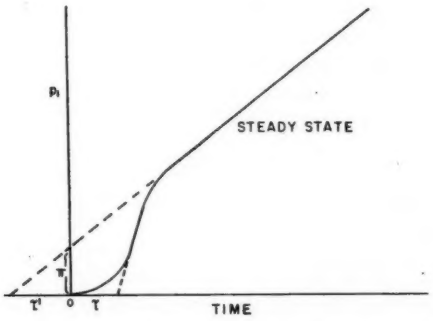

FIG. 1. Schematic plot of amount of product 1 (p_1) against time, in the general case.

The straight line obtained after steady state conditions have prevailed introduces, when extrapolated to the axes, two quantities that can be measured: τ', the intercept on the time axis, and π, the intercept of the p_1 axis.

From equation [19], which describes the steady state condition of the system, τ' can be obtained by making $p_1 = 0$, and solving for t. After substitution of the proper quantities for R, Q, M, N, and F, τ' becomes

[20] $$\tau' = \frac{k_3^2-k_1k_2s_0}{k_1k_3(k_2+k_3)(s_0+K'_m)}.$$

Two extreme cases regarding the relative magnitudes of k_2 and k_3 will be considered. In the first case, if $k_3 \gg k_2$, corresponding to only a fleeting existence of the complex ES_2, equation [20] reduces to

$$\tau' = 1/k_1(s_0+K_m) - k_2 s_0/k_3^2(s_0+K_m). \quad [21]$$

The first part of this expression is identical with that obtained in the case where only one complex is formed (1). The second part could be considered a correction term the magnitude of which depends on the relative magnitudes of $k_1 s_0$, k_2, and k_3.

In the second extreme case where $k_2 \gg k_3$, τ' becomes

$$\tau' = -s_0/k_3(s_0+K'_m) + k_3/k_1 k_2(s_0+K'_m). \quad [22]$$

In the second term of equation [22], k_3/k_2 is small by hypothesis. On the other hand, $1/k_1(s_0+K'_m)$ is usually very small (3). At any rate, it could be measured from the true induction period, τ, if it is not small (see Fig. 1, and equation [37]). In the cases where an induction period cannot be detected, the influence of the second term of equation [22] on τ' is negligible, as it is k_3/k_2 times an undetectably small quantity. Under those conditions, τ' becomes

$$\tau' = -s_0/k_3(s_0+K'_m). \quad [23]$$

If enough data are available to plot $1/\tau'$ against $1/s_0$, the intercept on the $1/\tau'$ axis of the straight line obtained would give $-k_3$. The slope of the straight line obtained is K'_m, the experimental Michaelis constant obtained under steady state conditions. Since a value for $k_3 e_0$ can readily be obtained from the steady state rate of the reaction, under the condition that $k_2 \gg k_3$ (see equation [7]), a value for the concentration of the enzyme e_0 can be calculated, in moles per liter, the units of p_1. In the case of pure enzymes, e_0 can be measured directly in grams per unit volume, and one can calculate the number of grams of enzyme reacting with 1 mole of substrate to form the complex ES_2. This would give the number of active sites per molecule of enzyme if the molecular weight of the enzyme was known from other methods.

Similar information could, of course, be obtained from the intercept on the p_1 axis. According to equation [19] the extrapolated value of p_1 at $t = 0$ is

$$\pi = [k_2^2 e_0 s_0^2/(k_2+k_3)^2(s_0+K'_m)^2] - k_2 k_3^2 e_0 s_0/[k_1(k_2+k_3)^2(s_0+K'_m)^2]. \quad [24]$$

In the case $k_3 \gg k_2$, π could become negative, depending on the relative magnitudes of k_2 and $k_1 s_0$. At best it is small compared to e_0.

In the case, $k_2 \gg k_3$, π becomes

$$\pi = e_0 s_0^2/(s_0+K'_m)^2 - k_3^2 e_0 s_0/k_1 k_2(s_0+K'_m)^2. \quad [25]$$

The second term of this expression becomes negligible unless $k_1 s_0 \ll k_3$, a somewhat improbable situation, as k_1 is usually unmeasurably large. With the condition that $k_2 \gg k_3$, π then reduces to

$$\pi = e_0 s_0^2/(s_0+K'_m)^2. \quad [26]$$

At high concentrations of substrate, compared to K'_m, the ratio $s_0^2/(s_0+K'_m)^2$ becomes practically equal to 1 and

$$\pi = e_0. \quad [27]$$

Hartley and Kilby (7) have reported that the extrapolation of the concentration of *p*-nitrophenol produced during the hydrolysis of *p*-nitrophenol acetate by chymotrypsin to zero time gives the molar concentration of the enzyme. Such an observation could be interpreted as evidence that chymotrypsin has but one active site.

At low concentrations of substrate compared to K'_m, similar considerations lead to somewhat more complex results that will not be discussed.

Equations [24] and [25] indicate that the intercept on the p_1 axis is very small unless k_3 is much smaller than k_2 and $k_1 s_0$. Unless these conditions are fulfilled, equation [18] is hardly of any use as the steady state is approached very rapidly and the influence of the exponential part is very small. For these reasons, a discussion of equation [18] will be limited to the cases where k_2 and $k_1 s_0$ are larger than k_3. Under these conditions

$$P = k_1(s_0+K_m) \quad [28]$$

$$Q = k_1 k_2(s_0+K'_m) \quad [29]$$

where K_m and K'_m are described as

$$K_m = (k_1+k_2)/k_1 \quad [30]$$

$$K'_m = k_3 K_m/k_2. \quad [31]$$

The series development of $\sqrt{(P^2-4Q)}$ leads to

$$F = -\frac{k_2(s_0+K'_m)}{s_0+K_m} - \cdots \quad [32]$$

$$G = -k_1(s_0+K_m)+k_2(s_0+K'_m)/(s_0+K_m) - \cdots \quad [33]$$

A further simplification can be obtained in F and G if experimental conditions are so chosen that s_0 is much larger than K'_m. The conditions $k_2 \gg k_3$ and equation [31] imply that such conditions could be realized and still have s_0 of a magnitude comparable to K_m. This leaves

$$F = -\frac{k_2 s_0}{s_0+K_m} - \cdots \quad [34]$$

$$G = -k_1(s_0+K_m)+k_2 s_0/(s_0+K_m) - \cdots \quad [35]$$

Under these conditions equation [18] becomes

$$p_1 = \pi+k_3 e_0 t+k_2(M/F)\exp[-k_2 s_0/(s_0+K_m)]t + k_2(N/G)\exp[-k_1(s_0+K_m)+k_2 s_0/(s_0+K_m)]t. \quad [36]$$

At the very beginning of the reaction, the second exponential will have a retarding effect on the appearance of the product P_1. Figure 2 is a theoretical plot of p_1 as a function of time according to equation [18]. It is obtained by assuming that $s_0 \gg K_m$ and assigning values of 100, 10, and 1 to $k_1 s_0$, k_2, and k_3 respectively. Under these conditions $F = -11.3$ and $G = -99.8$, which justifies, in part, the assumption that under the present conditions F and G can be approximated to the values given by equations [34] and [35].

The short induction period indicated in Fig. 2 can be calculated by expanding $\exp[(-k_2 s_0/(s_0+K_m)]t$ in series and taking the first two terms only, since t is small at the beginning of the reaction. The extrapolation to $p_1 = 0$ of the curve obtained when $\exp[-k_1(s_0+K_m)]t$ is negligibly small gives

$$\tau = 1/k_1(s_0+K_m). \quad [37]$$

In cases where both a measurable π, interpreted according to equation [25], and a measurable τ, interpreted according to equation [37] appear, values for both k_1 and k_2 can be obtained. Such cases are unknown, as far as we know. In the known cases where the mechanism described here could apply, the induction period is unmeasurably small (3). Such behavior implies that $\exp(Gt)$ is unmeasurably small even at the beginning of the reaction. Under such conditions, equation [35] becomes, assuming $k_2 \gg k_3$,

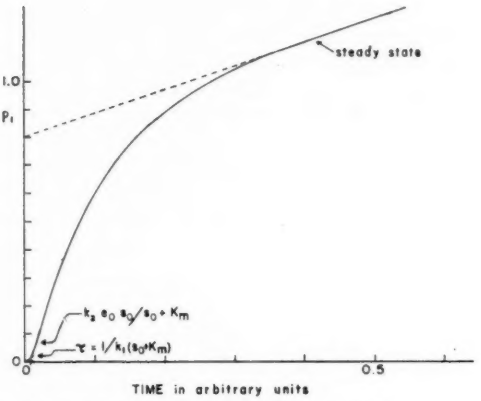

FIG. 2. Theoretical plot of p_1 as a function of time assuming $s_0 \gg K_m$ and $k_1 s_0 = 100$, $k_2 = 10$, $k_3 = 1$ $k_{-1} = 0.1$. The ordinate p_1 is in enzyme concentration units.

[38] $$p_1 = e_0 + k_3 e_0 t - e_0 \exp[-k_2 s_0/(s_0+K_m)]t.$$

If a physical property proportional to p_1 can be measured, k_2 and K_m can be evaluated from the values of $k_2 s_0/(s_0-K_m)$ at different concentrations of substrate, using the Guggenheim technique (8).

At the beginning of the reaction, the series development of the exponential part of equation [38] would give a good approximation of the function. From equation [38], one can then describe the initial rate of production of the first appearing product, P_1, by,

[39] $$p_1 = [k_3 + k_2 s_0/(s_0+K_m)]e_0 t.$$

The smaller k_3 becomes, compared to k_2, the better the approximation. Values for k_2 and K_m can be obtained from initial rate data using the ordinary techniques of enzyme kinetics (9). In so doing, one assumes that the concentration ES_1 is in a steady state right at the beginning of the reaction while the concentration of ES_2 reaches a steady state sometime later.

RÉSUMÉ

Une discussion théorique de la cinétique, dans le cas de réactions enzymatiques, d'une réaction du type

$$E+S \rightleftarrows ES_1 \rightarrow ES_2+P_1$$
$$ES_2 \rightarrow E+P_2$$

est présentée. Différentes situations expérimentales sont analysées en termes des simplifications qu'elles apportent et des renseignements qu'elles donnent sur le système. L'analyse du système permet de justifier la détermination des constantes cinétiques et en certains cas de donner une approximation de la masse de l'enzyme par site actif, si le mécanisme proposé ci-haut est appuyé par des données expérimentales suffisantes.

ACKNOWLEDGMENTS

We wish to acknowledge with thanks the continued financial support from the National

Research Council of Canada. We are indebted to Mr. G. E. Pelletier, who suggested several modifications to the present text.

REFERENCES

1. LAIDLER, K. J. Can. J. Chem. **33**, 1614 (1955).
2. OUELLET, L. and LAIDLER, K. J. Can. J. Chem. **34**, 146 (1956).
3. HARTLEY, B. S. and KILBY, B. A. Biochem. J. **50**, 672 (1952).
4. STEWART, J. A. and OUELLET, L. Can. J. Chem. **37**, 751 (1959).
5. GUTFREUND, H. and STURTEVANT, J. M. Biochem. J. **63**, 656 (1956).
6. MICHAELIS, L. and MENTEN, M. L. Biochem. Z. **49**, 333 (1913).
7. HARTLEY, B. S. and KILBY, B. A. Biochem. J. **65**, 288 (1954).
8. GUGGENHEIM, E. A. Phil. Mag. **2**, 538 (1926).
9. LINEWEAVER, H. and BURK, D. J. Am. Chem. Soc. **56**, 658 (1934).

A STOPPED-FLOW MIXING DEVICE FOR THE SPECTROPHOTOMETRIC STUDY OF RAPID REACTIONS[1]

JAMES A. STEWART[2] AND LUDOVIC OUELLET[3]

ABSTRACT

A simplified stopped-flow mixing device, which has been adapted to a Beckman DU spectrophotometer, is described. Removable storage syringes are used to inject the required solutions into the apparatus, while the operations of filling the reaction syringes, mixing the reactants, or standardization are achieved with T-bore stopcocks. Provision has been made in the design for interchangeable mixing chambers and observation cells. The temperature is controlled by circulating water through a suitable enclosure surrounding the reaction syringes. A zero-suppression method has been devised to record the extent of reaction.

The transient phase kinetics of several enzyme systems has been described from the experimental and theoretical point of view by Chance (1, 2, 3, 4, 5, 6, 7, 8), Beers (9, 10, 11), Gutfreund (12, 13, 14, 15, 16), and Laidler (16, 17). This type of investigation, which provides useful information not obtainable from steady state kinetics, has not been fully utilized probably because of the complex experimental technique. Therefore, this paper will attempt to develop a simplified technique for the study of transient phase kinetics employing the stopped-flow apparatus along the lines of other workers (1, 4, 5, 6, 11, 18, 19, 20, 21).

APPARATUS

A block diagram of the apparatus is shown in Fig. 1. A Beckman Model DU spectro-

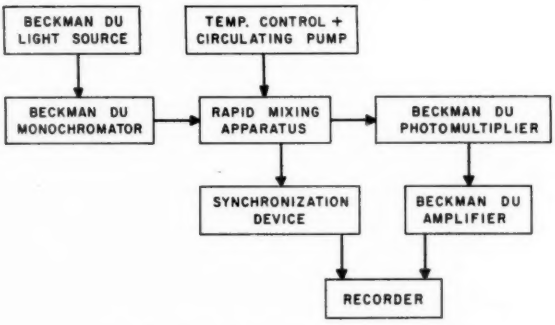

FIG. 1. Block diagram of the apparatus.

photometer equipped with a photomultiplier attachment and recording adapter (#5800) was used. The time constant of the circuit was decreased by altering the load resistance on the photomultiplier cell from 22 meg and 0.01 μf to 0.68 meg and 0.002 μf. The 510-ohm output resistor of the Beckman recording adapter was replaced with a 750-ohm potentiometer, so that the output impedance or sensitivity could be varied.

[1]*Manuscript received August 22, 1958.*
Contribution from the Department of Chemistry, University of Ottawa, Canada.
[2]*Present address: Laboratories of the Food and Drug Directorate, Department of National Health and Welfare, Ottawa, Canada.*
[3]*Present address: Department of Chemistry, Laval University, Quebec, Quebec.*

Stopped-flow Mixing Apparatus

The stopped-flow method was originally conceived by Chance (1) for the rapid mixing of enzyme and substrate. The apparatus to be described is in principle the same, but such features as a plunger-release mechanism, standardization, temperature control, magnetic stopcock at the outlet, the use of rubber "O" ring seals, removable storage syringes, and interchangeable observation tubes and mixing chambers have been added for greater ease in operation and construction.

The details of the apparatus, which is illustrated in Fig. 2, are as follows. The 1-ml

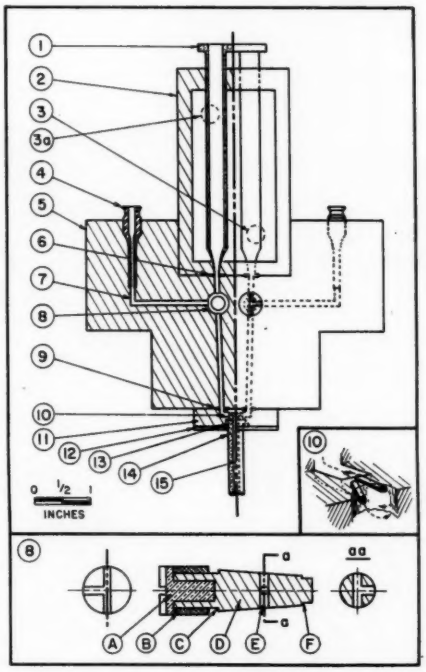

FIG. 2. The stopped-flow mixing apparatus.

reaction syringes "1" are held in the plexiglass enclosure "2" which acts as a constant-temperature bath, fitted with water inlet "3" and outlet "3*A*". The reaction syringes are filled from removable storage syringes located on hypodermic needles "4" embedded in the plexiglass section "5". The lower insert in Fig. 2 gives the details of the T-bore plug of the stopcock "8", which connects the veins "7" from storage syringe to reaction syringe, reaction syringe to mixing chamber, or storage syringe to mixing chamber. The T-slotted head of brass core "*A*" is positioned to coincide with T-bore "*E*" to aid in the alignment of the bore with the veins. An aluminum sleeve "*B*" secures the plexiglass plug "*D*" to brass core "*A*". External leakage of liquid is prevented by rubber "O" ring seals located at "*C*" and "*F*", which are held in position by pressure plates (not illustrated).

A three-dimensional sketch of the mixing chamber "10" is shown in the right-hand insert of Fig. 2. Here, each reactant enters through a pair of 0.5-mm jets that are located

between the tangent and diameter of the chamber and diagonal to each other (19). The mixed reactants pass into the observation cell "15" where the change in absorbance is measured photoelectrically. The present 2-mm observation cell is constructed of plexiglass, but provision has been made in the design for the use of quartz or pyrex observation tubes. These will be sealed in the plexiglass block "11" by a rubber O ring and pressure plate "12".

The plexiglass sections "2", "5", and "11" are fastened together with vertical screws,

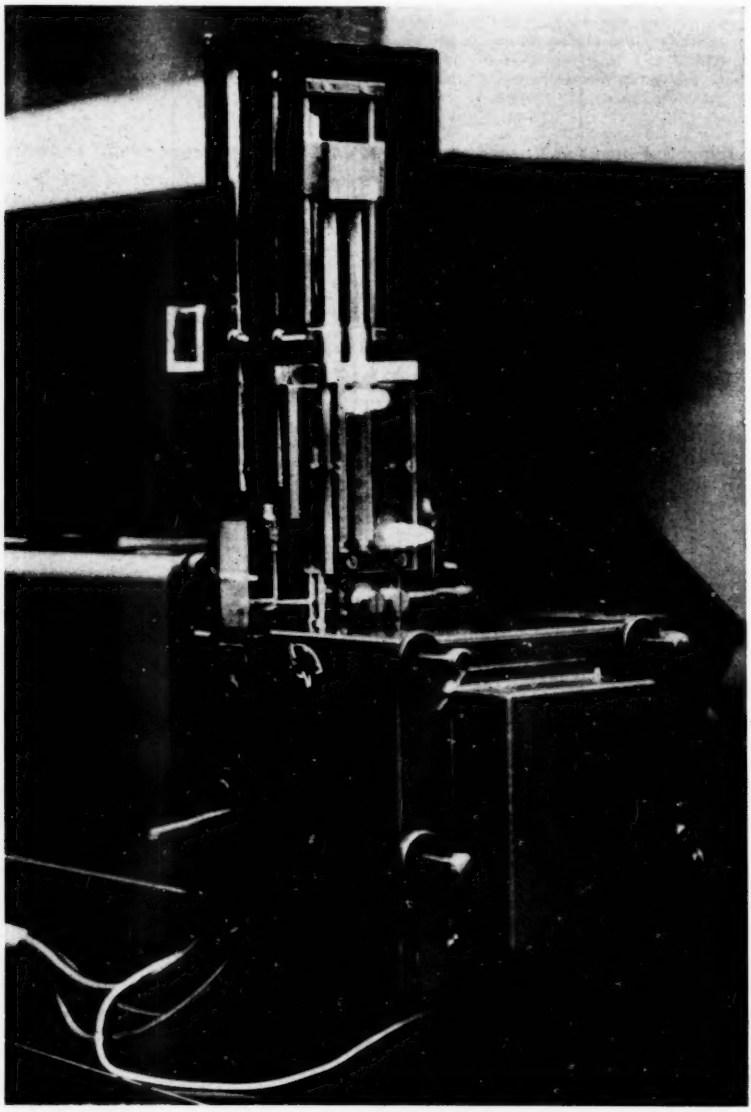

FIG. 3. The stopped-flow apparatus mounted in the Beckman DU.

and external leakage at the joins is prevented by rubber "O" ring seals at "6" and "9". The apparatus is attached to an aluminum plate which replaces the cell compartment of a Beckman DU spectrophotometer as illustrated in Fig. 3. This aluminum plate also supports the plunger and synchronization mechanism.

Plunger Holder and Release Mechanism

Equal portions of two reactants are driven manually from the reaction syringes into the observation cell by the mechanism shown in Fig. 4. A track consisting of two vertical rods carries a brass block that drives the plungers. A plunger-release plate restrains the

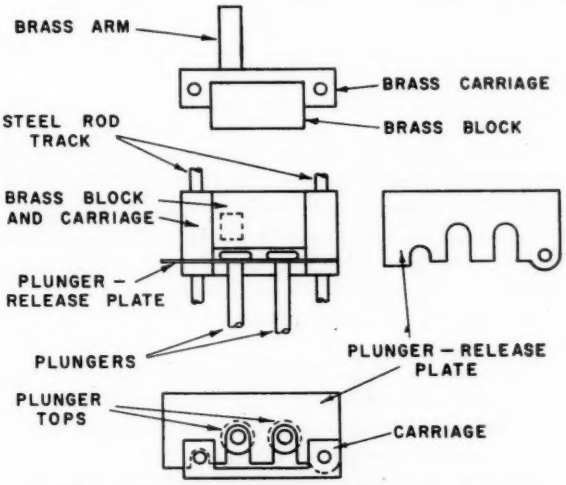

FIG. 4. The plunger holder and release mechanism.

downward motion of the plungers, and is hinged to one side of the track so that the plungers may be freed. This allows the reaction syringes to be filled by pressure from the storage syringes, or the plungers to be removed for the elimination of residual air by completely filling the syringes.

Synchronization Mechanism

The synchronization mechanism in Fig. 5 is used to synchronize the events of stopped

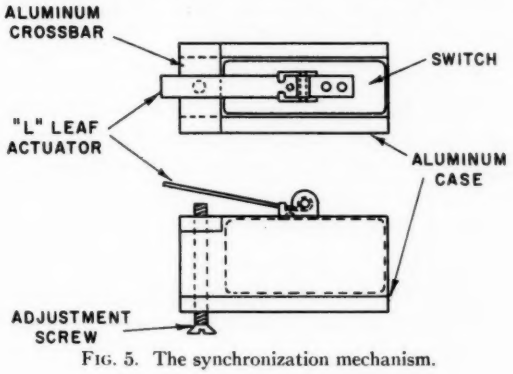

FIG. 5. The synchronization mechanism.

flow and the beginning of recording. This is accomplished by a brass arm on the carriage of the plunger mechanism (Fig. 4), which actuates the "L" leaf of a snap-action switch when it reaches the crossbar of the case surrounding the switch (Fig. 5). Synchronization is adjusted by a screw located in this cross bar.

In the "on" position the switch applies an electrical potential to initiate the sweep circuit of a cathode-ray oscillograph, the chart drive of a pen recorder, or the operation of a time-marker device. In the case where more than one potential is to be synchronized a fast acting four-pole-double-throw relay is incorporated in the circuit.

Temperature Control

Water from a thermostated bath capable of control to $\pm 0.1°$ C is circulated through the enclosure around the reaction syringes, Beckman thermospacers, and the lamp housing of the spectrophotometer.

Recorders

The cathode-ray oscillograph, the pen oscillograph, and the high-speed strip-chart recorder are all suitable for studying rapid reactions, each having its own particular advantage. The cathode-ray oscillograph is useful when a response of <0.01 second is required, while the pen oscillograph could be recommended above this range because of the direct-writing feature. In the case of certain reactions, which have been studied in this laboratory, the high-speed strip-chart recorder with a response of 0.25 second for a 10-inch deflection was found to be sufficient.

MODE OF OPERATION

Reactants kept in a constant temperature bath are transferred to the reaction syringes by means of suitable storage syringes. The reaction is recorded by manually driving the plunger mechanism, which forces the reactants into the mixing chamber and the observation cell. When the flow stops, a synchronized recorder produces the reaction trace.

The following zero suppression method was found to achieve the sensitivity required by the stopped-flow technique (5). With the phototube shutter closed (0% transmittance) the output voltage of the recording adapter is given an arbitrary value (300 mv available) using the suppression and dark current adjustments. The phototube shutter is then opened, and the slit of the monochromator varied until this output is zero. The latter may be chosen to correspond to 100% transmittance or a convenient percentage reaction with an appropriate standard solution in the observation cell. The first procedure is used when the reactants are colorless but the products colored, while the second is adapted to follow the disappearance of colored reactants.

APPLICATION

The apparatus described has been employed in a kinetic study of the enzymatic hydrolysis of *p*-nitrophenyl acetate with trypsin and is the subject of a subsequent paper (22). The stopped-flow method, however, has been used in a similar instance for the study of *p*-nitrophenyl acetate hydrolysis with chymotrypsin (15). Therefore, it was convenient to repeat part of this work as a check on technique.

Hydrolysis of p-Nitrophenyl Acetate with Chymotrypsin

Theoretical.—Measurements of the rate of appearance of *p*-nitrophenol at small values of t have been employed for this chymotrypsin system to evaluate F given in the relationship,

[1] $$P_1 = k'_3\, e_{0t} + e_0\,(1-\exp Ft) \qquad \text{(ref. 23)}$$

where P_1 is the concentration of p-nitrophenol, k'_3 is the apparent rate constant for deacetylation of enzyme, e_0 is the initial concentration of enzyme, t is the time, and $-F$ is the quantity to be determined. If equation [1] is treated as suggested by Guggenheim (24) the result is

[2] $$\log|r_1+r_3-2r_2| = \log \text{constant} + (Ft_1/2.303) \qquad \text{(ref. 15)}$$

where r_1, r_2, and r_3 are readings directly proportional to P_1 taken at the times t_1, $t_1+\Delta t$, and $t_1+2\Delta t$, respectively. Therefore, F can be determined from the slope of a plot of $\log|r_1+r_3-2r_2|$ against t_1.

EXPERIMENTAL

Enzyme.—Twice crystallized chymotrypsin (salt-free) was purchased from the Mann Research Laboratories, Inc., New York.

Substrate.—p-Nitrophenyl acetate was synthesized according to the method of Chattaway (25), and recrystallized from an ethanol–water solution m.p. 78–79°.

Buffers.—The appropriate buffered solutions were prepared from monosodium and disodium phosphate so that the reaction solutions contained 0.05 M phosphate.

Solvent.—To improve the solubility of the substrate 20% (v/v) isopropyl alcohol was used.

RESULTS

Figure 6 gives the Guggenheim plot for the reaction trace in Fig. 7 that was recorded

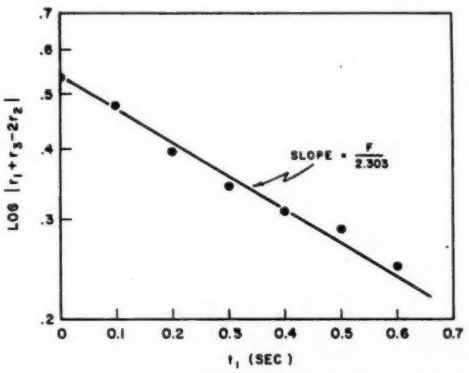

FIG. 6. A Guggenheim plot of the reaction trace for the chymotrypsin–NPA system.

TABLE I

The value of F obtained with different types of recorders for $S_0 = 5\times10^{-3}$ M at pH 7.8 and 25° C

Type of recorder	$-F$
Pen oscillograph (Brush BL201)	1.30 (15)
Pen oscillograph (Brush BL202)	1.33±0.07
Cathode-ray oscillograph (DuMont 403)	1.37±0.12
Strip-chart (Brown, Quarter Second)	1.35±0.08
Mean	1.34
Standard deviation	±0.02

with a high-speed strip-chart recorder. The same reaction was also recorded with a pen oscillograph and cathode-ray oscillograph equipped with a Polaroid Land camera. The values for F obtained from these records are listed in Table I along with the result estimated from the work reported previously. The mean result for a substrate concentration of 5×10^{-3} M and a pH 7.8 at 25° C is 1.34 ± 0.02. This is within the limit of error expected of the stopped-flow method.

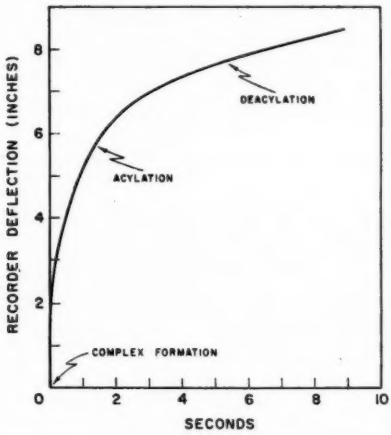

FIG. 7. A typical reaction trace recorded with a Brown "Quarter Second" recorder for 1 mg/ml chymotrypsin and 5×10^{-3} M NPA at pH 7.8.

ACKNOWLEDGMENTS

The authors are indebted to the National Research Council of Canada for a grant in aid of this work. We are grateful to Professor K. J. Laidler for his advice and interest in this research and to Mr. F. Giacobbi, who constructed many parts of the apparatus.

REFERENCES

1. CHANCE, B. J. Franklin Inst. **229**, 455, 613, 737 (1940).
2. CHANCE, B. J. Biol. Chem. **151**, 533 (1943).
3. CHANCE, B. Acta Chem. Scand. **1**, 236 (1947).
4. CHANCE, B. Biochem. J. **46**, 387 (1950).
5. CHANCE, B. Rev. Sci. Instr. **22**, 619 (1951).
6. CHANCE, B. Rapid reactions. *In* A. WEISSBERGER, *Editor*. Technique of organic chemistry. Vol. VIII. Interscience Publishers, Inc., New York. 1953. p. 690.
7. CHANCE, B., GREENSTEIN, D. S., and ROUGHTON, F. J. W. Arch. Biochem. Biophys. **37**, 311 (1952).
8. CHANCE, B. Arch. Biochem. Biophys. **71**, 130 (1957).
9. BEERS, R. F. and SIZER, I. W. J. Phys. Chem. **57**, 290 (1953).
10. BEERS, R. F. J. Phys. Chem. **58**, 197 (1954).
11. BEERS, R. F. Biochem. J. **62**, 492 (1956).
12. ROUGHTON, F. J. W. Discussions Faraday Soc. **17**, 116 (1954).
13. GUTFREUND, H. Discussions Faraday Soc. **20**, 167 (1955).
14. GUTFREUND, H. Trans. Faraday Soc. **51**, 441 (1955).
15. GUTFREUND, H. and STURTEVANT, J. M. Biochem. J. **63**, 656 (1956).
16. LAIDLER, K. J. Can. J. Chem. **33**, 1614 (1955).
17. OUELLET, L. and LAIDLER, K. J. Can. J. Chem. **34**, 146 (1956).
18. HARTRIDGE, H. and ROUGHTON, F. J. W. Proc. Roy. Soc. A, **104**, 376 (1923).
19. ROUGHTON, F. J. W. Rapid reactions. *In* A. WEISSBERGER, *Editor*. Technique of organic chemistry. Vol. VIII. Interscience Publishers, Inc., New York. 1953. p. 669.
20. GIBSON, Q. H. and ROUGHTON, F. J. W. Proc. Roy. Soc. B, **143**, 310 (1955).
21. SIRS, J. A. Trans. Faraday Soc. **54**, 201, 207 (1958).
22. STEWART, J. A. and OUELLET, L. Can. J. Chem. **37**, 751 (1959).
23. OUELLET, L. and STEWART, J. A. Can. J. Chem. **37**, 737 (1959).
24. GUGGENHEIM, E. A. Phil. Mag. **2**, 538 (1926).
25. CHATTAWAY, F. D. J. Chem. Soc. **134**, 2495 (1931).

THE TRYPSIN CATALYZED HYDROLYSIS OF *p*-NITROPHENYL ACETATE[1, 2]

JAMES A. STEWART[3] AND LUDOVIC OUELLET[4]

ABSTRACT

The hydrolysis of *p*-nitrophenyl acetate (NPA) by trypsin has been investigated in the early stage of the reaction using stopped-flow techniques. The influence of pH on the initial rate suggests competitive inhibition of the active site of the enzyme by hydrogen ions. The dissociation constant of the enzyme obtained from the kinetics of this reaction ($pK = 6.9$) indicates possible catalysis by an amino group or an imidazole group of the enzyme. Lysine methyl ester as an analogue of the enzyme catalyzes the hydrolysis of NPA under similar experimental conditions. The results are described in terms of an assumed mechanism and the nature of the catalytic site is discussed.

Hartley and Kilby (1, 2) first reported that the enzyme chymotrypsin was capable of catalyzing the hydrolysis of *p*-nitrophenyl acetate (NPA). From their results they concluded that the mechanism consisted of three distinct stages. The first stage is extremely rapid and concerns the combination of enzyme with substrate, the second stage is moderately rapid and involves the liberation of phenol and the acetylation of the enzyme, while the last stage, which is slow, liberates acetate with the consequent regeneration of enzyme.

Gutfreund and Sturtevant (3), employing stopped-flow techniques, showed that the rate constant for acetylation (second stage) of chymotrypsin with NPA was pH independent. This is contrary to their results for dinitrophenyl acetate (4) and the results of other workers (5) who report pH dependence.

The purpose of our investigation into the mechanism of trypsin catalyzed hydrolysis of NPA is mainly to clarify the problem as to whether or not the rate constant related to acetylation is pH independent, and compare the suggested mechanism with a mechanism recently proposed by Cunningham (6). His scheme, which emphasizes the hydroxyl group of a serine residue as primary site rather than the imidazolyl group of histidine, satisfies the available experimental evidence (7). However, when trypsin (8) or chymotrypsin (9) are treated with DFP^{32} (diisopropyl fluorophosphate) no histidine residue occurs in the vicinity of the phosphorylated serine, so that we would like to present some evidence that an amino group other than the imidazolyl might function as part of the catalytic site.

EXPERIMENTAL

Twice crystallized trypsin (salt-free) was obtained from the Mann Research Laboratories Inc., New York. The substrate *p*-nitrophenyl acetate was synthesized as described by Chattaway (10). All reactions were carried out in 20% (v/v) isopropyl alcohol at 25° C with 0.025 *M* phosphate as buffer. The pH values quoted refer to the buffer and were measured in the absence of alcohol, but in the presence of enzyme, using a Beckman Model G pH meter.

The rapid acetylation reaction was studied employing the stopped-flow apparatus

[1]*Manuscript received August 22, 1958.*
Contribution from the Department of Chemistry, University of Ottawa, Ottawa, and the Laboratories of the Food and Drug Directorate, Department of National Health and Welfare, Ottawa, Canada.
[2]*Presented at the Chemical Institute of Canada Conference, Toronto, May 1958.*
[3]*Present address: Laboratories of the Food and Drug Directorate, Department of National Health and Welfare, Ottawa, Canada.*
[4]*Present address: Department of Chemistry, Laval University, Quebec, Que.*

described previously (11), while the slow deacetylation reaction was followed with a Cary Model 11 spectrophotometer using the differential technique. The data were treated according to the suggested mechanism by the theoretical method outlined in a preceding paper (12).

RESULTS AND DISCUSSION

Effect of pH on Acetylation

The initial rapid production of *p*-nitrophenol, corresponding to the formation of acetyl-trypsin was recorded at several substrate and hydrogen-ion concentrations. The constant F (12) was then calculated from the reaction trace using the Guggenheim technique (13). A typical Lineweaver–Burk plot (14) of some of the results is given in Fig. 1, where the extrapolation of $1/F$ at infinite substrate concentration yields the same value for $1/k_2$ at two widely separated pH values. The fact that seven such plots between pH 6.2 and 7.8 produced the same result for $1/k_2$ strongly suggests competitive inhibition by hydrogen-ions. The same result, though not elucidated as competitive inhibition, was obtained with chymotrypsin (3). Similar to the usual Michaelis–Menten treatment, the slopes obtained from the Lineweaver–Burk plot in Fig. 1 involve K_m/k_2. According to Laidler (15), the variation of K_m/k_2 with pH provides the dissociation constants of the groups which comprise the active site of the enzyme. It should also be pointed out, as has been done previously (3), that should the three-step mechanism be general for other enzyme systems, then the standard Michaelis constant may consist of a rather large number of constants.

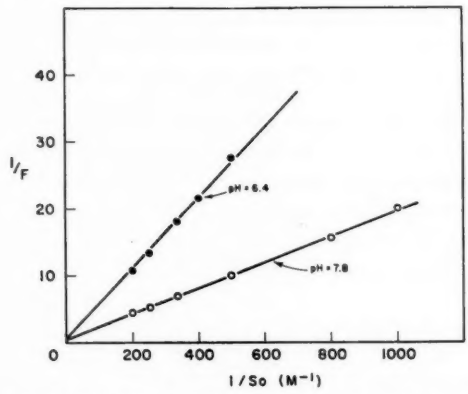

FIG. 1. A Lineweaver–Burk plot of the hydrolysis of NPA by trypsin (1 mg/ml) at pH 6.4 and 7.8.

The results given in Fig. 1 can be explained if we assume that hydrogen-ion competitively inhibits the initial combination of enzyme and substrate. With this in mind, the scheme for acetylation becomes,

(*a*) $$E + H^+ \underset{k_{-4}}{\overset{k_4}{\rightleftharpoons}} EH^+$$

(*b*) $$E + S \underset{k_{-1}}{\overset{k_1}{\rightleftharpoons}} ES_1$$

(*c*) $$ES_1 \xrightarrow{k_2} ES_2 + P_1$$

where E is the active form and EH^+ the inactive form of the enzyme, S is the substrate, ES_1 is the Michaelis complex, ES_2 is the acetylated enzyme, P_1 is the phenol, and k_1, k_{-1}, k_2, k_4, and k_{-4} are the appropriate rate constants. When this scheme is treated theoretically (12) and the effect of hydrogen-ion taken into account (15, 16, 17) $-F$, the quantity to be determined, formulates to

[1] $$F = -\frac{(k_2+k'_3)\,s_0+k'_3K'_m}{s_0+[(k'_3+k_2+k_{-1})/k_1](Ka+[H])/Ka}$$

when $k_2 \gg k'_3$

[2] $$F = -\frac{k_2 s_0}{s_0+K'_m}$$

where

[3] $$K'_m = K_m\left(\frac{Ka+[H]}{Ka}\right)$$

[4] $$K_m = \frac{k_2+k_{-1}}{k_1}$$

and

[5] $$Ka = k_{-4}/k_4.$$

Equation [2] may be also written as,

[6] $$-\frac{1}{F} = \frac{1}{k_2}+\frac{1}{s_0}\left(\frac{K_m}{k_2}+[H]\frac{K_m}{Ka\,k_2}\right).$$

Figure 2 was obtained by plotting the slopes of equation [6] against [H]. The resultant dissociation constant $Ka = 1.4\times10^{-7}$, which is related to the active site of the enzyme, was calculated from the intercept K_m/k_2 and the slope $K_m/k_2\,Ka$.

Equation [2] may be rearranged in still another fashion,

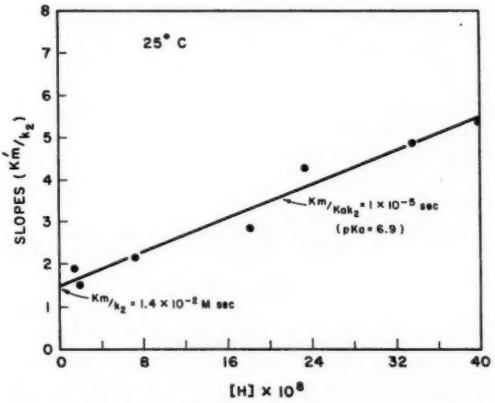

FIG. 2. The determination of K_m/k_2 and $K_m/Ka\,k_2$ for the trypsin–NPA system, from a plot of slopes against $[H^+]$.

[7] $$-\frac{1}{F}=\left(\frac{1}{k_2}+\frac{1}{s_0}\frac{K_m}{k_2}\right)+[\mathrm{H}]\frac{K_m}{s_0 Ka\, k_2}.$$

The constants k_2 and K_m were evaluated by plotting the intercepts of equation [7] against $1/s_0$, as illustrated in Fig. 3. The rate constant of acetylation $k_2 = 1.5$ sec^{-1} was estimated from the intercept $1/k_2$, which allowed a Michaelis constant $K_m = 2.1 \times 10^{-2}$ M to be determined from K_m/k_2, the slope of the line.

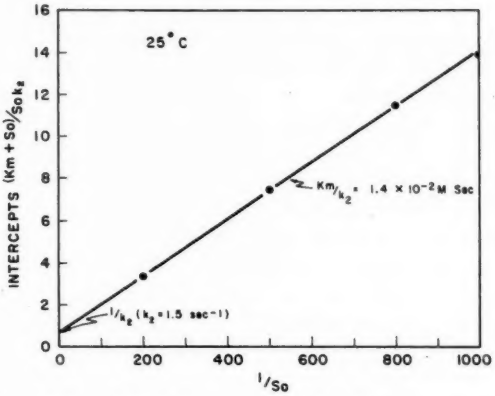

FIG. 3. The estimation of $1/k_2$ and K_m/k_2 by means of a plot of intercepts versus s_0, for trypsin catalyzed hydrolysis of NPA.

The results for k_2, Ka, and K_m are included in Table I, where the constants for trypsin and chymotrypsin are compared.

TABLE I

Kinetic constants for the enzymatic hydrolysis of *p*-nitrophenyl acetate

Constant	Trypsin	Chymotrypsin*
k_2 (sec^{-1})	1.5	3.1
K_m (M)	2.1×10^{-2}	6.8×10^{-3}
pK_a	6.9	6.6
pK'_a	7.0	7.3†
k_3 (sec^{-1})	0.013	0.025

*Calculated from the results of Gutfreund, H. and Sturtevant, J. M. Biochem. J. **63**, 656 (1956).
†6.8 for ester hydrolysis (ref. 5).

Effect of pH on Deacetylation

The reactions which represent deacetylation are:

(*d*) $$ES_2 \xrightarrow{k_3} E+P_2$$

(*e*) $$ES_2+H^+ \underset{k_{-5}}{\overset{k_5}{\rightleftharpoons}} ES_2H^+$$

where ES_2 is the unstable form and ES_2H^+ the stable form of the acetylated enzyme, P_2 is acetate, and k_3, k_5, and k_{-5} the appropriate rate constants. When t is large the rate is

[8] $$\dot{p}_1 = \dot{p}_2 = k'_3 e_0 \text{ (refs. 3, 10)},$$

where

[9] $$k'_3 = k_3\left(\frac{Ka'}{Ka'+[H]}\right)$$

and

[10] $$Ka' = k_{-5}/k_5.$$

The slow deacetylation reaction was studied spectrophotometrically by following the phenol produced after the rapid acetylation reaction had subsided. The results were conveniently corrected for the spontaneous hydrolysis of NPA by placing the reaction solution in the sample cell and the same solution less enzyme in the reference cell of a double beam spectrophotometer, and recording the difference in absorbance. The reaction was started by introducing equal portions of NPA simultaneously into both cells with hypodermic syringes. The necessary corrections were then applied to the records to take into account that the fraction of colored species of *p*-nitrophenol, i.e. $pK_a = 7.15$ (18), varies with pH.

In the above manner the rates at different hydrogen-ion concentrations, which are plotted as the reciprocal rate against [H] in Fig. 4, were obtained. This plot gives a dissociation constant $Ka' = 1\times10^{-7}$ for acetylated trypsin and compares favorably with the constant Ka, concerned with the active site. The rate constant for deacetylation, $k_3 = 1.3\times10^{-2}$ sec^{-1}, was determined from the intercept of Fig. 4; the extinction coefficient of *p*-nitrophenol was taken as 1.8×10^4 (19), and the molecular weight of trypsin as 21,000 (20).

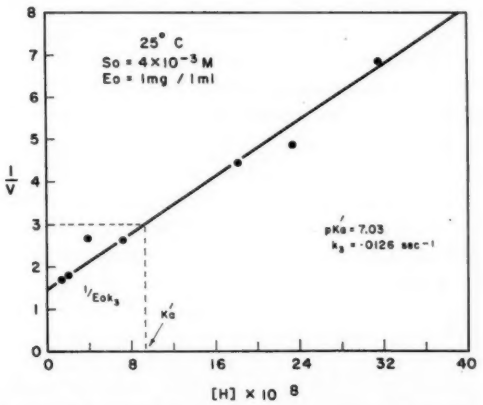

FIG. 4. A plot of the reciprocal rate of liberation of *p*-nitrophenol against $[H^+]$, for the determination of k_3e_0 and Ka' in the catalyzed hydrolysis of NPA by trypsin.

Mechanism of Hydrolysis

When the effect of proton inhibition is introduced, the result suggests a mechanism similar to that proposed by Cunningham (6). Quite different from former mechanisms his scheme advocates the hydroxyl group as primary site, rather than the imidazolyl which is now thought to be secondary. To facilitate a comparison of the two mechanisms those stages which correspond to reactions (*a*) to (*e*) are represented in the scheme outlined in Fig. 5. As our present experimental method does not detect the acyl-transfer

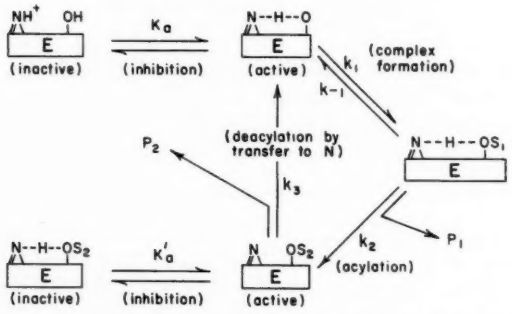

FIG. 5. The mechanism of enzymatic ester hydrolysis.

reaction, the absence of this transfer is the main difference in the two schemes. Thus, the rate constant k_3 for deacetylation is a composite constant involving two stages: the transfer of acetyl to nitrogen and its subsequent release.

In the scheme as shown in Fig. 5 the enzyme is inactive to complex formation unless a proton is released from the active site, and explains why inhibition is competitive rather than non-competitive. On examination of equation [1] it is seen that under certain conditions competitive inhibition may not be realized. This is especially true when the rate constants of acetylation and deacetylation are of the same order of magnitude. A Lineweaver–Burk plot of the data will not produce a straight line with constant intercept, and competitive inhibition may appear to be non-competitive.

The initial point of attack of substrate is the hydroxyl group of serine where the complex undergoes partial decomposition, releasing phenol. The hydroxyl group becomes acetylated, but before deacetylation can proceed there must be a transfer of the acetyl group to the nitrogen. The stability of certain acylated enzymes at low pH has been reported (5, 21, 22). This can be explained on the basis that transfer from the hydroxyl only takes place at higher pH values where the nitrogen does not have the inhibiting hydrogen intact. Therefore, proton inhibition at the deacylation stage accounts for this inactivity and stability of acetyltrypsin and chymotrypsin below a pH of 5 to 6.

A similar approach may be used to explain inhibition by certain organophosphorus compounds. For instance, in the case of DFP the hydroxyl group of a serine residue in the enzyme is phosphorylated, but transfer of this phosphoryl group to the nitrogen is difficult, resulting in an inactive enzyme.

Nature of the Catalytic Site

Tracer experiments show that DIP^{32} (diisopropyl phosphate) is attached to the hydroxyl group of a serine residue and no histidine (imidazole) occurs in the vicinity (8, 9). However, Westheimer (23) presents in detail the necessary orientation of the active site of chymotrypsin that enables the imidazolyl and hydroxyl groups to come together by folding. Also, spectrophotometric evidence has been published to show that acetyl-imidazolyl is an intermediate when acetyl-chymotrypsin decomposes (7).

The lack of histidine in the neighborhood of DIP^{32}–serine, and the differences in the pK values and the degree of activity of trypsin and chymotrypsin (see Table I) has led us to postulate that other groups might also function in partnership with the hydroxyl group to constitute an active site. As for model hydrolysis (24) the facts present the possibility that the basicity of the nitrogen containing group of the active site may

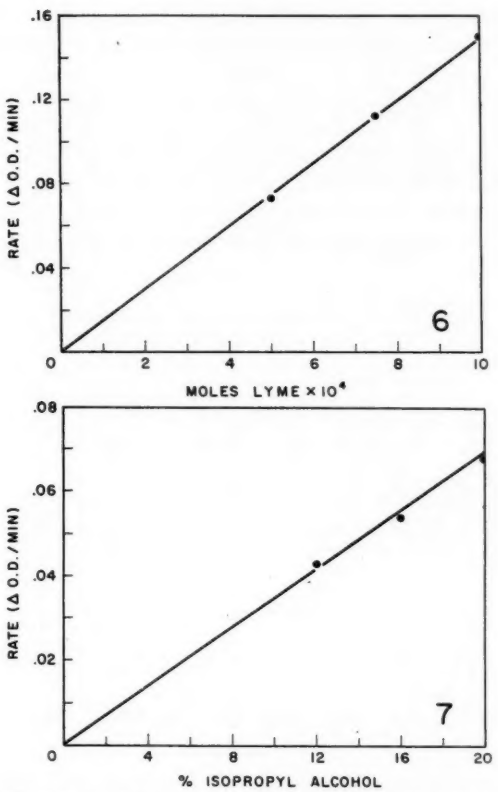

FIG. 6. The effect of LYME on the rate of hydrolysis of NPA in the presence of 20% (v/v) isopropyl alcohol.

FIG. 7. The effect of isopropyl alcohol on the rate of hydrolysis of NPA in the presence of 4×10^{-4} *M* LYME.

be the important factor. Since the p*K* of a free α-amino group in an ester is in the neighborhood of the p*K* for the active site of trypsin, lysine methyl ester (LYME) was tested and found to influence the rate of hydrolysis of NPA under conditions comparable to enzymatic hydrolysis. This effect is demonstrated in Fig. 6, where the rate of hydrolysis of NPA is proportional to the amino acid concentration. The same result was obtained by varying the isopropyl alcohol concentration and is given in Fig. 7. These results show that the aliphatic hydroxyl and amino groups could play a significant part in the constitution of an enzymatic site. Further evidence to support this hypothesis can be secured from the literature. Hartley and Kilby (2) have reported that the phenolic hydroxyl and the aliphatic amino groups may act as acceptors of the acetyl group. The work of Balls and co-workers reveals that chymotrypsin mediates the transfer of acetyl to ethanol (22) or trimethylacetyl to *n*-butanol (25), illustrating the importance of hydroxyl; while the significance of an amino group is shown by the transfer of acetyl from chymotrypsin to hydroxylamine (22) and the fact that certain monoacylated chymotrypsin derivatives are reactivated by tyrosine ethyl ester (25). Also, Wagner-Jauregg and Hackley (26) discovered during an investigation of the model hydrolysis

of organophosphorus inhibitors that certain amino and hydroxyl substituted pyridines, and such compounds as catechol, increased the rate of hydrolysis as compared to pyridine.

Finally, some results were obtained by infrared spectroscopy using the KBr-pellet technique which indicate the α-amino group is acetylated when NPA is allowed to hydrolyze in the presence of tyrosine ethyl ester (TYEE). From the infrared spectra in Fig. 8 it is seen that both acetyl-TYEE and the system of NPA hydrolyzed in the presence of TYEE possess appreciable absorbance at 1660 cm^{-1}, while TYEE and hydrolyzed NPA do not; thereby disclosing that tyrosine ethyl ester is acetylated during the hydrolysis of NPA.

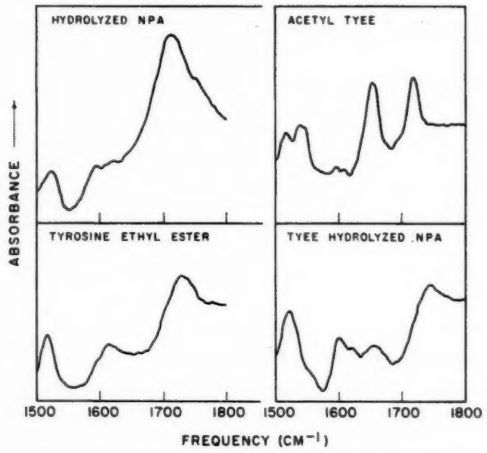

FIG. 8. The infrared spectra of freeze-dried solutions of hydrolyzed NPA, TYEE, acetyl-TYEE, and NPA hydrolyzed in the presence of TYEE; each containing 20% (v/v) isopropyl alcohol and 0.05 *M* phosphate pH 7.8.

CONCLUSIONS

The rate constant related to the acetylation stage during the trypsin or chymotrypsin catalyzed hydrolysis of NPA appears to be pH independent. The mechanism implied by the result is in agreement with the postulated mechanism of Cunningham. There is some degree of suggestion that this three-step scheme might be general, and in the instance of other enzyme systems the Michaelis constant may be a composite of a larger number of constants than formerly anticipated. Even though it has been shown that hydroxyl groups and amino groups influence the rate of hydrolysis of NPA, further investigations will be required before definitely establishing the nature of their relationship to enzymatic hydrolysis. This is particularly true in the case of the free α-amino group. Although the pK of this group in an ester and possibly a peptide would be in agreement with the pK reported for the active site of trypsin, free α-amino groups are believed to exist only in the terminal residues of proteins.

ACKNOWLEDGMENT

We wish to thank the National Research Council of Canada for their financial support of a portion of this research.

REFERENCES

1. HARTLEY, B. S. and KILBY, B. A. Biochem. J. **50**, 672 (1952).
2. HARTLEY, B. S. and KILBY, B. A. Biochem. J. **56**, 288 (1954).
3. GUTFREUND, H. and STURTEVANT, J. M. Biochem. J. **63**, 656 (1956).
4. GUTFREUND, H. and STURTEVANT, J. M. Proc. Natl. Acad. Sci. **42**, 719 (1956).
5. DIXON, G. H. and NEURATH, H. J. Biol. Chem. **225**, 1049 (1957).
6. CUNNINGHAM, L. W. Science, **125**, 1145 (1957).
7. DIXON, G. H. and NEURATH, H. J. Am. Chem. Soc. **79**, 4558 (1957).
8. DIXON, G. H., KAUFFMAN, D. L., and NEURATH, H. J. Am. Chem. Soc. **80**, 1260 (1958).
9. SCHAFFER, N. K., SIMET, L., HARSHMAN, S., ENGLE, R. R., and DRISKO, R. W. J. Biol. Chem. **225**, 197 (1957).
10. CHATTAWAY, F. D. J. Chem. Soc. **134**, 2495 (1931).
11. STEWART, J. A. and OUELLET, L. Can. J. Chem. **37**, 744 (1959).
12. OUELLET, L. and STEWART, J. A. Can. J. Chem. **37**, 737 (1959).
13. GUGGENHEIM, E. A. Phil. Mag. **2**, 538 (1926).
14. LINEWEAVER, H. and BURK, D. J. Am. Chem. Soc. **56**, 658 (1934).
15. LAIDLER, K. J. Trans. Faraday Soc. **51**, 550 (1955).
16. LAIDLER, K. J. Trans. Faraday Soc. **51**, 528 (1955).
17. LAIDLER, K. J. Trans. Faraday Soc. **51**, 540 (1955).
18. ROBINSON, R. A. and BIGGS, A. I. Trans. Faraday Soc. **51**, 901 (1955).
19. BIGGS, A. I. Trans. Faraday Soc. **50**, 800 (1954).
20. SEDLACEK, B. and BARTL, P. Chem. Listy, **49**, 996 (1955).
21. BALLS, A. K. and ALDRICH, F. L. Proc. Natl. Acad. Sci. **41**, 190 (1955).
22. BALLS, A. K. and WOOD, H. N. J. Biol. Chem. **219**, 245 (1956).
23. WESTHEIMER, F. H. Proc. Natl. Acad. Sci. **43**, 969 (1957).
24. BRUICE, T. C. and SCHMIR, G. L. J. Am. Chem. Soc. **79**, 1663 (1957).
25. MCDONALD, C. E. and BALLS, A. K. J. Biol. Chem. **227**, 727 (1957).
26. WAGNER-JAUREGG, P. and HACKLEY, B. E. J. Am. Chem. Soc. **75**, 2125 (1953).

THE STEREOCHEMISTRY OF THE PIMARIC ACIDS[1,2]

O. E. EDWARDS AND R. HOWE[3]

ABSTRACT

Isodextropimaric and dextropimaric acids have been shown to have the same stereochemistry at C_1, C_{11}, and C_{12}, but to be epimeric at C_7. A critical survey is made of the present evidence with regard to the stereochemistry at C_{13} in these acids. Preliminary experiments on the action of formic acid on isodextropimaric acid are reported.

In view of the current interest in the stereochemistry of the tetracarbocyclic diterpenes, e.g. rimuene (2, 3), phyllocladene (3, 4, 5, 6), mirene (3, 7), steviol (6, 8), cafestol (6, 9, 10) and gibberellic acid (11), and also the tetracarbocyclic diterpene alkaloids, e.g. the *Garrya* alkaloids (6, 10, 12), atisine (13), and ajaconine (14), the question of whether their close relatives, the pimaric acids, belonged to one steric group became of outstanding interest.

While the skeleton I (R_1 = vinyl; R_2 = methyl) and stereochemistry at C_1, C_{11}, and C_{12} of dextropimaric acid have been well established (15, 16), the stereochemistry at C_7 and C_{13} has remained in doubt. Isodextropimaric acid, which occurs with dextropimaric acid in the oleoresin of *Pinus palustris* (17), has been shown to have the same basic skeleton as dextropimaric acid by Harris and Sanderson (18). However, their

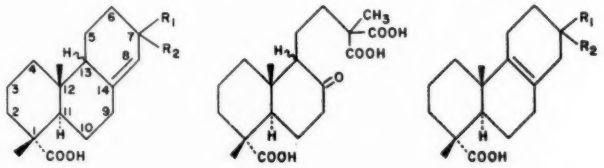

I II III

degradation products were optically inactive and the possibility existed that epimerization at the asymmetric center adjacent to the carbonyl group of the keto-tricarboxylic acid II might have taken place (3). Hence the only safe conclusion which may be drawn from their experiments is that isodextropimaric acid is identical at C_1, C_{11}, and C_{12} to dextropimaric acid, or bears an over-all mirror image relation to it at these centers.

The evidence presented below establishes that the two acids are identical at C_1, C_{11}, and C_{12}, and that they are epimeric at C_7 as originally suggested by Harris and Sanderson (18) on equivocal evidence, but allows no certain conclusion about the stereochemistry at C_{13}. Since our preliminary communication (1), Wenkert and Chamberlin (19), and Green, Harris, and Whalley (20) have announced the same and further conclusions (see below for a critical discussion).

As a preliminary to our work it was necessary to re-examine the properties of the dihydro- and tetrahydro-derivatives of both acids, because of the conflicting data in the literature. The vinyl double bond in both acids was readily reduced in the presence

[1]*Manuscript received December 16, 1958.*
Contribution from the Division of Pure Chemistry, National Research Council, Ottawa, Canada.
Issued as N.R.C. No. 5097.
[2]*A preliminary report of some of this work was published earlier (ref. 1).*
[3]*National Research Council of Canada Postdoctoral Fellow. Present address: Research Laboratory, I.C.I. Pharmaceutical Division, Fulshaw Hall, Alderly Rd., Wilmslow, Manchester, England.*

of presaturated palladized charcoal. Dihydroisodextropimaric acid was purified by chromatography on silica gel and recrystallization of its cyclohexylamine salt. It melted at 173–175° and had $[\alpha]_D$ −7°. (The literature values are m.p. 173–175°, $[\alpha]_D$ ±0° (EtOH) (18) and m.p. 173.5°, $[\alpha]_D$ −16° (chloroform–acetone, 1 : 1) (21).) The dihydrodextropimaric acid was isolated directly from Staybelite Resin by a modification[4] of the method of Hasselstrom and Bogert (22). It melted at 243–245° and had $[\alpha]_D$ +22°. The infrared spectrum of both acids (nujol mull) contained medium bands at 825 cm^{-1}, corresponding to the trisubstituted double bonds.

Dihydroisodextropimaric acid slowly took up 0.76 mole of hydrogen over Adams' catalyst in acetic acid giving a product with $[\alpha]_D$ +30°. This took up a further 0.27 mole of hydrogen in the presence of fresh catalyst. The tetrahydro-acid had m.p. 172–173° and $[\alpha]_D$ +24° (EtOH), +21° ($CHCl_3$). Ukita *et al.* (23) report a melting point of 172–172.5° (no rotation).

A similar hydrogenation of dihydrodextropimaric acid gave tetrahydrodextropimaric acid, m.p. 238–240°, $[\alpha]_D$ +18°, in agreement with Ruzicka *et al.* (24), who report a melting point of 236–237° (no rotation). Le-Van-Thoi and Ourgaud (25) report a melting point of 198° with $[\alpha]_j$ +55° for tetrahydrodextropimaric acid. This appears to be a mixture of Δ^{13}-dihydrodextropimaric acid (see below) and the tetrahydro-acid which we now report. (Their analytical figures fit $C_{20}H_{32}O_2$ rather than $C_{20}H_{34}O_2$.) When dihydrodextropimaric acid was allowed to absorb 0.25 mole of hydrogen the total product melted at 193–197° and had $[\alpha]_D$ +53° in excellent agreement with their product. On complete reduction this mixture gave pure tetrahydro-acid, m.p. 238–240°, $[\alpha]_D$ +19°.

In order to compare the asymmetry at C_7, methods were sought for eliminating or rendering identical the asymmetry at C_{13} in dextro- and isodextro-pimaric acids and their derivatives. The action of strong acids on the pimaric acids could possibly cyclize the diene to a tetracarbocyclic system, isomerize the nuclear double bond to the Δ^{13}-position, produce γ- and δ-lactones (e.g. IV and V), and convert the C_7-substituents to an isopropylidene group. In the isodextropimaric acid series, conditions have been found for producing all these changes except the cyclization of the diene system.

The easiest method of destroying the asymmetry at C_{13} appeared to be by isomerizing the $\Delta^{8,14}$-ethylenic bond to the Δ^{13}-position. When isodextropimaric acid was refluxed with *p*-toluenesulphonic acid in dry dioxane, the desired migration was slowly brought about,[5] but it was found to be a poor preparative method. The cleanest method of isomerizing the $\Delta^{8,14}$ double bond to the Δ^{13}-position was found to be by the action of hydrogen chloride in chloroform. The method was first applied to the dihydro-acids (I; R_1 = ethyl; R_2 = methyl) in order to prevent complicating reactions due to the vinyl group.

Dihydrodextropimaric acid (I; R_1 = ethyl; R_2 = methyl) and dihydroisodextropimaric acid (I; R_1 = methyl; R_2 = ethyl) were converted by hydrogen chloride in chloroform to their Δ^{13}-isomers (III), m.p. 181.3°, $[\alpha]_D$ +73°, and m.p. 107–108°, $[\alpha]_D$ +76.7° respectively. The infrared spectra of the products lacked the 825 cm^{-1} band characteristic of the starting materials and together with the hydrogenation evidence presented below leads to the Δ^{13}-assignment for the double bond.

Hydrogenation of Δ^{13}-dihydrodextropimaric acid in acetic acid with Adams' catalyst gave the same tetrahydrodextropimaric acid as reported above, m.p. 238–240°,

[4]*We cordially thank Dr. T. H. Sanderson, of Hercules Research Center, for the resin and for kindly furnishing details of the isolation method.*

[5]*We thank Dr. D. K. R. Stewart for characterizing the isodextropimaric acid, and for preliminary experiments on the isomerization with p-toluenesulphonic acid.*

$[\alpha]_D$ +19° as the only product. Similar conditions converted Δ^{13}-dihydroisodextropimaric acid to the same tetrahydroisodextropimaric acid as reported above, m.p. 172–173°, $[\alpha]_D$ +21°. Since dihydrodextropimaric acid is recovered unchanged after refluxing with glacial acetic acid for 5 hours, the possibility of group migration or skeletal rearrangement may be precluded in both the hydrogenation experiments and during the hydrogen chloride – chloroform treatment of the dihydro-acids.

It was reported above that the intermediate product isolated during the reduction of dihydroisodextropimaric acid had a rotation which was more positive than either the starting material or the final product. This provided a valuable clue that hydrogenation was accompanied by double-bond migration to give the Δ^{13}-dihydro-acid of high positive rotation and less facile reducibility. An interpretation of Le-Van-Thoi and Ourgaud's results was also afforded. We attempted, but found that it was not possible, to obtain pure Δ^{13}-dihydrodextropimaric acid from dihydrodextropimaric acid by isomerization on the catalyst surface; conditions favoring isomerization also brought about some reduction.

Dextropimaric acid has usually been considered to be stable to mineral acids (16), although Vesterburg (26) obtained some evidence that isomerization did occur when an ethereal solution of the acid was saturated with hydrogen chloride. Ruzicka and Balas (27) report the formation of three monohydrochlorides by long treatment of dextropimaric acid with acetic acid saturated with hydrogen chloride. When dextropimaric acid in chloroform was saturated with hydrogen chloride we found that the only product was the expected Δ^{13}-isomer, m.p. 131–132°, $[\alpha]_D$ +70°. The infrared spectrum revealed that the vinyl group had remained intact, while the trisubstituted ethylenic bond peak (825 cm^{-1}) had disappeared. Selective reduction of the vinyl group of the new Δ^{13}-acid gave the Δ^{13}-dihydrodextropimaric acid, m.p. 181–182°, $[\alpha]_D$ +75° reported above. Application of the hydrogen chloride method of isomerization to isodextropimaric acid, m.p. 162–164°, $[\alpha]_D$ ±0° produced the Δ^{13}-isomer, m.p. 106–107°, $[\alpha]_D$ +113°, the infrared spectrum showing peaks due to a vinyl group but none due to a trisubstituted ethylenic bond. Selective reduction of the vinyl group of the new Δ^{13}-acid gave Δ^{13}-dihydrodextropimaric acid, m.p. 107–108°, $[\alpha]_D$ +73° reported above.

Since our preliminary report of this work was published (1), Green, Harris, and Whalley (20) have reported Δ^{13}-isodextropimaric acid as having m.p. 118° and $[\alpha]_D$ +58°. Their isomerization appears to have been only partial, since we have prepared a synthetic mixture (*ca.* 1:1) of isodextropimaric acid and Δ^{13}-isodextropimaric acid having $[\alpha]_D$ +58° and found it to have m.p. 118–121°. In view of this the Δ^{13}-dihydroisodextropimaric acid which they report would also seem to be a mixture. Molecular rotation correlations based on the figures may well be meaningless.

We now turn our attention to the lactones produced by more vigorous acid treatment of the dihydrodextro- and dihydroisodextro-pimaric acids. Δ^{13}-Dihydrodextropimaric acid with concentrated sulphuric acid at −5° C gave the known γ-lactone (28) (IV; R_1

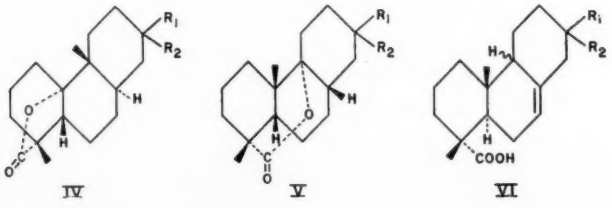

= ethyl; R_2 = methyl) m.p. and mixed m.p. 100°, $[\alpha]_D$ −15°, which was also obtained from dihydrodextropimaric acid. Similar conditions converted both dihydroisodextro and Δ^{13}-dihydroisodextropimaric acid to a new γ-lactone (IV; R_1 = methyl; R_2 = ethyl) m.p. 105–106°, $[\alpha]_D$ −9°. More vigorous acid treatment, i.e. concentrated sulphuric acid at 25° C converted the γ-lactone of dihydroisodextropimaric acid to a new δ-lactone (V; R_1 = methyl; R_2 = ethyl) m.p. 72–73°, $[\alpha]_D$ −40°, which could also be obtained directly from dihydroisodextropimaric acid under similar conditions. This δ-lactone differed from the known δ-lactone (28) (V; R_1 = ethyl; R_2 = methyl) from dihydrodextropimaric acid, m.p. 142°, $[\alpha]_j$ −45°. In one experiment, the action of *p*-toluenesulphonic acid on isodextropimaric acid in dioxane solution produced a new γ-lactone IV (R_1 = methyl; R_2 = vinyl), m.p. 128–130°, $[\alpha]_D$ −1° in very poor yield.

The fact that dihydrodextropimaric and dihydroisodextropimaric acids give different Δ^{13}-derivatives, γ-lactones, and δ-lactones proves conclusively that the acids are epimeric at C_7. The correspondence of ΔM_D on going from the Δ^{13}-dihydro-acids to the γ-lactones (−268° and −260° respectively) firmly indicates the *identical* stereochemistry at C_1, C_{11}, and C_{12} in both acids. The comparable rotational change on the transformation of Δ^{13}-dihydroabietic acid (III; R_1 = isopropyl; R_2 = H) to a γ-lactone (29) (IV; R_1 = isopropyl; R_2 = H) (ΔM_D −398°) provides additional proof that the stereochemistry of ring A of the pimaric acids is correctly shown in I.

Ukita and Tsumita (21) report the isolation from the fruits of *Juniperus japonica* of isodextropimaric acid and also a new pimaric acid, m.p. 162.5–165°, $[\alpha]_D$ −8.9°, which gives tetrahydroisodextropimaric acid, m.p. 172–173° on complete hydrogenation. This new acid cannot have the Δ^{13}-structure (III; R_1 = methyl; R_2 = vinyl) which they assign to it (23), since its properties are distinct from those of Δ^{13}-isodextropimaric acid (m.p. 106–107°, $[\alpha]_D$ +113°) reported here. Through the great kindness of Professor Ukita we have been able to make further observations on this new acid. Treatment of Ukita's acid in chloroform with hydrogen chloride converted it to Δ^{13}-isodextropimaric acid, m.p. 105–107°, $[\alpha]_D$ +110°, identical with that reported above. We conclude that Ukita's acid[6] may be $\Delta^{9,14}$-isodextropimaric acid (VI; R_1 = methyl; R_2 = vinyl) or its 13-epimer. The key compound (VII; R_1 = methyl; R_2 = ethyl) in Ukita's proof of structure was derived from the corresponding allyl alcohol, which must have arisen by

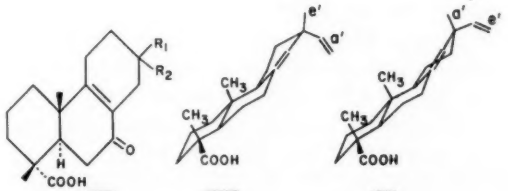

VII VIII IX

allylic oxidation and double bond migration during selenium dioxide oxidation of VI (R_1 = methyl; R_2 = ethyl). Fieser (30) has reported several examples of bond migration concomitant with selenium dioxide oxidations. The infrared spectrum of Ukita's acid has peaks at 1410, 1000, and 910 cm^{-1}, characteristic of a vinyl group, but shows only a shoulder at 825 cm^{-1} due to the trisubstituted ethylenic bond. However, the corre-

[6]*The naming of Ukita's acid will be deferred until the stereochemistry at C_{13} is known, when it can be named so as to indicate its relationship to isodextropimaric acid.*

sponding dihydro-acid with the vinyl group reduced, m.p. 154–157°, $[\alpha]_D$ +18° shows the expected trisubstituted ethylenic bond peak at 825 cm^{-1}.

The change in molecular rotation on reduction of the Δ^{13}-ethylenic bond of Δ^{13}-dihydrodextropimaric and Δ^{13}-dihydroisodextropimaric acid (ΔM_D −182° and −175° respectively) indicates that hydrogenation has taken place in the same stereospecific sense in both cases. Models indicate that approach of a catalyst surface will be much more facile from the α-face, regardless of the C_7 orientation. Assuming *cis*-addition of hydrogen, this leads to a structure for the tetrahydro-acids having the C_{13} and C_{14} hydrogen atoms α-orientated. It is interesting to note that ΔM_D for the conversion of rimuene to tetrahydro-rimuene (2) (+65°) agrees better with the ΔM_D for the similar change in the isodextropimaric acid series (+72°) rather than that in the dextropimaric acid series (−199°).

Having shown that dextropimaric and isodextropimaric acid are epimeric at C_7, it remains to decide the actual stereochemistry at C_7 for each acid and to elucidate the stereochemistry at C_{13}. Wenkert and Chamberlin (19) have studied the infrared spectra of the equilibrium mixtures of γ- and δ-lactones derived from dihydrodextropimaric and dihydroisodextropimaric acids. From the percentages of γ- and δ-lactones (5±0.6% and 95±0.6%) and (3.6±0.8% and 96.4±0.8%) respectively in each equilibrium mixture, they reach the conclusion that in dextropimaric acid the vinyl group is β-orientated, and therefore in isodextropimaric acid it must be α-orientated. This result is independent of the stereochemistry at C_{13}. However, in view of the very small observed difference in the percentages of the γ- and δ-lactones in each equilibrium mixture and the intrinsic difficulty in obtaining high precision in quantitative infrared spectrophotometry, it seems to us that one should be cautious in accepting these conclusions.

From surface tension measurements, Bruun (31, 32) had previously reached the same conclusion concerning the stereochemistry at C_7 in these acids but had tacitly assumed that the C_{13} hydrogen atom is α-orientated in both acids. This seems a reasonable assumption in view of the closeness of the collapse areas for dextropimaric and the abietic acids (44.2 → 44.6 sq. Å), and isodextropimaric (43.6 sq. Å).[7] However since Bruun ignored the effect of the $\Delta^{8,14}$-ethylenic bond on the conformation of ring C (VIII and IX), his conclusions with regard to the stereochemistry at C_7 based on the film balance studies and on the intensities of absorption due to the vinyl group in the infrared (34, 35) are not necessarily correct. Furthermore, following a recent mass spectrometric study of the resin acids, Bruun, Ryhage, and Stenhagen (36) have reached the conclusion that dextropimaric and isodextropimaric acids are epimeric at C_{13} in opposition to the conclusion indicated on the basis of the film balance work.

Green, Harris, and Whalley (20), following a method reported earlier by us, agree that dextropimaric and isodextropimaric acid are epimeric at C_7 and without giving any details conclude that they are probably also epimeric at C_{13}. In dextropimaric acid, they consider that the C_{13}-hydrogen atom is α-orientated, i.e., *trans*- to the C_{12} methyl group, because dextropimaric acid is said to be stable to mineral acids. We have already shown, however, that dihydrodextropimaric acid is readily isomerized by hydrogen chloride in chloroform, and now report that dextropimaric acid behaves in a similar manner.

In view of the above uncertainties, we consider that the stereochemistry at C_{13} remains unproved for dextropimaric and isodextropimaric acids.

[7]*While no close analogue is available a somewhat comparable change of molecular shape to that involved in changing from a 13α- to a 13β-hydrogen atom in the pimaric acids is found in the cholestanol → coprostanol transformation (33). Here the effect is to increase the collapse area by ca. 3 sq. Å.*

We have simultaneously measured the amount of migration in a given time of the $\Delta^{8,14}$-ethylenic bond of dihydrodextropimaric and dihydroisodextropimaric acid catalyzed by mineral acid. The conditions were not sufficiently reproducible from run to run to give the same values for any given time interval but for every run carried out dihydroisodextropimaric acid was found to isomerize faster than dihydrodextropimaric acid as shown by the representative values given in the table.

	% of Δ^{13}-isomer formed	
Time (min.)	Dihydrodextropimaric acid	Dihydroisodextropimaric acid
3	11	25
6	23	39
10	40	52
15	38	45
20	48	58
40	79	82
100	86	88

These results could point to a difference in stereochemistry at C_{13} in the two acids, but may also be a measure of the effect of the differing stereochemistry at C_7, i.e., a quasi-equatorial ethyl group becoming equatorial after migration would act as an additional driving force whereas a quasi-axial group becoming axial after migration would retard the process.

We are at present engaged in converting the vinyl group of both dextropimaric and isodextropimaric acid to a methyl group in order to eliminate the asymmetry at C_7, and thereby establish whether or not dextropimaric and isodextropimaric acid have similar or dissimilar stereochemistry at C_{13}.

Some preliminary observations have been made on the action of formic acid on isodextropimaric acid, under conditions which cyclize rimuene (X) to isophyllocladene (37) (XI). No acidic product was isolated from the reaction. The products characterized

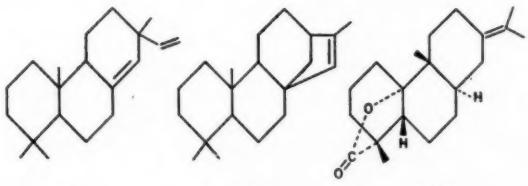

X XI XII

are an unsaturated γ-lactone of probable structure (XII), a hydrocarbon $C_{19}H_{29}$, clearly formed by decarboxylation of the β-γ-unsaturated acid which is intermediate in the formation of the γ-lactone XII, and also the known hydroxy-γ-lactone previously obtained (38) by the action of concentrated sulphuric acid on dextropimaric acid at −30° C. The γ-lactone (XII), m.p. 109.5–111°, $[\alpha]_D$ −54°, showed no absorption in the infrared at 825 cm^{-1} characteristic of a trisubstituted ethylenic bond, and when it was hydrogenated in acetic acid with Adams' catalyst, it formed the known saturated γ-lactone (IV; R_1 = isopropyl; R_2 = hydrogen) which may be obtained from any of the dihydroabietic acids by the action of concentrated sulphuric acid at −5° (39, 40). In order to obtain a reference sample of this γ-lactone, neoabietic acid was partially hydrogenated in ethanol solution using palladized charcoal (30%). A-Dihydroabietic

acid (29, 41), m.p. 149°, $[\alpha]_D$ +43°, was isolated in 25% yield and was converted by concentrated sulphuric acid at −5° into the γ-lactone IV (R_1 = isopropyl; R_2 = hydrogen). On similar treatment, the non-crystalline material from the hydrogenation afforded the same γ-lactone.

EXPERIMENTAL

Unless otherwise stated rotations were determined in absolute ethanol, and infrared spectra were determined on nujol mulls using a Perkin–Elmer model 21 double beam spectrophotometer.

Isodextropimaric Acid

WW pine gum rosin was converted to its 2-methyl-2-amino-1,3-propanediol salt in 2-butanone and the sparingly soluble salt of neoabietic acid collected (42). The mother liquors on concentration gave several crops of salt with low rotation. After three recrystallizations from 2-butanone this salt melted at 184–187° with slight preliminary sintering. The acid was liberated from the salt and recrystallized twice, giving a sample melting at 159–162° and having $[\alpha]_D$ −2±1° (*c*, 3.36). This was reconverted to the aminopropanediol salt, which after two recrystallizations melted at 184–187° after sintering slightly at 180°. The acid liberated from this had m.p. 160–163° and $[\alpha]_D$ 0° (*c*, 2.1). It did not depress an authentic specimen of isodextropimaric acid very kindly provided by Mr. R. V. Lawrence. It gave a methyl ester with diazomethane which crystallized from methanol as glistening plates, m.p. 61.5–62.5°.

Partial Hydrogenation of Isodextropimaric Acid

A solution of isodextropimaric acid (600 mg) in ethanol (25 ml) was hydrogenated in the presence of prereduced palladized charcoal catalyst (30%; 125 mg). Hydrogen (48 ml) was rapidly absorbed during 2 minutes, after which time absorption ceased abruptly. Calc. for 1 mole, 49 ml. The total product $[\alpha]_D$ −2° (*c*, 1.26; $CHCl_3$) was adsorbed on silica gel (15 g) and eluted with 50-ml portions of light petroleum – benzene (1:1) to give seven fractions as gums. Fractions 2 → 5 inclusive had similar rotations ($[\alpha]_D$ −4°) and were combined and recrystallized from methanol to give dihydroisodextropimaric acid as stout needles, m.p. 173–175° (450 mg), $[\alpha]_D$ −7° (*c*, 1.11), $[\alpha]_D$ −5° (*c*, 1.1; $CHCl_3$). Found: C, 78.61; H, 10.32. Calc. for $C_{20}H_{32}O_2$ (304): C, 78.94; H, 10.52. Infrared spectrum 1698 cm^{-1} (—COOH); 825 cm^{-1} (trisubstituted double bond).

The dihydro-acid (200 mg) in acetone was treated with cyclohexylamine (66 mg) in acetone to form the salt. After four recrystallizations from acetone the salt formed soft needles m.p. 203–206° (too insoluble for determination of rotation). Found: C, 77.56; H, 10.72. Calc. for $C_{21}H_{44}NO_2$ (402): C, 77.62; H, 10.95. The dihydro-acid regenerated from the pure salt had m.p. 173–175°, $[\alpha]_D$ −5° (*c*, 1.27; $CHCl_3$). The methyl ester formed plates m.p. 75° from methanol–water, $[\alpha]_D$ −5° (*c*, 2.01). Found: C, 78.89; H, 10.35. Calc. for $C_{21}H_{34}O_2$ (318): C, 79.25; H, 10.69.

Hydrogenation of Dihydroisodextropimaric Acid

A solution of dihydrodextropimaric acid (100 mg) in acetic acid (20 ml) was hydrogenated in the presence of Adams' catalyst (75 mg); 0.76 moles of hydrogen were absorbed in 24 hours. The total product, thrown out of methanol solution by water had m.p. 158–161°, $[\alpha]_D$ +30° (*c*, 0.96; $CHCl_3$) and showed some unsaturation with tetranitromethane. The total product in acetic acid (20 ml) was rehydrogenated using 125 mg of the catalyst. In 12 hours 0.27 moles of hydrogen were absorbed. The total product, thrown out of methanol solution by water, formed needles m.p. 163–167°, $[\alpha]_D$ +19°

(*c*, 1.15; $CHCl_3$). Chromatography on silica gel (3 g) using benzene as eluting solvent gave tetrahydroisodextropimaric acid as needles m.p. 172–173° (73 mg) from methanol–water, $[\alpha]_D$ +24° (*c*, 0.9), $[\alpha]_D$ +21° (*c*, 0.95; $CHCl_3$). Found: C, 78.46; H, 11.25. Calc. for $C_{20}H_{34}O_2$ (306): C, 78.37; H, 11.18%. Infrared spectrum 1700 cm^{-1} (—COOH). The methyl ester formed needles m.p. 68–69° from methanol–water, $[\alpha]_D$ +18° (*c*, 0.86). Found: C, 78.67; H, 11.08. Calc. for $C_{21}H_{36}O_2$ (320): C, 78.75; H, 11.26%.

Hydrogenation of Dihydrodextropimaric Acid

A solution of dihydrodextropimaric acid (117 mg) in acetic acid (35 ml) was added to Adams' catalyst (200 mg) which had been freshly reduced in acetic acid (5 ml). One mole of hydrogen was absorbed in 20 hours. The catalyst was removed by filtration and the acetic acid evaporated under reduced pressure. The crude product with m.p. 218–223° and $[\alpha]_D$ +20° (*c*, 1.13) was twice recrystallized from methanol to give tetrahydrodextropimaric acid as needles m.p. 238–240° (100 mg), $[\alpha]_D$ +18° (*c*, 1.1). Found: C, 78.41; H, 11.09. Calc. for $C_{20}H_{34}O_2$ (306): C, 78.37; H, 11.18%. Infrared spectrum 1699 cm^{-1} (—COOH).

Isomerization of Dihydrodextropimaric Acid on the Surface of a Catalyst

(*a*) A solution of dihydrodextropimaric acid (100 mg) in acetic acid (30 ml) was added to Adams' catalyst (20 mg) which had been freshly reduced in acetic acid (5 ml). One mole of hydrogen was absorbed in 20 hours. The crude product $[\alpha]_D$ +30° (*c*, 1.05) was recrystallized three times from methanol to give tetrahydrodextropimaric acid as needles m.p. and mixed m.p. 238–240° (60 mg), $[\alpha]_D$ +18° (*c*, 0.98). The mother liquors gave plates m.p. 177–180° (28 mg), $[\alpha]_D$ +39° (*c*, 0.86). A similar experiment to the above was carried out but without prereduction of the catalyst. The crude product with $[\alpha]_D$ +27° (*c*, 0.98) gave tetrahydrodextropimaric acid (65 mg) m.p. and mixed m.p. 238–240°, $[\alpha]_D$ +18° (*c*, 1.08), and also some plates m.p. 177–180° (20 mg), $[\alpha]_D$ +39° (*c*, 0.86). The material (45 mg) m.p. 177–180° obtained from the mother liquors of the above reductions was dissolved in acetic acid (30 ml) and added to Adams' catalyst (90 mg) which had been freshly reduced in acetic acid (5 ml). Two milliliters of hydrogen was absorbed in 20 hours. The total product $[\alpha]_D$ +17° (*c*, 0.74) was recrystallized from methanol to give tetrahydrodextropimaric acid as needles m.p. and mixed m.p. 238–240° (37 mg), $[\alpha]_D$ +18° (*c*, 1.0).

(*b*) A solution of dihydrodextropimaric acid (100 mg) in acetic acid (25 ml) was added to Adams' catalyst (20 mg) which had been freshly reduced in acetic acid (5 ml). Hydrogenation was allowed to proceed for 100 minutes after which time 1.9 ml of hydrogen had been absorbed. Calc. for 1 mole, 8.2 ml. The catalyst was removed by filtration and the acetic acid evaporated to give a solid m.p. 188–191°, $[\alpha]_D$ +54° (*c*, 1.17). When thrown out of methanol solution by water the total product formed prisms m.p. 193–197°, $[\alpha]_D$ +53° (*c*, 1.17). The constants of this material are approximately those m.p. 198°, $[\alpha]_J$ +55° reported by Le-Van-Thoi and Ourgaud (25) for tetrahydrodextropimaric acid. The above material m.p. 193–197° (63 mg) in acetic acid (20 ml) was added to Adams' catalyst (150 mg) freshly reduced in acetic acid (5 ml). Five milliliters of hydrogen was absorbed overnight. The crude product, $[\alpha]_D$ +20° (*c*, 0.92), was recrystallized twice from methanol to give tetrahydrodextropimaric acid as needles, m.p. and mixed m.p. 238–240° (48 mg), $[\alpha]_D$ +19° (*c*, 0.87).

(*c*) A solution of dihydrodextropimaric acid (100 mg) in acetic acid (25 ml) was added to Adams' catalyst (20 mg) which had been freshly reduced in acetic acid (5 ml). The mixture was shaken briefly once every minute for 1 hour under hydrogen. There was

no uptake of hydrogen and the starting material was recovered virtually unchanged, m.p. and mixed m.p. 240–242°, $[\alpha]_D$ +25° (*c*, 0.77).

(*d*) The above experiment was repeated except that this time the mixture was shaken briskly for 22 hours under nitrogen, after first reducing the catalyst in hydrogen. Starting material was recovered, m.p. and mixed m.p. 240–242°, $[\alpha]_D$ +21° (*c*, 1.06).

Isomerization of Isodextropimaric Acid Using p-Toluenesulphonic Acid

Isodextropimaric acid (440 mg) in dry dioxane (30 ml) was refluxed with *p*-toluenesulphonic acid (100 mg) under nitrogen for 4 hours and then allowed to stand overnight. The dioxane was evaporated, the viscous residue dissolved in chloroform, and washed free from *p*-toluenesulphonic acid using water. Evaporation of the dried chloroform solution gave a yellow gum $[\alpha]_D$ +82° (*c*, 2.05; $CHCl_3$). The gum was dissolved in ether and extracted with aqueous potassium carbonate, the carbonate soluble part being recovered by the addition of dilute hydrochloric acid. The acidic gum so obtained was adsorbed on a silica gel column (7.5 g) and eluted with benzene (50-ml portions) to give eight fractions. Fractions $2 \rightarrow 6$ inclusive in acetone gave solid when cooled to −10°. The solid was recrystallized four times from acetone–water to give Δ^{13}-isodextropimaric acid as clusters of prisms, m.p. 105–106° (105 mg), $[\alpha]_D$ +94° (*c*, 1.14; $CHCl_3$). Found: C, 79.74; H, 9.75. Calc. for $C_{20}H_{30}O_2$ (302): C, 79.49; H, 9.93. Infrared spectrum 1694 cm^{-1} (—COOH); 1413 cm^{-1}, and 908 cm^{-1} (vinyl group).

Several repetitions of this experiment under similar or slightly different conditions gave products having rotations between +45° and +55° from which it was not found possible to obtain pure Δ^{13}-isodextropimaric acid by either chromatography or fractional crystallization of the free acid or its cyclohexylamine or 2-aminopropan-1,3-diol salts. A better preparative method is given below.

Isomerization of Dihydrodextropimaric Acid Using Hydrogen Chloride

Dry hydrogen chloride was passed into a solution of dihydrodextropimaric acid (400 mg) in dry chloroform (50 ml) at −5° C for 4 hours. The chloroform solution was washed free from mineral acid with water and then dried (Na_2SO_4) and evaporated to give a gum (390 mg), $[\alpha]_D$ +75° (*c*, 0.95) which solidified. After five recrystallizations from methanol, Δ^{13}-dihydrodextropimaric acid formed plates, m.p. 182–183° (305 mg), $[\alpha]_D$ +73° (*c*, 1.00). Found: C, 79.05; H, 10.35. Calc. for $C_{20}H_{32}O_2$ (304): C, 78.94; H, 10.52. Infrared spectrum 1696 cm^{-1} (—COOH); no ethylenic absorption.

Isomerization of Dihydroisodextropimaric Acid Using Hydrogen Chloride

Dry hydrogen chloride was passed into a solution of dihydroisodextropimaric acid (210 mg) in dry chloroform (12 ml) at −5° C for 4 hours. The chloroform solution was extracted with aqueous potassium carbonate. The aqueous extract on acidification gave an acid gum (170 mg) $[\alpha]_D$ +74° (*c*, 1.03; $CHCl_3$). The gum was adsorbed on silica gel (4 g) and eluted with 30-ml portions of light petroleum – benzene (1:1) to give 10 fractions. Fractions $2 \rightarrow 8$ inclusive were combined and recrystallized three times from acetone–water to give Δ^{13}-dihydroisodextropimaric acid as needles, m.p. 107–108° (130 mg) $[\alpha]_D$ +76° (*c*, 0.92), $[\alpha]_D$ +74° (*c*, 0.99; $CHCl_3$). Found: C, 78.96; H, 10.41. Calc. for $C_{20}H_{32}O_2$ (304): C, 78.94; H, 10.52. Infrared spectrum 1696 cm^{-1} (—COOH); no ethylenic absorption. The methyl ester was a colorless oil, b.p. 130–135° at 2×10^{-2} mm, $[\alpha]_D$ +56° (*c*, 1.04). Found: C, 79.13; H, 10.58. Calc. for $C_{21}H_{34}O_2$ (318): C, 79.25; H, 10.69.

Rate of Isomerization Experiments

Twenty-five milligrams of each dihydropimaric acid in a finely powdered state were

simultaneously dissolved in 7-cc portions of ethanol-free dry chloroform previously saturated with hydrogen chloride at 0°. Dry hydrogen chloride was bubbled through the solutions maintained at 0°. Reaction time was measured from the time of complete solution. The reaction was quenched by three water washes, and the chloroform solution dried and evaporated. Rotations were done in ethanol on the total product. The results of a series of runs are summarized in the table.

Hydrogenation of Δ^{13}-Dihydrodextropimaric Acid

A solution of Δ^{13}-dihydrodextropimaric acid (83 mg) in acetic acid (16 ml) was hydrogenated in the presence of Adams' catalyst (166 mg); 1.07 moles of hydrogen were absorbed in 17 hours. The catalyst was removed by filtration and then the solvent was evaporated under reduced pressure. The product was dissolved in ether, washed with water, and dried. Evaporation of the ether gave a solid product (80 mg) $[\alpha]_D$ +17° (*c*, 1.15). The product was adsorbed on silica gel (2.5 g) and eluted with benzene–ether (19:1) in 20-ml portions to give four fractions. Fraction 1 had $[\alpha]_D$ +18° (*c*, 0.84) and fraction 4 had $[\alpha]_D$ +19° (*c*, 0.9). The four fractions were combined and recrystallized four times from methanol–water to give tetrahydrodextropimaric acid as needles, m.p. and mixed m.p. 238–240° (66 mg), $[\alpha]_D$ +19° (*c*, 0.84), identical with that obtained above.

Hydrogenation of Δ^{13}-Dihydroisodextropimaric Acid

A solution of Δ^{13}-dihydroisodextropimaric acid (100 mg) in acetic acid (20 ml) was hydrogenated in the presence of Adams' catalyst (200 mg); 1.05 moles of hydrogen were absorbed in 17 hours. The catalyst was removed by filtration and the solvent was evaporated under reduced pressure. The product was dissolved in ether, washed with water, and dried. The total product, thrown out of methanol solution by means of water, formed needles, m.p. 165–168°, $[\alpha]_D$ +21° (*c*, 1.11; $CHCl_3$) and gave no coloration with tetranitromethane. Chromatography on silica gel (3 g) and elution with benzene gave tetrahydroisodextropimaric acid, m.p. and mixed m.p. 172–173° (89 mg), $[\alpha]_D$ +21° (*c*, 1.07; $CHCl_3$), identical with that obtained above.

Isomerization of Dextropimaric Acid Using Hydrogen Chloride

Dry hydrogen chloride was passed into a solution of dextropimaric acid (100 mg) in dry chloroform (30 ml) at −5° C for 4 hours. The chloroform solution was washed free from mineral acid with water and then dried and evaporated to give a gum (95 mg), $[\alpha]_D$ +69° (*c*, 0.76). The gum was adsorbed on silica and eluted with 20-ml portions of benzene – light petroleum (3:2) to give 10 fractions. Fractions $2 \rightarrow 8$ inclusive had rotations between +69° and +71° and were combined to give Δ^{13}-dextropimaric acid as prisms, m.p. 131–132° (55 mg) from methanol–water, $[\alpha]_D$ +70° (*c*, 0.94). Found: C, 79.34; H, 9.97. Calc. for $C_{20}H_{30}O_2$ (302): C, 79.49; H, 9.93. Infrared spectrum 1697 cm^{-1} (—COOH); 1408 cm^{-1}, 995 cm^{-1}, and 908 cm^{-1} (vinyl group).

Partial Hydrogenation of Δ^{13}-Dextropimaric Acid

Δ^{13}-Dextropimaric acid (26.4 mg) in ethanol (7 ml) was hydrogenated in the presence of palladized charcoal catalyst (30%) (10 mg). Hydrogen (2.14 ml) was absorbed in 8 minutes after which time absorption ceased abruptly. Calc. for 1 mole, 2.15 ml. The total product $[\alpha]_D$ +75° (*c*, 0.85) was recrystallized three times from methanol–water to give Δ^{13}-dihydrodextropimaric acid as plates, m.p. and mixed m.p. 181–182°, $[\alpha]_D$ +75° (*c*, 0.94).

Isomerization of Isodextropimaric Acid Using Hydrogen Chloride

Dry hydrogen chloride was passed into a solution of isodextropimaric acid (1.4 g) in

dry chloroform (30 ml) at −5° C for 4 hours. The chloroform solution was washed free from mineral acid with water and then dried and evaporated to give a gum (1.36 g), $[\alpha]_D$ +91° (*c*, 1.0; $CHCl_3$). The gum was adsorbed on silica gel (30 g) and eluted with 50-ml portions of light petroleum – benzene (1:1) to give nine fractions as gums. Fractions 1 → 6 inclusive had rotations between +92° and +89° and were combined (0.97 g). After six recrystallizations from acetone–water, Δ^{13}-isodextropimaric acid was obtained as clusters of prisms, m.p. 106–107° (0.6 g), $[\alpha]_D$ +113° (*c*, 0.88), $[\alpha]_D$ +96° (*c*, 1.34; $CHCl_3$). Found: C, 79.29; H, 9.74. Calc. for $C_{20}H_{30}O_2$ (302): C, 79.49; H, 9.93. A further crop of 470 mg, m.p. 104–106°, was obtained from the residues. The methyl ester formed flattened needles, m.p. 70–71° from methanol–water, $[\alpha]_D$ +118° (*c*, 0.82). Found: C, 79.75; H, 9.95. Calc. for $C_{21}H_{32}O_2$ (316): C, 79.75; H, 10.13.

Partial Hydrogenation of Δ^{13}-Isodextropimaric Acid

Δ^{13}-Isodextropimaric acid (304 mg) in ethanol (20 ml) was hydrogenated in the presence of palladized charcoal catalyst (30%) (150 mg). Hydrogen (23.9 ml) was rapidly absorbed during 2 minutes, after which time absorption ceased abruptly. Calc. for 1 mole, 24.3 ml. The total product, $[\alpha]_D$ +68° (*c*, 1.32; $CHCl_3$) was adsorbed on silica gel (7.5 g) and eluted with 50-ml portions of light petroleum – benzene (1:1) to give seven fractions. Fractions 2 → 6 inclusive were combined and recrystallized three times from acetone–water to give Δ^{13}-dihydroisodextropimaric acid as needles, m.p. and mixed m.p. 107–108° (225 mg), $[\alpha]_D$ +73° (*c*, 0.99; $CHCl_3$).

γ-Lactone of Dihydrodextropimaric Acid

(*a*) *From dihydrodextropimaric acid.*—Dihydrodextropimaric acid (400 mg) was added gradually during 15 minutes to sulphuric acid (2.5 ml, d = 1.84) cooled to −5° C. After 1 hour the reaction mixture was worked up as described previously to give a neutral gum (380 mg), $[\alpha]_D$ −20° (*c*, 1.22), which solidified. The gum was adsorbed on silica gel (10 g) and eluted with 30-ml portions of benzene–ether (19:1) to give six fractions. Fractions 1 → 4 inclusive, when precipitated from methanol solution by water, formed plate-like crystals. These were combined and recrystallized from methanol–water to give the γ-lactone of dihydrodextropimaric acid as plates, m.p. 100°, $[\alpha]_D$ −15° (*c*, 1.17). Found: C, 78.66; H, 10.35. Calc. for $C_{20}H_{32}O_2$ (304): C, 78.94; H, 10.52. Infrared spectrum 1763 cm^{-1} (γ-lactone). Le-Van-Thoi and Ourgaud (28) report m.p. 100° $[\alpha]_j$ −17° (EtOH). The melting point was depressed to 97° on admixture with the γ-lactone of dihydroisodextropimaric acid.

(*b*) *From Δ^{13}-dihydrodextropimaric acid.*—Δ^{13}-Dihydroisodextropimaric acid (100 mg) was added gradually during 15 minutes to sulphuric acid (1 ml, d = 1.84) cooled to −5° C. After 1 hour the reaction mixture was worked up as described previously to give a neutral gum (98 mg), $[\alpha]_D$ −22° (*c*, 1.26), which crystallized on seeding. The product was adsorbed on silica gel (2.5 g) and eluted with benzene–ether (19:1) in 30-ml portions to give seven fractions. Fractions 1 → 5 inclusive were combined and recrystallized from methanol–water to give the γ-lactone of dihydrodextropimaric acid as plates, m.p. and mixed m.p. 100° (58 mg), $[\alpha]_D$ −15° (*c*, 1.07).

γ-Lactone of Dihydroisodextropimaric Acid

(*a*) *From dihydroisodextropimaric acid.*—Dihydroisodextropimaric acid (400 mg) was added gradually during 15 minutes to sulphuric acid (2.5 ml, d = 1.84) cooled to −5° C in a mixture of ice and salt. After being kept at −5° C for 1 hour the reaction mixture was decomposed by being poured into water containing chopped ice. The organic material

was extracted with ether and the extract washed with water to remove mineral acid. The ether extract was then washed with aqueous potassium carbonate (10%) to remove acidic material. The ether extract was washed with water, dried (Na_2SO_4), and evaporated to give a neutral gum (380 mg), $[\alpha]_D$ −19° (*c*, 1.1). The gum was adsorbed on silica gel (10 g) and eluted with 30-ml portions of benzene to give seven fractions. Fractions 1 → 4 inclusive, which when thrown out of methanol solution by water formed plate-like crystals, were combined and recrystallized from methanol–water to give the γ-lactone as plates, m.p. 105–106° (250 mg), $[\alpha]_D$ −90° (*c*, 1.59). Found: C, 78.57; H, 10.47. Calc. for $C_{20}H_{32}O_2$ (304): C, 78.94; H, 10.52. Infrared spectrum 1770 cm^{-1} (γ-lactone).

(*b*) *From* Δ^{13}*-dihydroisodextropimaric acid.*—Δ^{13}-Dihydroisodextropimaric acid (80 mg) was added gradually during 15 minutes to sulphuric acid (0.6 ml, d = 1.84) cooled to −5° C in a mixture of ice and salt. After being kept at −5° C for 1 hour the reaction mixture was worked up as described above to give a neutral gum (79 mg), $[\alpha]_D$ −18° (*c*, 1.01). The gum was adsorbed on silica gel (3 g) and eluted with benzene. The first fractions were recrystallized from methanol–water to give the γ-lactone as plates, m.p. and mixed m.p. 105–106° (43 mg), $[\alpha]_D$ −8° (*c*, 1.06).

δ-Lactone of Dihydroisodextropimaric Acid

(*a*) *From dihydroisodextropimaric acid.*—Dihydroisodextropimaric acid (170 mg) was added gradually during 15 minutes to sulphuric acid (3 ml, d = 1.84) at room temperature (23° C). After 5 hours the reaction mixture was poured into water containing chopped ice. The organic material was extracted with ether and washed with water to remove mineral acid. The ether extract was then washed with aqueous potassium carbonate (10%) to remove acidic material. The ether extract was washed with water, dried (Na_2SO_4), and evaporated to give a neutral gum (168 mg), $[\alpha]_D$ −31° (*c*, 1.14). The gum was adsorbed on silica gel (4 g) and eluted with 30-ml portions of benzene to give eight fractions. Fractions 4 → 8 inclusive, which when thrown out of methanol solution by water formed plate-like crystals, were combined and recrystallized from methanol–water to give the δ-lactone as plates, m.p. 74–75° (70 mg), $[\alpha]_D$ −40° (*c*, 0.93). Found: C, 79.05; H, 10.49. Calc. for $C_{20}H_{32}O_2$ (304): C, 78.94; H, 10.52. Infrared spectrum 1720 cm^{-1} (δ-lactone). A further crop of plates, m.p. 72–74° (30 mg) was obtained from the mother liquors.

(*b*) *From the γ-lactone.*—The γ-lactone (80 mg) was gradually added during 15 minutes to sulphuric acid (2 ml, d = 1.84) at room temperature (23° C). After 5 hours the lactonic material was isolated as described above to give a colorless gum (80 mg), $[\alpha]_D$ −29° (*c*, 0.93), which solidified on seeding. The total product was adsorbed on silica gel (2 g) and eluted with benzene in 30-ml portions to give four fractions. The last two fractions were combined and recrystallized from methanol–water to give the δ-lactone as plates, m.p. and mixed m.p. 73–74° (40 mg) $[\alpha]_D$ −39° (*c*, 0.97).

Isomerization of Ukita's Acid Using Hydrogen Chloride

Dry hydrogen chloride was passed into a solution of Ukita's acid (20 mg) in dry chloroform (15 ml) at −5° for 4 hours. The chloroform solution was washed free from mineral acid with water, and then dried, and evaporated to give a colorless gum (19 mg), $[\alpha]_D$ +108° (*c*, 0.79), which was twice recrystallized from acetone–water to give Δ^{13}-isodextropimaric acid as stout prisms (15 mg), m.p. and mixed m.p. 105–107°, $[\alpha]_D$ +110° (*c*, 1.08).

Partial Hydrogenation of Ukita's Acid

A solution of Ukita's acid (15.5 mg) in ethanol (7 ml) was hydrogenated in the presence

of pre-reduced palladized charcoal catalyst (30%, 3 mg); 1 mole of hydrogen (1.25 ml) was absorbed during 8 minutes and then absorption ceased. The crude product, m.p. 148–152° was recrystallized five times from methanol–water to give the dihydro-acid as prisms, m.p. 154–157° (9.4 mg), $[\alpha]_D$ +18° (*c*, 0.72). Found: C, 78.96; H, 10.31. Calc. for $C_{20}H_{32}O_2$ (304): C, 78.94; H, 10.52. Infrared spectrum 1700 cm^{-1} (—COOH); 825 cm^{-1} (trisubstituted double bond).

γ-Lactone of Isodextropimaric Acid

Isodextropimaric acid (200 mg) in dry dioxane (20 ml) was refluxed under nitrogen with *p*-toluenesulphonic acid (1 g) for 4 hours and then allowed to stand overnight. The dioxane was evaporated off and the viscous residue taken up in ether. Extraction of the ether solution with aqueous potassium carbonate (10%) gave only 15 mg of acidic material which was not further investigated. The ether layer was washed with water and dried (Na_2SO_4). On evaporation of the ether a neutral gum (180 mg), $[\alpha]_D$ −18° (*c*, 1.24), was obtained. The product was adsorbed on silica (4 g) and eluted with benzene in 20-ml portions to give five fractions. Fractions 4 and 5 gave some solid material with methanol–water and after several recrystallizations from methanol–water, the γ-lactone of isodextropimaric acid formed plates, m.p. 128–130° (15 mg), $[\alpha]_D$ −1° (*c*, 0.84). Found: C, 79.59; H, 9.90. Calc. for $C_{20}H_{30}O_2$ (302): C, 79.49; H, 9.93. Infrared spectrum: 1770 cm^{-1} (γ-lactone); 1480 cm^{-1}, 1000 cm^{-1}, 910 cm^{-1} (vinyl group).

Treatment of Isodextropimaric Acid with Formic Acid

Isodextropimaric acid (500 mg) was refluxed for 60 hours with formic acid (90%, 75 ml). The formic acid was evaporated under reduced pressure. Globules of oil which steam-distilled over were isolated by extracting the neutralized distillate with ether, and proved to be a mobile hydrocarbon (84 mg), $[\alpha]_D$ +4° (*c*, 0.79). The distillation residue was dissolved in ether and washed free from formic acid with water. The dried ether extract gave a brown gum (385 mg), $[\alpha]_D$ +18° (*c*, 1.5) on evaporation. Infrared spectrum ($CHCl_3$) 3520 cm^{-1} (—OH), 1780 cm^{-1} (γ-lactone), 1730 cm^{-1} (δ-lactone); absence of carboxyl and vinyl groups. The product was split into the following fractions by chromatography on neutral alumina (Grade IV, 10 g).

A. Hexane (20 ml) readily eluted a mobile hydrocarbon fraction (38 mg).

B. Hexane (200 ml) gave 10 fractions, $[\alpha]_D$ −43° to −34° which were combined (137 mg).

C. Benzene and chloroform eluted further fractions as gums (210 mg).

To fraction C was added material (60 mg) from the mother liquors of the recrystallization of fraction B. Further chromatography of this material on neutral alumina (Grade II, 5 g) gave the following fractions.

D. Hexane (100 ml) eluted material which crystallized from methanol–water (125 mg) $[\alpha]_D$ −28° (*c*, 0.98).

E. Benzene eluted non-crystalline material.

F. Benzene–chloroform (3:1) eluted material (25 mg), m.p. 170–172°, which crystallized spontaneously on evaporation of the solvent.

Investigation of the Fractions

A. The hydrocarbon fraction was combined with that from the steam distillate and warmed with aqueous sodium hydroxide (10%). The hydrocarbon, recovered by ether extraction, was dissolved in hexane and percolated through alumina. The hydrocarbon distilled as a colorless mobile oil, b.p. 90° at 0.05 mm, n_D^{24} 1.5125, $[\alpha]_D$ +6° (*c*, 1.09). Found: C, 88.21; H, 12.10. Calc. for $C_{19}H_{30}$: C, 88.30; H, 11.70.

B. The combined material (137 mg) was recrystallized twice from methanol–water and then four times from methanol to afford prisms, m.p. 109.5–111° (70 mg), $[\alpha]_D$ −52° (*c*, 0.97). Found: C, 79.12; H, 9.60. Calc. for $C_{20}H_{30}O_2$ (302): C, 79.49; H, 9.93. Infrared spectrum 1762 cm^{-1} (γ-lactone); no bands for ethylenic bonds.

When the above γ-lactone (24.4 mg) in acetic acid (6 ml) was hydrogenated in the presence of Adams' catalyst (10 mg), 0.96 mole of hydrogen was absorbed in 1 hour. The crystalline product, recrystallized from methanol–water afforded prisms, m.p. 131–132°, $[\alpha]_D$ −5° (*c*, 0.8). Found: C, 78.78; H, 10.32. Calc. for $C_{20}H_{32}O_2$ (304): C, 78.94; H, 10.52. This material is identical (mixed m.p. 131–132°) with the known γ-lactone obtained from any of the dihydroabietic acids (see below).

D. Fraction D was recrystallized from methanol–water to give a further crop of γ-lactone, m.p. 109.5–111° (47 mg).

E. No solid material could be isolated from this fraction.

F. Recrystallization of this fraction from methanol gave needles, m.p. 179–180°, $[\alpha]_D$ −6° (*c*, 0.9). Found: C, 75.08; H, 9.83. Calc. for $C_{20}H_{32}O_3$ (320): C, 74.96; H, 10.06. Infrared spectrum: 3548 cm^{-1} (—OH), 1764 cm^{-1} (γ-lactone). This is clearly the known hydroxy-γ-lactone from dextropimaric acid (38).

Partial Hydrogenation of Neoabietic Acid

Neoabietic acid (1.035 g) in ethanol (40 ml) in the presence of palladized charcoal (30%, 200 mg) rapidly absorbed 1.07 moles of hydrogen in 11 minutes, after which time absorption became comparatively slow. The ultraviolet spectrum of the product $[\alpha]_D$ +26° (*c*, 1.2) showed the presence of less than 1% of neoabietic acid. Chromatography on silica gel using hexane as eluting solvent gave 14 fractions. Fractions 1 → 6 having rotations ranging from +12° to +25° were combined (530 mg). Fractions 7 → 14 of $[\alpha]_D$ +37° gave A-dihydroabietic acid (29) on crystallization from methanol–water (98 mg), m.p. 149°, $[\alpha]_D$ +43° (*c*, 1.03). Found: C, 78.66; H, 10.27. Calc. for $C_{30}H_{32}O_2$ (304): C, 78.94; H, 10.52. Infrared spectrum: 1697 cm^{-1} (—COOH); 826 cm^{-1} (trisubstituted double bond).

Fractions 1 → 6, together with material (340 mg) from the mother liquors of the recrystallization of fractions 7 → 14, were converted to the piperidine salt and recrystallized from acetone. Two crops of the least soluble material, $[\alpha]_D$ +31° (*c*, 1.5) and $[\alpha]_D$ +27° (*c*, 0.9), were combined (350 mg) and reconverted to acid, $[\alpha]_D$ +35° (*c*, 0.94). Recrystallization from methanol–water afforded a further crop of A-dihydroabietic acid as needles (165 mg), m.p. 147–148°, $[\alpha]_D$ +39° (*c*, 0.99). The more soluble piperidine salt gave acid (580 mg), $[\alpha]_D$ +19° (*c*, 1.0).

γ-Lactone of A-Dihydroabietic Acid

A-Dihydroabietic acid (165 mg) was added gradually during 15 minutes to sulphuric acid (1 ml, d = 1.84) cooled to −5°. After 1 hour the reaction mixture was worked up as in the previous examples to give neutral material which crystallized spontaneously. Chromatography on alumina (Grade III, neutral) using hexane as eluting solvent gave the γ-lactone as prisms, m.p. 132°, $[\alpha]_D$ −4° (*c*, 1.04). Found: C, 78.96; H, 10.35. Calc. for $C_{20}H_{32}O_2$ (304): C, 78.94; H, 10.52. Infrared spectrum: 1758 cm^{-1} (γ-lactone).

The non-crystalline dihydroneoabietic acid $[\alpha]_D$ +19° afforded the same γ-lactone on similar treatment.

ACKNOWLEDGMENTS

We are indebted to Mr. R. V. Lawrence for a supply of pine gum and rosin, and

valuable advice on the isolation of the acids, and to Dr. T. F. Sanderson for a generous sample of dextropimaric acid, a gift of Staybelite resin, and valuable advice. We wish to thank Mr. A. Knoll for technical assistance, Mr. H. Seguin for the analyses, and Mr. R. Lauzon for determining the infrared absorption spectra.

REFERENCES

1. Edwards, O. E. and Howe, R. Chem. & Ind. 629 (1958).
2. Briggs, L. H., Cain, B. F., and Wilmshurst, J. K. Chem. & Ind. 599 (1958).
3. Wenkert, E. Chem. & Ind. 282 (1955).
4. Brandt, C. W. New Zealand J. Sci. Technol. B, **34**, 46 (1952).
5. Bottomley, W., Cole, A. R. H., and White, D. E. J. Chem. Soc. 2624 (1955).
6. Djerassi, C., Riniker, R., and Riniker, B. J. Am. Chem. Soc. **78**, 6362 (1956).
7. Briggs, L. H., Cawley, R. W., Loe, J. A., and Taylor, W. I. J. Chem. Soc. 955 (1950).
8. Mosettig, E. and Nes, W. R. J. Org. Chem. **20**, 884 (1955).
9. Haworth, R. D. and Johnstone, R. A. W. J. Chem. Soc. 1492 (1957).
10. Djerassi, C., Cais, M., and Mitscher, L. A. J. Am. Chem. Soc. **80**, 246 (1958).
11. Cross, B. E., Grove, J. F., MacMillan, J., and Mulholland, T. P. C. Proc. Chem. Soc. 221 (1958).
12. Wiesner, K., Armstrong, R., Bartlett, M. F., and Edwards, J. A. J. Am. Chem. Soc. **76**, 6068 (1954).
13. Dvornik, D. and Edwards, O. E. Chem. & Ind. 623 (1958).
14. Dvornik, D. and Edwards, O. E. Proc. Chem. Soc. 280 (1958).
15. Ruzicka, L., de Graaff, G. B. R., Goldberg, M. W., and Frank, B. Helv. Chim. Acta, **15**, 915 (1932).
16. Simonsen, J. and Barton, D. H. R. The terpenes. Vol. III. Cambridge University Press. 1952. p. 448.
17. Harris, G. C. and Sanderson, T. F. J. Am. Chem. Soc. **70**, 2079 (1948).
18. Harris, G. C. and Sanderson, T. F. J. Am. Chem. Soc. **70**, 2081 (1948).
19. Wenkert, E. and Chamberlin, J. W. J. Am. Chem. Soc. **80**, 2912 (1958).
20. Green, B., Harris, A., and Whalley, W. B. Chem. & Ind. 1084 (1958).
21. Ukita and Tsumita. J. Pharm. Soc. Japan, **72**, 1324 (1952).
22. Hasselstrom, T. and Bogert, M. T. J. Am. Chem. Soc. **57**, 2118 (1935).
23. Ukita, Tsumita, and Utsugi. Pharm. Bull. Japan, **3**, 441 (1955).
24. Ruzicka, L., Huyser, H. W., and Seidel, C. F. Rec. trav. chim. **47**, 363 (1928).
25. Le-Van-Thoi and Ourgaud, J. Bull. soc. chim. France, 205 (1956).
26. Vesterberg, K. A. Ber. **19**, 2167 (1886).
27. Ruzicka, L. and Balas, F. Ann. **460**, 202 (1928).
28. Le-Van-Thoi and Ourgaud, J. Bull. soc. chim. France, 202 (1956).
29. Velluz, L., Muller, G., Petit, A., and Mathieu, J. Bull. soc. chim. France, 401 (1954).
30. Fieser, L. F. J. Am. Chem. Soc. **75**, 4395 (1953).
31. Bruun, H. H. Acta Acad. Aboensis, Math. et Phys. **19**(3), 7 (1954).
32. Bruun, H. H. Finska Kemistsamfundets Medd. **63**, 22 (1954).
33. Adam, N. K., Askew, F. A., and Danielli, J. F. Biochem. J. **29**, 1786 (1935).
34. Bruun, H. H. Paperi ja Puu, **38**, 577 (1956).
35. Bruun, H. H. Paperi ja Puu, **39**, 221 (1957).
36. Bruun, H. H., Ryage, R., and Stenhagen, E. Acta Chem. Scand. **12**, 789 (1958).
37. Brandt, C. W. New Zealand J. Sci. Technol. **20**, 8 (1938).
38. Fleck, E. E. and Palkin, S. J. Am. Chem. Soc. **62**, 2044 (1940).
39. Barton, D. H. R. Chem. & Ind. 638 (1948).
40. Subluskey, L. A. and Sanderson, T. F. J. Am. Chem. Soc. **76**, 3512 (1954).
41. Lombard, R. and Ebelin, J. Bull. soc. chim. France, 930 (1953).
42. Loeblich, V. M. and Lawrence, R. V. J. Org. Chem. **21**, 610 (1956).

APPLICATIONS OF PROTON MAGNETIC RESONANCE SPECTRA IN FATTY ACID CHEMISTRY[1]

C. Y. Hopkins and H. J. Bernstein

ABSTRACT

An introductory study has been made of the proton magnetic resonance spectra of fatty acids, fatty acid esters, and natural glyceride oils. Characteristic signals were recorded for the hydrogens of such groupings as hydroxy, acetoxy, and epoxy; isolated, conjugated, and methylene-interrupted double bonds; and others. Examples are given of the application of this technique in identifying the fatty acids of natural glyceride oils. Semiquantitative estimations are shown to be feasible. Evidence for Nunn's formula for sterculic acid is discussed on the basis of the spectra of the acid and its derivatives.

Proton magnetic resonance measurements provide a new method of distinguishing certain groupings in fatty acid molecules. This preliminary study indicates that the method is of value in determining the structure of fatty acids and their derivatives and in estimating in a roughly quantitative manner the proportions of certain fatty acids in mixtures. Quantitative estimation is applicable in some degree to single mixed glycerides and to natural oils, which are mainly mixtures of mixed glycerides.

Small amounts of impurities are not likely to interfere, since components constituting less than 5% of the sample do not usually give a measurable signal.

In the present work measurements were made with a Varian V-4300 NMR spectrometer operating at a frequency of 40 Mc/s and equipped with a Varian Field Stabilizer. Each sample was dissolved in chloroform at sufficiently high concentration to give signals of moderate intensity. Some of the oxygenated acids were used at maximum solubility. Usually 0.2 to 0.5 g of sample was dissolved in 0.5 to 1.0 ml of chloroform. The sample tube was 5 mm o.d. and was set spinning by a jet of nitrogen.

Chemical shifts were measured from the dissolved chloroform signal or that of the long-chain CH_2 signal by the well-known side-band technique. All chemical shifts were referred to the long-chain CH_2 signal, the signals at lower applied field having negative values. All figures are displayed with applied magnetic field increasing toward the right.

MATERIALS

Oleic acid, methyl oleate, and methyl linoleate were prepared from natural oils by fractional distillation of the esters followed by low-temperature crystallization. 9,10-Diacetoxystearic acid was made by acetylating the pure dihydroxy acid. 12,13-Dihydroxyoleic acid was prepared from the seed oil of *Vernonia colorata* by Gunstone's procedure (1). Commercial ethyl ricinoleate was purified by low-temperature crystallization.

Vernonia oil and *Sterculia* oil were extracted in the laboratory from seed of *Vernonia colorata* and *Sterculia foetida* respectively. The other oils and the lauric acid were commercial products. Methyl 10,12-octadecadienoate was kindly supplied by Dr. O. S. Privett.

Sterculic acid was made by cold saponification of *Sterculia* oil, followed by repeated crystallization from acetone at low temperature. It was hydrogenated with palladium

[1]*Manuscript received December 16, 1958.*
Contribution from the Division of Pure Chemistry, National Research Council, Ottawa, Canada.
Issued as N.R.C. No. 5093.

catalyst. 9,11-Diketononadecanoic acid, m.p. 59–60°, was obtained by controlled oxidation of sterculic acid.

RESULTS AND DISCUSSION

Typical spectra are shown in Fig. 1. The saturated acid, lauric, shows the signals common to all fatty acids. The groupings and the position of the corresponding signals were as follows (parts per million): terminal CH_3, +0.43; CH_2 groups of the chain, 0; CH_2 adjacent (α) to the carboxyl group, −1.0. The position of the signal for the carboxy hydrogen (offscale to low field) is strongly affected by the degree of dilution and is not shown.

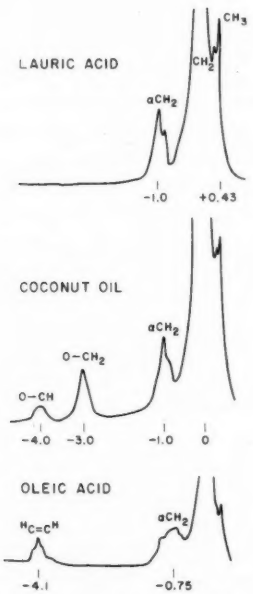

FIG. 1. Proton resonance spectra of a saturated acid, a highly saturated oil, and a monounsaturated acid. The signal for the acid proton is offscale to the left.

Coconut oil, consisting mainly of glycerides of saturated acids, shows the signals for terminal CH_3, CH_2 chain, and αCH_2, and also for the glyceryl residue.* The two $O-\underset{|}{CH_2}$ groups of the glyceryl radical appeared at −3.0 p.p.m. with intensity 4 (four protons) and the $O-\underset{|}{CH}$ at −4.0 p.p.m. with intensity 1.

Oleic acid produced a signal at −4.1 p.p.m. characteristic of the monounsaturated grouping CH=CH. The CH_2 groups adjacent to the double bond carbons contribute to the intensity of the signal at −0.75 p.p.m.

Double Bond Unsaturation

Characteristic signals for the various types of double bond groupings were observed. Those for simple monoenes, 1,4-dienes, and conjugated dienes are shown in Fig. 2.

**The identification of these signals followed by comparison with the spectrum of glyceryl triacetate.*

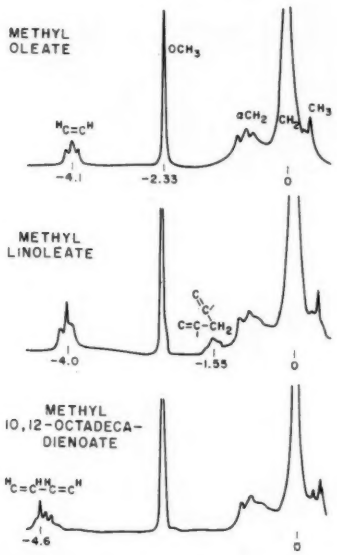

FIG. 2. Proton resonance spectra of methyl esters of a monoenoic acid, a non-conjugated dienoic acid, and a conjugated dienoic acid.

The CH_3 of the ester group in these compounds gave a sharp peak at -2.32 to -2.35 p.p.m. In the 1,4-diene, methyl linoleate, the signal at -1.55 p.p.m. for the CH_2 of the divinyl methane grouping has half the intensity of the signal for the two CH=CH groups, since the latter contain a total of four protons. In the 1,3-diene, methyl 10,12-octadecadienoate, the effect of conjugation on the ethylenic protons is to shift the signal to low field (-4.6 p.p.m.). The divinyl methane signal has disappeared.

Hydroxy- and Keto-acids

The —CHOH group in hydroxy acids is recognized by two signals, one for each hydrogen, at different frequencies (Fig. 3). Thus 12,13-dihydroxyoleic acid, in addition to the usual peaks shown by oleic acid, gave a signal at -2.2 p.p.m. due to the —CH—O groups. The position of the —OH signal varies with concentration (8), and is observed here at -4.8 p.p.m. In these experiments the concentration was not standardized. Accordingly, the —OH signal appeared at -1.2 p.p.m. in ethyl ricinoleate. The quartet and triplet characteristics of the ethyl group of the ethyl ester are clearly observed.

The spectrum of 9,11-diketononadecanoic acid indicates that enolization has taken place to a large extent. A diketone enolizes according to the mechanism:

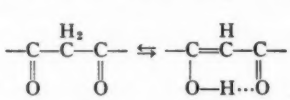

Keto Enol

The hydrogen-bonded signal of the enol form has been found in acetylacetone to appear at very low field (2). The signal at -4.1 p.p.m. corresponds to the C=CH group in the enol form and that at about -2.1 p.p.m. to the CH_2 group of the keto form. This

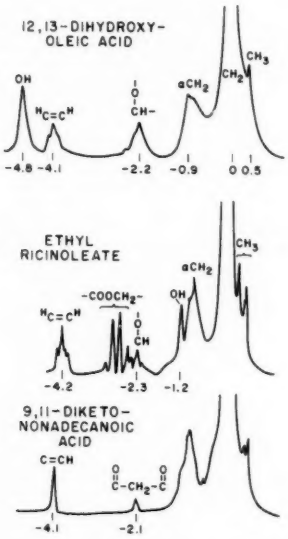

FIG. 3. Proton resonance spectra of compounds having hydroxy- and keto-groups.

is 2 p.p.m. to high field of the C=CH signal in acetylacetone also (2). From the relative areas under these signals (~1:3) the ratio of keto to enol concentration is about 1:6.

Epoxy Acids and Epoxy Oils

The epoxy group $-\underset{H}{\overset{O}{\overset{/\backslash}{C}}}-\underset{H}{C}-$ in the long-chain fatty acids produced a signal at −1.55 to −1.7 p.p.m. This has been shown in 9,10-epoxystearic acid and 12,13-epoxyoleic acid (3), and in 9,10,12,13-diepoxystearic acid.

Certain natural oils are known to contain 12,13-epoxyoleic acid as glyceride. However, detection of the epoxy group in these oils is complicated by the fact that linoleate is usually present and gives a signal at approximately the same position in the field. Thus the seed oil of *Vernonia colorata*, in which the fatty acids are approximately 70% epoxyoleic and 15% linoleic, gave a signal in the region of −1.65 p.p.m. which is due to the summation of the signals due to the epoxy group protons and the diene-activated CH_2 of the 1,4-dienoic acid (A, Fig. 4).

To resolve this difficulty, the oil was acetylated, thereby converting the epoxy group to diacetoxy. The residual intensity at −1.75 p.p.m. is due then to the contribution of the CH_2 group of the 1,4-diene, (B, Fig. 4). The acetylated oil produced a new signal at −2.3 p.p.m., attributed to the hydrogens adjacent to the acetyl groups. 9,10-Diacetoxystearic acid gave a signal at approximately the same position, −2.4 p.p.m. The triplet structure (spacing of 6.2 c/s) is probably due to spin–spin coupling with the hydrogens of the adjacent CH_2 group. The hydrogens of the two acetyl groups produced two sharp peaks in the vicinity of −0.8 p.p.m.

This acetylation procedure seems useful in detecting or confirming the presence of epoxy acids in natural oils where the amount exceeds 5% of the total acids.

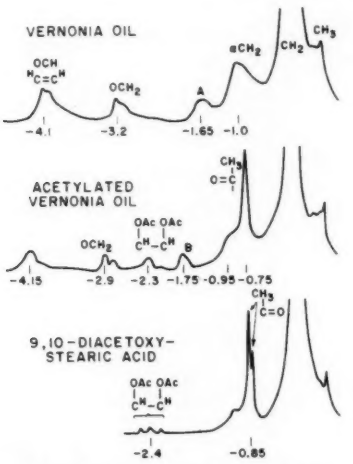

FIG. 4. Proton resonance spectra of an epoxy-acid oil, showing the effect of acetylation, and a simple diacetoxy acid.

Examination of Natural Fatty Oils

It is evident from the foregoing data that useful information on the components of natural glyceride oils can be obtained from proton magnetic resonance absorption measurements. The presence of free carboxyl, hydroxy, 1,4-diene, conjugated double bonds, and isolated double bonds can usually be determined by inspection of the spectra. By converting the oil to methyl esters and determining the spectrum of the mixed esters, the glycerol signals are eliminated and no longer interfere with the signal of the isolated double bonds.

Confirmation of the presence of the OH group can be obtained by acetylating, whereby the product gives a new signal due to the acetoxy group. Similarly, oils having a 1,4-diene grouping can be isomerized to the conjugated form, producing a new signal which is readily identified.

Quantitative applications are also possible. The intensity of a given signal is directly proportional to the number of protons contributing to it. By comparing the areas of peaks in the same spectrum, estimates can be made of the relative proportions of certain groupings in the sample. The glyceryl radical provides a useful internal reference standard for such calculations in examining the oils. Its signal A at -3.0 p.p.m. (Fig. 5) is due to the two —OCH groups and thus represents four protons. Its signal B at -4.0 (—OCH) represents only one proton.

On this basis, one can calculate the ratios of saturated: monoene: diene fatty acids in ordinary glyceride oils composed of these three types of acids. The degree of precision is of the order of ± 5 units %.

In the spectrum for cocoa butter (Fig. 5), the absence of a signal in the region of -1.55 p.p.m. shows that there is little or no 1,4-diene (actually about 2% of linoleate is present), so that for purposes of calculation the component acids are regarded as consisting of saturated and monoenoic acids. If the acid residues were entirely monoenoic the ratio of the area of B to the total area of A would be 7:4 ($3 \times$ CH=CH+OCH: $2 \times OCH_2$) since there would be three molecules of monoenoic acid to one of glycerol. The component

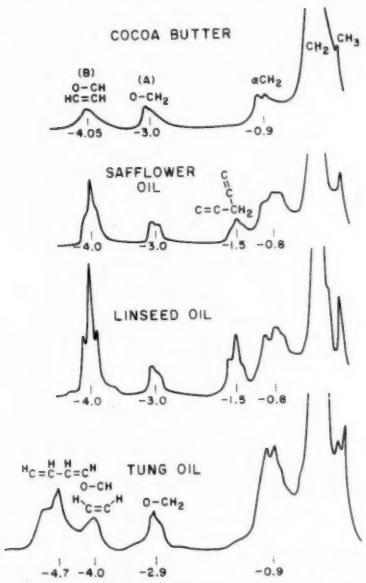

FIG. 5. Proton resonance spectra of typical oils. The increasing degree of unsaturation in the first three oils is indicated by the ratio of the areas of the B and A signals. In tung oil the total unsaturation is indicated by the peaks at −4.0 and −4.7 p.p.m.

of B due to the OCH group is one-quarter of the area of the A signal (one proton/four protons). Therefore, deducting one-quarter of the area of A from B gives the area due to the CH=CH groups. If the acids were entirely monoenoic, the ratio of this area to A would be 6:4. By actual measurement, the ratio was found to be about 2.4:4, hence the ratio of monounsaturated acids to total acids is about $(2.4 \div 6) : 1 = 0.4 : 1$ in this sample.

By extending this procedure to include the diene signal at −1.55 p.p.m., the ratios of saturated: monoene: diene in cottonseed or similar oils can be estimated. Similarly the proportion of conjugated acid, e.g. in tung oil, can be estimated by comparing the areas of the glyceryl signal and the signal at −4.7 p.p.m. In the curve for tung oil, the signal at −4.0 p.p.m. represents the non-conjugated ethylenic groups of oleic and linoleic acids present in the oil, in conjunction with the O—CH— glycerol signal.

cis- and trans-Groupings

Two pairs of *cis–trans* isomeric compounds were examined, viz. oleic and elaidic acids, and *cis-* and *trans*-9,10-epoxystearic acid. 12,13-Epoxyoleic acid, prepared by the action of peracetic acid on linoleic acid, was also compared with *Vernonia colorata* oil, which contains *cis*-12,13-epoxyoleic acid as glyceride. The difference in the positions of the double bond signals and the epoxy group signals in these pairs of compounds was not great enough to be significant. However, the possibility of a significant difference between *cis-* and *trans*-groupings under more exactly controlled conditions is not excluded.

Constitution of Sterculic Acid

The spectra of sterculic acid and some of its derivatives were examined to obtain evidence for the structure of the acid, which has been in dispute (4, 5).*

**Shortly after our work was completed, the proton resonance spectrum of sterculic acid was reported by Rinehart, Nilsson, and Whaley (6).*

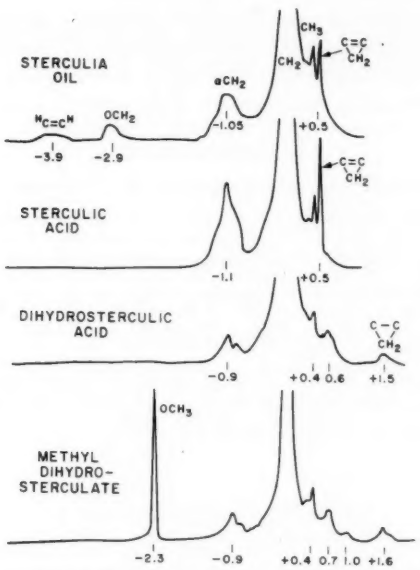

FIG. 6. Proton resonance spectra of *Sterculia* oil, sterculic acid, and two derivatives. The signal of the CH_2 group of the cyclopropane ring is at +1.5 p.p.m.

In our experiments, *Sterculia foetida* oil showed a signal of low intensity at −3.9 p.p.m. attributable to the unsaturated linkages of the small percentage of ordinary unsaturated acids in the glycerides. Sterculic acid itself, prepared by cold saponification of the oil and crystallization of the acids at low temperature, gave no signal in the region expected for isolated double bonds. Hence the proposed formula (5)

$$CH_3(CH_2)_8\underset{\diagdown\,\diagup}{CH}\!-\!CH\!-\!CH\!=\!CH(CH_2)_7COOH$$
$$\quad\;\; CH_2$$

I

is judged to be incorrect. Absence of the signal for the CH_2 group of the cyclopropane ring in the region of +1.5 p.p.m. is further evidence for the rejection of formula I.

The signal at +0.5 p.p.m., attributed by Rinehart and co-workers (6) to the cyclopropene ring of Nunn's formula

$$CH_3(CH_2)_7C\!=\!C\!-\!(CH_2)_7COOH,$$
$$\quad\;\; \diagdown\,\diagup$$
$$\quad\;\; CH_2$$

II

can scarcely be regarded as positive proof of structure II until the position of this signal has been confirmed by examining model compounds of similar structure. However, hydrogenation of sterculic acid to dihydrosterculic acid undoubtedly gives a cyclopropane ring, as confirmed by synthesis (7) and the magnetic resonance spectrum of dihydrosterculic acid (Fig. 6) gives a signal at 1.5 p.p.m., which is characteristic of the CH_2 group in a cyclopropane ring.* Since this signal is absent in the spectrum of sterculic acid,

**Unpublished results (H.J.B.).*

formula I is clearly inadmissible and the NMR evidence strongly supports formula II. The spectra of dihydrosterculic acid and its methyl ester were identical except for the carboxy and ester signals respectively. The signal at 0.7 p.p.m. has not been positively identified but is possibly associated with the CH groups of the cyclopropane ring.

ACKNOWLEDGMENT

We wish to acknowledge the assistance of J. R. Nicholson in obtaining the NMR spectra.

REFERENCES

1. GUNSTONE, F. D. J. Chem. Soc. (London), 1611 (1954).
2. JARRET, H. S., SADLER, M. S., and SHOOLERY, J. N. J. Chem. Phys. **21**, 2092 (1953).
3. CHISHOLM, M. J. and HOPKINS, C. Y. Can. J. Chem. **35**, 358 (1957).
4. NUNN, J. R. J. Chem. Soc. 313 (1952).
5. VARMA, J. P., NATH, B., and AGGARWAL, J. S. Nature, **175**, 84 (1955).
6. RINEHART, K. L., JR., NILSSON, W. A., and WHALEY, H. A. J. Am. Chem. Soc. **80**, 503 (1958).
7. HOFMANN, K., OROCHENA, S. F., and YOHO, C. W. J. Am. Chem. Soc. **79**, 3608 (1957).
8. COHEN, A. D. and REID, C. J. Chem. Phys. **25**, 790 (1956).

EFFECT OF PRESSURE ON THE SPONTANEOUS AND THE BASE-CATALYZED HYDROLYSES OF EPOXIDES[1]

J. KOSKIKALLIO[2] AND E. WHALLEY

ABSTRACT

The effect of pressures up to 3000 atm on the spontaneous and the base-catalyzed hydrolyses of ethylene and propylene oxides has been determined. It is that expected from the accepted mechanisms. The volumes of activation of ion–molecule reactions that probably occur without major change in polarity are reviewed. For all reactions that have been studied so far in which a C–O bond is formed the volumes of activation are about -5 to -10 cm^3 mole^{-1}.

1. INTRODUCTION

Epoxides hydrolyze spontaneously and by acid and base catalysis (1, 2, 3). We have already described (4) the effect of pressure on the acid-catalyzed reaction, and in this paper the effect of pressure on the base-catalyzed and the spontaneous hydrolyses is described.

2. EXPERIMENTAL METHODS

The epoxides, the pressure technique, and the method of analysis for epoxide were as described in a previous paper (4). At 1 atm, 5-ml sealed ampoules were used for the rate measurements. The concentration of epoxide was about 0.1 *M* at the start of each run. About seven samples were taken during each run.

Spontaneous hydrolysis.—The rates of hydrolysis in a buffer solution containing 0.001-*M* 2,4,6-trimethylpyridine and 0.0015-*M* 2,4,6-trimethylpyridinium perchlorate (3) (pH 7.3) were taken to be the rates of the spontaneous hydrolysis. There was a difference of only a few per cent between the rates in the buffer and in pure water.

Alkaline hydrolysis.—The alkali was carbonate-free sodium hydroxide and was usually about 0.01 *M*. The first-order rate constant k is given by

$$k = k_0 + k_b c_{OH^-},$$

where k_0 and k_a are the rate constants for the spontaneous and the base-catalyzed reactions and c_{OH^-} is the concentration of hydroxyl ion at the temperature and pressure of the experiment. The calculation of k_b is straightforward. The compression and thermal expansion of the solution were assumed to be the same as those of pure water (5).

3. RESULTS

The experimental rate constants for the spontaneous hydrolysis of ethylene and propylene oxides are given in Table I and those for the base-catalyzed hydrolysis of ethylene oxide are given in Table II. Previous measurements at 1 atm are given for comparison; the agreement is good.

The rate constants at 1 atm for the spontaneous hydrolysis were fitted graphically to the Arrhenius equation, and the Arrhenius energy E_A and the enthalpy $\Delta H^{\ddagger}$ and entropy $\Delta S^{\ddagger}$ of activation were obtained. We found:

[1]*Manuscript received December 19, 1958.*
Contribution from the Division of Applied Chemistry, National Research Council, Ottawa, Canada.
Issued as N.R.C. No. 5070.
[2]*N.R.C. Postdoctorate Fellow 1957–58. Present address: Department of Chemistry, University of Helsinki, Helsinki, Finland.*

$$E_A = 19.5 \pm \sim .2 \text{ kcal mole}^{-1},$$

$$\Delta H^{\ddagger} = 18.9 \pm \sim .2 \text{ kcal mole}^{-1},$$

and

$$\Delta S^{\ddagger} = -23.6 \pm \sim .6 \text{ cal deg}^{-1} \text{ mole}^{-1},$$

the errors being estimated. Our value of E_A agrees well with Lichtenstein and Twigg's (2), 19.0±.3 kcal mole^{-1}.

TABLE I

Spontaneous hydrolysis of ethylene and propylene oxides

			$10^4 k_0$/sec^{-1}		
Oxide	Temp.	p/atm	This work	Ref. (1)	Ref. (3)
Ethylene	20° C	1	(0.332)*	0.413	0.36
	25° C	1	0.58		
		1000	1.07		
		2000	1.71		
		3000	2.58		
	60° C	1	19.2		
		500	27.2		
		1000	36.6		
		2000	59.1		
		3000	86.5		
	70° C	1	43.9	43.1	
		1000	86.3		
		2000	135		
		3000	206		
Propylene	25° C	1	0.69		
		3000	3.32		
	60° C	1	21.1		
		3000	95.2		

*The value in parentheses is extrapolated using the Arrhenius equation.

TABLE II

Base-catalyzed hydrolysis of ethylene oxide at 60° C

		$10^3 k_b$/l. mole^{-1} sec^{-1}	
p/atm	c_{OH^-}/mole l.$^{-1}$	This work	Ref. (2)
1	0.0102	2.76	(2.79)*
1	0.0195	2.81	
1	0.0390	2.84	
500	0.0097	3.19	
1000	0.0102	3.64	
1000	0.0196	3.58	
2000	0.0102	4.31	
2000	0.0196	4.56	
3000	0.0098	5.71	
3000	0.0106	5.33	

*The value in parentheses is interpolated.

The rate constants as a function of pressure at constant temperature for both the spontaneous and the base-catalyzed hydrolyses are shown in Fig. 1. The volumes of activation at 1 atm were obtained graphically; values found were, for the spontaneous hydrolysis,

at 25° C $\Delta V^{\ddagger} = -15.9 \pm \sim 1$ cm³ mole^{-1},

at 60° C $\Delta V^{\ddagger} = -18.9 \pm \sim 1$ cm³ mole^{-1},

and

at 70° C $\Delta V^{\ddagger} = -19.9 \pm \sim 1$ cm³ mole^{-1};

for the base-catalyzed hydrolysis

at 60° C $\Delta V^{\ddagger} = -7.0 \pm \sim 1$ cm³ mole^{-1}.

The errors are estimated.

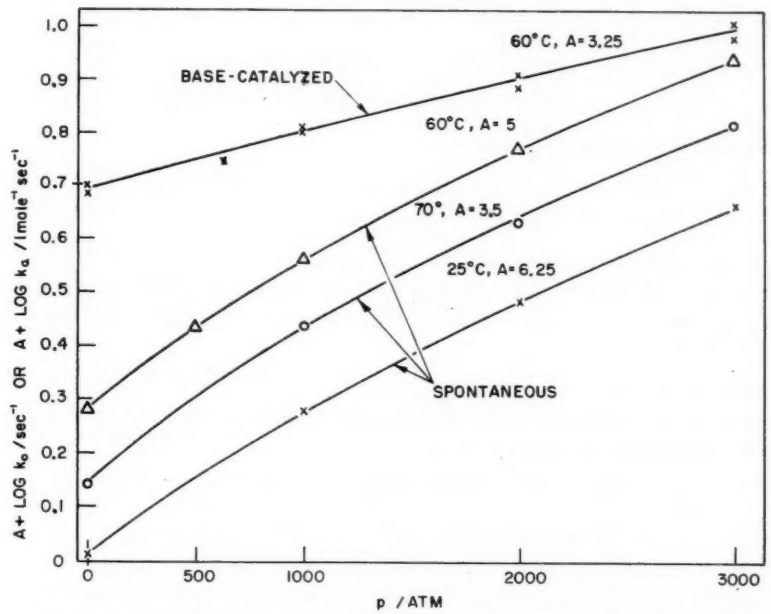

FIG. 1. Effect of pressure on the spontaneous and the base-catalyzed hydrolyses of ethylene oxide.

4. DISCUSSION

Spontaneous Hydrolysis

The volume of activation for the spontaneous hydrolysis of ethylene oxide at 60° C is $-18.9 \pm \sim 1$ cm³ mole^{-1}. The mechanism is very likely to be (6)

[4.1] $$H_2O + \begin{matrix} H_2C \\ | \\ H_2C \end{matrix}\!\!>\!O \xrightarrow{\text{slow}} H_2O^+\!-\!CH_2 \,|\, H_2C\!-\!O^- \xrightarrow{\text{fast}} \begin{matrix} CH_2OH \\ | \\ CH_2OH \end{matrix}.$$

There are two effects causing a decrease of volume when the transition state is formed, the conversion of a van der Waals' interaction between water and epoxide into a partial valence bond, and the increased electrostriction of the solvent due to the separation of charges in the transition state (7). The contribution of valence-formation to the volume-decrease will presumably be similar to that in similar reactions in which no major change of electrostriction is expected. We show below that the contribution of valence-formation to the volume of activation is expected to be about -5 to -10 cm³ mole^{-1}. The con-

tribution of valence-formation in reaction [4.1] is, therefore, likely to be about $\frac{1}{3}$ to $\frac{1}{2}$ of the total volume of activation; the remaining $\frac{2}{3}$ to $\frac{1}{2}$ is presumably due to electrostriction of the solvent.

Although the volume of activation for the spontaneous hydrolysis of propylene oxide cannot be calculated for lack of data, it is of the same order of magnitude as that for ethylene oxide, and is presumably the sum of similar contributions.

A volume of activation can be divided into an enthalpy effect and an entropy effect thus

$$[4.2] \qquad \Delta V^{\ddagger} = (\partial \Delta H^{\ddagger}/\partial p)_T - T(\partial \Delta S^{\ddagger}/\partial p)_T.$$

Using the relations

$$[4.3] \qquad (\partial \Delta S^{\ddagger}/\partial p)_T = -(\partial \Delta V^{\ddagger}/\partial T)_p,$$

$$[4.4] \qquad (\partial \Delta H^{\ddagger}/\partial p)_T = -T^2\,[\partial(\Delta V^{\ddagger}/T)/\partial T]_p,$$

we find from our measurements that

$$\partial \Delta H^{\ddagger}/\partial p = 19 \pm \sim 10 \text{ cm}^3 \text{ mole}^{-1} \text{ at } 25\text{–}70^\circ \text{ C and 1 atm},$$
$$T\partial \Delta S^{\ddagger}/\partial p = 38 \pm \sim 10 \text{ cm}^3 \text{ mole}^{-1} \text{ at } 25\text{–}70^\circ \text{ C and 1 atm}.$$

Thus both the enthalpy and the entropy of activation increase as the pressure is increased, the entropy term dominating the enthalpy term and determining the sign of $\Delta V^{\ddagger}$. Similar reactions, in which charges are created in the transition state, behave similarly (8, 9, 10).

Base-catalyzed Hydrolysis

The volume of activation for the base-catalyzed hydrolysis at 60° C is $-7.0 \pm \sim 1$ cm^3 mole^{-1}. The mechanism of the reaction is

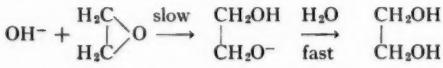

There are two contributions to the volume of activation, the formation of a new partial valence bond between oxygen and carbon and the extension of an existing C–O bond in the epoxide, and the decreased electrostriction of the solvent due to the dispersion of the negative charge between two oxygen atoms thus

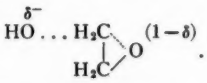

The value, -7.0 cm^3 mole^{-1}, is presumably the sum of these effects.

It is important to establish the sum of these effects for a number of similar reactions for the following reason. In a bimolecular reaction between a molecule and an ion the main contributors to the volume of activation are valence-formation and charge-dispersion as described above and electrostriction of the solvent due to newly separated charges. If the loss of volume due to valence-formation and charge-dispersion can be estimated then it should be possible to determine whether a major separation of charge occurs in the transition state. Laidler and Chen (11) have done this by assuming that the loss in volume due to valence formation is unimportant. We now examine the available evidence on the volumes of activation of ion–molecule reactions. The volume of activation will probably not depend strongly upon whether the ion is positively or negatively

charged. In order to reduce the possibility of increased polarity in the transition state we will omit reactions that occur near a highly polarizable group such as a carbonyl group. The available information on the volumes of activation of such reactions is summarized in Table III. For some of the reactions only rough rate constants were obtained; for example, David and Hamann (15) claim an accuracy no greater than 30% in the rate constants. It is worthwhile to include these only because there are so few data at present and even rough values are better than none.

TABLE III

Volumes of activation of reactions that probably occur without major change in polarity

Reaction	Solvent	Temperature	$\Delta V^{\ddagger}$/cm³ mole⁻¹	Ref.
$C_2H_4O + OH^- \rightarrow C_2H_4(OH)O^-$	H_2O	60° C	$-7\pm\sim1$	This work
$C_2H_4O + H_3O^+ \rightarrow C_2H_4(OH)O^+H_2$	H_2O	0° C	$-5.9\pm\sim1$	4
		15° C	$-7.4\pm\sim1$	4
		25° C	$-7.9\pm\sim1$	4
		40° C	$-8.9\pm\sim1.3$	4
$CH_2.C_2H_3O + H_3O^+ \rightarrow CH_3C_2H_3(OH)O^+H_2$	H_2O	0° C	$-8.4\pm\sim1.3$	4
$(CH_3)_2.C_2H_2O + H_3O^+ \rightarrow (CH_3)_2C_2H_4(OH)O^+H_2$	H_2O	0° C	$-9.2\pm\sim1.7$	4
$(C_2H_5)_2O + H_3O^+ \rightarrow C_2H_5O^+H_2 + C_2H_5OH$	H_2O	161.2° C	$-8.5\pm\sim2$	12
$CH_3Br + \begin{cases} OH^- \\ OC_2H_5^- \end{cases} \rightarrow \begin{cases} CH_3OH \\ CH_3OC_2H_5 \end{cases} + Br^-$	'80%' C_2H_5OH in water	0° C	~-7	13*
			~-8	14*
$C_2H_5Br + OCH_3^- \rightarrow C_2H_5OCH_3 + Br^-$	CH_3OH	30° C	~-9	13*
$C_2H_5I + OC_2H_5^- \rightarrow (C_2H_5)_2O + I^-$	C_2H_5OH	30° C	~-5	8*
$CH_2ClCO_2^- + OH^- \rightarrow CH_2(OH)CO_2^- + Cl^-$	H_2O	40° C	$-8.2\pm\sim2$	15*
		60° C	$-6.6\pm\sim2$	15*
		80° C	$-9.4\pm\sim2$	15*
$n\text{-}C_3H_7Br + Br^{82-} \rightarrow n\text{-}C_3H_7Br^{82} + Br^-$	'90%' C_2H_5OH in H_2O	19° C	~-12	16
$n\text{-}C_3H_7I + I^{131-} \rightarrow n\text{-}C_3H_7I^{131} + I^-$	"	"	~-13	16

*The values of $\Delta V^{\ddagger}$ cited were obtained graphically from data in the reference.

All the reactions in Table III except the halogen-exchange reactions result in the formation of a bond between carbon and oxygen. The loss of volume is about -5 to -10 cm³ mole⁻¹. It seems reasonable to conclude, therefore, on the basis of present evidence that the volume of activation of ion–molecule reactions in which a C–O bond is formed and in which no major increase in the polarity occurs is about -5 to -10 cm³ mole⁻¹.

REFERENCES

1. Bronsted, J. N., Kilpatrick, M., and Kilpatrick, M. J. Am. Chem. Soc. **51**, 428 (1929).
2. Lichtenstein, J. and Twigg, G. H. Trans. Faraday Soc. **44**, 905 (1948).
3. Long, F. A., Pritchard, J. D., and Stafford, F. E. J. Am. Chem. Soc. **78**, 2663, 2667 (1956).
4. Koskikallio, J. and Whalley, E. Trans. Faraday Soc. **55**, (1959) (In press).
5. Bridgman, P. W. Proc. Am. Acad. Arts Sci. **48**, 309 (1912).
6. Ingold, C. K. Structure and mechanism in organic chemistry. Cornell Univ. Press, Ithaca, N.Y. 1953. p. 343.
7. Hamann, S. D. Physico-chemical effects of pressure. Butterworth Scientific Publications, London. 1957. Chap. 9.
8. Gibson, R. O., Fawcett, E. W., and Perrin, M. W. Proc. Roy. Soc. A, **150**, 223 (1935).
9. Weale, K. E. Discussions Faraday Soc. **22**, 122 (1956).
10. Perrin, M. W. and Williams, E. G. Proc. Roy. Soc. A, **159**, 162 (1937).
11. Laidler, K. J. and Chen, D. Trans. Faraday Soc. **54**, 1026 (1958).
12. Koskikallio, J. and Whalley, E. Can. J. Chem. **37**, 788 (1959).
13. David, H. G. and Hamann, S. D. Trans. Faraday Soc. **50**, 1188 (1954).
14. Strauss, W. Australian J. Chem. **10**, 38 (1957).
15. Williams, E. G., Perrin, M. W., and Gibson, R. O. Proc. Roy. Soc. A, **154**, 684 (1936).
16. Gonikberg, M. G., Miller, V. B., Neĭman, M. B., D'yachkovskiĭ, F. S., Lickhtenshteĭn, G. I., and Opekunov, A. A. Zhur. Fiz. Khim. **30**, 784 (1956).

PRESSURE EFFECT AND MECHANISM IN ACID CATALYSIS

IV. THE HYDROLYSIS OF DIETHYL ETHER[1]

J. KOSKIKALLIO[2] AND E. WHALLEY

ABSTRACT

The acid-catalyzed hydrolysis of diethyl ether has been measured in the temperature range 120–160° C at low acid concentrations; the entropy of activation is $-9.0\pm\sim2.5$ cal deg^{-1} mole^{-1}. The effect of pressures up to 3000 atm has been measured at 161.2° C; the volume of activation at 1 atm is $-8.5\pm\sim2$ cm^3 mole^{-1}. These two results show that the slow step is bimolecular. The rate in concentrated acids was measured at 119° C; the rate was much more nearly proportional to the acidity function h_0 than to concentration of acid. This is contrary to the predictions of the Zucker–Hammett hypothesis, which is therefore not valid for the hydrolysis of diethyl ether.

1. INTRODUCTION

Diethyl ether hydrolyzes to ethanol by acid catalysis (see ref. 1 for review). The reaction is presumed to involve a pre-equilibrium proton-transfer to the ether though there is no compelling evidence for this. Two possible slow steps are the unimolecular decomposition of the conjugate acid (A-1 mechanism)

$$R_2OH^+ \rightarrow R^+ + ROH, \qquad [1.1]$$

or its bimolecular substitution (A-2 mechanism)

$$H_2O + R_2O^+H \rightarrow RO^+H_2 + ROH. \qquad [1.2]$$

There is no firm evidence about which mechanism is followed, though Long and Paul (2) have noted that the entropies of activation calculated from the measurements of Skrabal and Zahorka (3) are positive and say that this suggests that the mechanism for primary and secondary ethers is A-1. It was shown in Part I of this series of papers (4) that there are no grounds for thinking that entropies of activation of A-2 reactions cannot be positive, and consequently, the conclusion of Long and Paul is not valid.

It has been shown (4, 5, 6) that the A-1 and A-2 mechanisms can be distinguished by measuring reaction rates under pressure, and in this paper the technique is applied to the hydrolysis of diethyl ether. The measurements of Skrabal and Zahorka (3) of the hydrolysis of diethyl ether catalyzed by 0.5-*M* *p*-toluenesulphonic acid indicate a rapid variation with temperature of the Arrhenius energy and of the entropy of activation, and rates over a temperature range have been measured in an attempt to verify this. Measurements of the rates over a range of acid concentrations have been made in order to examine the validity of the Zucker–Hammett hypothesis.

2. EXPERIMENTAL METHODS

Because the rates of hydrolysis are slow it is necessary to measure them at fairly high temperatures, and the range 120–160° C has been used. Because ether is very volatile and not very soluble in water it is most important to avoid having a vapor-space above the reaction mixture in order to avoid loss of reactant from the solution. Consequently, all reported rate measurements were done in such a way that there was no

[1]*Manuscript received December 19, 1958.*
Contribution from the Division of Applied Chemistry, National Research Council, Ottawa.
Issued as N.R.C. No. 5092.
[2]*National Research Council Postdoctorate Fellow, 1957–58. Present address: Chemistry Department, University of Helsinki, Helsinki, Finland.*

vapor-space. Some rate measurements were made using sealed ampoules as reactors, and vapor was present. The apparent rate constants were badly reproducible and were only a fraction of those obtained as described below, in which there was no vapor-space above the solution.

All reagents used were of analytical quality. The usual catalyst was perchloric acid in concentrations up to 5.65 *M*. A few runs were done with sulphuric acid and hydrochloric acid as catalysts.

High-pressure Technique

The high-pressure equipment was essentially that used in previous work (5), except that the acid solution at the high temperature needed (up to 160° C) reacted with stainless steel so that stainless-steel tubing could not be used to connect the hypodermic syringe to the valve. Consequently, a batch method was used. The reactors were 10-cm³ hypodermic syringes that had the outlets sealed off and the pistons sawn off short. The reaction mixture was thus in contact with glass only. The tubes were placed in the pressure vessel, which was then closed and placed in the thermostat, and the pressure was applied. After a suitable reaction time, which was usually 1 day or more, the vessel was cooled and opened and the three samples were analyzed. There was no evidence of oil entering the reactor or of solution leaving it. The heating of the pressure vessel after it was introduced into the bath had a half life of about 4 minutes as determined from the change in pressure in the closed system. In calculating the reaction time 20 minutes were allowed for warming.

Analysis

The rate of the reaction was followed by analyzing the ethanol produced by oxidizing it to acetic acid with potassium dichromate and sulphuric acid. Five milliliters of the reaction mixture, which was initially about 0.05 *M* in diethyl ether, were put into a mixture containing 3 ml of 96% sulphuric acid and 5 ml of potassium dichromate solution which contained about 50% excess over that required for the oxidation. The mixture was thermostated at 50° C for 20 minutes and then about 100 cm³ of distilled water and 10 cm³ of 0.1-*M* potassium iodide solution were added. The iodine liberated was titrated with 0.4-*N* sodium thiosulphate. The difference between the titer and that of a blank is proportional to the amount of ethanol present in the sample. During the oxidation of the ethanol the ether present is also slowly oxidized. When the unhydrolyzed diethyl ether solution was analyzed by the above method about 4% of the diethyl ether was oxidized; in partly hydrolyzed samples the amount of oxidation was proportionately less. A correction for this was applied to the ethanol analyses. If the sample contained much acid then less sulphuric acid was added when the sample was analyzed in order not to increase the rate of oxidation of ether and thus the correction needed.

The amount of ether initially present in the solution was found by completely oxidizing the ether to acetic acid with potassium dichromate. For this purpose samples of the solution were mixed with the potassium dichromate solution and sulphuric acid and kept in sealed ampoules in a thermostat at 99° C for 1–2 days. When a solution of acetic acid, potassium dichromate, and sulphuric acid, in the same concentrations as above was heated at 99° C for 10 days no oxidation occurred. The amount of ether found by analysis agreed with the amount calculated from the weight of ether in the sample. The 0.05-*M* solution of ether in water was also completely hydrolyzed by heating with 5.7-*M* sulphuric acid for 22 hours at 120°. The amount of ethanol found in this sample agreed within about 2% with the amount found by direct oxidation of ether.

3. RESULTS

The first-order rate constants k were calculated from the results of two analyses for ethanol. Those obtained from runs at different reaction times agreed within about 10%. The second-order constants k_a for runs with dilute acid were corrected for compression and thermal expansion of the solution by extrapolating the densities of water obtained from the literature (7); the correction factors are given in Table I. The second-order constants agreed within about 10%, and those for dilute acids are summarized in Table I. The first-order constants for concentrated solutions of acids are summarized in Table II. The accuracy is probably about 10%.

TABLE I

The second-order rate constants for the hydrolysis of diethyl ether catalyzed by perchloric acid

Temp.	p/atm	c_{HClO_4}/mole l.$^{-1}$	$(\rho_{20°,1\ atm})/\rho_{t,p}$*	$10^6 k_a$/l. mole^{-1} sec^{-1}
119.2°	50	0.198	1.06	1.46
130.4°	50	0.198	1.07	4.36
140.8°	50	0.198	1.08	10.8
151.8°	50	0.198	1.09	26.2
161.2°	50	0.0495	1.10	74
161.2°	50	0.099	1.10	81
161.2°	50	0.198	1.10	75
161.2°	400	0.099	1.09	79
161.2°	1000	0.0495	1.07	99
161.2°	1000	0.099	1.07	102
161.2°	2000	0.0495	1.03	113
161.2°	2000	0.099	1.03	112
161.2°	2000	0.198	1.03	102
161.2°	3000	0.0495	1.01	131
161.2°	3000	0.099	1.01	132
161.2°	50	0.060†	1.10	82

*$\rho_{20°,\ 1\ atm}$ and $\rho_{t,p}$ are the densities of the solvent at 20° C and 1 atm and temperature t and pressure p respectively.
†Hydrochloric acid was used as catalyst.

TABLE II

The first-order rate constants of the hydrolysis of diethyl ether in concentrated aqueous acids at 120.1° C and 50 atm

Acid	c_{acid}/mole l.$^{-1}$	$10^6 k$/sec^{-1}
$HClO_4$	0.198	0.30
	1.12	1.85
	2.26	5.7
	3.05	10.7
	4.14	21.8
	5.65	73
H_2SO_4	3.57	10.7
HCl	3.20	17.5

An Arrhenius plot of the second-order constants is given in Fig. 1, in which the vertical lines at each point show a 10% error. The best straight line through the points is shown; it yields for the Arrhenius energy E_A and the entropy of activation $\Delta S^{\ddagger}(= R \ln\{(A/1.\ \text{mole}^{-1})(h/ekT)\}$ where A is the Arrhenius frequency factor, R is the gas-constant, h is Planck's constant, k is Boltzmann's constant, and T is the temperature)

$$E_A = 31.0 \pm \sim 1 \text{ kcal mole}^{-1},$$

$$\Delta S^{\ddagger} = -9.0 \pm \sim 2.5 \text{ cal deg}^{-1} \text{ mole}^{-1}.$$

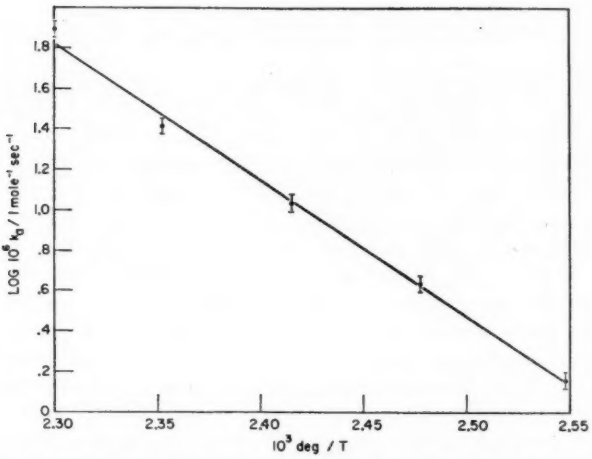

FIG. 1. Log k_a vs. $1/T$ for the acid-catalyzed hydrolysis of diethyl ether between 119 and 161° C.

The points at the highest two temperatures do not fit well with this line, though a good line of slightly smaller slope can be drawn through all but the highest-temperature point, which is about 30% higher than the extrapolated line. It is possible that the Arrhenius energy and the entropy of activation are increasing at the higher temperatures, but the accuracy of the rate constants is not high enough to be sure of it.

The second-order rate constants at 161° C are plotted against pressure in Fig. 2. They

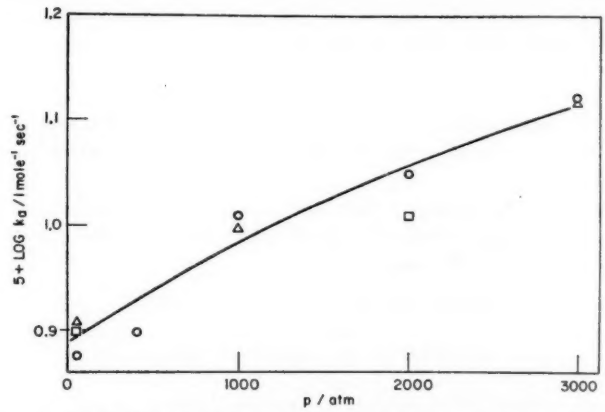

FIG. 2. Log k_a vs. p for the hydrolysis of diethyl ether catalyzed by perchloric acid at 161.2° C. The concentration of catalyst was: triangles, 0.0495 M; circles, 0.099 M; squares 0.198 M.

were fitted by the method of least squares to the equation

$$\log k_a = a+bp+cp^2,$$

and the activation volume $\Delta V^{\ddagger}$ at 1 atm obtained from

$$d \ln k/dp = -\Delta V^{\ddagger}/RT = 2.303b.$$

We found

$$\Delta V^{\ddagger} = -8.5 \pm \sim 2 \text{ cm}^3 \text{ mole}^{-1} \text{ at } 161^\circ \text{ C, 1 atm.}$$

Our rate constants are in very poor agreement with those of Skrabal and Zahorka (3). Our measurements extrapolated to 95° C give $10^6 k_a = 0.34$ l. mole^{-1} sec^{-1} at 50 atm; Skrabal and Zahorka give for 95° C and 1 atm $10^6 k_a = 0.044$ l. mole^{-1} sec^{-1}, nearly $\frac{1}{8}$ of our value. Skrabal and Zahorka give the rate constant at 125° C, obtained by extrapolation, as 0.0785×10^{-6} l. mole^{-1} sec^{-1}; our interpolated value is 2.57×10^{-6} l. mole^{-1} sec^{-1}, 33 times Skrabal and Zahorka's value. Reduction of our rate constants from 50 atm to 1 atm would make little difference to this disagreement. They also found that in the range 65–95° C the Arrhenius law was not obeyed, the apparent Arrhenius energy decreasing with temperature, whereas we find that it is obeyed in the range 120–150° C, though there may be an *increase* in E_A above this temperature. A partial explanation of this disagreement may be as follows. Skrabal and Zahorka attempted to render small and constant the effect of the vapor-space on the rate constant by keeping the volume of the vapor-space 2 cm^3 and of reaction mixture 12 cm^3. However, the amount of ether in the vapor-space relative to that in the solution will increase as the temperature increases and this will cause the apparent rate constant to be lower than the true rate constant by an amount that increases with increasing temperature. This is at least in the right direction to account for Skrabal and Zahorka's variation of Arrhenius energy with temperature.

In a few cases the reaction mixtures were analyzed for ethylene using the method of Christensen *et al.* (8). Within the experimental error of about 0.3% of the ether initially present no ethylene was found under the following conditions: (i) 14 hours at 120° C and 50 atm in 3.57-*M* sulphuric acid with 49% of the ether hydrolyzed, and (ii) 4 hours at 120° C and 50 atm in 5.65-*M* sulphuric acid with 67% of the ether hydrolyzed. Also, the fact that ether hydrolyzed completely at 120° C, within the experimental error of 2%, to ethanol shows that ethylene is not an important product at 120° C.

DISCUSSION

The second-order constants are independent of acid concentration in dilute acids within experimental error, confirming the much less extensive measurements of Skrabal and Airoldi (9).

As pointed out in the introduction there are two likely mechanisms for the hydrolysis of ether, the A-1 mechanism which is steps [1], [2*a*], and [3*a*], and the A-2 mechanism which is steps [1], [2*b*], and [3*b*], below.

$$(C_2H_5)_2O + H_3O^+ \rightleftharpoons (C_2H_5)_2O^+H + H_2O, \qquad [1]$$

$$(C_2H_5)_2O^+H \xrightarrow{\text{slow}} C_2H_5OH + C_2H_5^+, \qquad [2a]$$

$$C_2H_5^+ + 2H_2O \xrightarrow{\text{fast}} C_2H_5OH + H_3O^+, \qquad [3a]$$

$$(C_2H_5)_2O^+H + H_2O \xrightarrow{\text{slow}} C_2H_5OH + C_2H_5O^+H_2, \qquad [2b]$$

$$C_2H_5O^+H_2 + H_2O \xrightarrow{\text{fast}} C_2H_5OH + H_3O^+. \qquad [3b]$$

The measured volume or entropy of activation is the sum of the volume or entropy change of step [1] and the volume or entropy of activation of the slow step [2*a*] or [2*b*]. It was shown in Part I of this series of papers (4) that the volume change of step [1] is probably small, so that the experimental volume of activation is determined mainly

by the volume of activation of step [2]. If [2*a*] is the slow step then the transition state is bigger than the reactants and the volume of activation is positive or close to zero; this occurs in the acid-catalyzed hydrolysis of sucrose (4), dimethoxymethane, diethoxymethane, dimethoxyethane, and triethoxymethane (5). If [2*b*] is the mechanism then the conversion of a van der Waals' bond between water and the conjugate acid of the ether to a partial valence bond in the transition state results in a decrease of volume, and the volume of activation is expected to be negative by about 5–10 cm^3 $mole^{-1}$; this occurs in the acid-catalyzed hydrolysis of methyl acetate (4), ethylene oxide, propylene oxide, and isobutylene oxide (6). Similar arguments, which were developed in Part I, apply to the entropy of activation, except that the standard entropy change of the proton-transfer step (1) may be quite high. Consequently, we concluded that an A-1 reaction should have a positive entropy of activation and an A-2 reaction can have either a positive or a negative entropy of activation.

The volume of activation is $-8.5\pm\sim2$ cm^3 $mole^{-1}$, showing that the mechanism is A-2. The entropy of activation is $-9.0\pm\sim2.5$ cm^3 $mole^{-1}$, and this confirms the A-2 mechanism.

It is possible that if increases in E_A and $\Delta S^{\ddagger}$ are beginning to occur at the higher temperatures, as is indicated but not proved by our measurements, an A-1 mechanism is beginning to occur. More work is needed on this point. However, it seems certain that the A-2 mechanism, which is detected by the volumes of activation at 161° C and by the entropy of activation over the range 119°–160°, holds at 120° C.

If the Zucker–Hammett hypothesis (10, 2), that when rates in concentrated acids are proportional to Hammett's acidity function h_0 the mechanism is A-1 and when rates are proportional to concentration of hydrogen ion the mechanism is A-2, is correct then the rate of hydrolysis of diethyl ether should be proportional to concentration of strong acid. Values of H_0 ($= -\log h_0$) are not known for perchloric acid in water at the

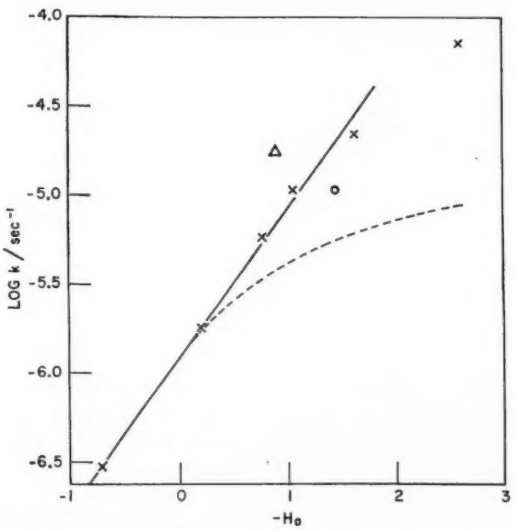

FIG. 3. Log k at 120.1° C and 50 atm vs. $-H_0$ at 25° C and 1 atm for the hydrolysis of diethyl ether catalyzed by acids. The acid was: crosses, perchloric acid; circle, sulphuric acid; triangle, hydrochloric acid. If log k ∝ log c_{H^+} the points would fall near the dashed line.

temperature and pressure of the measurements, 120.1° C and 50 atm. We have used, therefore, the values appropriate to 25° C and 1 atm (11). These will certainly not be accurate for 120.1° C and 50 atm, but the difference will probably not be enough to invalidate the following discussion. In Fig. 3, log k/sec^{-1} is plotted against $-H_0$, and for comparison the curve that would be obtained if the rate were proportional to concentration of acid is shown. It is quite evident that log k is much more nearly proportional to H_0 than to log c_{H^+}, though the rate at high acidities is somewhat less than strict proportionality would give. The rate in 5.65-M perchloric acid is 8.5 times faster than if it were proportional to c_{HClO_4} and 0.4 times faster than if it were proportional to h_0.

Though there is some uncertainty in the values of H_0 for 120° C and 50 atm, it seems very likely that the Zucker–Hammett hypothesis is not valid for the hydrolysis of diethyl ether. It failed also for the hydrolysis of ethylene oxide (6). The method is inherently empirical, and, since two reactions are now known for which it fails, we must conclude that the relation between rates and h_0 and hydrogen-ion concentration does not distinguish between A-1 and A-2 mechanisms.

Taft, Deno, and Skell, in a recent review (12), refer to work (13) that is not yet fully published that also refutes the Zucker–Hammett hypothesis.

REFERENCES

1. Burwell, R. L. Chem. Revs. **54**, 615 (1954).
2. Long, F. A. and Paul, M. A. Chem. Revs. **57**, 935 (1957).
3. Skrabal, A. and Zahorka, A. Monatsh. Chem. **63**, 1 (1933).
4. Whalley, E. Trans. Faraday Soc. (In press).
5. Koskikallio, J. and Whalley, E. Trans. Faraday Soc. (In press).
6. Koskikallio, J. and Whalley, E. Trans. Faraday Soc. (In press).
7. Bridgman, P. W. Proc. Am. Acad. Arts Sci. **66**, 185 (1931).
8. Christensen, D. E., Hansen, E., and Cheldelin, V. H. Ind. Eng. Chem. Anal. Ed. **11**, 114 (1939).
9. Skrabal, A. and Airoldi, H. Monatsh. Chem. **45**, 13 (1924).
10. Zucker, L. M. and Hammett, L. P. J. Am. Chem. Soc. **61**, 2791 (1939).
11. Paul, M. A. and Long, F. A. Chem. Revs. **57**, 1 (1957).
12. Taft, R. W., Deno, N. C., and Skell, P. S. Ann. Rev. Phys. Chem. **9**, 287 (1958).
13. Boyd, R. H. and Taft, R. W. Abstr. Am. Chem. Soc. 132nd Meeting. 1957. p. P76.

REACTION OF TRICHLOROACETONITRILE WITH PRIMARY AND SECONDARY AMINES

PART II. INFRARED SPECTRA OF N-SUBSTITUTED TRICHLOROACETAMIDINES[1, 2]

JOHN C. GRIVAS[3] AND ALFRED TAURINS

ABSTRACT

A correlation between the infrared absorption spectra and the structure of 13 N-mono- and N-di-substituted trichloroacetamidines is presented. N-Alkyl- and N-aryl-trichloroacetamidines associate strongly in the liquid and solid phases, and exist only in the imino form in non-polar solvents. They can be characterized by a strong band (amidine II band) at 1510–1525 cm^{-1} and 1570–1580 cm^{-1} respectively which is attributed to the deformation vibration $\delta(\rangle N—H)$ of the secondary amino group. The degree of association of N-substituted trichloroacetamidines changes in the following order of substitution:

N-alkyl- > N-aryl- > N-dialkyl.

INTRODUCTION

The free secondary amino group shows only one NH stretching absorption band between 3500 and 3300 cm^{-1}, but hydrogen bonding of this group sometimes gives rise to a second band at lower frequencies. A somewhat narrower frequency range (3400–3200 cm^{-1}) has been established for the stretching vibration, ν(N—H), of the unassociated imino group =NH as is expected from the fact that the environment around the NH group is almost always the same. The deformation vibration, δ(NH), of both secondary amino and imino groups occur between 1650 and 1550 cm^{-1}, but they are usually too weak to be used for identification purposes (1). In the aromatic amines this absorption is complicated by the fact that it occurs in the same region as the aromatic ring vibrations and often causes a modification of these. Certain combinations of structural features are likely to enhance the intensity of the deformation vibration, δ(NH), just as the NH deformation is believed by some authors to be enhanced by the presence of the carbonyl group, with a result of appearance of the amide II band. That has been recently substantiated by Barr and Haszeldine (2), who assigned the deformation vibration, δ(NH), to a strong band near 1500 cm^{-1} showed by secondary perfluoroalkylamines. The same mode has also been reported to be responsible for the absorption near 1510 cm^{-1}, which was observed in the spectra of the secondary aromatic amines (3).

Amidines of the general formula (I)

$$\begin{array}{l} R—C—NHR'' \\ \quad\| \\ \quad NR' \end{array}$$

I

show also the free stretching vibrations ν(NH), between 3440 and 3470 cm^{-1}, but a considerable amount of chemical evidence indicates that monosubstituted and symmetrically disubstituted amidines having different groups at the nitrogen atom exhibit tautomerism (4). Further support for this evidence has been provided by the infrared

[1]*Manuscript received January 7, 1959.*
Contribution from the Department of Chemistry, McGill University, Montreal, Que., with financial assistance from the National Research Council, Ottawa.
[2]*Part I: Grivas, J. C. and Taurins, A. Can. J. Chem.* **36**, *771 (1958).*
[3]*Holder of the National Research Council Studentship, 1957–59.*

studies of the amidines (I), which showed a second weaker absorption, not vanishing upon dilution, near 3400 cm^{-1} (5, 6).

Fabian, Delaroff, and Legrand (5) observed a rather strong band near 1515 cm^{-1} with solutions of the N-alkyl-N′-phenylbenzamidines. This absorption was displaced by 30–40 cm^{-1} toward the higher frequencies in solid state. This led to the conclusion that it was owing to the NH deformation vibration. However, in some cases, the band was confused with the aromatic ring modes which also occur near 1500 cm^{-1}.

Acetamidines (I) with R′,R″ = aryl groups have been reported to exhibit four bands in the region 1550–1200 cm^{-1}, which were effected by the breaking of the hydrogen bonding and deuteration (6). Two of them, near 1540 and 1330 cm^{-1}, were assumed to originate from the coupling of the deformation vibrations, δ(NH), with the antisymmetric mode of the group —C(=N)N, and the other two at 1440 and 1220 cm^{-1} from the coupling mode of the δ(NH) with the ν(N—R).

The C=N stretching vibration has been firmly established as a very strong band between 1690 and 1640 cm^{-1} for open chain compounds. Pickard and Polly (7) quote this absorption at 1655–1615 cm^{-1} for ketimines of the structure $\begin{matrix} R \\ R' \end{matrix}\!\!>\!C{=}NH$. The range of the ν(C=N) is somewhat larger for the substituted amidines (1685–1590 cm^{-1}) and the position or intensity of this band seems to depend on the degree of substitution and the presence of electron-attracting groups attached to the amidine system (5).

The C—N stretching vibrations occur in a wide range together with the C—C skeletal vibrations. This makes the assignments uncertain in many cases. However, Colthup (8) gives a range 1100–1200 cm^{-1} for C_{alk}—N deformation frequency for the secondary aliphatic amines. This was confirmed by Hadži and Škrbljak (3), who mentioned a strong band between 1170 and 1140 cm^{-1} to be associated with skeletal vibrations, in which the C_{alk}—N bonds participate strongly. Colthup's table shows also that the $\nu(C_{ar}—N)$ of amines of the type $_{ar}$—NH—$_{alk}$ occurs at 1350–1280 cm^{-1}, and that the second band of medium intensity at 1240–1290 cm^{-1} should correspond to the $\nu(C_{alk}—N)$ of the same type of secondary amines. Finally, the $\nu(C_{ar}—N)$ was recently located at 1240–1260 cm^{-1} for a series of secondary aromatic amines (3).

EXPERIMENTAL

The trichloroacetamidines subjected to infrared analysis are represented by the formulae II and III:

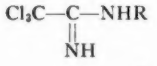

II R = alkyl, phenyl, or substituted phenyl,

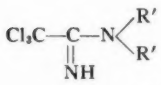

III R′ = alkyl.

The methods of preparation of trichloroacetamidines have been described previously (9). The solid substances were investigated in potassium bromide pellets. Liquid substances were examined by spraying a thin layer between sodium chloride plates. Solutions of the amidines were prepared by dissolving 10 mg of the substance in 1 ml of tetra-

TABLE I

Positions of absorption maxima (cm^{-1}) in the infrared spectra of N-substituted trichloroacetamidines

No.	Trichloro-acetamidine	State*	(N—H)	(N=H)	Hydrogen-bonded NH	(CH_2) and (CH_3)	(C=N)	(C=C) aromatic	(N—H) amidine II	(C=C) aromatic	(C_{ar}—N)	(C—N) HN=C—N	(C_{alk}—N)
1	N-Methyl	L	3490s	3300vs†	3200(sh)–3045s	2950s, 2905s	1635vs		1522vs			1313vs	1152vs
2	N-Ethyl	L	3465s	3340vs‡	3280(sh)–3050s	2970m, 2940s, 2875s	1637vs		1515vs			1314vs	1168vs
		Sol	3465m	3350w	None	2970m, 2930m, 2870w	1642vs		1510vs			1308m	
3	N-*n*-Butyl	L	3445s	3325vs	3200(sh)–3040m	2920vs, 2850s	1633vs		1515vs			1313s	1155vs
4	N-*n*-Amyl	L	3440m	3320s‡	3180(sh)–3030m	2915vs, 2845s	1632vs		1513vs			1312s	1155s
		Sol	3455m	3350w	None	2950(sh), 2925vs, 2855s	1642vs		1512vs				
5	N-Benzyl	S	3330m	3205s‡		2915vw, 2890vw	1635vs	1602m	1545vs	1495s		1338s	1168vs
		Sol	3475m	3370w			1642vs	1602m	1510s	1500sh			
6	N-Phenyl	S	3485s	3370s	3270(sh)–3150vw		1657vs	1594vs	1584vs	1483s	1337s	1237m	
		Sol	3520m	3415m	None		1672vs	1594vs	1580vs	1484s	1327s	1240m	
7	N-*o*-Tolyl	Sol	3500s	3400s		2915vw, 2860(sh)	1670vs	1596s	1577s	1483vs	1327s	1239m	
8	N-*m*-Tolyl	S	3470m	3365m	3320m–3160(sh)	2915vw, 2860(sh)	1652vs	1595vs	1585vs	1486s	1337s	1265m	
		Sol	3500m	3400m	None	2915vw, 2860(sh)	1670vs	1595vs	1580vs	1484s			
9	N-*p*-Tolyl	S	3480m	3370m	3150w	2915w–2850w	1660vs	1610s(sh)	1580vs	1504vs	13375	1237s	
		Sol	3505m	3400m	None	2918w–2860vw	1667vs	1611m	1580vs	1505vs			
10	N-*p*-Ethoxyphenyl	S	3450m	3360m	3330m–3110m	2990m, 2930m, 2890vw	1660vs	1606vs	1627vs	1507vs	1332	1232vs	
		Sol	3500m	3400m	None	2980m, 2920(sh), 2895w	1667vs	1604m	1577vs	1503vs	1322s	1236vs	
11	N,N-Dimethyl	L		3340m		2895s	1603vs					1267vs	1090vs
		Sol		3360m		2895s, 2820(sh)	1607vs					1267vs	
12	N,N-Diethyl	L		3380s		2985vs, 2945vs, 2885s	1593vs						
		Sol		3380m		2985vs, 2945vs, 2880m	1600vs						
13	N-Morpholyl	L		3360m								1275vs	1117vs
		Sol		3365m		2975m–2920m, 2900m–2858s	1601vs					1277vs	

*L, liquid; S, solid; Sol, solution.
†A wide band between 3250 and 3350 cm^{-1}.
‡Wide bands.

chloroethylene. Sodium chloride cells of 1 mm thickness were used. The infrared spectra were recorded with a Perkin–Elmer Model 21 double beam spectrophotometer equipped with a sodium chloride prism. The settings at the instrument were as follows: resolution 927, gain 5, speed 4.5, response 1, suppression 0. The results have been summarized in Tables I and II.

TABLE II

Positions of absorption maxima (cm^{-1}) in the infrared spectra of N-substituted trichloroacetamidines

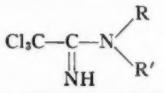

Assignments	R = H R′ = Alkyl	R = H R′ = Aryl	R,R′ = Alkyl
Free $\nu(\rangle N—H)$	3440–3480	3490–3520	
Free $\nu(=N—H)$	3300–3370	3390–3420	3360–3380
Bonded (N—H) (*trans*)	3180–3300	3270–3330	
Bonded (N—H) (*cis*)		3100–3160	
$\nu(C=N)$	1630–1650	1650–1670	1590–1610
Free $\delta(\rangle NH)$ (amidine II band)	1510–1525	1570–1580	
$\nu(C_{ar}—N)$		1320–1340	
$\nu(C—N)$ in HN=C—N	1300–1340	1230–1270	1260–1280
$\nu(C_{alk}—N)$	1150–1170		1090–1120(?)
$\nu(C—C)$ in $Cl_3C—C$	1025–1070		

RESULTS AND DISCUSSION

I. Region 4000–1800 cm^{-1}

If trichloroacetamidines existed in two tautomeric forms IV*a* and IV*b*

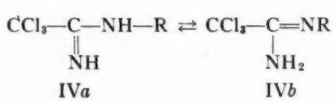

IV*a* IV*b*

present in dilute solutions then more than two absorption bands should appear between 3500 and 3200 cm^{-1}. Or, if the tautomeric equilibrium had been displaced to the right completely (IV*b*), two absorption bands characteristic of the stretching vibrations of the primary amino group should appear, although modified by the double bond at the α-carbon atom. However, the infrared spectra of the N-monosubstituted trichloroacetamidines revealed only two, very sharp, absorptions at 3450–3520 cm^{-1} and at 3350–3415 cm^{-1} in dilute solutions. The intensity of the two bands showed a general increase on passing from N-alkyl- to N-phenyl-derivatives, where both were almost of the same intensity. The second absorption band was of a much lower intensity in the spectra of the N-alkyl-trichloroacetamidines. No inflections were recorded. The results indicate that amidines do not exhibit any tautomerism at least not in dilute tetrachloroethylene solutions.

Furthermore, a comparison of the infrared spectra of N-dialkyl substituted trichloroacetamidines with those of the N-alkyl homologues revealed that the first and the second stretching band of the imino group =NH appear in the same regions and are very close to each other. Thus, in dilute solution N-ethyl- and N-amyl-trichloroacetamidines showed the second band at 3350 and 3347 cm^{-1} respectively, whilst the

N-dimethyl-, N-diethyl, and N-morpholyl-derivatives exhibited only one band of the free =NH group in this region at 3362, 3382, and 3365 cm^{-1} respectively.

The NH stretching vibration of the secondary amino group was thus assigned to the 3450–3520 cm^{-1} band and the ν(NH) of the imino group to 3350–3415 cm^{-1} absorption. Further evidence in favor of the above assignments was obtained from the position of the ν(C=N) in different types of substitution, which will be discussed later in this paper.

The infrared spectra of all the compounds show that hydrogen bonding is involved to a considerable extent in liquid and solid phases, except the liquid N-dialkyl substituted amidines. The general trend of the displacement of the $\nu(\rangle NH)$ and ν(=NH) to the higher frequencies is shown when the substances are diluted, in accordance with what is expected from a breaking of hydrogen bonding. This displacement is very slight for the change from the liquid to the solution and it is more pronounced in the case of the solid derivatives.

More than two bands appear in the spectra of solid or liquid compounds in addition to the two NH vibrations; their behavior resembles that of the secondary amides, since they disappear upon dilution. Many of the liquids examined possess a weak absorption near 3040 cm^{-1} and it is expected that other bands exist because of the fact that the ν(=NH) band is very broad and exhibits one or two inflections. Its intensity is also higher than the $\nu(\rangle NH)$ while the opposite is true with the spectra obtained by solutions of these substances.

The existence of these absorption bands in addition to the $\nu(\rangle NH)$ and ν(=NH) was established in four of the six solid amidines examined; i.e. N-(*p*-ethoxyphenyl)-trichloroacetamidine absorbed rather strongly at 3450, 3360, 3330, and 3110 cm^{-1}. The last two bands vanished upon dilution, while the first two were displaced to 3498 and 3398 cm^{-1} respectively. Solid N-(*m*-tolyl)trichloroacetamidine showed absorption maxima at 3470, 3365, 3320, and 3160 cm^{-1}; these four bands were replaced by only two strong absorptions at 3500 and 3400 cm^{-1} in dilute solution. The 3050 cm^{-1} weak absorption observed with the N-alkyl-trichloroacetamidines may be confused with the stretching motion of the aromatic C—H group with the N-phenyl derivatives.

Of the two hydrogen atoms of the imino and secondary amino groups, the first one seems to be involved in hydrogen bonding to a greater extent since it is the band near 3350 cm^{-1} which undergoes greater transformation on changing from the condensed phase to the solution. Although more work is necessary in this field, it can be assumed that the absorption near 3300 and 3150 cm^{-1} are due to hydrogen bonding and originate from a *trans* and *cis* arrangement respectively. These absorption bands correspond to the dimer and polymer structures (V and VI), from which the dimer may be stabilized by resonance occurring in a fashion similar to that observed with the carboxylic acids.

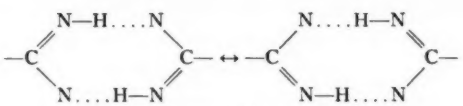

V

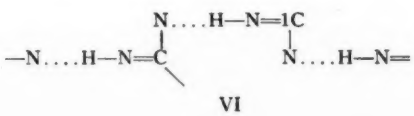

VI

In conclusion, secondary amidines possess hydrogen bonding to a smaller extent than secondary amides and the N-alkyl-trichloroacetamidines are more strongly associated than the N-aryl derivatives.

II. Region 1800–1200 cm^{-1}

(*a*) *The Stretching, ν(C=N), Absorption*

These vibrations were easily recognizable in all the spectra taken, since they appeared as a very strong band between 1590 and 1670 cm^{-1} and did not show any appreciable change in intensity and position, whether the sample was a solid, a liquid, or a solution. The small displacement (5–25 cm^{-1}) to the lower wave lengths upon dilution is quite characteristic in all cases and excludes the possibility of being any NH bending vibration. The position of the ν(C=N) seems to be a function of substitution on the amino nitrogen atom. Thus N-alkyl-trichloroacetamidines absorbed between 1630 and 1645 cm^{-1}, whereas the N-dialkyl compounds at 1590–1610 cm^{-1}. The opposite shift to higher frequencies (1650–1670 cm^{-1}) was recorded with the N-phenyl-trichloroacetamidines.

This behavior can be easily explained and it comes as additional evidence for the non-existence of tautomerism in the amidines examined. Amidines are the resonance hybrid of the following structures (VII).

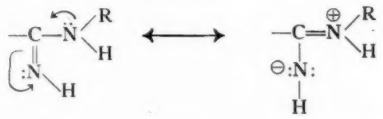

VII

Substitution of the amino hydrogen atom by another alkyl group increases the electron density around the amino nitrogen atom owing to the greater +Is effect. As a consequence the contribution of the polar structure increases, the double bond character of the C=NH double bond decreases, and hence causes a displacement of the ν(C=N) to the lower frequencies which is in fact observed. When R is an electron-attracting group (phenyl) its −Is effect should oppose such an electron movement and depress the resonance within the amidino group. As a result N-phenyl derivatives should absorb at higher frequencies than the corresponding N-alkyl derivatives in agreement with our findings. If tautomerism exists, one of the two tautomers (IX) should be present.

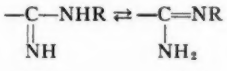

VIII IX

In this case the resonance hybrid can be represented as (X)

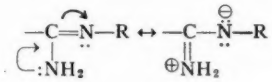

X

and the pattern of the displacement going from the N-alkyl- to the N-dialkyl- and N-phenyl-trichloroacetamidines is expected to be the opposite of that observed.

(*b*) *The Amidine II Band*, δ(N—H)

The second very strong absorption in this region appeared near 1515 cm^{-1} for all N-alkyltrichloroacetamidines, and was absent from all the infrared spectra of N-dialkyl derivatives. This immediately suggested that it could be related to the δ(NH) of the secondary amino group. The displacement of this band (1–5 cm^{-1}) to the lower frequencies upon dilution was negligible, since association is weak in the liquid phase, but was indicative of an NH deformation frequency. A rather pronounced shift to lower frequencies was recorded for the N-benzyl derivative, the only aliphatic solid which showed a strong displacement. This compound had a very strong band at 1545 cm^{-1}, in addition to the aromatic absorptions at 1602 and 1495 cm^{-1}. The 1545 cm^{-1} band was displaced to 1510 cm^{-1} upon dilution and the 1495 cm^{-1} absorption peak appeared as a distinct inflection of this band.

In the case of the N-aryl derivatives, the δ(NH) seems to be located near 1580 cm^{-1}, in addition to the two aromatic vibrations. A normal aromatic stretching mode, nevertheless, has been identified between 1600 and 1560 cm^{-1}; although it is always weak, external conjugation increases its intensity, when it becomes a readily recognizable medium band (1).

This possibility was excluded on the following grounds:

(1) The band is very strong in all the spectra.

(2) In the case of the solid N-(*p*-ethoxyphenyl)-trichloroacetamidine, which associates strongly it appeared at 1627 cm^{-1} as a strong absorption, whereas it was found at 1578 cm^{-1} upon dilution.

(3) Richards and Thompson (10) reported only two bands for the aromatic modes near 1600 and 1500 cm^{-1} with the N-aryl acetamides, for which a similar increase in intensity of the 1560–1600 cm^{-1} frequency could be expected.

(4) Since the resonance within the amidine system C(=NH)—NH is opposed to that arising from the aromatic ring, such a conjugation should be reduced greatly, if it existed at all. The assignment of the δ(NH) to the 1515 cm^{-1} absorption for the N-alkyl-trichloroacetamidines and to the 1580 cm^{-1} for the N-aryl analogues might be supported by the findings of Barr and Haszeldine and Hadži and Škrbljak, who located the δ(NH) of the secondary aromatic amines and the secondary perfluoroalkylamines in the same region. It is obvious that the otherwise weak δ(NH) is enhanced through resonance which imposes a partial positive charge on the nitrogen atom.

(*c*) *The Stretching*, ν(C—N), *Frequencies*

Amidines should give rise at least to two absorption bands related mainly to the C—N stretching vibrations. It was clearly understood that only two absorptions of strong and very strong intensity were suitable for the ν(C—N) vibrations in the 1400–1100 region for the N-aryl-substituted trichloroacetamidines, i.e. the 1330 cm^{-1} band for the $\nu(C_{ar}—N)$ and the 1240 cm^{-1} for the ν(C—N) of the amidino grouping. Both values agree with those given by Cothup's table and permit the assumption that the phenyl group "localizes" the C=N double bond to some extent; in agreement with our observation the C=N groups in the phenyl derivative absorb at higher frequencies than the N-alkyl- and N-dialkyl-derivatives.

The ν(C—N) of N-alkyl-trichloroacetamidines occur at higher frequencies; alkyl groups facilitate the resonance within the amidine system, thus imposing a partial double bond character to its (C—N) bond, which therefore should absorb at higher frequencies than the $C_{alk}—N$ bond. This was revealed from a comparison of the infrared spectra recorded for the different classes of substituted amidines on the one hand and from

their absorption in the ultraviolet region on the other. Indeed the amidine ν(C—N) was found to be located near 1310 cm^{-1}, very close to the $\nu(C_{ar}—N)$ in the aromatic compounds, whereas the 1150–1170 cm^{-1} strong absorption should involve mainly $\nu(C_{alk}—N)$ modes, with the N-alkyl-trichloroacetamidines.

No general conclusion could be drawn, for the N-disubstituted derivatives. Nevertheless, a strong band near 1270 cm^{-1} was attributed to the amidine ν(C—N) absorption and the $\nu(C_{alk}—N)$ could be related also to a strong band occurring near 1100 cm^{-1}. It should be pointed out that the ν(C—C) of the $Cl_3C—C$ group was definitely found near 1050 cm^{-1}, in agreement with the spectrum obtained for the trichloroacetonitrile which was used in the preparation of the amidines mentioned above and with the data found in the literature (11).

REFERENCES

1. Bellamy, L. J. The infrared spectra of complex molecules. 2nd ed. Methuen & Co. Ltd., London. 1958.
2. Barr, D. A. and Haszeldine, R. N. J. Chem. Soc. 4169 (1955).
3. Hadzi, D. and Skrbljak, M. J. Chem. Soc. 843 (1957).
4. Shriner, L. R. and Newman, W. F. Chem. Revs. **35**, 378 (1944).
5. Fabian, J., Delaroff, V., and Legrand, M. Bull. soc. chim. France, **287**, 287 (1956).
6. Prevorsek, D. Compt. rend. **244**, 2599 (1957).
7. Pickard, P. L. and Polly, G. W. J. Am. Chem. Soc. **76**, 5169 (1954).
8. Colthup, B. N. J. Opt. Soc. Am. **40**, 397 (1950).
9. Grivas, J. C. and Taurins, A. Can. J. Chem. **36**, 771 (1958).
10. Richards, E. R. and Thompson, W. H. J. Chem. Soc. 1248 (1947).
11. Wait, C. S., Jr. and Janz, J. Cr. J. Chem. Phys. **26**, 1554 (1957).

A SURVEY OF THERMODYNAMIC PARAMETERS FOR SOLVOLYSIS IN WATER[1]

R. E. ROBERTSON, R. L. HEPPOLETTE,[2] AND J. M. W. SCOTT[2]

ABSTRACT

A method is suggested for determining the standard state entropies ($S^0_{\ddagger}$) of the transition state for the neutral hydrolysis of esters in water. This has required the development of methods for approximating initial state parameters where experimental data are lacking.

Characteristic linear correlations between the entropy and enthalpy of activation are observed for hydrolysis in water, as well as for the bimolecular halide exchange reaction in acetone and for acid–base equilibria. Explanations are advanced to explain the observed trends.

From the derived standard state entropies, a method for estimating the charge development in the transition state for the methyl and isopropyl halides is proposed. With this further detailed knowledge of the transition state in the methyl halide series, reasonable values of the activation enthalpy can be calculated from available thermochemical data.

Correlations of kinetic data for reactions in solution have normally been attempted in terms of relative rates and some function of the reactant (1, 2), the solvent (3, 4, 5), or both (6, 7). There is no doubt that the effect of structural changes on the reactivity can be estimated quite fairly by relative rates, provided neither a detailed understanding of the activation process (8, 9) nor a quantitative description of the transition state is required. The next stage of refinement, however, will require a consideration of the derived thermodynamic parameters which characterize the activation process and the transition state. In principle this will require not only that rate data be determined over a wider range of temperature and with greater accuracy (10, 11) than has frequently been judged necessary but also that the corresponding parameters for the solvated initial state of the ester as well as those characterizing the gaseous state be available (8). Differences in the absolute values of the parameters so derived may then be properly analyzed and so provide a quantitative measure of the effect of structure on reactivity. The procedure may be outlined as follows. Consider the reaction:

[1] $$RX_{gas} \xrightarrow{\delta_s F} RX_{solution} \xrightarrow{\Delta F^{\ddagger}} RX_{transition\ state}.$$

For each ester in the gaseous state there will be an equation of the form

[2] $$F^0_g = E^0 + H^0_g - T\,S^0_g$$

where

$$H^0_g = \int_0^T C_p\,dT$$

and

$$S^0_g = \int_0^T C_p/T\,dT;$$

$S^0_0 = 0$ (third law) but E^0 is indeterminate. Similarly for the solution of the gaseous ester, there will be a corresponding equation with appropriate subscripts incorporating parameters derived from the temperature dependence of the Henry's Law constant

[1]*Manuscript received November 21, 1958.*
Contribution from the Division of Pure Chemistry, National Research Council, Ottawa, Canada.
Issued as N.R.C. No. 5103.
[2]*National Research Council of Canada Postdoctorate Fellow.*

(omitting the zero point energy) and similarly for the transition state. Thus the entropy of the transition state will be a summation of the terms

$$S^0_{\ddagger} = S^0_g + \delta_s S^0 + \Delta S^{\ddagger} \quad [3]$$

and an analysis of changes in $S^0_{\ddagger}$ as a consequence of structural changes will obviously require a consideration of the sum of the changes in each of the contributing terms. Such an analysis has been previously indicated by Moelwyn-Hughes for methyl bromide (12).

The general plan of this paper then follows eq. [3].

1. We propose a simple empirical method for estimating S^0_g values for certain series of esters where these are lacking.

2. Similarly an empirical method is given which provides parameters for the solution processes where the temperature dependences for the corresponding Henry's Law constants are unknown.

3. The entropy and enthalpy values ($\Delta S^{\ddagger}$, $\Delta H^{\ddagger}$) for the solvolytic process are correlated and related to changes in structure and to the role of the solvent.

4. The problem of charge development which is of such importance in connection with 3 is dealt with in a separate section.

5. Finally the parameters are combined as indicated in eq. [3] to give a limited characterization of the transition state for some alkyl halides and the activation energies for the methyl halides are calculated.

Values for S^0_g

The values of S^0_g (p = 1 atmosphere) have been listed for the methyl halides (13) but not for the other alkyl halides with which we are concerned in this paper. An isolated value has been given for tertiary butyl bromide by Howlett (14). Hence we have used a simple method for the estimation of gas phase entropies based on the S^0_g values of the corresponding hydrocarbons (15) for the isopropyl and tertiary butyl halides.

A term $\delta_x = S^0_g(\text{Me-X}) - S^0_g(\text{Me-H})$ is defined which gives the contribution to the standard state gaseous entropy obtained by replacing a hydrogen atom in the hydrocarbon by a halogen atom. Values for δ_x so calculated based on known values of the methyl halide (13) are given in Table I.

TABLE I

The $\delta_x S^0_g$ contribution of halogen atoms to the standard state entropy of the methyl halides (p = 1 atm)*

Halogen	$\delta_x S^0_g$ e.u.
F	8.8
Cl	11.47
Br	14.24
I	16.35

*It is only for the methyl halides that all the terms on the R.H.S. of eq. [3] have been determined experimentally. As a consequence values for S^0_g and $\delta_s S^0$ for other compounds must be regarded as tentative, especially those for S^0_g, since these have been obtained, by an approach which is undoubtedly oversimplified. Since this paper was written, a much more detailed treatment of the calculation of standard state entropies in cases where experimental values are lacking has been given by Benson and Buss (64) as well as in a recent monograph by Janz (65). It must be emphasized that this lack of precise data in no way alters the broad conclusions which we wish to establish, nor do we suggest that this is the only possible mode of treating these quantities.

To calculate S^0_g(R-X), S^0_g was combined with δ_x in the following manner:

$$S^0_g(\text{RX}) = S^0_g(\text{R-H}) + \delta_x. \quad [4]$$

As a check on the method, the values for ethyl chloride and for *t*-BuBr were calculated, since these were both known.

Calc.	Lit.
S^0_g(EtCl) = 66.32	65.9 (ref. 13)
S^0_g(*t*-BuBr) = 84.66	80.52 (ref. 14)

Clearly the errors involved for these simple molecules are not too serious. The required values for other compounds determined by this method are recorded in Table VI and compared where possible with the corresponding values calculated by Franklin (16). There is a constant difference of *ca.* 2.6 e.u. between Franklin's values for the isopropyl halides and the values calculated by the above simplified method, but the values for the *t*-BuCl and *t*-BuBr are essentially identical.

Certain special cases arise in which a relative characterization of $F^0_{\ddagger}$ can be obtained without reference to F^0_g. Consider a reaction of a single substrate solvolyzing in a series of solvents or solvent mixtures such as the recent study of the solvolysis of *t*-butyl chloride by Winstein and Fainberg (4):

$$F^0_{\ddagger} = F^0_g + \delta_s F + \Delta F^{\ddagger}. \qquad [5]$$

Since only one compound is involved, for a change of solvent,

$$\delta_M F^0_{\ddagger} = \delta_M \delta_s F + \delta_M \Delta F^{\ddagger}, \qquad [6]$$

i.e. the changes in $F^0_{\ddagger}$ derive only from changes in the solution and activation processes. The use of this relation can be illustrated by reference to the recent data of Winstein and Fainberg (4) for the solvolysis of *t*-butyl chloride in methanol–water mixtures.

By means of the cycle

$$\begin{array}{lcl} F^0_g & (RX)_g \xrightarrow{\Delta F^0_g} & (R\oplus\ldots\ldots X^{\ominus})_g \quad F^0_i \\ & \uparrow \delta_t F \qquad\qquad & \delta_s F_i \downarrow \\ F^0_s & (RX)_s \xrightarrow[\Delta F^0_{\ddagger}]{} & (R\oplus\ldots\ldots X^{\ominus})_s \quad F^0_{\ddagger} \end{array}$$

Winstein and Fainberg attempt a separation of the various changes in F^0_s and $F^0_{\ddagger}$ which are due to changes in the solvent. For example it is obvious that by combining the two relations from the above cycle

$$\delta_s F_i = F^0_{\ddagger} - F^0_i \qquad [7]$$

$$F^0_i = F^0_g + \Delta F^0_g \qquad [8]$$

the following relation is obtained for each solvent

$$\delta_s F_i = F^0_{\ddagger} - F^0_g - \Delta F^0_g \qquad [9]$$

and the effect of a change of solvent will be measured by difference

$$\delta_M \delta_s F_i = \delta_M F^0_{\ddagger} - \delta_M \Delta F^0_g, \qquad \delta_M F^0_g = 0. \qquad [10]$$

Clearly changes in $\delta_s F_i$ can only be compared with changes in $\delta_M F^0_{\ddagger}$ if the corresponding $\delta_M \Delta F^0_g$ values are known to $\rightarrow 0$. There is some reason to conclude that the extent of ionization along the MeOH–H_2O mixtures may vary and consequently further discussion of Winstein and Fainberg's dissected values must be postponed until further data are available. While such an approach may be useful in studying the effect of changes in

solvent, it cannot be extended to a study of the effect of structural differences on reactivity in the absence of a knowledge of the corresponding changes in F_g^0.

TABLE II

Free energy changes for the solvolysis of *t*-butyl chloride in methanol–water mixtures $T = 298.16°$ K

Solvent	$\Delta F^{\ddagger}$	$\delta_s F^*$	$F_{\ddagger}^0$	δ_M
MeOH	25.80	+3.15	$28.95+F_g^0$	10.40
90.17 MeOH/H_2O	24.72	+2.76	$27.48+F_g^0$	8.93
80.09 MeOH/H_2O	23.80	+2.35	$26.15+F_g^0$	7.60
70.45 MeOH/H_2O	23.15	+1.94	$25.09+F_g^0$	6.54
H_2O	19.49	−0.94 (−1.05)†	$18.55+F_g^0$	0

*Winstein and Fainberg values are corrected to the hypothetical standard state used in this paper. This involves a correction of $298.16\times19.53 = 5.823$ kcal. In this and succeeding work we shall use a standard state of 1 mole per liter in both liquid and gaseous state implying $p = 24.466$ atm at 298.16° K. This will involve a correction when comparing our data with those based on other standard states as follows:

Standard states summary

Source	c_g	c_s	p	Conversion factor
1. This paper	1 mole liter^{-1}	1 mole liter^{-1}	22.446 atm	—
2. Glew and Moelwyn-Hughes (17)	1 mole/1.8594×10^4 liter	1 mole liter^{-1}	1 mm Hg	$19.53 = R \ln (760\times22.415)\times(298.16/273.16)$
3. NBS Circular 500 (13)	1 mole/24.466 liter	—	1 atm	$6.35 = R \ln (24.466)$
4. NBS Circular C 461 (15)	1 mole/24.466 liter	—	1 atm	$6.35 = R \ln (24.466)$

†This value was calculated from an extension of the Barclay–Butler Rule (see below).

Initial State Solvation Differences

The solution process for non-electrolytes in water is dominated by the large water–water (*b–b*) interaction in contrast to similar solutions in non-associated solvents where (18) the solute–solute (*a–a*) interactions appear to govern the observed $\delta_s H$ and $\delta_s S$ values. Detailed discussions of aqueous solutions of non-electrolytes have been given by Bernal and Fowler (19), Eley (20), Frank and Evans (21), Glew and Moelwyn-Hughes (17), Feats and Ives (22). The outstanding features of such solution processes may be summarized as follows: (1) large positive ΔC_p values, (2) comparatively large negative $\delta_s H$ and $\delta_s S$ values which are found to be related for any series of alkyl groups attached to a common polar group X by a linear relation of the form

$$\delta_s H = \beta\delta_s S+\gamma, \qquad [11]$$

(3) changes in $\delta_s H$ and $\delta_s S$ appear to follow changes in the size of the solvation shell. The constant (γ) for any given series will include those specific differences in $\delta_s F$ arising as a consequence of differences in the interaction of the anionic portion of the ester with the solvent. The above regularities may be rationalized as follows. A hole must be created in the water for the solute. This will obviously vary with the size of the solute and will be related to the latent heat of evaporation as follows:

$$\delta_c H = (V_{\text{solute}}/V_{H_2O})\ 10.4 \text{ kcal} \qquad [12]$$

with corresponding values for $\delta_c S$, while through any series $\delta_R\delta_c F \approx 0$. But this cannot be the controlling step in the solution process, since the observed values of $\delta_s H$ and $\delta_s S$ are negative, suggesting a freezing process. This conclusion is supported by the sign of the $\delta_s C_p$ for the solution process of non-electrolytes which is positive and increases with the size of the solute. These facts were noted by Eley (20) and subsequently formed

the basis of the "iceberg hypothesis" suggested by Frank and Evans (21) and developed even more specifically by Glew and Moelwyn-Hughes (17). In effect, the mere presence of a cavity removes a measure of librational freedom (20) over an area proportional to the surface area of the solute and thus leads to increased interaction between those water molecules in the solvation shell. This increased interaction as a consequence of loss of librational freedom results in the changes in $\delta_s H$ and $\delta_s S$ and $\delta_s C_p$ which are opposite in sign, and being greater in magnitude than the corresponding values for cavity formation determine the observed sign of these parameters. Finally, solute–solvent interaction must be considered. Since the alkyl groups have low polarizability (with the exception of those containing unsaturated groups) this interaction will largely depend on the polarizability (23) of the anionic portion of the ester leading to the following increasing order of interaction:

$$F < Cl < Br < I < NO_3 < \text{sulphonates} \backsim \text{phosphates}.$$

This solvent–solute interaction will make a specific negative contribution to $\delta_s F$, which is constant throughout any given series. Since it will be less than $(b\text{–}b)$ interaction this $(a\text{–}b)$ interaction will alter the solvation parameters in the sense

$$[13] \qquad -\delta_x\delta_s F_{ab} = -\delta_x\delta_s H_{ab}; \quad T\,\delta_x\delta_s S_{ab} \approx 0\,.$$

That this is but a first approximation is evident from a consideration of $\delta_s H$ and $\delta_s S$ for ethane–ethylene; MeF, MeCl, and MeBr. These regularities as well as certain deviations are illustrated in Fig. 1, which shows the correlation of $\delta_s H$ vs. $\delta_s S$ values characterizing the solution of a series of hydrocarbons, alcohols, and a series of esters. The values for the latter and some of the former have been approximated by a method to be described below.

Estimation of $\delta_s H$ and $\delta_s S$

The determination of the temperature dependence of the Henry's Law constants for the esters reported here is a long arduous task, where it is at all possible (17). While an attempt will be made to determine values for key compounds, an approximate method was needed as an interim guide for the interpretation of the kinetic data available. The proposed method is based on the interpretation of the solvation process discussed above and on the further assumption that those regularities which formed the basis of the Barclay–Butler rule (24), and hold for the alkane and alcohol series, will also be true for intermediate series. It must be emphasized that the values so determined (Tables III, IV, and VI—excluding the methyl halides) are no better than these assumptions. Frank and Evans (21) comment on the difference in slope between the alcohols and the less polar compounds while Adon, Cox, and Herrington (25) and Glew and Robertson (26) showed a definite separation between the $\delta_s H$ vs. $\delta_s S$ plots for various series of solutes. ΔF in the eq. [14]

$$[14] \qquad \delta_s S = \frac{\delta_s H}{T} - \left(\frac{\delta_s F}{T}\right)$$

depends on polarity but $\delta_s F/T$ is found to remain remarkably constant for a given series. The regularities already noted support the assumption that through each point in the $\delta_s H$–$\delta_s S$ plot corresponding to RX where R = methyl we may draw a line such that

$$[15] \qquad \delta_s S = \beta\delta_s H$$

where $\beta = f(1/T)$ and T will have a value intermediate between that for alcohols, T

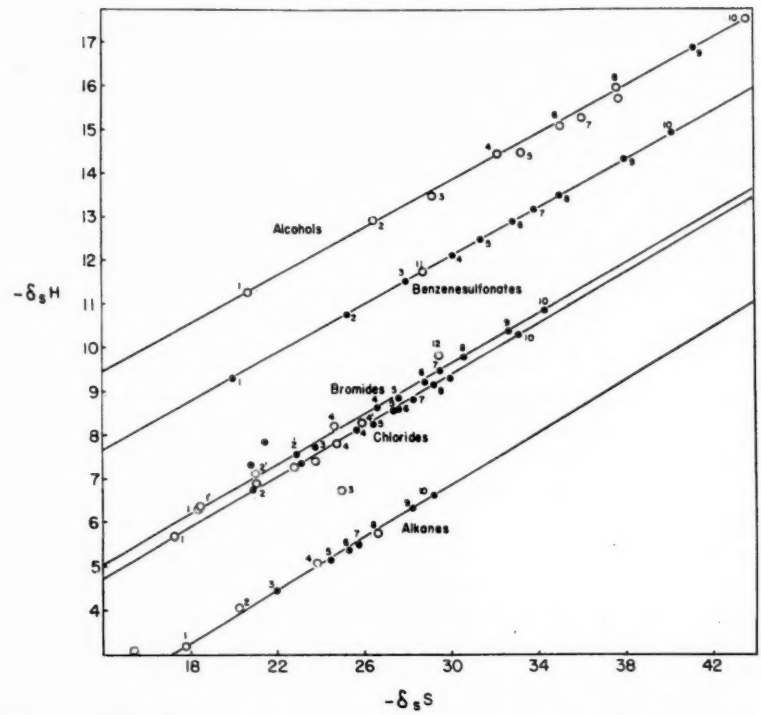

FIG. 1. Estimation of solvation parameters for compounds in water. The numbers refer to Table IV. ○Experimental. ●Estimated.

= 273, and that for the alkanes, $T = 300$, the variation being assumed proportional to separation along the $\delta_s H$ axis. If the Henry's Law parameters are known for a single member of a series, the $\delta_s H$ vs. $\delta_s S$ plot may be assumed to pass through this point with a slope as given above. Since the solution parameters for the methyl halides were known (17), the corresponding plots were drawn and a line joining methane and methanol was found to approximate to the MeBr and MeI points. The intersection on the chloride and fluoride line did not coincide with the experimental methyl point and the values were accordingly adjusted on the assumption that the deviation was due to some constant $\delta_s H$–$\delta_s S$ contribution associated with X. Lines joining ethane–ethanol, propane–propanol, butane–butanol gave the corresponding EtX, PrX, and BuX points. Since Butler gave $\delta_s H$ vs. $\delta_s S$ values for many alcohols, the above assumptions were used to extend the hydrocarbon plot and so to the corresponding RX values (Table III). The values $\delta_s H$ vs. $\delta_s S$ for ethylamine (27) similarly provide a basis for obtaining the corresponding values for the amines. The only experimental points for comparison are those calculated by Glew (28) from data for EtCl by Nicloux and Scotti-Foglieni (29) and for the *n*-Pr, *i*-Pr bromides and iodides from 1906 data by Rex (30). With the exception of isopropyl chloride the values fall in the predicted range. However, since the experimental values are not consistent among themselves, e.g. $\delta_s S$ (EtCl) < $\delta_s S$ (EtBr), $\delta_s S$ (EtI), $\delta_s S$ (*n*-PrCl) < $\delta_s S$ (EtBr) contrary to what would be expected from relative sizes and polarizabilities (23), we do not regard the deviations between predicted and experimental

values as significant, and anticipate that more precise data will yield parameters which lie closer to the predicted points. It will be noted that any error in $\delta_s H$ will lead to a compensating error in $\delta_s S$ and displacement along the given plot.

TABLE III

Estimated thermodynamic parameters† for gas solution equilibria of RX

	X					
	–H		–Cl		–Br and –I	
R	$-\delta_s H$	$-\delta_s S$	$-\delta_s H$	$-\delta_s S$	$-\delta_s H$	$-\delta_s S$
1. Methyl	3.2	17.7	5.7	17.1	6.4	18.3
2. Ethyl	4.1	20.0	6.7	21.0	7.0	23.0
4. *n*-Propyl	5.1	23.7	8.1	25.7	8.6	26.5
3. Isopropyl	4.5	22.0*	7.4	23.1	7.8	24.3
8. *n*-Butyl	5.7	26.5	9.1	29.2	9.7	30.5
7. Isobutyl	5.5	25.8	8.9	28.2	9.5	29.5
6. *sec*-Butyl	5.4	25.2*	8.2	27.6	9.2	28.7
5. *t*-Butyl	5.1	24.5	8.2	26.3	8.8	27.5
9. Neopentyl	6.3	28.2	9.9	32.0	10.3	32.5
10. *n*-Pentyl	6.6	29.2	10.3	33.1	10.8	34.3
11. Ethyl acetate						
12. Chloroform						

*Hypothetical.
†See footnote Table I.

Some idea of the influence of the considerable differences in $\delta_s H$ and $\delta_s S$ through a series on the corresponding parameters for the activation process ($\Delta H^{\ddagger}$, $\Delta S^{\ddagger}$) can be judged for the normal series by comparison of the corresponding terms from weak acid–base equilibria studies. In these cases there can be no doubt of the degree of charge development in the ionic form, while in the solvolytic process the transition state has been variously estimated by some to have a charge of $\frac{1}{2}\epsilon$ and others $\rightarrow 1\epsilon$ (see below) (9, 31, 32).

Acid–Base Equilibria Entropy and Enthalpies

The initial state data for the amines can be determined as described above. Those for the acids may be determined if we assume that acetic acid is colinear with ethane and ethanol and determine the $\delta_s H$–$\delta_s S$ point along this line corresponding to $\delta_s F = 1.50$ kcal. The slope of the acid ionization plot was determined as before and, from the predicted values for propionic and butyric acids, $\delta_s F$ values were calculated which agreed (Table IV) within experimental error with the values given by Butler (27). Entropy and enthalpy values for the process of acids and amines and for the corresponding equilibria are recorded in Table IV. A comparison of $\delta_s H/\delta_s S$ with the corresponding $\Delta H/\Delta S$ shows that while the former becomes increasingly negative as the chain lengthens the corresponding ΔS values rapidly converge to a value -24 e.u. The obvious conclusion is that on ionization, reorganization of a solvent will only occur over a limited volume. In any comparison, solvation differences to be significant must occur within this volume (33, 34, 35).

This same consideration will enter into discussions of kinetic parameters where we wish to take account of initial state solvation differences, e.g. the Franklin cycle (see below). Here, too, the development of charge in the activation process results in reorganization of solvent about the "seat of reaction" only, a volume difficult of definition but obviously influenced by the degree of charge development and the structure con-

TABLE IV

Parameters for hydration and equilibria* for a series of acids and amines

Compound	$\delta_s H$	$\delta_s S$	$\Delta H_{ionization}$	$\Delta S_{ionization}$
Formic			− 40	−17.3
Acetic	−14.9	−27.9	−100	−22.1
Propionic	−16.6	−33.9	−170	−22.9
Butyric	−15.91	−40.1	−700	−24.4
Isobutyric	−17.85	−38.80	−799	−24.9
NH_3			1.094	−18.1
$MeNH_2$	−11.45	−22.30	431	−14.0
$EtNH_2$	−12.91	−27.9	− 41	−15.5
n-$PrNH_2$	−14.5	−33.51	−229	−16.5
n-$BuNH_2$	−15.96	−38.9	−453	−17.0
Me_2NH	−13.75	−30.75	1660	− 9.2

*Ref. 36.

tiguous to the bond being broken. Only in the case of such simple compounds as the methyl halides can we assume that this volume includes the entire primary solvation shell characteristic of the initial state. A recognition of the above limitation becomes extremely important when thermodynamic parameters such as the entropy of hydration of ions are being correlated with parameters derived from rate data (10). For the halides it will be noted that the correlation between the $\Delta S^{\ddagger}$ and $\delta_s S$ ion (Fig. 2) is permitted because the complete solvent shell about the forming halide ion in the activation process is influenced just as it is about the corresponding ion. However, the same correlation need not necessarily hold for the nitrate, methanesulphonate, or the benzenesulphonate groups for, although the initial state solvation involves the complete group, the entire solvation shell need not be affected in the transition state (66).

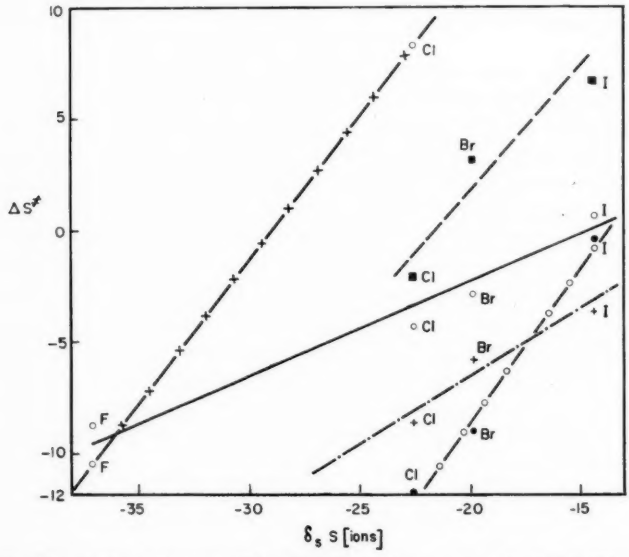

FIG. 2. Correlation between $\Delta S^{\ddagger}$ and $\delta_s S$[ions] for a series of alkyl halides.
—×—×—× *t*-Butyl (50° C) ——— Methyl (25° C)
— — — Isopropyl (25° C) —o—o—o Allyl (50° C)
—·—·—· Ethyl (50° C)

A distinction must clearly be made between such comparisons as suggested in the previous paragraph and the problem of determining the thermodynamic parameters characterizing the transition state. In such calculations the experimental parameters for the solvation process will enter quite naturally as indicated by eq. [3].

Kinetic Parameters

In Table V are collected a series of parameters characterizing the uncatalyzed solvolysis of esters which have been studied in pure water with sufficient accuracy to warrant comparison. For these compounds, where an accurate determination of $\Delta C_p^{\ddagger}$ had been made, the evaluation of $\Delta H^{\ddagger}$ and $\Delta S^{\ddagger}$ for any temperature between 0 and 100° is convenient. For compounds where $\Delta C_p^{\ddagger}$ can only be estimated the following technique was used.

TABLE V*a*

Summary of activation parameters (at 323.16° K) for the solvolysis of a series of methanesulphonates, benzenesulphonates, and alkyl halides hydrolyzing in water

	Benzene sulphonates		Methane sulphonates		Fluorides		Chlorides		Bromides		Iodides	
	$\Delta H^{\ddagger}$	$\Delta S^{\ddagger}$	$\Delta H^{\ddagger}$	$\Delta S^{\ddagger}$	$\Delta H^{\ddagger}$	$\Delta S^{\ddagger}$	$\Delta H^{\ddagger}$	$\Delta S^{\ddagger}$	$\Delta H^{\ddagger}$	$\Delta S^{\ddagger}$	$\Delta H^{\ddagger}$	$\Delta S^{\ddagger}$
Methyl	20.597	−11.58(1)	20.441	−14.08(3)	25.591	−12.21(5)	25.263	−8.89(6)	24.142	−6.65(6)	25.950	−3.94(6)
Ethyl	21.161	−10.30(1)	21.120	−12.31(3)			24.960	−5.24(6)	24.26	−7.10(6)	25.606	−3.61(6)
Isopropyl	20.791	−3.86(1)	21.424	−3.55(4)			24.960	−5.25(6)	24.36	−1.43(6)	25.527	+1.86(6)
t-Butyl					22.61	−11.36(4)	21.94	+8.32(7,8)				
n-Propyl	20.606	−12.33(1)	20.600	−11.7(3)					23.282	−10.12(10)		
n-Butyl	19.900	−14.7(2)	20.400	−15.00(3)								
n-Amyl	20.100	−13.9(2)										
Isobutyl	23.700	−6.6(2)	24.200	−6.1(3)					26.59	−2.64		
Neopentyl	26.000	−2.8(2)	25.700	−3.5(3)					32.201	−1.37(4)		
Allyl			17.750	−12.21(3)			20.009	−11.68(9)	21.166	−8.91(9)	22.91	−5.34(9)
Benzyl							20.388	−12.35(9)				

1. Ref. (54)
2. Ref. (55)
3. Ref. (56)
4. Ref. (57)
5. Ref. (59)
6. Ref. (45)
7. Ref. (60)
8. Ref. (62)
9. Ref. (58)
10. Ref. (61)

TABLE V*b*

Heat capacity data for the calculation of $\Delta H^{\ddagger}$ and $\Delta S^{\ddagger}$ in V*a*

The following values have been obtained in three different ways:
1. by means of the three-parameter equation (ref. 54),
2. by a plot of E_A vs. T,
3. estimated on the basis of known values by methods 1 or 2 for similar compounds.

Heat capacity of activation ($\Delta C_p^{\ddagger}$ = cal/mole/deg)

	Benzene sulphonate	Methane sulphonate	Fluoride	Chloride	Bromide	Iodide
Methyl	−33.4 (1)	−37.6 (1)	−69 (1)	−52.0 (1)	−46.5 (1)	−56.6 (1)
Ethyl	−34.5 (1)	−36.7 (1)		−50 (3)	−50 (3)	−50 (3)
Isopropyl	−41.2 (1)	−27.4 (1)		−38.5 (1)	−56.4 (1)	−59 (1)
t-Butyl			−50 (3)	−45 (3)		
n-Propyl	−31.3 (1)	−28.8 (2)			−50 (3)	
n-Butyl	−30 (3)	−26.5 (2)				
n-Amyl	−30 (3)					
Isobutyl	−30 (3)				−50 (3)	
Neopentyl	−30 (3)	−23.7 (2)			−50 (3)	
Allyl		−35 (3)		−50.1 (1)	−59 (1)	−46.7 (2)
Benzyl				−40.4 (1)		

*The references for the above parameters are the same as for the corresponding compounds in Table V*a*.

The rates were determined over a small temperature range, e.g. 40°–50°–60°. The Arrhenius E_A was determined by the method of least squares and this will correspond in the case quoted to E_{50} (mid-point in the experimental range). Since

$$\Delta H^{\ddagger}_{50} = E_{A\,50} - R \times 323.16 \quad [16]$$

then from k_{50} and $\Delta H^{\ddagger}_{50}$, the $\Delta S^{\ddagger}_{50}$ follows from the absolute rate equation (37). It should be noted that this method does not require any knowledge of $\Delta C_p^{\ddagger}$ and will give results at 50° C of accuracy comparable to those for which $\Delta C_p^{\ddagger}$ has been determined.

Where reactivities made 50° inconvenient or impossible as a mid-point for a series (cf. technique 1 above) e.g. neopentyl bromides or *t*-butyl chloride, $\Delta H^{\ddagger}_T$ and $\Delta S^{\ddagger}_T$ were determined for the mid-point (T) of the experimental range. To evaluate $\Delta H^{\ddagger}_{50}$ and $\Delta S^{\ddagger}_{50}$ we used the formula

$$\Delta H^{\ddagger}_{T+\Delta T} = \Delta H^{\ddagger}_T + \Delta C_p^{\ddagger} \Delta T \quad [17]$$

$$\Delta S^{\ddagger}_{T_1} - \Delta S^{\ddagger}_{T_2} = \Delta C_p^{\ddagger} 2.3026 \, (\log T_1/T_2). \quad [18]$$

This requires a knowledge of $\Delta C_p^{\ddagger}$ for the respective compounds. Here we are guided by experience, the estimated values being shown in Table V*b*. When $\Delta H^{\ddagger}$ and $\Delta S^{\ddagger}$ values are plotted (Fig. 3) a series of linear relations are apparent, revealing definite

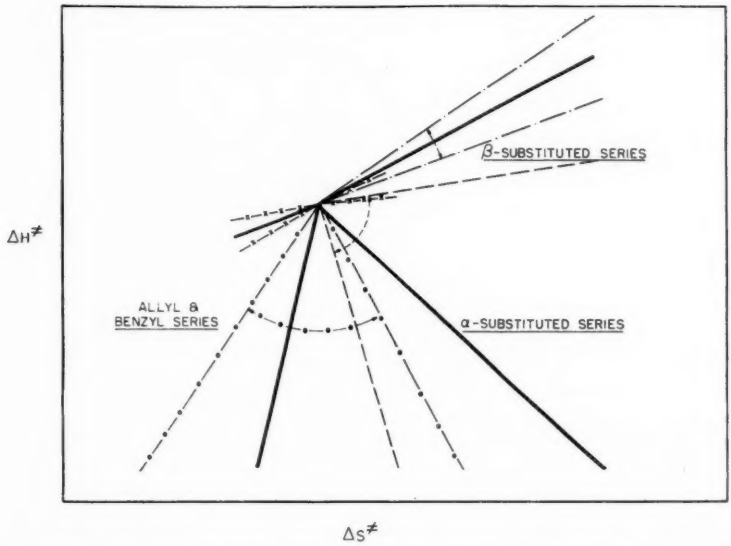

FIG. 3. General profile illustrating the effect of structure on the entropy and enthalpy of activation, for solvolysis reactions in water. The heavy lines indicate average trends; dotted lines indicate specific variations with changing anions.

correlations between the relative values of these parameters and the structure of the alkyl group. Specifically, the values of these coefficients for the α-methyl, β-methyl, straight chain, and unsaturated esters lie on distinct lines which radiate approximately from the methyl group. Functional relationships between $\Delta H^{\ddagger}$ and $\Delta S^{\ddagger}$ for other systems have been noted frequently and an extensive review on this subject has been published by Leffler (38). Hinshelwood (39) has suggested that such correlations are a consequence

of differences in the lifetime of the transition state but such a suggestion would set kinetic processes apart from the very similar correlations observed in acid–base equilibria (see above and Fig. 4) and those for parameters derived from solution processes. Leffler

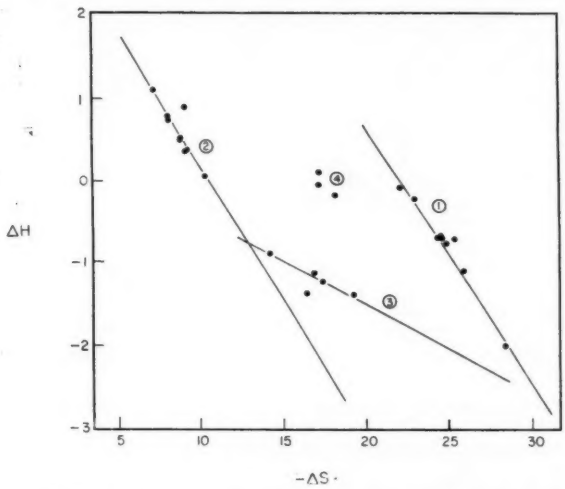

FIG. 4. Linear correlation for the thermodynamic parameters characterizing the dissociation of weak acids: 1, aliphatic acids; 2, amino acids; 3, halogeno-substituted acetic acids; 4, hydroxy acids.

noted that as a consequence of the reorganization of the solvent, on the basis of the Born equation one would expect a linear relation between $\Delta H^{\ddagger}$ and $\Delta S^{\ddagger}$. It would appear that the same argument can be used to include the corresponding changes in enthalpy and entropy arising from solute–solvent interaction as a consequence of other types of force fields involved in the activation process. However, the implication that the linear $\Delta H^{\ddagger}$ and $\Delta S^{\ddagger}$ correlations may be rationalized in terms of differences in solvation is probably an oversimplification. These parameters derived from kinetic studies must include internal as well as solvation differences and a linear correlation in the former implies a similar correlation in the latter or the assumption that the internal contributions to $\Delta H^{\ddagger}$ and $\Delta S^{\ddagger}$ are constant throughout any particular series. In order to rationalize the differences in the slopes of the $\Delta H^{\ddagger}$ and of $\Delta S^{\ddagger}$ correlation (Fig. 3) from our solvolytic data in water, it is convenient to examine, first, the corresponding plot derived from the results published by Ingold and co-workers for the halide exchange reaction in acetone (41). In these latter reactions we may assume that nucleophilic interaction is the dominant factor in the activation process, and the correlation between $\Delta H^{\ddagger}$ and $\Delta S^{\ddagger}$ from these data (Fig. 5) can be rationalized in terms of steric hindrance to nucleophilic attack (41) or a combination of polar and steric effects with the latter predominating (42). Solvation differences must be present, but are probably less specific in organic solvents than in water.

In contrast to the halide exchange reaction, solvation effects are undoubtedly the controlling factor for hydrolysis of esters in water, and the differences evident between the correlation of reaction parameters in Fig. 5 for the halide exchange and in Figs. 3, 6, and 7 for the solvolytic reaction must be rationalized in terms of this change in the controlling factors. From the standpoint of solvation there is also the difference in charge

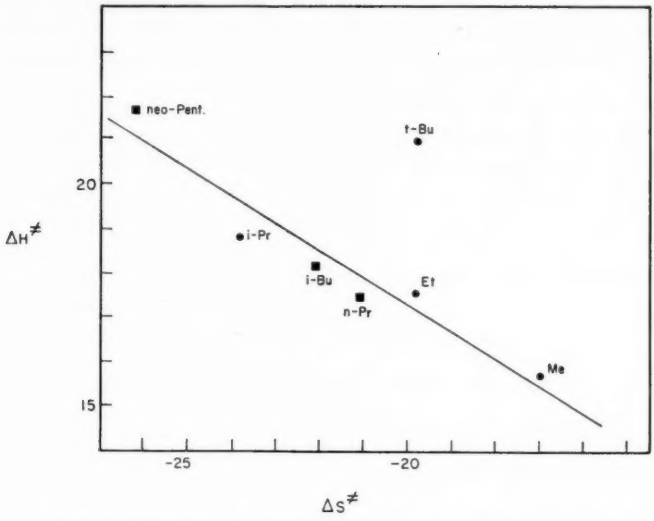

FIG. 5. Effect of structure on the entropy and enthalpy of activation for a bimolecular reaction.

type of the activation process but this is not considered responsible for the trends in the halide exchange parameters. Changes in initial state solvation, as a consequence of β-methylation for any series of esters, will result in successively moving the solvent farther from the carbon at the seat of reaction. The net result will be that, on thermal activation, interaction between the solvent and this carbon will be reduced. Consequently there will be less reorganization of the solvent about the developing carbonium ion in comparison to the reorganization of solvent about the less substituted alkyl group and hence a more positive entropy ($\Delta S^{\neq}$) for the former than for the latter.

Bond making between a particular solvent molecule and the alkyl group will likewise reduce $\Delta H^{\neq}$. Loss of such interaction will have to be compensated for by increased thermal activation and increased solvent interaction with the forming anion, but from the results we must conclude that the effect of this increased interaction on the entropy is not sufficient to compensate for the gain in entropy as a consequence of the decrease in quantum mechanical interaction with the carbonium carbon.

In the halide exchange reaction considered above the dominant driving force came from one direction only—the attack of the nucleophile. In solvolysis, by contrast, as one type of interaction is rendered less effective by structural changes in the alkyl group, alternative paths with higher activation energies become available. The effect of β-methylation in both cases was to raise the enthalpy ($\Delta H^{\neq}$) thus reducing the rate of reaction. The striking difference between the two series is evident in the accompanying entropy changes. Where bond making is dominant, the effect of β-methylation is to impose more stringent requirements on the transition state, leading to more negative entropies and further reducing the rate. In solvolysis, by contrast, as quantum mechanical interaction is reduced through structural change, alternative paths of reaction become available at higher temperatures which are characterized by less reorganization of the solvent and more positive entropy, which to a considerable degree compensates for the higher enthalpy. This difference between the two series can be illustrated by a com-

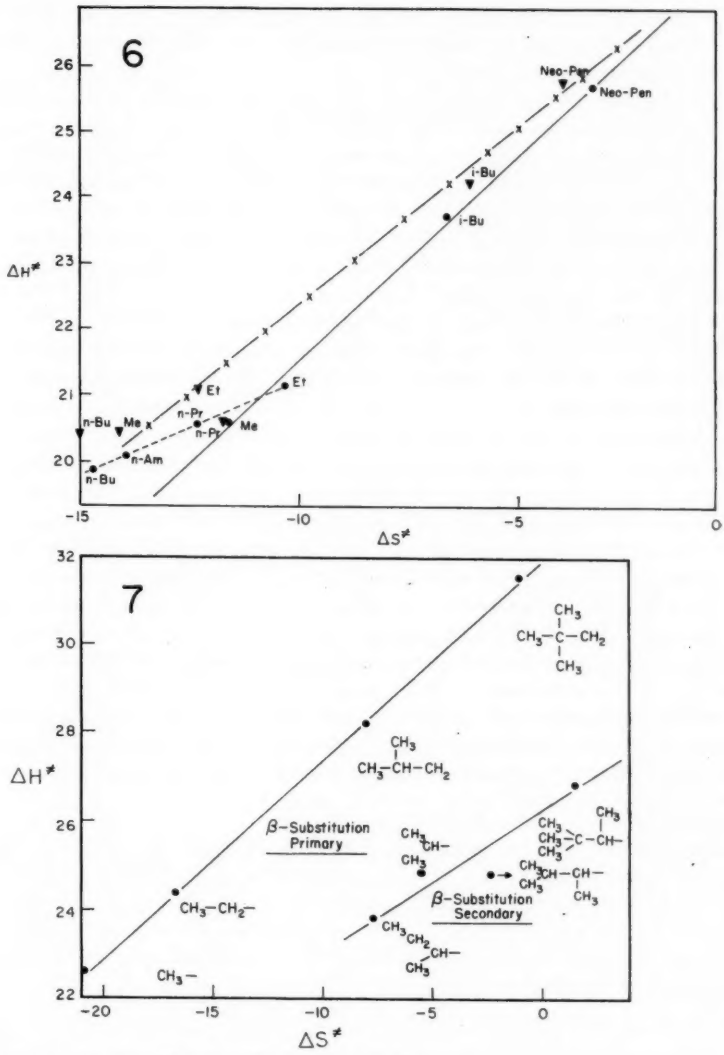

FIG. 6. Correlation of $\Delta H^{\ddagger}$ and $\Delta S^{\ddagger}$ for hydrolysis in water.
—X—X—X Methanesulphonates β-series
———— Benzenesulphonates β-series
— — — Benzenesulphonates *n*-series

FIG. 7. Effect of structure on the entropy and enthalpy of activation for solvolysis in acetic acid (ref. 63).

parison of the relative rates $k_{\text{methyl}}/k_{\text{neopentyl}} = 7.7\times10^{6}$ for halide exchange between Cl^- and the alkyl bromides, while the corresponding ratio from solvolysis at 80° C is 16.4. It is noted that the above argument neglects the positive shift in entropy resulting from increased charge development as well as initial state solvation differences.

Such an analysis would lead to the prediction that the values of $\Delta H^{\ddagger}$ and $\Delta S^{\ddagger}$ for the hydrolysis of the normal series of esters would lie close to those corresponding to the

ethyl ester. Since this is not found for the benzenesulphonates (Fig. 6) we must conclude that where steric factors are approximately constant, the effect of other factors such as initial state differences becomes apparent.

Changes in the entropy and enthalpy of activation through the β-substituted primary series of toluenesulphonates solvolyzing in acetic acid (63) show the same general trends both in magnitude and sign (Fig. 7) as was found for the benzenesulphonates hydrolyzing in water. The somewhat reduced slope for the linear $\Delta H^{\ddagger}$ vs. $\Delta S^{\ddagger}$ relation for the former may arise from the reduced importance of quantum mechanical interaction as a consequence of the shift from water to acetic acid as a solvolyzing medium. The difference between the alpha and the beta series arises first from the possibility in the former of a driving force for the reaction arising from an increased tendency toward a change in hybridization from sp^3 to sp^2, which in itself would account for a lowering of the enthalpy and a positive shift in entropy. Secondly, because there is branching close to the seat of reaction, the effect of added α-methyls will exclude solvent more effectively, resulting in an even larger proportional effect by comparison with the β-esters. In addition, in so far as the initial state of the isopropyl or *t*-butyl ester is in some degree more ionic in the initial state than is the corresponding beta compound, then this will further emphasize the difference in entropy between the two series. The combined effect of the above factors will lead to a larger positive shift in the entropy of activation through the alpha series than the corresponding beta series. The difference in the complexity of the contributing factors in the two series is further reflected in the range of values for the parameters through the various series for which data are available to us; contrast the wider range for the alpha than for the beta groups (Figs. 3, 8). In the allyl and benzyl series, where varying charge development in the initial state can alter with the nature of the anionic portion of the molecules, a wider range is also found. Here, however, because the steric factors about the seat of the reaction are relatively constant, the observed changes occur largely in the enthalpy, and solvation differences probably arise from differences in charge development characteristic of the transition state.

Charge Development in the Transition State

In the preceding sections we have shown how to estimate the values of S_g^0 and $\delta_s S$ where they are not known and are now in a position to combine these values with the experimentally determined $\Delta S^{\ddagger}$ according to eq. [3] to get the standard state entropies which characterize the transition state. These values are recorded in Table VI. With the above data available it is now possible to estimate the degree of charge development present in the transition state as follows.

TABLE VI

Summary of thermodynamic parameters for the alkyl halides at 298.16° K

Compound	S_g^0	$\delta_s S$	$\Delta S^0_{\ddagger}$	$S^0_{\ddagger}$
MeF	46.95	−14.11	−8.70	24.14
MeCl	49.62	−17.13	−4.31	28.18
MeBr	52.39	−18.30	−2.91	31.18
MeI	54.50	−18.32	+0.61	36.79
i-PrCl	69.63	−23.08	−2.15	44.40
i-PrBr	72.40	−24.25	+3.11	51.26
i-PrI	74.51	−24.27	+6.67	56.91
t-BuCl	75.54	−26.33	+11.94	61.15

NOTE: We may assume that $\Delta S^{\ddagger} = \Delta S^0_{\ddagger}$, since the $K^{\ddagger}$ from which $\Delta S^{\ddagger}$ is derived is independent of concentration units (37)—in general this will not be true (see Appendix).

If the transition state is quasi-ionic it is reasonable to assume

[19] $$S^0_{\ddagger} \propto S^0_{R}{}^{\oplus} + S^0_{X}{}^{\ominus}.$$

Making this equation more explicit we may write

[20] $$S^0_{\ddagger} = \mu S^0_{R}{}^{\oplus} + \alpha S^0_{X}{}^{\ominus} + c$$

where μ and α and c are constants.

The existence of similar relationships has been noted previously by Hudson and Saville (44) and by Evans and Hamman (10) but has not been set down explicitly as above. The latter, for example, showed a trend between the entropy of solvation for bromide and iodide and the corresponding entropy of activation for two alkyl halides, but such a comparison cannot be strictly true because it fails to take account of initial state differences. It will be noted that these initial state differences are included in the $S^0_{\ddagger}$ and this must be regarded as the main justification for stressing the importance of this term in comparison with the more easily available $\Delta S^{\ddagger}$ value from kinetic measurements.

TABLE VII

Estimation of standard state entropies of alkyl cations

	$S^0(R^{\oplus})$*	$S^0(R^{\oplus})$†
Me	28.32	—
i-Pr	33.34	57.9 (16)
t-Bu	47.98	63.9 (16)

*Calculated from experimental data.
†Semitheoretical values computed by Franklin (ref. 16).

If a plot of the $S^0_{\ddagger}$ values is made against the standard state entropy of the corresponding halogen ions (Fig. 9), two linear relationships are apparent, the methyl and isopropyl series forming two distinct lines. In the methyl halide series the three halides recently measured in this laboratory (45) gave a linear relationship which loses its precision with the methyl fluoride. This, however, might have been anticipated from the large extrapolation of the rate data required to calculate $S^0_{\ddagger}$ (298.16) for the latter compound. The parameters for these linear plots were determined by the method of least squares (neglecting the fluoride in the methyl series) leading to eqs. [21] and [22].

[21] Methyl $$S^0_{\ddagger} = 0.671\ S^0(X^{\ominus}) + 19.00$$

[22] Isopropyl $$S^0_{\ddagger} = 0.962\ S^0(X^{\ominus}) + 32.07$$

Observed and calculated entropies from these equations are compared in Table VIII, where the standard state entropies of the corresponding halogen ions are also given (13).

TABLE VIII

Comparison of observed and calculated standard state entropies by equations [21] and [22]

		Methyl halides		Isopropyl halides	
	$S^0(X^{\ominus})$	$S^0_{\ddagger obs}$	$S^0_{\ddagger calc}$	$S^0_{\ddagger obs}$	$S^0_{\ddagger calc}$
F	−2.3	24.14	—		
Cl	13.17	28.18	27.83	44.4	44.73
Br	19.29	31.18	31.94	51.26	50.62
I	26.14	36.97	36.54	57.91	57.22

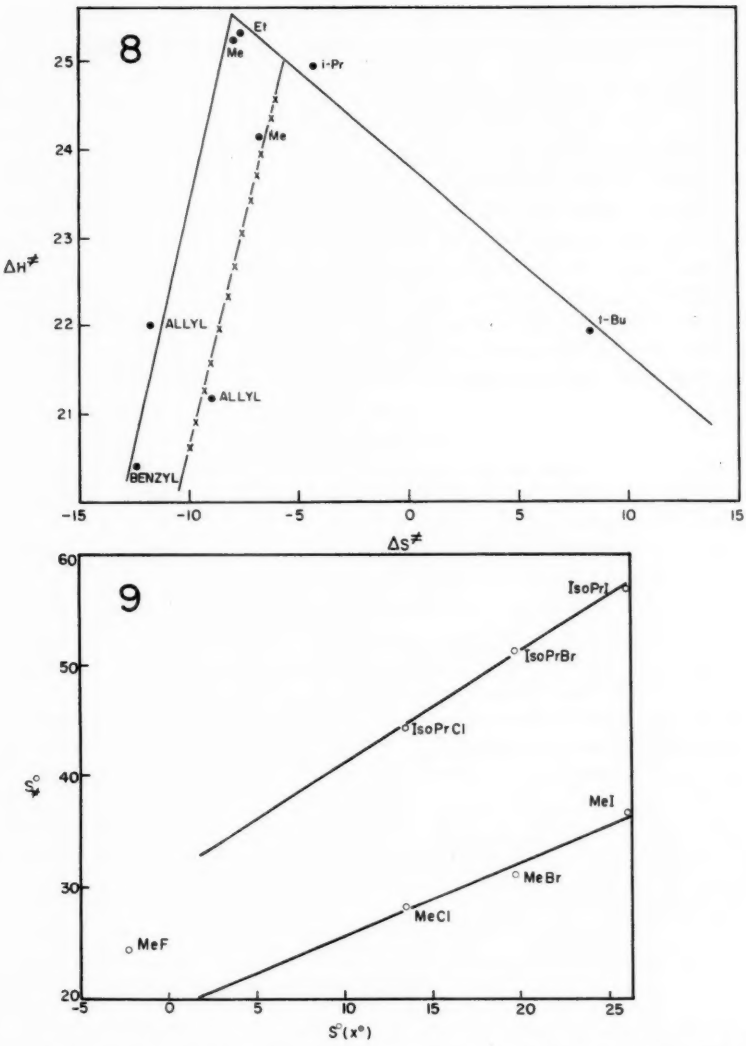

FIG. 8. Correlation of enthalpy and entropy of activation for α-substituted and unsaturated alkyl halides
——●—— Chlorides —×—×—× Bromides

FIG. 9. Correlation of $S^{0}_{\ddagger}$ and $S^{0}(X^{\ominus})$ for methyl and isopropyl halides.

If we make the assumption that $\mu = \alpha$ and $c = 0$ we can calculate the standard state entropies of the methyl, isopropyl, and *t*-butyl cations ($\alpha = 1$ for the *t*-Bu series).

The coefficients of $S^{0}(X\ominus)$ in the above equations are consistent with the view that the anions are not completely formed in the transition state. Since $\alpha(\text{Me}) < \alpha(i\text{-Pr})$ it would seem that the tendency toward complete ionization increases with α substitution, as is normally assumed. We may safely assume $\alpha = 1$ for the *t*-butyl halides and from this we may calculate $S^{0}(t\text{-Bu}^{\oplus})$ for the single reasonably accurate value we have in the

t-butyl series (*t*-BuCl). To give α any further significance must be largely speculative, since it requires a knowledge of how $S^0(X^{\ominus})$ will vary with partial charge development.[3] Currently two views are adopted. Laidler considers (46) $S^0(X^{\ominus}) \propto Z^2$ (Z = charge) and Powell and Latimer (47) consider $S^0(X^{\ominus}) \propto Z$. In this paper we shall adopt Laidler's conclusion because of the successful application by Mason (48) of the Z^2 relationship in discussing the entropy factors in the solvolysis of arylmethyl chlorides.

Thus from eqs. [21] and [22] the charge development for the methyl halides in the transition state is $(0.671)^{\frac{1}{2}}\epsilon = 0.82\epsilon$ and for the isopropyl halides is $(0.962)^{\frac{1}{2}}\epsilon = 0.98\epsilon$.

The Activation Energy for the Methyl Halides

With a guide to the charge development in the methyl halide series it becomes worth while to attempt to calculate again the activation energy for this series. (See for previous work Ogg and Polanyi (49), Evans (32), and Franklin (16).)

Following Franklin we use the cycle:

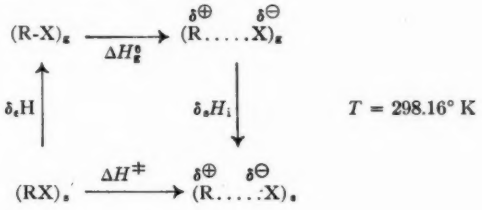

For this calculation we shall require:

(*a*) $\delta_s H$, the heat of escape of the gaseous methyl halides from solution. This has been measured by Glew and Moelwyn-Hughes (17).

(*b*) ΔH_g^0, the heat of partial ionization of R-X in the gas phase. Calculations for complete ionization are well known (42) (Table IX).

(*c*) $\delta_s H_i$, the combined heats of solution of $R^{\oplus}$ and $X^{\ominus}$ from the gas phase to solution.

The heats of solution for the halide ions have been listed by Latimer, Pitzer, and Slansky (50). These values, it must be noted, are somewhat arbitrary in that they require the total heat of solution of a *pair* of ions to be split up. How this should best be accomplished has not yet been made clear (cf. Moelwyn-Hughes (51)).

TABLE IX

Energies for the ionization of the methyl halides in the gas phase at 298.16° K

Compound	ΔH_g^{0*}	$\Delta H_g^{0\dagger}$	
MeF	247.2	—	—
MeCl	223.3	220	223
MeBr	215.2	215	214
MeI	207	208	204

*This paper.
†Streitwieser (ref. 42).

The heat of solvation of the methyl cation represents a much more difficult problem. On a purely electrostatic basis Franklin (16) has estimated the heat of solution as −61 kcal/mole. This value treats the methyl cation as a thermodynamically stable entity

[3]*We are fully aware that other interpretations of the constant α are possible but these will be dealt with in a later communication.*

when it is in water. This is certainly erroneous, i.e. the methyl cation does not correspond to an ion of given radius and complete octet. We have arrived at an estimate of the heat of solution of the methyl cation which combines both the heat of solvation and the heat of reaction. We consider that both these energy terms are available as driving forces in kinetics. The heat of solvation represents the purely electrostatic portion whilst the heat of reaction is derived from backside attack of the water molecule.

Following Mason (48) we shall apply an equation of the form

[23] $$\Delta H^{\ddagger} = \delta_s H + \alpha^{\frac{1}{2}} \Delta H_g^0 + \alpha \delta_s H_1$$

$\alpha^{\frac{1}{2}}$ being equal to the charge development in the transition state.

Values for ΔH_g^0

These have been calculated by Stevenson and quoted by Streitwieser (42). We have recalculated these values from available data (13) using the ionization potential for the methyl radical as 230 kcal/mole and the heat of formation of methyl fluoride as 64 kcal/mole, kindly provided by Dr. Bernstein of these laboratories.

Heat of Solution of the Methyl Cation

Consider the combined processes

$$\begin{array}{ccc} CH_3^{\oplus}(g) + H_2O(g) & \xrightarrow{\Delta H_b} & CH_3OH(g) + H^{\oplus}(g) \\ \downarrow \delta_s H_a & \searrow \Delta H & \downarrow \delta_s H_c \\ CH_3^{\oplus}(s) + H_2O(s) & \xrightarrow{\Delta H_d} & CH_3OH(s) + H^{\oplus}(s) \end{array}$$

We may assume

[24] $$\delta_s H_a + \Delta H_d = \Delta H_b + \delta_s H_c = \Delta H \,.$$

Now $\delta_s H_a = \delta_s H(CH_3^{\oplus}) + \delta_l H$ (latent heat of condensation of water),

ΔH_d = heat of reaction of 'solvated' methyl cation to give alcohol + solvated proton. Both processes may be considered to be exothermic, since the 'solvated' methyl cation would not be expected to be thermodynamically stable.

Since $\Delta H_b + \delta_s H_c$ are easily computed we can determine $\Delta H_d + \delta_s H(CH_3^{\oplus})$.

$$\begin{aligned} \Delta H_b &= \Delta H_f^0(H_g^+) + \Delta H_f^0(CH_3OH_g) - \Delta H_f^0(CH_{3_g}^+) - \Delta H_f^0(H_2O)_g \\ &= 367.1 - 48.1 - 262.0 + 57.8 \text{ kcals} \\ &= 114.8 \text{ kcals.} \end{aligned}$$

The heat attending the dissolution of 1 gram molecule of hydrohalic acids *as ions* is given by Moelwyn-Hughes (51). The heats of solution of the separate halogen ions have been given by Latimer, Pitzer, and Slansky (50), therefore

[25] $$\delta_s H\,(H^{\oplus}) = \delta_s H\,(H^{\oplus} X^{\ominus}) - \delta_s H\,(X^{\ominus}) \,.$$

Combining the above data according to eq. [25] we obtain a mean value for the enthalpy of hydration for the proton of 254.6 kcal/mole.

Latent heat of condensation of water = -10.4 kcal.
Heat of solution of MeOH = -10.7 kcal.
$\Delta H_d + \delta_s H\,(CH_3^{\oplus}) - (-10.4) = 114.8 - 10.7 - 254.6.$
$\Delta H_d + \delta_s H\,(CH_3^{\oplus}) = -140.1$ kcal.

We can now approximate to $\delta_s H_i$ in the Franklin cycle (previous section) by combining the above figure with the heat of solvation for the appropriate anion (Latimer).

In Table X we have recorded the various quantities which are required to calculate the enthalpy of activation according to eq. [23]. Values for $\delta_s H_i$ are given by the equation

$$\delta_s H_i = \Delta H_d + \delta_s H\ (CH_3^{\oplus}) + \delta_s H\ (X^{\ominus}).$$

Two values of α have been used: $\alpha = 0.67$ as determined by the relationship (21) for the methyl halides and a slightly higher value $\alpha = 0.74$. The value of $\Delta H^{\ddagger}$ calculated is extremely sensitive to the value of α adopted. It will be seen from Table X that the value of $\Delta H^{\ddagger}$ so calculated is in reasonable agreement with experiment, from which we may conclude that in the transition state the water molecule is strongly bonded (both covalently and electrostatically) to the carbon atom undergoing substitution.

TABLE X

Theoretically computed values for $\Delta H^{\ddagger}$ and associated data at 298.16° K

Compound (RX)	$\delta_s H_i(X^{\ominus})$	$\delta_s H$	ΔH_g^0 (1)	ΔH_g^0 (2)	$\delta_s H_i$ (1)	$\delta_s H_i$ (2)	Calc. $\Delta H^{\ddagger}$ (1)	Calc. $\Delta H^{\ddagger}$ (2)	Obs. $\Delta H^{\ddagger}$
MeF	−122.6	4.4	202.7	212.6	−176.0	−194.4	31.1	32.6	27.3
MeCl	−88.7	5.7	183.1	192	−153.3	−169.3	35.5	28.4	26.5
MeBr	−81.4	6.3	176.5	185.1	−148.4	−163.9	34.4	27.5	25.3
MeI	−72.1	6.4	169.7	178	−142.2	−157.0	33.9	27.4	27.4

$\delta_s H_i$ (1) is equal to $\alpha[\Delta H_d + \delta_s H_i\ (CH_3^{\oplus}) + \delta_s H_i\ (X^{\ominus})]$ where $\alpha = 0.67$.
$\delta_s H_i$ (2) is equal to $\alpha[\Delta H_d + \delta_s H_i\ (CH_3^{\oplus}) + \delta_s H_i\ (X^{\ominus})]$ where $\alpha = 0.74$.

ΔH_g^0 (1) is equal to $\alpha^{\frac{1}{2}} \Delta H_g^0$ where $(\alpha)^{\frac{1}{2}} = 0.82$: ΔH_i^0 given in Table IX.

ΔH_g^0 (2) is equal to $\alpha^{\frac{1}{2}} \Delta H_g^0$ where $(\alpha)^{\frac{1}{2}} = 0.86$: ΔH_i^0 given in Table IX.

The extension of the above calculations to the isopropyl and *t*-butyl and allyl and benzyl halides has not been carried out for a variety of reasons which are both practical and theoretical. On the practical side the approximate evaluation of the charge development in the *t*-butyl halides from the standard state entropies of activation ($S_{\ddagger}^0$) is impossible because of their high reactivity. Theoretical objections to any such calculation are equally great.

It will be noted that the ΔH_g^0 values for the isopropyl, *t*-butyl, allyl, and benzyl are considerably less than those for the corresponding methyl halides. This drop in ΔH_g^0 is mainly due to a decrease in the ionization potential of the corresponding radical accompanied by a relatively small bond energy decrease (52). The lowering of the ionization potential is attributed to resonance in the alkyl radical. This is a perfectly reasonable explanation for the gas phase reaction.

In solution, however, the charge stabilization of the forming cation can occur in two distinct ways. First, the localized charge can be solvated, or second, the delocalized charge can be stabilized by solvation. It has been shown in a most elegant paper by Mason (48) that the effect of charge delocalization is to lower the free energy of solvation to a considerable degree. A rough calculation for the benzyl cation indicates that the solvation of the delocalized charge plus the resonance energy is less than the solvation energy of the localized charge by as much as 20 kcal.

The tropylium ion, however, provides a striking example where resonance stabilization, implying delocalized charge, is more favorable than the solvation of the localized charge.

Even in this case, where resonance stabilization is large (53), there is a definite tendency to revert to the alcohol

$$C_7H_7^{\oplus} + 2H_2O \rightleftharpoons C_7H_7OH + H_3O^{\oplus} \qquad K_{25} = 1.8\times10^{-5}$$

a reaction analogous to the specific localized solvation of a resonating carbonium ion. From the above it would appear that great care must be exercised in rationalizing changes in reactivity as arising from resonance contributions to the transition state, since the solvation of the localized charge may represent a more favorable reaction path. The reasons why we hesitate to use Stevenson's ΔH_g^0 for the gas phase reaction

$$(RX)_g \rightarrow R_g^{\oplus} + X_g^{\ominus}$$

can now be stated for the cases where R = *i*-Pr, *t*-Bu, allyl, and benzyl.

Stevenson's values contain the whole of the resonance energy, since there can be no other mode of stabilization of the positive charge in the gas phase. The only case where ΔH_g^0 can be related to solution kinetics is in the methyl halide series where resonance is negligible in the forming alkyl cation.

The above discussion of the effect of charge delocalization on the free energy of solvation suggests some important criticisms of the calculations by Franklin (16). The errors in calculating the heats and entropies of solvation of the alkyl cations in terms of their relative dimensions only has already been noted. Franklin has also used the values for ΔH_g^0 which contain the resonance energy of the forming cation, although no account has been taken of the effect of this charge distribution on the solvation parameters which as a consequence would be considerably reduced. Thus Franklin's calculations give reasonable results due to a fortuitous cancellation of several errors (4). There is good reason from the $S_{\pm}^0$ vs. $S^0(X^{\ominus})$ relationship (see above) to believe that in water only reactive compounds have reached complete ionization in the transition state ($\alpha = 1$) which Franklin assumes for all compounds. However, Franklin's calculations appear to be correct in principle and should be capable of giving good results with the proviso that the appropriate values for the thermochemical quantities required are available and the transition state is carefully defined.

It will be obvious that the argument presented here rests on the correctness of the assumption (common to all such applications of thermodynamics to kinetic data) that the transition state may be treated as though in equilibrium with the average initial state. We are unaware of any evidence to suggest that such an assumption is unjustified. It will be equally obvious that the work presented here is made possible by the happy combination of accurate kinetic data and reasonable values for the initial state parameters. While it should be possible in principle to extend this treatment to all systems, in practice almost none of the necessary data are available. In this respect we hope that this paper may point the way as well as emphasize the tremendous challenge in this field for both the experimentalist and the theoretician. Yet even if all the necessary thermodynamic parameters were determined for the reactions of interest, a detailed understanding of the activation process would still require that a satisfactory model be constructed, which would satisfy the energetic requirements so determined. In this connection it would appear that the variations in the entropy and enthalpy factors discussed above, in the particular case of hydrolysis, throw far more light on the nature of the transition state than could possibly be derived from a comparison of free energies. While hardly surprising, this needs to be emphasized as a justification for the greatly increased experimental requirements. The above treatment is presented, therefore, not as a panacea,

but rather as an illustration of what can be done under very favorable experimental conditions and as an example of an essential link in the development of a quantitative treatment of the relation between structure and reactivity for reactions in solution.

ACKNOWLEDGMENT

We wish to acknowledge the criticism and suggestions which we received from Professors K. J. Laidler and P. M. Laughton.

REFERENCES

1. HAMMETT, L. P. Physical organic chemistry. McGraw-Hill Book Company, Inc., New York. 1940. Chap. 7.
2. BRONSTED, J. M. Chem. Revs. **5**, 322 (1928).
3. GRUNWALD, E. and WINSTEIN, S. J. J. Am. Chem. Soc. **70**, 846 (1948).
4. WINSTEIN, S. and FAINBERG, A. J. Am. Chem. Soc. **79**, 5937 (1957).
5. HUDSON, R. F. and BROWN, D. A. J. Chem. Soc. 3352 (1953).
6. SWAIN, C. G. and SCOTT, C. B. J. Am. Chem. Soc. **75**, 141 (1953).
7. MILLER, S. I. (In press).
8. EVANS, M. G. and POLANYI, M. Trans. Faraday Soc. **32**, 1333 (1936).
9. INGOLD, C. K. Structure and mechanism in organic chemistry. Cornell University Press, Ithaca, N.Y. 1953. Chap. 6.
10. EVANS, A. G. and HAMMAN, S. D. Trans. Faraday Soc. **47**, 25 (1951).
11. BENSLEY, B. and KOHNSTAM, G. J. Chem. Soc. 287 (1956).
12. MOELWYN-HUGHES, E. A. Proc. Roy. Soc. (London), A, **220**, 386 (1953).
13. NATIONAL BUREAU OF STANDARDS. Selected values of thermodynamic properties, Circ. 500 (1952).
14. HOWLETT, K. J. Chem. Soc. 2834 (1957).
15. NATIONAL BUREAU OF STANDARDS. Selected values of properties of hydrocarbons, Circ. 461 (1947).
16. FRANKLIN, J. L. Trans. Faraday Soc. **48**, 443 (1952).
17. GLEW, D. N. and MOELWYN-HUGHES, E. A. Discussion Faraday Soc. 15, 1953.
18. EVANS, M. G. Discussions Faraday Soc. 166 (1936).
19. BERNAL, J. D. and FOWLER, E. J. Chem. Phys. **1**, 515 (1933).
20. ELEY, D. D. Trans. Faraday Soc. **40**, 184 (1944).
21. FRANK, H. S. and EVANS, M. W. J. Chem. Phys. **13**, 507 (1945).
22. FEATS, F. S. and IVES, D. J. G. J. Chem. Soc. 2798 (1956).
23. MORRISON, T. S. and JOHNSTONE, N. B. J. Chem. Soc. 3441 (1954).
24. BARCLAY, I. M. and BUTLER, J. A. V. Trans. Faraday Soc. **34**, 1445 (1938).
25. ADON, R. J. L., COX, J. D., and HERRINGTON, E. F. G. J. Chem. Soc. 3188 (1954).
26. GLEW, D. N. and ROBERTSON, R. E. J. Phys. Chem. **60**, 332 (1956).
27. BUTLER, J. A. V. Discussions Faraday Soc. 229 (1936).
28. GLEW, D. N. Private communication.
29. NICLOUX, M. and SCOTTI-FOGLIENI, L. Ann. physiol. physicochim. biol. **5**, 434 (1929).
30. REX, A. Z. physik. Chem. **55**, 355 (1906).
31. EYRING, H. and STEARNS, A. E. J. Chem. Phys. **3**, 778 (1935).
32. EVANS, A. G. Reactions of organic halides in solution. Manchester University Press, Manchester. 1945.
33. HAMMOND, G. S. and HOGLE, D. S. J. Am. Chem. Soc. **77**, 3384 (1955).
34. ROBERTSON, R. E. Can. J. Chem. **33**, 1536 (1955).
35. GODDARD, E. D., HOEVE, C. A. J., and BENSON, G. C. J. Phys. Chem. **61**, 593 (1957).
36. LANDSMAN, D. A. Thesis, St. Andrews, 1955.
37. GLASSTONE, S., LAIDLER, K. J., and EYRING, H. The theory of rate processes. McGraw-Hill Book Company, Inc., New York. 1941. Chap. 1.
38. LEFFLER, J. J. Org. Chem. **20**, 1202 (1955).
39. HINSHELWOOD, C. N. Kinetics of chemical change. Oxford University Press. 1940. Chap. 9.
40. BLACKADDER, D. A. and HINSHELWOOD, C. N. J. Chem. Soc. 2728 (1958).
41. INGOLD, C. K. Quart. Revs. (London), **11**, 1 (1957).
42. STREITWIESER, A. Chem. Revs. **56**, 571 (1956).
43. WYNNE-JONES, W. F. K. and EYRING, H. J. Chem. Phys. **3**, 492 (1935).
44. HUDSON, R. F. and SAVILLE, B. J. Chem. Soc. 4114 (1956).
45. HEPPOLETTE, R. L. and ROBERTSON, R. E. (In press).
46. LAIDLER, K. J. Can. J. Chem. **34**, 1107 (1956).
47. POWELL, R. E. and LATIMER, W. M. J. Chem. Phys. **19**, 1139 (1951).
48. MASON, S. F. J. Chem. Soc. 808 (1958).
49. OGG, R. A. and POLANYI, M. Trans. Faraday Soc. **31**, 604 (1935).
50. LATIMER, W. M., PITZER, K. S., and SLANSKY, C. M. J. Chem. Phys. **7**, 108 (1939).
51. MOELWYN-HUGHES, E. A. Physical chemistry. Pergamon Press, London. 1957. Chap. 18.
52. LANE, M. R., LINNETT, J. W., and OSWIN, H. G. Proc. Roy. Soc. (London), A, **216**, 361 (1953).
53. DOERING, W. VON E. and KNOX, L. H. J. Am. Chem. Soc. **76**, 3203 (1954).
54. ROBERTSON, R. E. Can. J. Chem. **35**, 613 (1957).
55. LAUGHTON, P. M. and ROBERTSON, R. E. Can. J. Chem. **33**, 1207 (1955).

56. BARNARD, P. W. C. and ROBERTSON, R. E. Unpublished work.
57. ROBERTSON, R. E. Unpublished work.
58. SCOTT, J. M. W. and ROBERTSON, R. E. Unpublished work.
59. GLEW, D. N. and MOELWYN-HUGHES, E. A. Proc. Roy. Soc. (London), A, **211**, 254 (1952).
60. TOMMILA, E., MATTI TIILIKAINEN, and VOIPIO, A. Ann. Acad. Sci. Fennicae, A, **11**, 65 (1955).
61. FIERENS, P. J. C. and KRUYS, P. Bull. soc. chim. Belges, **64**, 542 (1955).
62. LAUGHTON, P. M. and ROBERTSON, R. E. Can. J. Chem. **34**, 1714 (1956).
63. WINSTEIN, S., MORSE, B. K., GRUNWALD, E., SCHREIBER, K. C., and CORSE, J. J. Am. Chem. Soc. **74**, 1113 (1952).
64. BENSON, S. W. and BUSS, J. H. J. Chem. Phys. **29**, 546 (1958).
65. JANZ, G. J. Estimation of thermodynamic properties of organic compounds. Academic Press, Inc., New York. 1958.
66. EVERETT, D. H. Discussions Faraday Soc. **24**, 220 (1957).

APPENDIX

The following scheme for the thermodynamic operators has been adopted. For all chemical reactions (i.e. for parameters derived from rates and equilibria) the symbol Δ carries its usual meaning. For changes in thermodynamic quantities arising from physical or structural changes the following operators have been used:

δ_M = change in medium,
δ_c = change from liquid to gas,
δ_R = change in structure of alkyl group,
δ_X = change in structure of anionic portion of solute,
δ_s = change from gas to solution.

The subscript i, e.g. $\delta_s H_i$, refers to the change in enthalpy in passing ions from gaseous phase to solution. For ionogenic reactions occurring in the gas phase, terms such as ΔF_g^0 and ΔH_g^0 have been used.

Terms such as $\Delta F_{\ddagger}^0$ have been used to designate the free energy of activation with respect to a defined standard state. The thermodynamic parameters derived from rate studies and collected in this paper will be independent of the standard state and hence $\Delta F_{\ddagger}^0 = \Delta F^{\ddagger}$.

STERIC INHIBITION OF RESONANCE
II. BOND LENGTHS IN MESO-SUBSTITUTED ANTHRACENES*

JAMES TROTTER†

The crystal structures of several meso-substituted anthracenes have recently been determined by X-ray diffraction methods (1) and reasonably accurate values of the molecular dimensions have been obtained. These detailed investigations have shown that the molecules of 9,10-dibromo- and 9,10-dichloro-anthracene are completely planar (2, 3). In the 9-nitro and 9,10-dinitro derivatives, however, the bulkier nitro groups are markedly tilted out of the aromatic planes about the C–N bonds (4), and correlation with the characteristic nitro group infrared frequencies suggests resultant decreases in resonance interaction between the nitro groups and the aromatic π-electrons (5). The angles of tilt alone do not give directly quantitative measures of the decreases in the conjugation compared with planar models, but resonance involving ionic structures, of type I for 9-nitroanthracene for example, would impart a considerable amount of double bond character to the C–N bond, and in addition cause variations in the N–O bond lengths when compared with those in aliphatic nitro compounds, and in the bond lengths in the anthracene nucleus compared with those in the unsubstituted molecule. It has been shown that in picryl iodide the C–N distances ortho to the iodine atom correspond to single bonds, indicating resonance inhibition, while the conjugated para C–N bond is very much shorter, suggesting a considerable amount of resonance interaction (6). Examination of the bond length variations in meso-substituted anthracenes therefore may give a quantitative account of the resonance interaction, and also indicate the amount of resonance inhibition due to steric effects in those molecules with bulky substituents, such as nitro groups, in the 9 and 10 positions.

The bond lengths, together with the standard deviations, in the molecules studied are compared in Table I with the bond lengths in anthracene (7, 8), the labelling of the carbon–carbon bonds being shown in the diagram. The values in the substituted anthracenes are quoted to 0.001 Å for comparison, although as the standard deviations indicate, the accuracy is much lower than this. The C–Br, C–Cl, C–N, and N–O distances in non-conjugated molecules are included under anthracene.

TABLE I

Bond lengths and standard deviations in meso-substituted anthracenes (Å)

Bond	Anthracene	9,10-Dibromo	9,10-Dichloro	9,10-Dinitro	9-Nitro
a	1.366±0.004	1.409±0.027	1.382±0.015	1.350±0.011	1.399±0.008
b	1.433±0.003	1.417±0.027	1.411±0.015	1.413±0.011	1.434±0.008
c	1.399±0.003	1.374±0.027	1.397±0.015	1.399±0.011	1.400±0.008
d	1.419±0.006	1.463±0.038	1.401±0.021	1.400±0.016	1.413±0.011
e	1.436±0.004	1.471±0.038	1.460±0.021	1.452±0.016	1.437±0.011
C–Br	(1.91)	1.928±0.027	—	—	—
C–Cl	(1.76)	—	1.739±0.016	—	—
C–N	(1.47)	—	—	1.450±0.015	1.482±0.015
N–O	(1.22)	—	—	1.241±0.009	1.216±0.009

Issued as N.R.C. No. 5068.

†*National Research Council Postdoctorate Fellow.*

Exocyclic Bonds

Since there is no resonance inhibition in the completely planar halogen derivatives, ionic structures (II) ought to make a contribution to the ground state of the molecule. However, the weight of structures of this type, with a positive charge on the halogen atom, is quite small, and only a small contraction of the carbon–halogen bond lengths below the single bond distances would be expected. The C–Cl bond distances in 9,10-dichloroanthracene are slightly less than the normal single bond length, but the difference is scarcely significant. The ionic structures, however, are highly polar and, although their weights are small, they reduce the dipole moment in 9-bromoanthracene, for example, in comparison with a non-conjugated molecule (methyl bromide = 1.78 D, bromobenzene = 1.52 D, 9-bromoanthracene = 1.50 D).

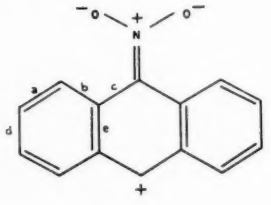

I

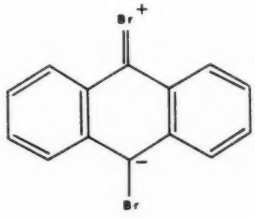

II

In 9-nitroanthracene the nitro group is tilted 85° out of the plane of the aromatic rings, and the C–N bond length (1.48 Å) corresponds to a single bond, indicating that there is little or no resonance between the anthracene nucleus and the nitro group. The C–N bond lengths in 9,10-dinitroanthracene, where the tilt of the nitro groups is 64°, are 1.45 Å, so that in this molecule there is a measurable amount of resonance interaction in spite of the large deviations from planarity. A quantitative measure of the resonance, however, requires a knowledge of the C–N bond length in a fully conjugated molecule such as nitrobenzene, and this length has not been accurately measured. (The conjugated C–N bond lengths in picryl iodide (6) and *p*-nitraniline (9) have been given as 1.35 Å and 1.41 Å respectively.) The C–N bond distances in 9,10-dinitroanthracene are much closer to the single bond length than to the distances in these fully conjugated molecules, so that while there is resonance interaction between the anthracene nucleus and the nitro group, it is much less than in completely planar aromatic nitro compounds. The N–O bond lengths in these nitroanthracenes also suggest that there is little or no resonance between the aromatic rings and the nitro group in 9-nitroanthracene, and a small but measurable interaction in 9,10-dinitroanthracene.

C–C Bonds

Examination of Table I shows that there are no really significant differences between the carbon–carbon bond lengths in the meso-substituted anthracenes studied and those in the unsubstituted molecule, indicating that contributions of ionic structures are too small to effect any measurable changes in the dimensions of the anthracene skeleton.

1. TROTTER, J. Acta Cryst. **11**, 564 (1958).
2. TROTTER, J. Acta Cryst. **11**, 803 (1958).
3. TROTTER, J. Acta Cryst. **12**, 54 (1959).
4. TROTTER, J. Acta Cryst. (In press).
5. TROTTER, J. Can. J. Chem. **37**, 351 (1959).

6. HUSE, G. and POWELL, H. M. J. Chem. Soc. 1398 (1940).
7. SINCLAIR, V. C., ROBERTSON, J. M., and MATHIESON, A. McL. Acta Cryst. **3**, 251 (1950).
8. CRUICKSHANK, D. W. J. Acta Cryst. **9**, 915 (1956).
9. DONOHUE, J. and TRUEBLOOD, K. N. Acta Cryst. **9**, 960 (1956).

RECEIVED OCTOBER 24, 1958.
DIVISION OF PURE PHYSICS,
NATIONAL RESEARCH COUNCIL,
OTTAWA, CANADA.

A CRYSTALLINE DERIVATIVE OF 2-*O*-(4-*O*-METHYL-α-D-GLUCOPYRANOSYLURONIC ACID)-D-XYLOPYRANOSE

T. E. TIMELL

2-*O*-(4-*O*-Methyl-α-D-glucopyranosyluronic acid)-D-xylopyranose, the structure of which was first established by Jones and Wise (1), has so far been isolated from some thirty natural plant products. Since no crystalline derivative of this amorphous compound has hitherto been known, it has been characterized by identification of the products obtained on hydrolysis of the original and of the methylated acid. A crystalline *p*-nitrobenzoate of the derived 2-*O*-(4-*O*-methyl-α-D-glucopyranosyl)-glycerol has been prepared (2) but the acetate of the 2-*O*-(4-*O*-methyl-α-D-glucopyranosyl)-D-xylitol is reported to be amorphous (3). A crystalline tetraacetate of the methyl ester methyl glycoside of the aldobiouronic acid has now been prepared and characterized.

Partial hydrolysis of a 4-*O*-methyl glucuronoxylan from white birch wood yielded 2-*O*-(4-*O*-methyl-α-D-glucopyranosyluronic acid)-D-xylopyranose, the structure of which had previously (4) been unequivocally established. Treatment of the derived methyl ester methyl glycoside with acetic anhydride in pyridine gave a sirup, a portion of which crystallized immediately from an ethyl ether solution. After recrystallization, white, small crystals were obtained, easily soluble in acetone, chloroform, ethyl acetate, and tetrahydrofuran, but only sparingly so in ethyl ether and ethanol. The methyl 2-*O*-[methyl-(2,3-di-*O*-acetyl-4-*O*-methyl-α-D-glucopyranosyl) uronate]-3,4-di-*O*-acetyl-D-xylopyranoside had m.p. 200–201° C, $[\alpha]_D^{20}$ +100° in chloroform, and was further characterized through its infrared spectrum and its X-ray diffraction pattern. The residual sirup had a specific rotation slightly lower than that of the crystalline portion (+85°). The data reported by Smith and co-workers (5) for the methyl ester methyl glycoside pentaacetate of two related, anomeric aldobiouronic acids would otherwise suggest that the xylopyranoside moiety was present in the β-configuration. Preparation of methyl ester methyl glycoside tetraacetates of specimens of the same aldobiouronic acid obtained from various natural products gave crystalline compounds with properties identical with those of the present derivative. The corresponding benzoate and *p*-nitrobenzoate esters were amorphous and could not be induced to crystallize.

EXPERIMENTAL

2-O-(4-O-Methyl-α-D-glucopyranosyluronic acid)-D-xylopyranose

A 4-*O*-methyl glucuronoxylan (200 g) from white birch wood (6) was dissolved in 72% sulphuric acid (100 ml). After 24 hours at room temperature, the solution was diluted to 4000 ml and boiled under reflux for 9 hours. Neutralization with barium

hydroxide, filtration through Celite, and evaporation and treatment with Darco G-60 charcoal and Amberlite IR-120 exchange resin yielded a pale yellow solution which was added to a column of Dowex 1-X4 anion exchange resin (acetate form). Neutral sugars were eluted with water (16 liters) after which sugar acids were removed with 30% aqueous acetic acid (16 liters). Evaporation of the acidic eluate yielded a sirup (25 g) which was resolved on 60 sheets of Whatman No. 3 MM filter paper with a solvent system consisting of ethyl acetate – acetic acid – water (9:2:2 v/v). The three main components, namely galacturonic acid, an aldobiouronic acid, and 4-*O*-methyl glucuronic acid (4), were eluted with water from the appropriate strips. Evaporation, treatment with Darco G-60 and Amberlite IR-120, and evaporation to dryness from methanol of the aldobiouronic acid gave a chromatographically pure, white, amorphous powder (10 g), $[\alpha]_D^{20}$ +108° (*c*, 1.0 in water). Anal. Calc. for $C_{12}H_{20}O_{11}$: OCH_3, 9.1%; equiv. wt., 340. Found: OCH_3, 9.2%; equiv. wt., 368.

*Methyl 2-O-[Methyl(4-O-methyl-α-*D*-glucopyranosyl)uronate]-*D*-xylopyranoside*

A portion of the above aldobiouronic acid (1.2 g) was boiled under reflux with 2.5% methanolic hydrogen chloride for 10 hours. After neutralization with silver carbonate, filtration through Celite, and evaporation, a white, fluffy powder was obtained (1.3 g, 100%), $[\alpha]_D^{20}$ +77° (*c*, 1.5 in water). Anal. Calc. for $C_{14}H_{24}O_{11}$: OCH_3, 25.3%. Found: OCH_3, 25.6%.

*Methyl 2-O-[Methyl(2,3-di-O-acetyl-4-O-methyl-α-*D*-glucopyranosyl)uronate]-3,4-di-O-acetyl-*D*-xylopyranoside*

The methyl ester methyl glycoside of the aldobiouronic acid (1.2 g) was dissolved in dry pyridine (75 ml), and redistilled acetic anhydride (25 ml) was added. After 24 hours at room temperature, the solution was poured into ice water (800 ml) and the aqueous solution was extracted with chloroform. The chloroform was extracted three times with ice-cold, 10% hydrochloric acid and subsequently three times with saturated sodium bicarbonate solution. After drying over anhydrous sodium sulphate, the chloroform solution was evaporated to yield a pale yellow sirup (1.70 g, 97%), which was dissolved in boiling ethyl ether (50 ml). On cooling of the solution, crystals immediately formed. The volume was adjusted to 25 ml and crystallization was allowed to proceed at −4° C for 24 hours. The white crystals obtained (0.32 g, 18.3%), m.p. 193–197° C (corrected), $[\alpha]_D^{20}$ +100° (*c*, 1.4 in chloroform), were dissolved in 20 ml of hot, anhydrous ethanol, followed by cooling and addition of the same volume of ethyl ether. The crystals formed (0.20 g) had m.p. 200–201° C, $[\alpha]_D^{20}$ +100° (*c*, 1.5 in chloroform). Anal. Calc. for $C_{22}H_{32}O_{15}$: C, 49.2%; H, 6.02%; OCH_3, 17.3%; $OCCH_3$, 40.1%; mol. wt., 536.3. Found: C, 49.7%; H, 5.93%; OCH_3, 17.0%; $OCCH_3$, 39.8%; mol. wt., 532.

The infrared spectrum of the compound exhibited absorption maxima at the following frequencies (cm^{-1}): 2940, 1745, 1440, 1370, 1225, 1050, 965, 920, 885, 790, 745, and 655. The X-ray powder diagram had the following interplanar lattice spacings in Å:* 8.92 (vs), 6.69 (s), 6.02 (s), 5.29 (s), 4.69 (vs), 4.07 (vs), 3.36 (s), 3.01 (s), 2.62 (m), 2.34 (m), 2.23 (m), 2.10 (m), 1.98 (m), 1.85 (m), 1.75 (w).

The residual sirup had $[\alpha]_D^{20}$ +85° (*c*, 1.5 in chloroform). It could not be induced to crystallize further. Its infrared spectrum was similar, albeit not identical with that of the crystalline portion.

1. Jones, J. K. N. and Wise, L. E. J. Chem. Soc. 2750, 3389 (1952).
2. Gorin, P. A. J. and Perlin, A. S. Can. J. Chem. **36**, 999 (1958).

**The author is grateful to Dr. R. St. J. Manley for providing the X-ray data.*

3. WHISTLER, R. L. and RICHARDS, G. N. J. Am. Chem. Soc. **80**, 4888 (1958).
4. GLAUDEMANS, C. P. J. and TIMELL, T. E. J. Am. Chem. Soc. **80**, 941, 1209 (1958).
5. MONTGOMERY, R., SMITH, F., and SRIVASTAVA, H. C. J. Am. Chem. Soc. **78**, 2837, 6169 (1956).
6. GLAUDEMANS, C. P. J. and TIMELL, T. E. Svensk Papperstidn. **60**, 869 (1957); **61**, 1 (1958).

RECEIVED DECEMBER 24, 1958.
MCGILL UNIVERSITY AND
PULP AND PAPER RESEARCH INSTITUTE OF CANADA,
MONTREAL, QUEBEC.

ABSOLUTE CONFIGURATION OF (−)-HOMOSTACHYDRINE*

A. V. ROBERTSON† AND LÉO MARION

Wiehler and Marion (1) isolated and identified a new alkaloid from alfalfa. The laevorotatory compound, which they called (−)-homostachydrine, was shown to be one of the enantiomers of the methyl betaine of pipecolic acid (piperidine-2-carboxylic acid). The proof of structure followed from the identity of the infrared spectra, X-ray powder diagrams, and chromatographic behavior of (−)-homostachydrine hydrochloride and the synthetic hydrochloride of racemic pipecolic acid methyl betaine.

We have now determined the configuration‡ of (−)-homostachydrine by methylating L-(−)-pipecolic acid. The methyl betaine hydrochloride had $[\alpha]_D$ −13°, identical with the value for the natural product (1). Thus (−)-homostachydrine belongs to the L-series of amino acids, and since (−)-pipecolic acid has been correlated with L-aspartic acid (2), the absolute configuration of the betaine is as shown in the formula.

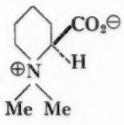

EXPERIMENTAL

Melting points are corrected. The infrared absorption spectra were measured in nujol mulls on a Perkin–Elmer double beam spectrometer model 21B.

L-(−)-*Pipecolic Acid*

Pure synthetic (±)-pipecolic acid hydrochloride was available in this laboratory (1). The acid was resolved with (−)-tartaric acid, $[\alpha]_D^{25}$ −14.2° (7% in water), according to the method of Schweet, Holden, and Lowy (3) (cf. Leithe, ref. 4). (−)-Pipecolic acid-(−)-bitartrate had constant optical activity after three crystallizations, $[\alpha]_D^{25}$ −20.0° (8% in water). After decomposing the diastereoisomer on Amberlite IR-4B ion exchange resin (3), the (−)-pipecolic acid had m.p. 271–272° (copper block) and $[\alpha]_D^{25}$ −25.8° (5% in water). These constants are in good agreement with reported values for natural and synthetic (−)-pipecolic acid (5).

L-(−)-*Homostachydrine Hydrochloride*

(−)-Pipecolic acid was methylated using the procedure of Wiehler and Marion for

*Issued as N.R.C. No. 5081.
†*National Research Council of Canada Postdoctorate Fellow.*
‡*Dr. H. C. Beyerman, Technische Hogeschool, Delft, has also independently established the configuration of homostachydrine, and is publishing his results in Rec. trav. chim. Pays-Bas.*

the racemic acid (1). The hydrochloride of the methyl betaine which was recrystallized by adding hot ethyl acetate to a boiling solution of the compound in absolute ethanol had m.p. 217–218° (gas evolution) and $[\alpha]_D^{25}$ −13.0° (2% in ethanol). The infrared spectrum and the X-ray powder diagram of the synthetic (−)-homostachydrine hydrochloride were identical in all respects with those of the hydrochloride of the natural material. Similarly, the synthetic and natural samples were chromatographically pure, and indistinguishable from each other, having R_F 0.58 in *n*-butanol – concentrated hydrochloric acid – water (100:20:39) and R_F 0.56 in 95% ethanol – concentrated aqueous ammonia (95:5).

We thank Dr. Maria Przybylska and Mr. R. Lauzon of these laboratories for the X-ray powder diagrams and for the infrared absorption spectra, respectively.

1. Wiehler, G. and Marion, L. Can. J. Chem. **36**, 339 (1958).
2. King, F. E., King, T. J., and Warwick, A. I. J. Chem. Soc. 3590 (1950).
3. Schweet, R. S., Holden, J. T., and Lowy, P. H. J. Biol. Chem. **211**, 517 (1954).
4. Leithe, W. Ber. **65**, 927 (1932).
5. Harris, G. and Pollock, J. R. A. Chem. & Ind. 462 (1953).

Received December 30, 1958.
Division of Pure Chemistry,
National Research Council,
Ottawa, Canada.

SEPARATION OF NICKEL AND COBALT BY PAPER CHROMATOGRAPHY*

Gerhard R. Weidmann

The R_F values of Ni and Co have been determined for *n*-tributyl phosphate (TBP) adjusted with concentrated hydrochloric acid of various concentrations. TBP is as suitable for the separation of Ni and Co by paper chromatography as other solvents mentioned in the literature (1, 2, 3). Before use the reagent was shaken with nitric acid to remove mono- and di-butyl phosphate (4), then distilled and adjusted with HCl of different molarities. Afterwards the organic phase was separated and mixed with methanol in the ratio 2:1 and 1:1.

PROCEDURE

The chromatograms were developed by ascending chromatography. The paper used was Schleicher and Schüll No. 4023*b* (Whatman No. 1). Solutions of Ni- and Co-chlorides each in quantities of 20γ were put on the paper. The process ran 4 hours at a temperature of 22° C. The flow of Co was easily identified by its blue color. On the following pictures Co was marked with α-nitroso-β-naphthol. Ni was identified with an alcoholic solution of dimethyl glyoxime.

RESULTS

The R_F values of Co recorded in Table I show a close dependence on increasing concentration of HCl used to equilibrate the TBP. Ascending concentration of HCl reduces the distance of Co from the liquid front, i.e. the R_F values increase. When working with

**Private contribution.*

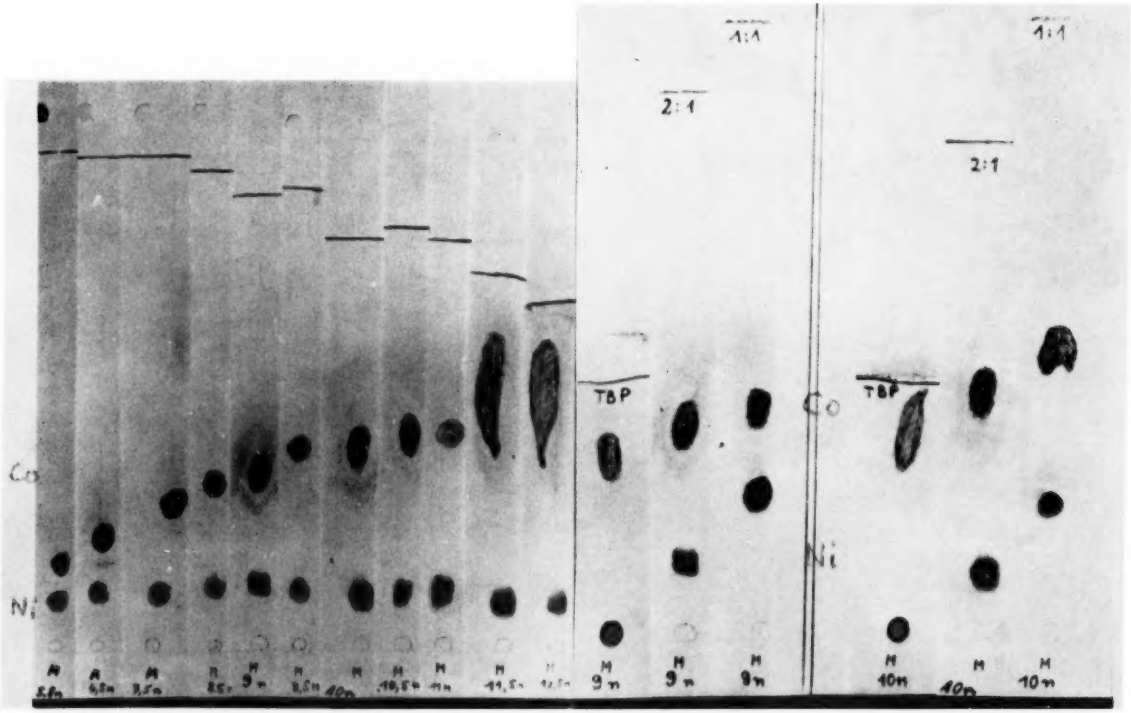

FIG. 1. Flow of Co using TBP/methanol mixture in the ratio 2:1 as a solvent.

FIG. 2. Different flow rates of Co and Ni depending on use of either pure HCl equilibrated TBP or with an admixture of methanol as a solvent.

highly concentrated HCl, Co will almost reach the liquid front. In this case Co does not flow as a spot any more, but has a long diffuse tail (see Fig. 1). Similar results are obtained when chromatographing Co using TBP as a solvent without admixture of methanol (see Fig. 2).

TABLE I

R_F of Co using a TBP/methanol mixture in the ratio 2:1

TBP adjusted with N HCl	5.5	6.5	7.5	8.5	9.0	9.5	10	10.5	11	11.5	12	12.5
R_F of Co	0.16	0.23	0.28	0.34	0.38	0.43	0.46	0.48	0.52	0.59	0.66	0.74

As Table II shows, the R_F values resulting thereof are considerably higher than those obtained using TBP/methanol mixtures.

TABLE II

R_F values of Co

TBP adjusted with N HCl	Ratio TBP/methanol		
	1:1	2:1	TBP pure
9 N	0.36	0.37	0.7
10 N	0.46	0.46	0.85
12.5 N	—	0.74	—

Previous tests have shown that Ni is not extracted by TBP from an aqueous solution. This effect is apparent in the chromatogram. Figure 2 shows that, when using pure HCl equilibrated TBP, Ni is immobile; and in TBP/methanol mixtures the flow rate is roughly proportional to the quantity of methanol present.

SUMMARY

Sharp chromatographing separations of Ni and Co can be obtained using HCl–equilibrated TBP. It is recommended that the TBP be treated with 9 to 10 molar HCl, and mixed with methanol in the proportion 2:1.

1. Burstall, F. H., Davies, G. R., Linstead, R. P., and Wells, R. A. J. Chem. Soc. 516 (1950).
2. Burstall, F. H. *et al.* J. Chem. Soc. 1497 (1952).
3. Lederer, E. Chromatography. Elsevier Publishing Company, New York. 1954.
4. Burger, L. L. and McClanahan, E. D. I/EC 50, 153 (1958).

Received December 8, 1958.
Coburg/Bavaria,
Kanonenweg 33,
West Germany.

QUENCHING AND VIBRATIONAL-ENERGY TRANSFER OF EXCITED IODINE MOLECULES

B. Stevens

From their investigation of the effect of foreign gases on the emission spectrum of I_2 $^3\Pi$ ($v' = 26$), Arnot and McDowell (1) obtain collisional transfer coefficients which are

some 10–15 times greater than expected from simple collision theory if a value of 10^{-8} second is assumed for τ_0, the radiative lifetime of the excited I_2 molecule.

In the same way, Polanyi (2) concludes that the collisional transfer efficiencies of H_2 and D_2 are 1 in 55 and 1 in 11 respectively if τ_0 is taken as 3×10^{-7} second. Recently, Arnot and McDowell (3) have corrected Polanyi's results for self-quenching and show that these are consistent with collisional transfer coefficients of 3.9 (H_2) and 7.7 (D_2) times greater than the theoretical values on the assumption that $\tau_0 = 10^{-8}$ second.

Neither Polanyi nor Arnot and McDowell observed self-transfer bands in the absence of foreign gases. In view of the high efficiency of I_2 as third body in I atom recombination (4) a non-quenching collision would be expected to lead to vibrational-energy transfer, and the absence of self-transfer bands may be taken as strong evidence that the collisional efficiency, p, of self-quenching is unity. A similar argument was put forward by Vartanyan (5) in connection with the O_2 quenching of aniline vapor fluorescence.

In their recent note, Arnot and McDowell (3) quote a value of 2.0×10^5 liter mole^{-1} for the I_2 self-quenching constant k_S/k_F measured presumably at 20° C, the temperature of their transfer experiments. Thus from

$$\frac{k_S}{k_F} = p\tau_0 \frac{N}{1000}(r_1+r_2)^2\left\{8\pi RT\left(\frac{1}{M_1}+\frac{1}{M_2}\right)\right\}^{\frac{1}{2}} = 2.0\times10^5 \text{ liter mole}^{-1}$$

with $p = 1$; $r_1 = r_2 = 2.7$ Å; $T = 293°$ K; N = Avogadro number; k_S = self-quenching rate constant; and $k_F = 1/\tau_0$ = radiative decay constant, we have

$$\tau_0 = 1.6\times10^{-6} \text{ second.}$$

This value of τ_0 is some 100 times longer than that usually associated with fluorescence emission but in view of Mulliken's assignment of $^3\Pi$ to this excited state of I_2, (6), the emission is by current definition (7) a phosphorescence of short lifetime due to the heavy atom effect (8). The Z dependence of radiative intersystem transition probabilities would lead us to expect a value closer to $\sim2\times10^{-6}$ second for Cd $^3P_1$ than to $\sim1\times10^{-7}$ second for Hg $^3P_1$.

Experimental transfer coefficients k_T/k_F obtained by Arnot and McDowell both from their own and from Polanyi's results are compared with the theoretical values computed on the basis $\tau_0 = 1.6\times10^{-6}$ second in Table I. k_T is the rate constant for collisional transfer from the 26th vibrational level of I_2*. The collisional transfer efficiency p_T is now intermediate between the values $\ll 1$ obtained from sound dispersion data in the region $v \sim 0$, and unity associated with third body effects on atom recombination in the region $v \sim \infty$. Eliaschevich (9) also adopted the value $\tau_0 = 10^{-8}$ second for the excited I_2

TABLE I

Coefficients for the transfer of vibrational energy from excited I_2 molecules at 20° C

Gas	k_T/k_F liter mole^{-1} Experimental	Theoretical	p_T	Ref.
H_2*	1.9×10^4	7.8×10^5	0.02	2, 3
D_2*	2.7×10^4	5.6×10^5	0.05	2, 3
He	5.31×10^4	5.17×10^5	0.10	1
Ne	2.69×10^4	2.66×10^5	0.10	1
A	1.64×10^4	2.28×10^5	0.07	1
O_2	1.5×10^4	2.2×10^5	0.07	1

*$T = 27°$ C.

molecule, which is reduced by self-quenching under his experimental conditions to 3.3×10^{-9} second, and obtained collisional transfer coefficients up to 100 times greater than the theoretical values. If $\tau_0 = 1.6 \times 10^{-6}$ second, the reduced lifetime due to self-quenching under the conditions he used is 9.0×10^{-7} second and his transfer coefficients should be reduced by a factor of 270, which brings them into line with the results in Table I.

It is of interest to compare the transfer efficiencies p_T with quenching efficiencies p_Q which may be obtained from the quenching constants k_Q/k_F in the same way; (k_Q is the collisional quenching rate constant). Unfortunately Arnot and McDowell do not give their numerical values for the quenching constants but for He and A these may be calculated from Figs. 3 and 4 (1), in which the slope is given by

$$(k_Q/k_F)/\{1+(k_S/k_F)[I_2]\}.$$

The relevant data are given in Table II along with values obtained for H_2 and D_2 by Arnot and McDowell (3) from Polanyi's results (2). The lower transfer efficiency p_T

TABLE II

Coefficients for quenching of excited I_2 molecules at 20° C

Gas	k_Q/k_F liter mole^{-1}		p_Q
	Experimental	Theoretical	
H_2*	8.4×10^3	7.84×10^5	0.01
D_2*	1.46×10^4	5.60×10^5	0.03
He	3.12×10^4	5.17×10^5	0.06
A	1.01×10^5	2.28×10^5	0.44

*T = 27° C.

for A compared with He may be explained if the higher quenching efficiency p_Q of A is taken into account. Comparable values $p_T{}^0$ obtained on the basis of non-quenching collisions are

$$p_T{}^0 = p_T/(1-p_Q),$$
$$= 0.10 \text{ for He, } 0.13 \text{ for A.}$$

The low transfer efficiency of O_2 can probably be explained in the same way.

It should be noted that the above calculations involve two assumptions. In the first place the collision diameters of the excited and unexcited iodine molecules are assumed to be equal, which is almost certainly not the case. The collision radius calculated from the self-quenching constant taking $\tau_0 = 10^{-8}$ second is 65.6 Å compared with 2.7 Å for the unexcited molecule. This value is unrealistic if quenching is due to a collision-induced predissociation of the excited molecule but could presumably be approached if quenching involves a sensitized predissociation of the quenching molecule as Polanyi has suggested (2). In the absence of direct measurements of τ_0 there is more justification for assigning a value of 2.7 Å to the excited molecule than for assuming a value of 10^{-8} second for its radiative lifetime in view of the electronic transition involved. Use of the larger collision diameter and shorter lifetime would not significantly affect the values of p_T and p_Q given, since in the expression from which they are obtained, the quantity $\tau_0(r_1+r_2)^2$ remains virtually unaltered.

A more serious objection may be made to the second assumption that the collision diameter of the excited I_2* molecule is the same both for quenching and for vibrational-

energy transfer, particularly if quenching is due to sensitized predissociation at super-kinetic distances. If, however, the quenched molecule predissociates following the collisional removal of 3 or 4 vibrational quanta then quenching and vibrational-energy transfer have similar requirements and the error introduced by this second assumption may not be serious.

1. ARNOT, C. and MCDOWELL, C. A. Can. J. Chem. **36**, 114 (1958).
2. POLANYI, J. C. Can. J. Chem. **36**, 121 (1958).
3. ARNOT, C. and MCDOWELL, C. A. Can. J. Chem. **36**, 1322 (1958).
4. CHRISTIE, M. I., HARRISON, A. J., NORRISH, R. G. W., and PORTER, G. Proc. Roy. Soc. A, **231**, 446 (1955).
5. VARTANYAN, A. T. Izvest. Akad. Nauk S.S.S.R. Ser. Fiz. **3**, 341 (1938).
6. MULLIKEN, R. S. Revs. Modern Phys. **4**, 1 (1932).
7. LEWIS, G. N. and KASHA, M. J. Am. Chem. Soc. **66**, 2100 (1944).
8. MCCLURE, D. S. J. Chem. Phys. **17**, 905 (1949).
9. ELIASCHEVICH, M. Physik. Z. Sowjetunion, **1**, 510 (1932).

RECEIVED DECEMBER 8, 1958.
DEPARTMENT OF CHEMISTRY,
THE UNIVERSITY,
SHEFFIELD 10,
ENGLAND.

NOTES TO CONTRIBUTORS

Canadian Journal of Chemistry

MANUSCRIPTS

General.—Manuscripts, in English or French, should be typewritten, double spaced, on paper 8½×11 in. **The original and one copy are to be submitted.** Tables and captions for the figures should be placed at the end of the manuscript. Every sheet of the manuscript should be numbered. Style, arrangement, spelling, and abbreviations should conform to the usage of recent numbers of this journal. Greek letters or unusual signs should be written plainly or explained by marginal notes. Characters to be set in bold face type should be indicated by a wavy line below the characters. Superscripts and subscripts must be legible and carefully placed. Manuscripts and illustrations should be carefully checked before they are submitted. Authors will be charged for unnecessary deviations from the usual format and for changes made in the proof that are considered excessive or unnecessary.

Abstract.—An abstract of not more than about 200 words, indicating the scope of the work and the principal findings, is required, except in Notes.

References.—These should be designated in the text by a key number and listed at the end of the paper, with the number, in the order in which they are cited. The form of the citations should be that used in this journal; in references to papers in periodicals, titles should not be given and only initial page numbers are required. The names of periodicals should be abbreviated in the form given in the most recent *List of Periodicals Abstracted by Chemical Abstracts*. All citations should be checked with the original articles and each one referred to in the text by the key number.

Tables.—Tables should be numbered in roman numerals and each table referred to in the text. Titles should always be given but should be brief; column headings should be brief and descriptive matter in the tables confined to a minimum. Vertical rules should not be used. Numerous small tables should be avoided.

ILLUSTRATIONS

General.—All figures (including each figure of the plates) should be numbered consecutively from 1 up, in arabic figures, and each figure referred to in the text. The author's name, title of the paper, and figure number should be written in the lower left corner of the sheets on which the illustrations appear. Captions should not be written on the illustrations.

Line drawings.—Drawings should be carefully made with India ink on white drawing paper, blue tracing paper, or co-ordinate paper ruled in blue only; any co-ordinate lines that are to appear in the reproduction should be ruled in black ink. Paper ruled in green, yellow, or red should not be used. All lines must be of sufficient thickness to reproduce well. Decimal points, periods, and stippled dots must be solid black circles large enough to be reduced if necessary. Letters and numerals should be neatly made, preferably with a stencil (**do NOT use typewriting**), and be of such size that the smallest lettering will not be less than 1 mm high when the figure is reduced to a suitable size. Many drawings are made too large; originals should not be more than 2 or 3 times the size of the desired reproduction. Wherever possible two or more drawings should be grouped to reduce the number of cuts required. In such groups of drawings, or in large drawings, full use of the space available should be made; the ratio of height to width should conform to that of a journal page (5¼×7¾ in.) but allowance must be made for the captions. **The original drawings and one set of clear copies (e.g. small photographs) are to be submitted.**

Photographs.—Prints should be made on glossy paper, with strong contrasts. They should be trimmed so that essential features only are shown and mounted carefully, with rubber cement, on white cardboard, with no space between those arranged in groups. In mounting, full use of the space available should be made. **Photographs are to be submitted in duplicate;** if they are to be reproduced in groups one set should be mounted, the duplicate set unmounted.

REPRINTS

A total of 50 reprints of each paper, without covers, are supplied free. Additional reprints, with or without covers, may be purchased at the time of publication.

Charges for reprints are based on the number of printed pages, which may be calculated approximately by multiplying by 0.5 the number of manuscript pages (double-space typewritten sheets, 8½×11 in.) and including the space occupied by illustrations. Prices and instructions for ordering reprints are sent out with the galley proof.

Contents

Notes:

Printed in Canada *by* University of Toronto Press